



UNIVERSITAT^{DE}
BARCELONA

Water-in-Water Emulsions for Obtaining Enzyme-Loaded Microgels and Encapsulated Emulsions

Yoran Beldengrün



Aquesta tesi doctoral està subjecta a la llicència **Reconeixement 3.0. Espanya de Creative Commons.**

Esta tesis doctoral está sujeta a la licencia **Reconocimiento 3.0. España de Creative Commons.**

This doctoral thesis is licensed under the **Creative Commons Attribution 3.0. Spain License.**

Encapsulation of enzymes into protective matrices is of interest in drug delivery or industrial processes, to control the release of the enzyme or protect it from harsh environments. We are studying the encapsulation of lactase (β -Gal) into drug delivery vehicles, templated by water-in-water (W/W) emulsions.

In the first system, the sodium carboxymethylcellulose (NaCMC) / bovine serum albumin (BSA) mixtures, phase behavior was analyzed and emulsions were formed. Ca^{2+} crosslinked selectively NaCMC, while the trivalent ions Fe^{3+} and Al^{3+} crosslinked both polymers, thus also the entire emulsion. By dropping the emulsion into the trivalent crosslinker solutions, encapsulated emulsions could be obtained, which consist of BSA gel beads that contain encapsulated NaCMC emulsion droplets. Freeze-drying of those beads lead to particles with pores, whose size corresponded to that of the emulsion droplets. Bead size was minimized by using the electrospraying technique. Stability of those encapsulated emulsions and incorporation of enzymes into them was studied.

In the second system, the gelatin/maltodextrin mixtures, phase behavior was analysed in detail. Microgels were formed from the gelatin-in-maltodextrin emulsions by cooling and crosslinking the gelatin droplets with genipin. Those microgels could also be kept in a dry form, obtained by freeze-drying the suspension. Responsiveness and stability of microgels under various physicochemical conditions was studied. Next, various immobilisation methods of the enzyme β -Gal were tested, to achieve highest encapsulation yield and activity recovery. Enzymes remained active over at least one month inside the microgels and enzyme-leakage decreased at higher crosslinking rates. Of interest is the fact that the enzyme remained active after a complete cycle of freeze-drying and rehydration of enzyme-loaded microgel particles.

The crosslinked gelatin microgels were not able to preserve enzyme activity under simulated gastric fluid temperature and pH conditions. It was shown however that they have protective effect on enzyme activity at pH 5.8 and 37 °C. These can be considered as preliminary results for their possible use in e.g. industrial production of lactose-hydrolyzed milk, which has similar pH and temperature conditions.

PhD Thesis realized at [IQAC-CSIC \(2014-2018\)](#)

PhD Student: Yoran Beldengrün

Director: Dr. Jordi Esquena Moret

Tutor: Dr. María José García Celma

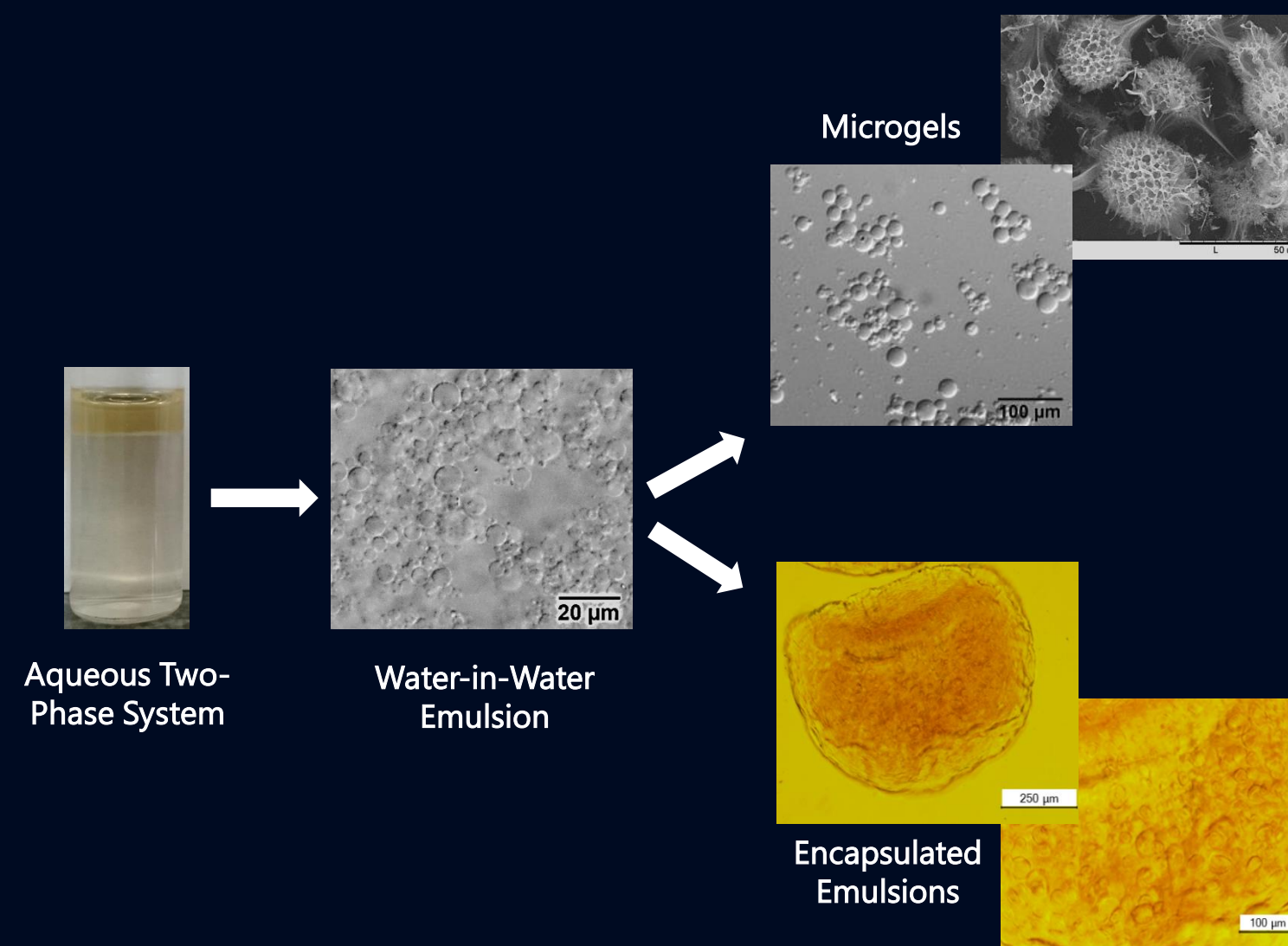
2018 (Barcelona)

PhD Thesis

Yoran Beldengrün

Water-in-Water Emulsions for Obtaining Enzyme-Loaded Microgels and Encapsulated Emulsions

Yoran Beldengrün



UNIVERSITAT DE BARCELONA

FACULTAT DE FARMÀCIA I CIÈNCIES DE L'ALIMENTACIÓ

**WATER-IN-WATER EMULSIONS FOR OBTAINING ENZYME-LOADED
MICROGELS AND ENCAPSULATED EMULSIONS**

Yoran Beldengrün
2018

UNIVERSITAT DE BARCELONA

FACULTAT DE FARMÀCIA I CIÈNCIES DE L'ALIMENTACIÓ

Programa de doctorat de Recerca, Desenvolupament i Control de Medicaments

**WATER-IN-WATER EMULSIONS FOR OBTAINING ENZYME-LOADED
MICROGELS AND ENCAPSULATED EMULSIONS**

Memòria presentada per Yoran Beldengrün per optar al títol de doctor per la universitat de
Barcelona

Director:
Jordi Esquena Moret

Doctorand:
Yoran Beldengrün

Tutora:
María José García Celma

Yoran Beldengrün
2018

Acknowledgements

I'm writing those acknowledgments from the plane to Berlin, where I will be spending some preparation days for my next career step, working in Science Diplomacy for the Israeli-Palestinian Conflict.

It's a perfect moment to look back and acknowledge all what this PhD thesis and persons involved in it have contributed to my personal and professional development.

First of all, and most importantly, I want to deeply thank the director of my PhD Thesis, Jordi Esquena, who gave me the opportunity to realise this PhD in the Surface Chemistry group of the IQAC-CSIC. Thanks for guiding me through the research, teaching me new scientific concepts and assistance in the moments of writing.

A special thanks goes also to Maria José Garcia Celma, my tutor of the PhD Thesis, for all assistance, especially in the interaction with the University of Barcelona.

Thanks to Conxita Solans and Carlos Rodriguez for co-leading with Jordi the Colloid and Interfacial Chemistry Center, bringing interesting researchers to our center and thanks for all the scientific interchanges we had.

In September 2014 I arrived freshly in Barcelona, did not speak yet good the language and also needed a scientific introduction to work in our lab facilities. Many people helped me thereby.

I want to thank therefore Susana and Jonathan, who patiently introduced me to the daily work in the lab, explaining me methods, introducing me to instrument use and teach me how to follow the qualitative guidelines. Concerning, introduction to life in Barcelona I want to thank Laura and Rodrigo, who were of great assistance. Thanks Laura, for having helped me out with the many personal and professional administrative paperwork. Without your help, I would have been completely lost.

Thanks to Rodrigo, for having given me a perfect welcome, by letting me stay in your apartment the first months in Barcelona, going out together for drinks or organise barbecues on your terrace. I also truly enjoy your positive energy, high scientific curiosity, and interest in sharing it, which I think is primordial in research. Same goes for Jeremie, thanks for the scientific interchanges we had and the good moments we also spent outside the lab. Thanks to both of you, for having also contributed to Scientists Dating Forum.

Emiliano, I think it goes without saying, that I'm extremely glad for having spent the second half of my PhD sharing the office with you. We share many passions of life, so if we would not have met in the lab, at some moment our life paths would have crossed anyways and we would have started our friendship outside lab 2301.

Those close to 4 years of PhD allowed me to collaborate with so many people, and I want to, on first place, send my gratitude to all undergraduate students, whose research I supervised during my time in Barcelona:

Thanks Laura for your important work on the NaCMC/BSA system and the encapsulation of the enzyme into beads. I admired your high motivation and capacity to plan and execute independently complex experiments. Same goes to Jordi; great job investigating the influence of salts of the Hofmeister Series on the phase behaviour of gelatin/maltodextrin mixtures. Being enrolled in a PhD program now, confirms the great passion for research I saw in you. Thanks Maite, for your work on phase behaviour of gelatin/maltodextrin emulsions at different pH conditions. It's great to see your motivation to having

done internships also extracurricularly. Cristina Miquel, you were the first undergraduate student, which I could supervise over a prolonged period of time. Thanks for initiating our research on the NaCMC/BSA system and setting the ground for all our further studies. I admired how organised you were in your work. Lastly thanks to the students Sara Poletti and Juan Maldonado, both from Texas, who came for few summer months to Europe, to collaborate with us in the laboratory, in between your weekly travels all over the continent. I hope you enjoyed this introduction to work and life in a research laboratory. I want to thank you for your great help in analysing gelatin/maltodextrin emulsions, Sara, and encapsulating emulsions into microgels, Juan.

Thanks to all other colleagues of the Colloid and Interfacial Chemistry Center, for making my time at work so pleasant: Adaris, Albert, Aurora, Baltazar, Carmen, Cristina, Elena, Eva, Ferran, Gabriela, Maria M^a Carmen, Marta, Montse, Natalia, Romà, Sheila, Théo, Tirso and Vanessa.

I indirectly also collaborated with the many partners from the MSCA-ITN BIBAFOODS network and enjoyed the scientific and personal exchanges we had during all our common trainings and secondments. I want to highlight thereby those persons at whom I could do a secondment or who came to our laboratory for a research stay:

Thanks a lot to Andreea Pasc, for your supervision during my 2 month research stay at the Université de Lorraine. You are a great team leader and I want to thank you for your great scientific input. It was a pleasure visiting the school of your children, teaching them science as a clown. One of my highlights of my science communication activities I did in my last years.

Thanks to Ileana, Fernanda and Nadia for all your help during my stay in the lab of the Université de Lorraine. Also thanks to all others of the Université de Lorraine, who made my 2 months at you so pleasant and who helped me out in my research. It was pleasure welcoming you in our research group in Barcelona, Poonam and Ileana. I was very glad sharing the office and free time with you those months. Thanks Sofia for your help with the Raman measurements the days during which I was in Alcalá de Henares. Thanks to Gemma Montalvo for welcoming me in your lab, and your help with corrections of the article.

Thanks to Jens Risbo, Henriette Hansen and the rest of the coordinating team of BIBAFOODS, for having lead this research consortium. At this place, I also want to thank the EU grant who helped to finance this research: Marie Skłodowska Curie Initial Training Networks (FP7-PEOPLE-2013-ITN-606713, BIBAFOODS project).

Further thanks go to Joan Grimalt, Gemma Fabrias and Lluís Fajarí who agreed to contract me for some additional months, in exchange of me doing some communication and project management work for the CID-CSIC.

I also want to thank the jury of my PhD Defense: Andreea Pasc, Carlos Rodriguez and Elvira Escribano. And Conxita Solans and Alicia Maestro as possible substitute. Thanks for your time to have a critical read through this thesis and I am looking forward to our discussion the day of the defense.

Thanks to M^a Luisa García, coordinator of my PhD program, for your assistance in the entire procedure of depositing the PhD Thesis.

Finally, I want to thank my parents who stood by my side, during the entire PhD thesis, having supported and advised me in the many situations I went through.

Table of Contents

| | |
|--|-----------|
| Summary | 12 |
| Abbreviations | 14 |
| Symbols and Units | 15 |
| 1 Introduction | 19 |
| 1.1 Relevance of Research..... | 19 |
| 1.1.1 Lactase Non-persistence and Lactose Intolerance..... | 19 |
| 1.2 General Introduction to Emulsions..... | 21 |
| 1.3 Water-in-Water Emulsions..... | 25 |
| 1.3.1 Historical Background to Studies on Water-in-Water Emulsions..... | 25 |
| 1.3.2 Phase Behaviour in Aqueous Mixtures..... | 26 |
| 1.3.3 Associative Phase Separation..... | 27 |
| 1.3.4 Segregative Phase Separation..... | 28 |
| 1.3.5 Thermodynamics of polymer mixtures..... | 29 |
| 1.3.5.1 Flory-Huggins, Lattice Theory..... | 30 |
| 1.3.5.2 Excluded Volume / Depletion Interactions Model..... | 32 |
| 1.3.6 Effects of Physicochemical Parameters on Phase Behaviour in W/W Emulsions..... | 36 |
| 1.3.7 Phase Behaviour..... | 39 |
| 1.3.8 Stabilisation of W/W Emulsions..... | 41 |
| 1.3.9 Applications of W/W Emulsions..... | 43 |
| 1.4 Microgels..... | 44 |
| 1.4.1.1 Microgel preparation methods..... | 45 |
| 1.4.1.2 Microgel formation from W/W emulsions..... | 48 |
| 1.4.2 Controlled Release Properties..... | 50 |
| 1.4.2.1 Temperature-triggered Release..... | 50 |
| 1.4.2.2 Electrostatic-triggered Release..... | 51 |
| 1.4.2.3 Triggered Release by Specific Compounds..... | 51 |
| 1.4.2.4 Triggered Release by Degradation..... | 52 |
| 1.5 Oral Delivery of Enzymes..... | 53 |
| 1.6 Immobilisation of Enzymes..... | 54 |
| 1.6.1 Immobilisation of Enzymes into Microgels..... | 55 |
| 1.6.2 Immobilisation of Lactase for Oral Delivery..... | 57 |
| 1.7 Polymers used and their Mixtures..... | 58 |
| 1.7.1 Sodium Carboxymethylcellulose..... | 58 |

| | | |
|----------|--|-----------|
| 1.7.2 | Bovine Serum Albumin..... | 59 |
| 1.7.3 | NaCMC/BSA Emulsions..... | 59 |
| 1.7.4 | Gelatin | 60 |
| 1.7.5 | Genipin | 62 |
| 1.7.6 | Crosslinking Mechanism:..... | 64 |
| 1.7.7 | Maltodextrin | 66 |
| 1.7.8 | Gelatin/Maltodextrin Mixtures..... | 68 |
| 2 | Main Objectives and Working Plan | 75 |
| 3 | Material and Methods..... | 79 |
| 3.1 | Material..... | 79 |
| 3.2 | Instruments..... | 82 |
| 3.3 | Methods | 84 |
| 3.3.1 | NaCMC/BSA Emulsions as Template for Microgel Formation..... | 84 |
| 3.3.1.1 | Stock Solutions of Polymers | 84 |
| 3.3.1.2 | Study of Phase Behaviour of NaCMC/BSA Mixtures | 84 |
| 3.3.1.3 | Formation of Capsules with Multivalent Ions | 84 |
| 3.3.1.4 | Electrospraying the NaCMC/BSA Emulsion | 85 |
| 3.3.1.5 | Evaluation of pH-Stability of Capsules..... | 86 |
| 3.3.1.6 | Immobilisation of Enzymes into NaCMC/BSA Emulsion Beads..... | 86 |
| 3.3.2 | Properties of Gelatin, Maltodextrin and Genipin | 86 |
| 3.3.2.1 | Reaction of Genipin with Water, Maltodextrin and Gelatin | 86 |
| 3.3.2.2 | Influence of Temperature and Time on Crosslinking of Genipin..... | 86 |
| 3.3.2.3 | Gelatin Sol-Gel Transition Temperature | 87 |
| 3.3.2.4 | Measurement of Swelling of Gelatin-Genipin Macrogels..... | 87 |
| 3.3.2.5 | Density of Gelatin and Maltodextrin..... | 87 |
| 3.3.2.6 | Measurement of UV Spectra of Gelatin, Genipin and Maltodextrin..... | 88 |
| 3.3.2.7 | Concentration Measurement of Maltodextrin and Gelatin by Optical Rotation..... | 88 |
| 3.3.2.8 | Labelling Polymers..... | 89 |
| 3.3.3 | Phase Behaviour of Water/Gelatin/Maltodextrin System | 92 |
| 3.3.3.1 | Determination of Phase Diagram | 92 |
| 3.3.3.2 | Study of Influence of Temperature on Phase Behaviour..... | 92 |
| 3.3.3.3 | Turbidity Study of Gelatin/Maltodextrin Mixtures | 93 |
| 3.3.3.4 | Raman Spectroscopy of Maltodextrin/Gelatin Mixtures..... | 93 |
| 3.3.3.5 | Observation of Emulsions by Optical Microscopy..... | 93 |
| 3.3.4 | Gelatin Microgel Preparation | 94 |
| 3.3.4.1 | Microgel Preparation..... | 94 |

| | | |
|----------|--|------------|
| 3.3.4.2 | Purification Methods of Microgels..... | 94 |
| 3.3.4.3 | Freeze-Drying of Microgels | 95 |
| 3.3.4.4 | Observation of Freeze-Dried microgels under SEM..... | 95 |
| 3.3.4.5 | Resuspension of Freeze-Dried Microgels..... | 95 |
| 3.3.5 | Characterisation of Microgel Particles | 95 |
| 3.3.5.1 | Study of Influence of time between emulsification and cooling down | 96 |
| 3.3.5.2 | Size Determination of Emulsion Droplets / Microgels by Microscope..... | 96 |
| 3.3.5.3 | Size Determination of Microgels by Light Diffraction Particle Size Analyser..... | 96 |
| 3.3.5.4 | Study of the Influence of Preparation Parameters on Microgel Size..... | 97 |
| 3.3.5.5 | Study of the Influence of Physicochemical Parameters on microgel size/morphology | 98 |
| 3.3.6 | Encapsulation of Enzymes into the Gelatin Microgels | 100 |
| 3.3.6.1 | Measurement of Enzyme Activity..... | 100 |
| 3.3.6.2 | Measurement of Enzyme Concentration | 101 |
| 3.3.6.3 | Study Enzyme Compatibility of Crosslinker and Microgels..... | 103 |
| 3.3.6.4 | Different Encapsulation Methods..... | 103 |
| 3.3.6.5 | Determination of Enzyme Encapsulation Efficiency | 106 |
| 3.3.6.6 | Enzyme Long-Term Stability in Microgels..... | 107 |
| 3.3.6.7 | Freeze-Drying of Enzyme-Loaded Microgels..... | 107 |
| 3.3.6.8 | Study of Enzyme stability under simulated gastric pH and body temperature conditions | 108 |
| 4 | Results and Discussion | 111 |
| 4.1 | NaCMC/BSA Emulsions as Template for Microgel Formation..... | 111 |
| 4.1.1 | Phase Behaviour of the NaCMC/BSA/Water System..... | 111 |
| 4.1.2 | Formation of Emulsions | 114 |
| 4.1.3 | Formation of Capsules with Multivalent Ions | 115 |
| 4.1.4 | Crosslink NaCMC/BSA Emulsion with Ca ²⁺ to obtain NaCMC Microgels | 117 |
| 4.1.5 | Crosslinking of NaCMC/BSA Emulsions with Trivalent Ions | 117 |
| 4.1.6 | Stability of Crosslinked Emulsions and Beads at pH 1.2 and 6.5 | 119 |
| 4.1.7 | Immobilisation of Enzymes into NaCMC/BSA Emulsion Beads | 122 |
| 4.2 | Using Gelatin/Maltodextrin Emulsions as Templates for Crosslinked Gelatin Microgel Formation | 124 |
| 4.2.1 | Crosslinking Reaction of Genipin | 124 |
| 4.2.1.1 | Reaction of Genipin with Water, Maltodextrin and Gelatin | 124 |
| 4.2.1.2 | Study Influence of Temperature and Time on Crosslinking of Genipin | 125 |
| 4.2.2 | Study of Gelatin Macrogel Gelling and Swelling | 127 |

| | | |
|---------|--|-----|
| 4.2.2.1 | Determination of Gelatin Sol-Gel Transition Temperature..... | 127 |
| 4.2.2.2 | Study of Gelation of Genipin-Crosslinked Gelatin | 128 |
| 4.2.2.3 | Study of Swelling of Gelatin-Genipin Macrogels | 130 |
| 4.2.3 | Identification and Quantification of Gelatin and Maltodextrin | 131 |
| 4.2.3.1 | Density of Gelatin and Maltodextrin solutions..... | 131 |
| 4.2.3.2 | UV Spectra of Gelatin and Maltodextrin..... | 132 |
| 4.2.3.3 | Measure Concentration of Maltodextrin and Gelatin by Optical Rotation..... | 133 |
| 4.2.3.4 | Labelling of Polymers | 137 |
| 4.2.4 | Phase Behaviour of Water/Gelatin/Maltodextrin System | 141 |
| 4.2.4.1 | Kinetics of Phase Separation in Gelatin-Maltodextrin Mixtures..... | 144 |
| 4.2.4.2 | Identification of Solid Phase in Gelatin/Maltodextrin Mixtures | 148 |
| 4.2.4.3 | Morphology of Solid Precipitate | 151 |
| 4.2.4.4 | Influence of Temperature on Phase Diagram..... | 152 |
| 4.2.5 | Properties of Gelatin-Maltodextrin Emulsion | 153 |
| 4.2.6 | Obtaining Microgels from Gelatin/Maltodextrin Emulsion | 157 |
| 4.2.6.1 | Preliminary study 1: Gelation of Gelatin Droplets..... | 157 |
| 4.2.6.2 | Preliminary Study 2: Remove Maltodextrin, before Gelling Gelatin..... | 157 |
| 4.2.6.3 | Final Protocol: Gelation of Gelatin Droplets and Purification of Microgel Suspension | 160 |
| 4.2.6.4 | Filtration..... | 161 |
| 4.2.6.5 | Dialysis..... | 162 |
| 4.2.6.6 | Centrifugation..... | 163 |
| 4.2.6.7 | Summary | 165 |
| 4.2.7 | Freeze-Drying of Microgels | 167 |
| 4.2.7.1 | Morphology of Microgels after Freeze-Drying..... | 168 |
| 4.2.7.2 | Influence of Freeze-Drying Conditions on Freeze-Dried Product | 170 |
| 4.2.7.3 | Influence of Microgel Composition on Freeze-Drying | 171 |
| 4.2.7.4 | Redispersion of Freeze-Dried Microgels..... | 171 |
| 4.2.8 | Characterisation of Microgel Particles | 173 |
| 4.2.8.1 | Flocculation of Microgels in Suspension | 173 |
| 4.2.8.2 | Deflocculating aggregated Microgel by Sonication of Microgels..... | 174 |
| 4.2.8.3 | Size Determination of Microgels: Microscopy versus Laser Diffraction..... | 175 |
| 4.2.8.4 | Influence of Preparation Parameters on Microgel Size | 177 |
| 4.2.8.5 | Long Term Stability of Microgels..... | 183 |
| 4.2.8.6 | Influence of pH on Microgel size..... | 183 |
| 4.2.8.7 | Influence of Salt concentration on Microgel size..... | 185 |

| | | |
|----------|---|------------|
| 4.2.8.8 | Stability of Microgels at 37 °C and in Simulated Gastric Fluid | 186 |
| 4.3 | Enzyme Encapsulation into Crosslinked Gelatin Microgels..... | 187 |
| 4.3.1 | Analysing Enzyme Concentration, Activity and Location..... | 187 |
| 4.3.1.1 | Determination of Enzyme Concentration..... | 187 |
| 4.3.1.2 | Enzyme Activity Measurement..... | 190 |
| 4.3.1.3 | Fluorescence Labelling of Lactase with FITC | 191 |
| 4.3.2 | Enzyme Compatibility with Crosslinker and Microgels | 191 |
| 4.3.2.1 | Enzyme Activity in Presence of Genipin and Gelatin..... | 191 |
| 4.3.2.2 | Enzyme Activity in Suspension of Crosslinked Microgels..... | 192 |
| 4.3.3 | Activity Loss of Enzymes during Encapsulation Process | 193 |
| 4.3.4 | Encapsulation Yield and Activity Recovery of different Encapsulation Methods..... | 194 |
| 4.3.4.1 | Addition of enzyme after microgel formation (Method Gen(E)/Enz(M))..... | 194 |
| 4.3.4.2 | Addition of the enzyme together with the gelatin solution | 196 |
| 4.3.5 | Enzyme Long-Term Stability in Microgels..... | 198 |
| 4.3.6 | Freeze-Drying and Rehydration of Enzyme-Loaded Microgels | 199 |
| 4.3.7 | Enzyme stability under simulated gastric pH and body temperature conditions..... | 201 |
| 5 | Conclusions | 207 |
| 6 | Recommendations for Future Research..... | 213 |
| 7 | Bibliography | 217 |
| 8 | Annexes | 239 |
| 8.1 | Calibration Curve of Ortho-Nitrophenol..... | 239 |
| 8.2 | Size Determination of Microgels: Microscopy versus Laser Diffraction – Number Size Distribution of crosslinked Microgels | 240 |
| 8.3 | Publications..... | 241 |
| 8.4 | Contributions at Conferences..... | 275 |
| 8.5 | Undergraduate Students Supervised | 276 |

Summary

Lactose intolerance is associated with a deficiency of lactase (β -Gal), which is normally produced within the brush border of the small intestine. It catalyzes the hydrolysis of lactose (β -D-galactopyranosyl-(1 \rightarrow 4)-D-glucose) into d-glucose and d-galactose. Exogenous supply of this enzyme allows the digestion of dairy products by persons having hypolactasia, which affects 70% of the world population. However β -Gal in its free form is usually deactivated under gastrointestinal tract conditions. Therefore, encapsulation of the enzyme into protective matrices of various materials has been subject of previous studies. We are studying the encapsulation of β -Gal into drug delivery vehicles, templated by water-in-water emulsions.

Water-in-water emulsions are colloidal dispersions made of two immiscible aqueous phases that are in thermodynamic equilibrium, in absence of both oil and surfactant. This makes them of interest for environment friendly industrial processes, in which organic solvents are replaced by aqueous ones, and for designing biocompatible and food grade delivery vehicles. Moreover, gelled droplets in the micron range, microgels, can be obtained by gelling and crosslinking the dispersed phase of W/W emulsions.

In this Thesis two distinct W/W emulsion systems were selected to serve as templates: sodium carboxymethylcellulose (NaCMC) / bovine serum albumin (BSA) mixtures and gelatin/maltodextrin mixtures.

In the first system, the NaCMC/BSA mixture, phase behavior of the polymer mixture was analyzed, showing that this system can form W/W emulsions under basic pH conditions (pH 11-13). Emulsions with droplets between 5-20 μ m were obtained, depending on the composition of the emulsion. At higher viscosities coalescence was reduced and droplet size decreased, providing for some samples stability for over 20 days. The ability of divalent Ca^{2+} and trivalent Al^{3+} and Fe^{3+} cations to crosslink the biopolymers of the emulsion was analysed. Ca^{2+} crosslinked selectively NaCMC, while the trivalent ions crosslinked both polymers, thus also the entire emulsion. By dropping the emulsion into the crosslinker solutions, encapsulated emulsions could be obtained, which consist of BSA gel beads that contain encapsulated NaCMC emulsion droplets. Freeze-drying of those beads lead to particles with pores, whose size corresponded to that of the emulsion droplets. Bead size was minimized down to \sim 600 μ m by electrospraying the emulsion into the ion solutions. These beads, composed of both polymers, BSA and NaCMC, remained stable when simulating pH conditions experienced during the passage from food to the stomach over to the intestine, making it an interesting delivery vehicle for oral delivery of active molecules. The challenges of immobilizing enzymes into this type of encapsulated emulsions have been studied and discussed.

In the second system, the gelatin/maltodextrin aqueous mixtures, the aim was to obtain gelatin microgels, crosslinked with genipin, to serve as enzyme carriers. Therefore, in a first step, gelling and swelling properties of gelatin macrogels crosslinked with genipin, was studied and an understanding of the parameters influencing the crosslinking rate was obtained.

Next, the phase behavior of gelatin/maltodextrin mixtures in water was analysed at 50 $^{\circ}\text{C}$ and three distinct zones could be found, depending on the concentration of the polymer components. At low polymer concentrations one liquid phase was found, increasing the concentration, lead to one liquid and a solid phase and at some critical concentrations the mixtures phase separated into two liquid phases coexisting with a solid phase. The formation of the two liquid phases and the solid phase was studied and the origin of the solid phase investigated.

Different types of simple emulsions were formed from the gelatin-maltodextrin mixtures, and also spontaneous formation of multiple emulsions, from simple gelatin-in-maltodextrin emulsions upon cooling was observed.

Microgels were formed from gelatin-in-maltodextrin emulsions, by cooling and crosslinking the dispersed gelatin droplets with genipin. The microgel suspensions were purified by centrifugation and resuspension in the aqueous solvent. Microgels could also be kept in a dry form, by freeze-drying the suspensions. When rehydrating them, they preserved their original morphology and particle size distribution.

Preparation parameters affecting the gelatin droplets, thus microgels, were investigated, reaching sizes as small as 6 μm . Those microgels had a slight swelling response at pH values different from their isoelectric point ($\text{pI} \approx 5$) and shrank at increasing ionic strength. Crosslinking increased their stability in simulated gastric pH and temperature conditions.

Various incorporation methods of the enzyme β -Gal were tested. The highest encapsulation yield of 64 % was achieved when the enzyme was added to gelatin and then forming the emulsion together with genipin. Higher crosslinking degrees increased encapsulation yields. These conditions lead however also to the highest activity loss, due to direct contact between genipin and the enzyme, which partly deactivated the enzyme. Considering the activity loss, the highest activity recovery (51 %), which corresponds to active enzyme remaining inside the microgels, was achieved for microgels crosslinked with 5 mM genipin during 1h at 30 °C. The enzyme remained active over at least one month, however a challenge was leakage of the enzyme from the microgels over time, which occurred faster at lower crosslinking rates. Therefore, of interest is the fact that the enzyme remained active after a complete cycle of freeze-drying and rehydration of enzyme-loaded microgel particles.

The enzyme-loaded crosslinked gelatin microgels were not able to preserve enzyme activity under simulated gastric fluid temperature and pH conditions (37 °C, pH 3). It was shown however that crosslinked microgels have some protective effect on enzyme activity at pH 5.8 and 37 °C. These can be considered as preliminary results for the possible use of those β -Gal-loaded microgels in e.g. industrial production of lactose-hydrolyzed milk, which has similar pH and temperature conditions.

Abbreviations

| | |
|----------------------|--|
| β-Gal | Beta-galactosidase |
| BSA | Bovine Serum Albumine |
| CLSM | Confocal Laser Scanning Microscope |
| ConA | Concanavalin A |
| DF | Dilution Factor |
| DE | Dextrose Equivalent |
| DMF | Dimethylformamide |
| DMSO | Dimethyl sulfoxide |
| FDA | Food and Drug Administration |
| FITC | Fluorescein isothiocyanate |
| Gel | Gelatin |
| Gen(E)/Enz(E) | Method of enzyme encapsulation: Addition of enzyme before microgel formation and crosslinking during emulsification |
| Gen(E)/Enz(M) | Method of enzyme encapsulation: Addition of enzyme after microgel formation and crosslinking during emulsification |
| Gen(M)/Enz(E) | Method of enzyme encapsulation: Addition of enzyme before microgel formation and crosslinking after microgel formation |
| GI | Gastrointestinal |
| GRAS | Generally regarded as safe |
| HLB | Hydrophilic-lipophilic balance |
| IQR | Interquartile Range |
| IP | Interphase |
| L | Liquid |
| M | Microgel |
| MD | Maltodextrin |
| MW | Molecular weight |
| MWCO | Molecular weight cut-off |
| NaCMC | Sodium carboxymethylcellulose |
| NG | Nucleation and growth |
| ONP | Ortho-nitrophenol |
| ONPG | Ortho-Nitrophenyl-β-galactoside |
| O/W | Oil-in-water |
| O/W/O | Oil-in-water-in-oil |
| PDMS | Polydimethylsiloxane |
| PEM | Phosphate EDTA Magnesium |
| PEG | Polyethyleneglycol |
| PGA | Polyglutamic acid |
| PLL | Polylysine |
| PNIPAm | Poly(N-isopropylacrylamide) |
| RI | Refractive Index |
| RITC | Rhodamine B isothiocyanate |
| rpm | Revolutions per minute |
| S | Solid |
| SD | Spinodal decomposition |
| SEM | Scanning electron microscope |

| | |
|--------------|------------------------------------|
| SGF | Simulated Gastric Fluid |
| SR | Swelling Ratio |
| UV | Ultraviolet |
| VEGF | Vascular Endothelial Growth Factor |
| VIS | Visible |
| W/O | Water-in-oil |
| W/O/W | Water-in-oil-in-water |
| W/W | Water-in-water |

Symbols and Units

| | |
|---------------------------------------|--|
| A | Rotation constant |
| A_{mg} | Enzyme activity within the microgel dispersions |
| A_{sn} | Enzyme activity in supernatant |
| A_{tot} | Total enzyme activity |
| A_i | i^{th} Osmotic virial coefficient |
| A.U. | Arbitrary unit |
| α | Optical rotation |
| $\alpha_i(\lambda)$ | Specific optical rotation per unit concentration |
| c | Concentration |
| c_p | Polymer concentration |
| γ | Surface tension |
| D | Diffusion coefficient |
| D[4,3] | De Brouckere volume mean diameter |
| Da | Dalton |
| deg | Degree |
| ΔG_M | Free mixing energy |
| H | Total enthalpy |
| ΔH_M | Mixing enthalpy |
| k | Boltzmann constant |
| kat | Katal |
| λ | Wavelength |
| λ_0 | Dispersion constant |
| M | Molar mass |
| N | Total number of lattices (Lattice Theory) |
| N_A | Avogadro constant |
| N_i | Number of molecules of type i (Lattice Theory) |
| η | Viscosity |
| °C | Celsius Degree |
| pI | Isoelectric Point |

| | |
|---|--|
| Ω | Number of ways for placing the molecule onto lattice (Lattice Theory) |
| φ | Volume fraction |
| R | Universal gas constant |
| r | Distance between the centres of the particles (Depletion Interactions Model) |
| Π_p | Osmotic pressure of the polymer solution |
| S | System entropy |
| σ_c | Colloid particle diameter |
| σ_p | Polymer diameter |
| ΔS_M | Mixing entropy |
| θ | Contact angle of adsorbed particles on a liquid-liquid interface |
| T | Temperature |
| T_{gel} | Gelling temperature |
| $T_{\text{gel} \rightarrow \text{sol}}$ | Liquefaction temperature |
| V_c | Particle volume of the colloidal particle |
| V_0 | Overlap volume |
| $W(\mathbf{r})$ | Potential of mean force |
| w_{12} | Interaction energy between molecule 1 and 2 |
| $\text{wt}\%$ | Weight percent |
| χ_{12} | Flory–Huggins parameter |
| z | Number of nearest neighbours (Lattice Theory) |

Chapter 1

INTRODUCTION

1 Introduction

1.1 Relevance of Research

1.1.1 Lactase Non-persistence and Lactose Intolerance

Lactose is a disaccharide usually found in milk, but is also present in forsythia flowers and some tropical shrubs (Brüssow, 2013). Humans can not absorb lactose into the intestine, and require therefore, first, its hydrolysis to its component monosaccharides, D-Galactose and D-Glucose. This is done by the brush-border enzyme lactase, also called β -galactosidase (β -gal) (Figure 1.1). Lactase activity can be detected from week 8 of gestation at the mucosal surface in the human intestine and is at its peak by birth. Lactase activity is essential during weaning, but starts to progressively decrease in the first months of life (lactase non-persistence), as a consequence of the maturational down-regulation of lactase expression (Vesa, Marteau, & Korpela, 2000).

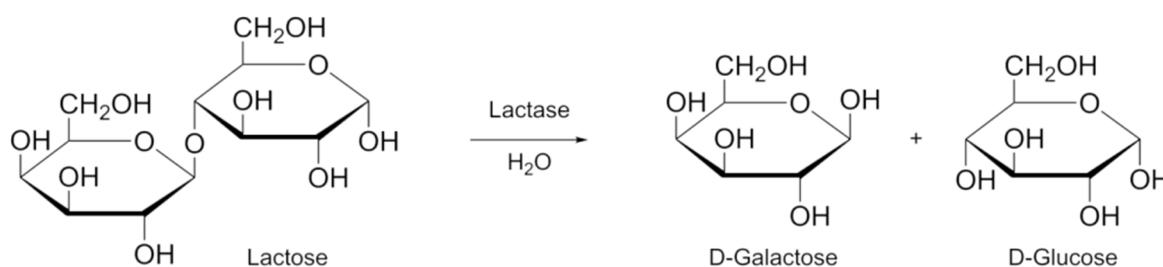


Figure 1.1 Enzymatic hydrolysis of lactose to galactose and glucose by the enzyme lactase (Figure reproduced from (Samuel, 2012))

This downregulation happens in 65–70% of humans (Ingram, Mulcare, Itan, Thomas, & Swallow, 2009). But a mutation, presumably resulting from strong positive selection in populations with a long history of cattle domestication lead to lactase persistence in some part of the population. Those people maintain the ability to digest dairy products into adulthood. Lactase persistence is high in northern European populations (>90% in Scandinavia) and decreases across southern Europe and the Middle East

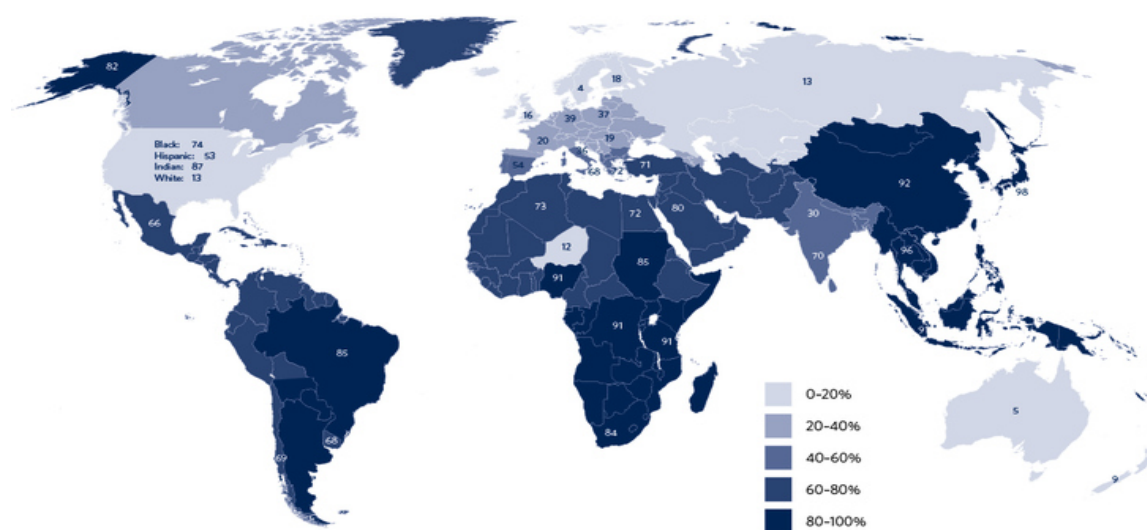


Figure 1.2 Global map of Lactase Non-Persistence (Figure reproduced from (Pereltsvaig, 2013))

(~50% in Spain, Italy and Arab populations). Lowest level of lactase persistence can be found in Asia and most of Africa (~1% in Chinese, ~5%–20% in West Africa) (Swallow, 2003) (Figure 1.2).

A decrease in lactase activity can also come in adulthood (secondary lactase deficiency), as a consequence of gastrointestinal infection, inflammatory bowel disease, abdominal surgery or other health issues.

Whatever the cause, lactase deficiency results in lactose not being able to be absorbed by the intestinal tract. The osmotic load leads to increased water content in the intestine, which can lead to diarrhea. Unabsorbed lactose is transported to the colon, where it is fermented by the colonic microbiome to short chain fatty acids and gas (H₂, CO₂ and CH₄). This contributes to some symptoms such as bloating and flatulence (Deng, Misselwitz, Dai, & Fox, 2015). Gastrointestinal symptoms because of lactose malabsorption is defined as lactose intolerance, a term which should not be confounded with lactase non-persistence.

Lactose non-persistence can be diagnosed over several ways (Misselwitz et al., 2013):

- Genetic test of polymorphism of lactase gene (Santonocito et al., 2015)
- Increase of glucose blood-level
- Increase of hydrogen in breath
- Enzymatic activity of lactase enzyme in biopsy sample

There are various ways by which lactose intolerance can be treated.

It was shown that lactose-fermenting organisms were proliferated, if lactase non-persistent individuals consumed regularly dairy food. The mimicked prebiotic effect lead that the colonic bacteria adapted to the condition with an increase in fecal lactase activity and decreased hydrogen production (Levitt, Wilt, & Shaukat, 2013). A similar strategy is based on the ingestion of probiotics that alter the intestinal flora (Deng et al., 2015).

Totally omitting dairy products, reduced the symptoms, however has the disadvantage of losing a major source of calcium and proteins. Thus, industrially treating milk with lactase to reduce its lactose content is a way to allow lactase non-persistence patients to continue consuming dairy product. Lactose-free products alter however the taste of the food, as glucose and galactose produced by lactose hydrolysis are sweeter than the original sugar.

Lastly, lactase can be administered orally, as an oral enzyme replacement therapy. Peroral lactase substitution with β -galactosidase preparations is a well-established strategy for the management of lactose intolerance. The enzyme can be obtained from bacterial, yeast, fungal, plant or recombinant sources (Husain, 2010). Most commonly used, generally recognized as safe-listed, are β -galactosidase isolated from yeast, e.g. *Kluyveromyces marxianus*, *Kluyveromyces lactis* or *Kluyveromyces fragilis*, or from fungi, such as *Aspergillus niger* and *Aspergillus oryzae*. Depending on the source, the enzyme has different properties (especially pH and temperature optimum), as summarized in (Saqib, Akram, Halim, & Tassaduq, 2017). In particular, the optimum pH of lactase obtained from fungi is 3.5 to 4.5, while enzymes from yeasts have an optimum pH between 6.5 and 7.0.

Solid lactase preparations, in capsules and tablets, are administered immediately before or together with the lactose-containing meal. Tablets administered in this way were shown to be successful in reducing the severity of the symptoms (Montalto et al., 2006), however are less effective than prehydrolysed milk.

Various studies showed that in vivo conditions, such as digestive proteases and gastro-intestinal pH were not suitable for the commercially available lactase digestive supplements. O'Connell and Walsh found that the enzymes were completely inactivated when subjected to gastric conditions for 1 min (O'Connell & Walsh, 2006). Furthermore, those tablets do not provide a long-term release of the enzyme.

Aim of this work is to develop a novel oral delivery method of lactase, by encapsulating lactase into microgels, prepared by a template of a water-in-water (W/W) emulsion. An introduction to water-in-water emulsions, microgels and oral delivery of enzymes and how those three fields can be combined is given in the following sections.

1.2 General Introduction to Emulsions

Emulsions are thermodynamically unstable colloidal dispersions of two immiscible liquid phases, with one of the liquids dispersed in the other, in form of small spherical droplets. Emulsions do not form spontaneously from equilibrium phases, because of their thermodynamic instability, and they can be kinetically stable dispersions, preventing phase separation.

Depending on droplet size, two types of emulsions are generally differentiated (T. Tadros, Izquierdo, Esquena, & Solans, 2004; Vold, 1965):

Macroemulsions: Those conventional emulsions typically have droplets with diameters between 0.1 and 100 μm . As the droplets have sizes similar to the wavelength of light, they tend to be optically turbid or opaque (solutions strongly scatter the light).

Nano-emulsion: Nano-emulsions are considered to be a type of emulsion that contains very small droplets, with mean diameters between 20 nm and 200 nm, which makes them transparent (T. Tadros et al., 2004). In addition, even though they are still thermodynamically unstable systems, they have much better stability to gravitational separation and aggregation than macroemulsions.

Microemulsions, defined as thermodynamically stable systems that incorporated both oil and water, are single-phase systems not considered as emulsions. They form spontaneously, generally have droplets between 5 and 50 nm, which makes the system to appear highly transparent.

Besides the above classification according to size, emulsions are also classified based on two other criteria: the nature of the phases (oil or water) and the number of phases, which coexist (simple or multiple emulsion).

W/O or O/W Emulsions:

Emulsions containing an oil phase dispersed in an aqueous phase are called oil-in-water (O/W) emulsions, whereas systems which consist of water droplets dispersed in a continuous oily phase are denoted as water-in-oil (W/O) emulsion. These emulsions are generally stabilised by surfactants or particles. In the case of surfactant-stabilised emulsions, the nature of the emulsion (O/W or W/O) is

mostly defined by the Bancroft rule, “The phase in which an emulsifier is more soluble constitutes the continuous phase” (Bancroft, 1912). Thus, surfactants are classified according to their hydrophilic-lipophilic balance (HLB) number, which is a scale based on the relative percentage of hydrophilic to lipophilic groups in the surfactant molecule.

In the case of emulsions stabilised by particles, so-called Pickering emulsions, the nature of the emulsion results from the contact angle of particles on the liquid-liquid interface. If the contact angle with respect to the water phase is smaller than 90° , O/W emulsions are obtained, elsewise W/O emulsions are obtained for contact angles $>90^\circ$.

O/O Emulsions:

O/O emulsions can be formed either by two non-miscible nonpolar/polar aprotic organic solvents, one acting as a continuous and the other as the dispersed phase, such as DMF or acetonitrile in alkanes (Klapper, Nenov, Haschick, Müller, & Müllen, 2008), or two molecules miscible in the same solvent, but not between each other, such as polystyrene and polybutadiene in chloroform (Asano, So, & Lodge, 2016). Other examples of O/O emulsions include components, such as fluorocarbons and silicon oils, which are both often immiscible with hydrocarbons. Stability of those non-aqueous emulsions has been an issue, but they can be properly stabilised by surfactants able to absorb at oil-oil interphases (Imhof & Pine, 1997). A typical example are fluorocarbon droplets stabilised by partly fluorinated molecules. O/O emulsions have shown to be useful in the formulation of drugs where the presence of water is undesirable, for the preparation of porous materials and in the creation of electro-optical displays.

W/W Emulsions:

Water-in-water (W/W) emulsions are colloidal dispersions made of two immiscible aqueous phases that are in thermodynamic equilibrium, in absence of both oil and surfactant (Vold, 1965). This type of emulsions will be described in great detail in section 1.3.

Multiple Emulsions:

Multiple emulsions are polydisperse systems, in which O/W and W/O emulsions coexist, which are stabilised by lipophilic and hydrophilic surfactants (A. Y. Khan, Talegaonkar, Iqbal, Ahmed, & Khar, 2006). The dispersed phase contains thus droplets of smaller size, denoted as a primary emulsion, generally of the other component. The most common multiple emulsions are oil-in-water-in-oil (O/W/O) or water-in-oil-in-water (W/O/W) emulsions, but exist as well O/W/W (Matalanis, Lesmes, Decker, & McClements, 2010), W/W/O (Yasukawa, Kamio, & Ono, 2011) or W/W/W emulsions (Song, Sauret, & Shum, 2013). They are usually prepared by the double emulsion technique, which consist of first forming a stable primary emulsion of small droplets, which is then introduced into a homogenous water or oil phase, to form the secondary emulsion. This second step of emulsification requires a gentle shear, in order not to destroy the primary emulsion.

Emulsion stability

The thermodynamically unfavourable mixtures of macro- and nanoemulsions break down over time, as a result of a variety of physicochemical mechanisms (T. F. Tadros, 2009), which are illustrated in Figure 1.3:

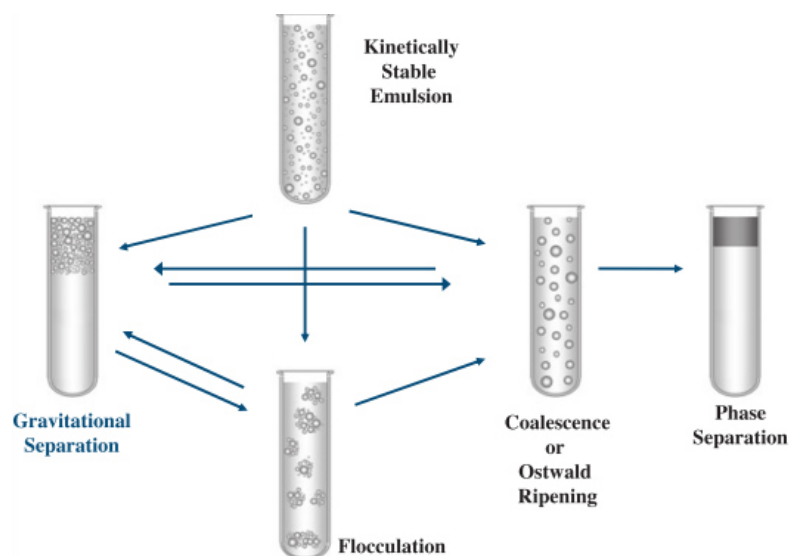


Figure 1.3. Instability mechanisms that occur in emulsions: gravitational separation, flocculation, coalescence and Ostwald ripening (Figure reproduced from (D. J. McClements, 2010))

Creaming and Sedimentation (Gravitational Separation)

Gravitational separation usually occurs through external forces, which exceed the Brownian motion of the droplets. As a consequence larger droplets move either to the top (creaming, if their density is smaller than the one of the continuous phase), or to the bottom (sedimentation, if their density is greater). Liquid oils have usually a lower density than water, thus creaming occurs for O/W emulsions, whereas sedimentation is more prevalent for W/O emulsions.

Flocculation

In the process of flocculation droplets aggregate to larger units, without change in primary droplet size, as a result of van der Waals attractions between them. Flocculation happens if there is not sufficient repulsion between the droplets, to keep them apart. To overcome the attraction of the droplets, they can be stabilised electrostatically, for example by using ionic surfactants. At high surface or zeta potential the electrical double layer introduces a repulsive energy, which overcomes the attractive van der Waals attraction. High electrolyte concentrations shield this electrical double layer, which promotes in turn flocculation. Alternatively, droplets can be stabilised sterically, using non-ionic surfactants or polymers.

Coalescence

When two droplets come into close contact, the liquid film between the droplets thins and disrupts, leading to eventual rupture. Moreover, there is a fluctuation of the liquid droplet surfaces, forming surface waves, which at big amplitude leads the surfaces of the droplets to join, due to strong van der Waals attractions. As a result, two or more droplets fuse to form larger droplets. Repetition of this process can eventually lead to complete separation of the emulsion into two distinct liquid phases.

The film fluctuations originate from a disjoining pressure, which balances the excess normal pressure. Electrostatic repulsion, steric repulsion and van der Waals attraction contribute to this pressure. Thus, as for flocculation, steric and electrical stabilisation can prevent coalescence. Furthermore, the film fluctuation can be dampened by enhancing the Gibbs elasticity which is a function of surface tension and surface area. Smaller droplets have lower surface fluctuations and are thus less likely to get destabilised by coalescence (T. F. Tadros, 2013).

Ostwald Ripening

Ostwald Ripening arises from the fact, that if two liquids have some form of mutual solubility, diffusion takes place of the disperse phase molecules from smaller, through the continuous phase, to larger droplets. Smaller droplets have a greater vapour pressure, thus greater solubility when compared to larger droplets. As a consequence, with the time, the smaller droplets get dissolved and their molecules diffuse to and are deposited on the larger droplets. The pressure difference between small and large droplets is the driving force for diffusion and can be obtained from the Laplace equation: $P = 2\frac{\gamma}{r}$, where P is the Laplace pressure, γ is the surface tension and r the droplet radius.

The rate of diffusion is increased at lower viscosity of the continuous phase, which increases the diffusion rate, as described by the Stokes-Einstein equation: $D = k_b T / 6\pi\eta r$ where, D is the diffusion coefficient of a droplet and η is the continuous phase viscosity. As in coalescence, Ostwald ripening eventually leads to bulk phase separation.

Due to those thermodynamic instabilities of emulsions, various measures exist to convey them sufficiently long kinetic stability. Therefore usually substances known as stabilizers, e.g., emulsifiers, texture modifiers, weighting agents, and ripening retarders are added to prevent phase separation (D. J. McClements, 2010).

1.3 Water-in-Water Emulsions

1.3.1 Historical Background to Studies on Water-in-Water Emulsions

Water-in-water emulsions were first described more than 100 years ago, in 1896, by Beijerinck (Beijerinck, 1896) (Figure 1.4). He studied the growth of bacteria on starch, and he was preparing soluble starch for culturing bacteria. When mixing the starch solutions with gelatin, he observed droplet formation within the solution. By dyeing starch with iodine, he found that the emulsions were composed of two different aqueous solutions. He furthermore observed that the nature of the continuous and dispersed phase can be controlled by the polymer ratio, and the droplet size in the dispersed phase could be controlled by agitation.

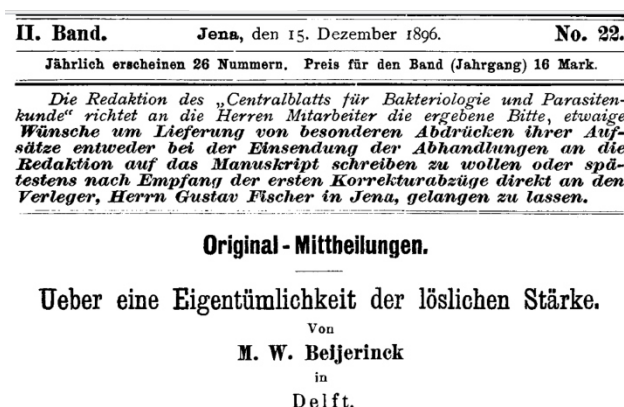


Figure 1.4. Article of Beijerinck, in which for the first time water-in-water emulsions were described. Title (german): “Concerning the peculiarity of soluble starch”

Only two years later, in 1898, a similar phenomenon was found by Bütschli in a similar system (Bütschli, 1898), which was composed of a mixed solutions of water, gelatin and autoclaved starch.

Beijerinck in another paper published in 1910 (Beijerinck, 1910), described that aqueous mixtures of the polysaccharide agar and the protein gelatin also showed the formation of droplets, similar to the gelatin/starch system. He correctly stated that in both cases one phase was rich in gelatin, but contained small amount of starch/agar, and that the other phase was in contrast, rich in starch/agar and depleted in gelatin. Moreover, he observed that the compositions of the dispersed droplets and dispersion medium, can be reversed by changing the relative concentration of biopolymers in the system. In the gelatin/starch mixtures phase separation was observed in a wide range of biopolymer concentrations, exceeding 0.1 % and that the system maintained phase separated, even under heating or intense mixing. Finally, coalescence of the dispersed droplets was slow, and thus remained in dispersion.

Deeper studies into mixtures of gelatin solutions with solutions of different starches were performed by Ostwald and Hertel in the late 20's (Ostwald & Hertel, 1929). The aim was to investigate the effects of pH, various salts, starch origin and concentrations of biopolymers on phase separation. Potato starch required higher concentrations than cereal starches for phase separation of mixed gelatin-starch solutions. Furthermore, the volume fraction of cereal starch phase, in the aqueous mixture with gelatin, was minimal at neutral pH and increased in basic or acidic pH. Systems containing potato starch remained however single phase at both acidic and basic pH. Salts affected the phase separation in agreement with their position in the Hofmeister series.

In the 50's and 60's some more studies were devoted to the thermodynamic incompatibility of proteins and polysaccharides (Dobry, 1948; Doi, 1965) and analyzed mixtures, such as the gelatin-amylopectin-

water system. It was in 1965 when, a systematic study of the thermodynamic incompatibility of proteins and polysaccharides began (Grinberg & Tolstoguzov, 1997). The knowledge about phase behavior of those mixtures was of key importance for the development of novel formulated foods or improving existing food processing. The study was initiated and part of an extensive research and development program of the USSR Academy of Sciences. The results of this extensive study have been summarized in 1997 by Grinberg and Tolstoguzov (Grinberg & Tolstoguzov, 1997).

1.3.2 Phase Behaviour in Aqueous Mixtures

Water-in-water emulsions are colloidal dispersions made of two immiscible aqueous phases that are in thermodynamic equilibrium, in absence of both oil and surfactant (Vold, 1965).

They gain in interest, due to the tendency towards environment friendly industrial processes, in which organic solvents are replaced by aqueous ones. Low-fat foods are another application, as water-water interfaces may give similar properties as oil-water interfaces. As a third area, W/W emulsions may be of interest as templates for drug delivery systems with controlled release of pharmaceuticals to the body. Water-water phase separation can be found in a large variety of systems, such as aqueous mixtures of polymers, surfactants and polymers and, polymers and electrolytes and surfactant solutions.

Surfactants in an aqueous environment have a strong tendency to self-aggregate to spherical micelles and may grow to rods, which is mainly caused by the attractive hydrophobic interaction between the hydrocarbon chains (details can be found in (Kronberg, Holmberg, & Lindman, 2014)). Those aggregates may respond to changes in the solution conditions by altering their conformation, which results in change in size, balance between exposed hydrophobic/hydrophilic chains etc. All of which affects the compatibility with other polymers or surfactants in solution. Piculell and Lindman studied in details the interaction of surfactants and polymers in solution (Piculell & Lindman, 1992). If surfactants are mixed with polymers containing hydrophobic units, mixed micelles can be formed. For other cases, such as mixtures of non-ionic surfactants with non-ionic polymers, no strong attraction are shown and at sufficiently concentrated mixtures phase separation was observed, such as in the case of $C_{12}E_8$ and Dextran (Piculell & Lindman, 1992). In mixtures of non-ionic polymers (e.g. ethyl- (hydroxyethyl) cellulose) and ionic surfactants (e.g. sodium dodecyl sulphate) the phase separation depends strongly on counterion entropy, thus also on the ionic strength of the solution. Furthermore, as in any of the other systems, phase separation is favoured at conditions above the cloud point of the surfactant, which can be regulated by e.g. temperature and salts, depending on the nature of the surfactant (Kronberg et al., 2014; Piculell & Lindman, 1992).

In the next chapters we will explain in details the phase separation phenomena of polymer mixtures, as this will be the focus of our research.

When mixing two polymers, there are three types of possible phase behaviours:

1. Complete miscibility, in the case of weak interactions between the two kinds of polymers
2. Associative phase separation, with formation of a precipitate/coacervate, because of strong attractive interactions between the two polymers (Figure 1.5 a).
3. Segregative phase separation induced by repulsive interactions between the polymers (Figure 1.5 b).

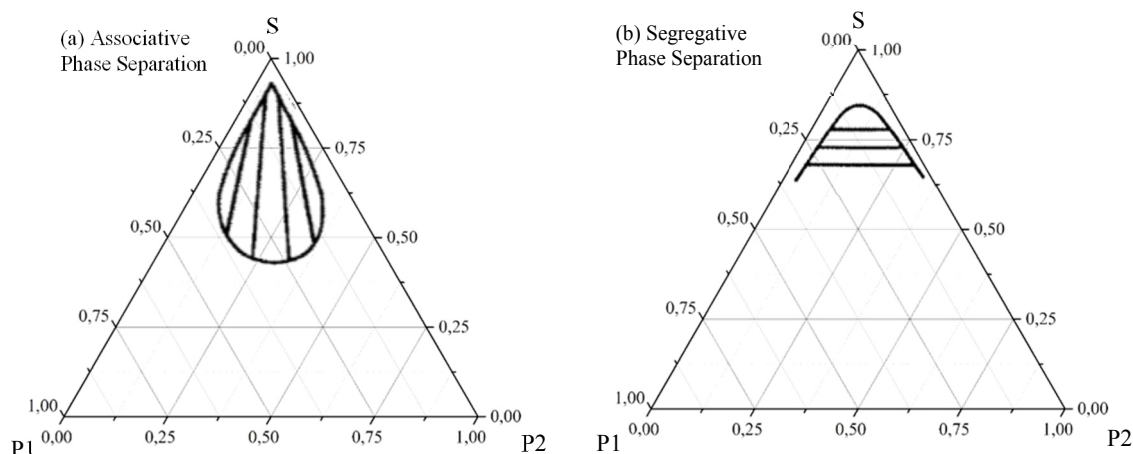


Figure 1.5. Schematic ternary phase diagrams, which illustrate associative (a) and segregative (b) phase separation in mixed hydrophilic polymer systems. For associative phase separation, points inside the two-phase region, separate along the tie-lines into a region rich in both polymers, and one, dominated by high solvent concentrations. In the case of segregative phase-separation, mixtures inside the two-phase region separate in two phases, both rich in one of the respective polymers. S: solvent (water); P1: Polymer 1; P2: Polymer 2.

The various phenomena that can lead to phase separation are summarised in Figure 1.6 and in the section below. The figure illustrates the different colloidal systems that can be observed, depending mainly on the interactions between the two polymers. Attractive interactions lead to associative phase separation, while repulsive interaction lead to segregative phase separation.

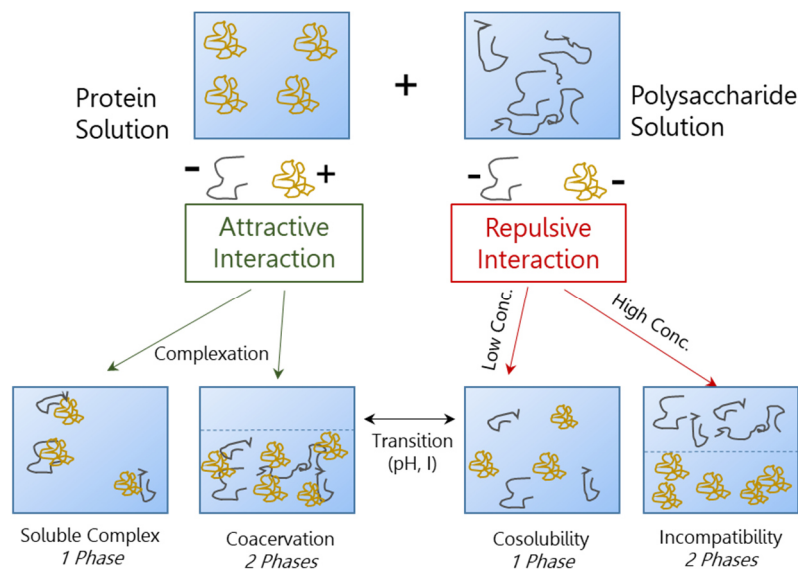


Figure 1.6. Possible interactions in a mixture of two biopolymers, leading either to aggregative (left) or segregative phase separation (right). Physicochemical alterations in the system can transform a system from an one-phase to two-phase region, or even from associative to segregative interactions. Adapted from (Matalanis et al., 2010).

1.3.3 Associative Phase Separation

Associative interactions take place, for the cases, in which two polymers experience attractive forces induced by opposite charges or if there is hydrogen bonding between them (Figure 1.6). Attractive forces

between the polymers will lead to ionic complexes, mutual neutralisation of chains bearing opposite charges and thus increasing hydrophobicity of junction forming zones (Tolstoguzov, 2003). Depending on the system composition either a one-phased soluble complex or a two-phased coacervate or precipitate may be formed. Coacervates have loose open structures containing a high amount of water, whereas precipitates have dense structures that hold less water (D. McClements, 2014). One of the phases will thus contain mainly the polymer complexes and the other phase contains mainly the solvent. The complexation between polymer 1 and polymer 2 is on the one side entropy driven, due to the liberation of counterions and water molecules and on the other side enthalpy driven, due to the decrease in electrostatic free energy in the system (Semenova & Dickinson, 2010). Associative interactions between proteins and polysaccharides have been used as flocculants for precipitation of suspensions containing proteins, for protein fractionation or to encapsulate oil (Lundin, Williams, & Foster, 2003). Some examples of polyelectrolyte mixtures, which experience association phase separation, can be seen in Table 1.1.

Table 1.1. Some examples of aqueous polymer mixtures, which undergo associative phase separation

| Polymer 1 | Polymer 2 | Reference |
|------------------|------------------------|---|
| Gelatin | Arabic Gum | (Burgess & Carless, 1985) |
| Gelatin | Carboxymethylcellulose | (Lii, Tomasik, Zaleska, Liaw, & Lai, 2002) |
| Gelatin | Pectin | (Joseph & Venkataram, 1995) |
| Gelatin | Carrageenan | (Michon, Cuvelier, Launay, Parker, & Takerkart, 1995) |
| Chitosan | Xanthan | (Chu, Sakiyama, & Yano, 1995) |
| Chitosan | Carrageenan | (Shumilina & Shchipunov, 2002) |

1.3.4 Segregative Phase Separation

More than 100 mixed aqueous mixtures, containing proteins and polysaccharides in aqueous solution, are known to experience phase separation, with formation of two aqueous immiscible phases (Grinberg & Tolstoguzov, 1997). Some examples of polymer mixtures, which experience segregative phase separation, can be seen in Table 1.2.

Table 1.2. Some illustrative examples of aqueous polymer mixtures, which undergo segregative phase separation

| Polymer 1 | Polymer 2 | Reference |
|--------------------------------|-------------------------------|--|
| PEG | Dextran | (Stenekes, Franssen, van Bommel, Crommelin, & Hennink, 1998) |
| Gellan | κ -carrageenan | (Wolf, Scirocco, Frith, & Norton, 2000a) |
| Alginate | Sodium Caseinate | (Capron, Costeux, & Djabourov, 2001) |
| Gelatin | Hydroxypropyl methylcellulose | (Esteghlal, Niakosari, Hosseini, Mesbahi, & Yousefi, 2016) |
| Gelatin | Maltodextrin | (Kasapis, Morris, Norton, & Clark, 1993a) |
| Sodium Carboxy-methylcellulose | Bovine Serum Albumin | (Grinberg & Tolstoguzov, 1997) |

This segregative phase separation can occur by thermodynamic incompatibility between a charged polymer 1 and a neutral or charged polymer 2 (Doublrier, Garnier, Renard, & Sanchez, 2000). Two main factors can contribute to the thermodynamic incompatibility between the two macromolecules.

The main one is their difference in hydration, which can be explained in terms of the Flory-Huggins interaction parameters between the two polymers and their respective interactions with water (Clark, 2000). Usually, the most charged polymer is highly hydrated, and it expels the less hydrated polymer.

The second factor that induces phase segregation in two immiscible aqueous phases is the “excluded volume” or “steric exclusion” effect. In this case, repulsive interactions of short range (0.2-0.3 nm) arise from the overlap of the macromolecule’s electron clouds. The relative spatial arrangement of pairs of segments on the macromolecules is restricted, which leads to a reduction in the mixing entropy of the system. It finally implies that above a critical concentration of polymers, there is an osmotic driving force that favours separation of the system into two aqueous phases, each one enriched in one of the polymers. Size and shape of the biopolymer molecule are determinant factors in those steric interactions (D. McClements, 2014; Semenova & Dickinson, 2010).

Because of that, phase segregation is promoted by differences in molecular weight, and many systems that show aqueous phase segregation consist of a charged polymer with very high molecular weight, mixed with a non-charged polymer with lower molecular weight (Figure 1.6).

1.3.5 Thermodynamics of polymer mixtures

Predicting phase behaviour of two polymers in solution is complex and various models have been developed to describe as detailed as possible interactions in the mixture. Most of them are based on two basic models: the osmotic virial expansions and lattice theories. Both of them have their limitations

which will be discussed, however they serve to understand the basic mechanisms of phase separation of two polymers in solution.

1.3.5.1 Flory-Huggins, Lattice Theory

The thermodynamics of polymers in solutions differ from ordinary binary mixtures. This stems from the size difference between solvent and polymer molecules. Solvent molecules can freely move around in a mixture of two liquids, while the bulkier polymer segments encounter some restrictions in a polymer solution. Therefore, it can be concluded that a single solvent molecule has a far higher entropy compared to a polymer segment. The lower entropy contribution to the free energy of mixing has some consequences on the ability to form stable mixtures of polymer solutions.

Flory and Huggins (Flory & Krigbaum, 1951; Huggins, 1942) proposed a model to predict the free energy of mixing and phase behaviour of polymer systems. A brief introduction to the basics of this model is given, summarising concepts of different articles (Frank, 2001; Horst & Wolf, 2002; Johansson, Karlström, Tjerneld, & Haynes, 1998; D. McClements, 2014; Schmitt, Sanchez, Desobry-Banon, & Hardy, 1998).

This theory is based on a statistical approach using a lattice model onto which individual molecules can be placed (Figure 1.7). The total number of lattices is N , while there are N_1 molecules of type 1 and N_2 molecules of type 2.

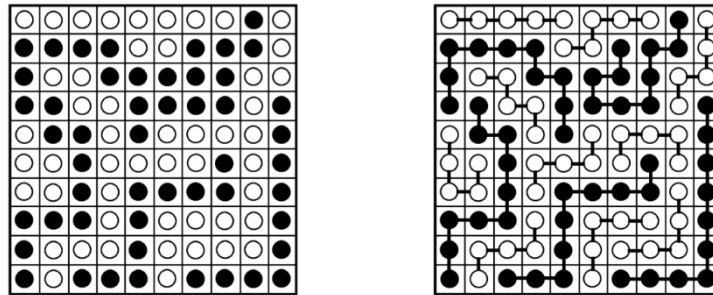


Figure 1.7. Lattice model for a low molecular weight compound (left side) compared to a mixture of 2 different polymers in solution (right side). (Figure reproduced from (Horst & Wolf, 2002)).

Each single one of those molecules occupies n_1 , respectively n_2 lattice sites. Molecule 1 is generally considered as the solvent and n_1 is thus considered to be 1. The volume fraction φ_1 of one of the molecules is

$$\varphi_1 = \frac{n_1 \cdot N_1}{N} = \frac{V_1}{V_1 + V_2} \quad (1.1)$$

V_1 and V_2 are the volumes of the individual molecules in solution.

The number of ways that this given system may come about, thus the thermodynamic probability, can be related to the entropy of the system through the Boltzmann Equation:

$$S = k \ln \Omega \quad (1.2)$$

With k , the Boltzmann constant and Ω , in this case, the number of ways for placing the molecule onto the lattice. After calculating the probabilities of placing a polymer/solvent molecules into the lattice,

considering N_i and n_i , Ω can be obtained (for details: (Frank, 2001)). From the entropies S_{11} and S_{22} of pure systems and S_{12} for binary systems, the mixing entropy ΔS_M can be calculated:

$$\Delta S_M = S_{12} - S_{11} - S_{22} \quad (1.3)$$

$$\Delta S_M = -R \left(\frac{\phi_1}{n_1} \ln \phi_1 + \frac{\phi_2}{n_2} \ln \phi_2 \right) \quad (1.4)$$

This result explains aforementioned fact that the entropy of mixing gets smaller for bigger polymers (bigger n) and that the mixing entropy is always positive.

The enthalpy of a polymer mixture can be derived in the following manner:

$\Delta w = 2w_{12} - w_{11} - w_{22}$ is the energy needed when changing polymer-polymer and solvent-solvent interactions for polymer-solvent interactions, with w being the interacting energy. This factor depends amongst others on changes in van der Waals, electrostatic, hydrogen bond and hydrophobic interactions (D. McClements, 2014).

Assuming that solvent molecule has z nearest neighbours, it will have $z \cdot \phi_1$ solvent and $z \cdot \phi_2$ polymer molecules in its vicinity. The total interaction energy of the solvent will be

$$z\phi_1 w_{11} + z\phi_2 w_{12} \quad (1.5)$$

And the total contribution for the $N_1 n_1 = N\phi_1$ solvent molecules in the system is

$$\frac{1}{2} z N \phi_1 [(1 - \phi_2) w_{11} + \phi_2 w_{12}] \quad (1.6)$$

Dividing by two to remove double counting.

The same procedure is done to calculate the total interaction energies for polymer molecules, which gives

$$\frac{1}{2} z N \phi_2 [(1 - \phi_1) w_{22} + \phi_1 w_{12}] \quad (1.7)$$

Summing up those interaction energies gives us the enthalpy H

$$H = \frac{1}{2} z N \phi_1 \phi_2 [2w_{12} - w_{11} - w_{22}] + \frac{1}{2} z N \phi_1 w_{11} + \frac{1}{2} z N \phi_2 w_{22} \quad (1.8)$$

Then total mixing enthalpy ΔH_M , considering $\phi_2 = 0$ for H_{11} and $\phi_1 = 0$ for H_{22} , is thus

$$\Delta H_M = H_{12} - H_{11} - H_{22} \quad (1.9)$$

$$= \frac{1}{2} z N \phi_1 \phi_2 \Delta w \quad (1.10)$$

By introducing the Flory-Huggins or molecular interaction parameter, which is specific for each solvent-polymer interaction, $\chi_{12} = \frac{z\Delta w}{2kT}$ and considering that $N = N_A$ and $R = kN_A$ we get finally for the mixing enthalpy.

$$\Delta H_M = RT \chi_{12} \phi_1 \phi_2 \quad (1.11)$$

The sign of the enthalpy depends on the Flory-Huggins parameter and more concretely on Δw . χ_{12} is equal to zero in ideal solutions when polymer-solvent are equal to polymer-polymer and solvent-solvent interactions. Molecular interactions which are unfavourable to mixing have a molecular interaction

parameter which is positive (i.e., $\chi_{12} > 0$), whereas systems where the molecular interactions are favourable, it is negative (i.e., $\chi_{12} < 0$).

The free mixing energy (ΔG_M) is the thermodynamic term, which determines if the polymer solution mixes or phase separates, and is the following

$$\Delta G_M = \Delta H_M - T\Delta S_M \quad (1.12)$$

$$\Delta G_M = RT \left[\chi_{12} \phi_1 \phi_2 + \left(\frac{\phi_1}{n_1} \ln \phi_1 + \frac{\phi_2}{n_2} \ln \phi_2 \right) \right] \quad (1.13)$$

it has to be noted that above equation is applicable for a single type of polymer in solution. For the case of two polymers the additional *Flory-Huggins* parameters, χ_{13} , and χ_{23} (the second polymer is denoted with index 3) have to be taken into account. The high molecular weight of the polymers (high n), thus the low entropy, indicates that it is predominantly the enthalpy and thus the interaction between the polymers which decides if phase separation occurs. Several groups were able to demonstrate, by fitting the tie-lines of phase diagrams to theoretical models, that the phase separation could be predicted according to theories based on Flory-Huggins parameters (Clark, 2000; Johansson et al., 1998).

It has to be noted that the Flory Huggins model is valid for non-charged polymers or at ionic strengths which are sufficiently high to screen the electrostatic interactions (Semenova & Dickinson, 2010). Some work has been carried out with the aim of taking the electrostatic interactions specifically into account (Yu & Arons, 1994). Furthermore, in reality the polymers are not free to sample any part of the lattice, as proteins and polysaccharides have secondary and tertiary structures or have a rigid conformation. Some authors argue that the model based on the osmotic second virial coefficients offer a greater universal applicability for the thermodynamic description of biopolymer mixtures (Semenova & Dickinson, 2010). Therefore, this model is presented next.

1.3.5.2 Excluded Volume / Depletion Interactions Model

This depletion interaction model is based on the assumption that the solution is a mixture of colloidal spheres, which behave as hard spheres, and non-adsorbing flexible polymers (Figure 1.8). This can be considered valid in the case of large globular macromolecules (e.g. micellar casein, BSA or large aggregates of heat-denaturated proteins) and flexible elongated polymers (e.g. neutral or charged polysaccharides). The addition of the polymers to the dispersion of colloidal spheres, will induce an attraction between the spheres. This attraction arises from depletion zones around the colloids, which are a result from a loss of conformational entropy of the polymer chains in vicinity of the surface of the colloidal particle (Lekkerkerker & Tuinier, 2011). This was first observed by Asakura and Oosawa in 1954 (Asakura & Oosawa, 1954) and then studied in more detail by Vrij in 1976 (Vrij, 1976). A brief introduction to the basics of this model is given, summarising concepts of different articles (Doublier et al., 2000; Semenova & Dickinson, 2010; Tolstoguzov, 2003; R. Tuinier, 1999; Remco Tuinier, Fan, & Taniguchi, 2015; Vrij, 1976).

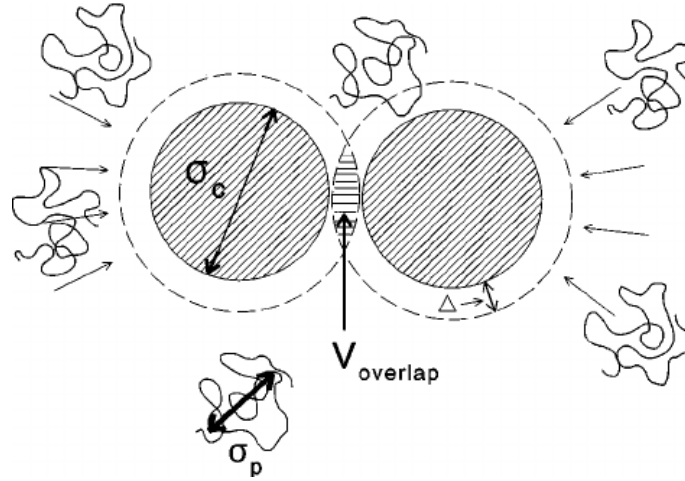


Figure 1.8. The depletion interaction model studies the interaction in a mixture of spherical colloids with diameter σ_c and polymer with diameter σ_p . The depletion layer Δ leads to an overlap volume V_{overlap} between both spheres.

The model starts from the principle that the potential of mean force $W(r)$ between the two particles is the sum of the free energies of attraction (A) and repulsion (R):

$$W(r) = W_A(r) + W_R(r) \quad (1.14)$$

r is defined as the distance between the two centers of the particles. Vrij (Vrij, 1976) developed a thermodynamic model to derive this attractive interparticle potential. They found that the potential is proportional to the overlap volume of the depletion layers V_O and the osmotic pressure of the polymer solution Π_p . According to the limiting Van't Hoff's law, the osmotic pressure depends on the polymer concentration c_p and molar mass M :

$$\Pi_p = RT \frac{c_p}{M} \quad (1.15)$$

The overlap volume V_O is a function of the distance between the centres of the particles, the polymer diameter σ_p (twice the depletion layer thickness) and the colloid particle diameter σ_c

$$V_O(r) = \frac{1}{6} \pi (\sigma_c + \sigma_p)^3 \left[1 - \frac{3r}{2(\sigma_c + \sigma_p)} + \frac{r^3}{2(\sigma_c + \sigma_p)^3} \right] \quad (1.16)$$

This expression applies for $\sigma_c \leq r \leq (\sigma_c + \sigma_p)$, thus from the two colloidal particles in direct contact ($r = \sigma_c$) to the distance, at which the polymer is located between the two particles $r = \sigma_c + \sigma_p$. The potential is thus:

$$\begin{aligned} W(r) &= +\infty, & 0 < r < \sigma_c \\ &= -\Pi_p V_O(r), & \sigma_c \leq r \leq (\sigma_c + \sigma_p) \\ &= 0, & r > (\sigma_c + \sigma_p) \end{aligned} \quad (1.17)$$

In this equation the potential depends mainly on the polymer concentration, size, molecular weight and the colloidal particle size. The respective graph is depicted in Figure 1.9.

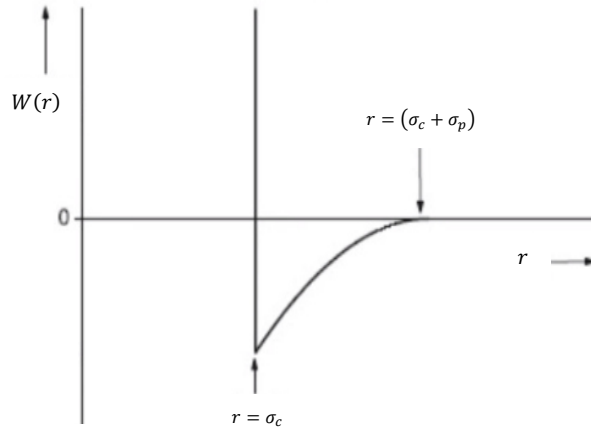


Figure 1.9. Attractive interparticle potential as a function of the distance r between the two colloidal particles. The minimum of the energy, thus the thermodynamically most favourable state is when the colloids are in closest contact to each other ($r = \sigma_c$).

The minimum of energy, thus the highest attraction force between the colloids, is at $r = \sigma_c$, which is when the space between both colloidal particles is depleted from the polymer. Thus, there is a polymer-induced attraction between two particles, which can lead to phase separation into a colloid-rich and polymer-rich phase. The colloid concentration limit, at which phase separation occurs, thus the localisation of the binodal¹ line, can be calculated, however is not straightforward. More simple is the calculation of the spinodal¹, which is when the osmotic compressibility of the colloid $\partial\Pi_c/\partial\varphi$ becomes zero (with φ the phase volume).

$$\frac{\partial\Pi_c}{\partial\varphi} = 0 \quad (1.18)$$

As the spinodal line lies close to the binodal line, as an approximation it can be considered as the phase boundary. The virial expansion of Π_c is:

$$\frac{\Pi_c V_c}{k_b T} = \varphi + A_2 \varphi^2 + A_3 \varphi^3 + \dots \quad (1.19)$$

Where, V_c is the particle volume of the colloidal particle, A_2 the second and A_3 the third osmotic virial coefficient. A_3 and higher order terms can be neglected for low volume fractions ($\varphi < 0.2$). The osmotic pressure of the colloid is thus

$$\Pi_c = \frac{k_b T}{V_c} (\varphi + A_2 \varphi^2) \quad (1.20)$$

$$\frac{\partial\Pi_c}{\partial\varphi} = \frac{k_b T}{V_c} (1 + 2A_2 \varphi) \quad (1.21)$$

With the above condition for the spinodal line ($\frac{\partial\Pi_c}{\partial\varphi} = 0$) we get

¹ Detailed explications of binodal and spinodal lines can be found in the section 1.3.7.

$$A_2^{sp} = -\frac{1}{2\phi^{sp}} \quad (1.22)$$

Where ϕ^{sp} is the volume fraction at the spinodal. The osmotic second virial coefficient can either be measured or calculated. From statistical mechanics, the relation between A_2 and $W(r)$ can be established (Vrij, 1976):

$$A_2 = \frac{2\pi}{v_c} \int_0^\infty r^2 \left(1 - e^{\frac{W(r)}{k_B T}}\right) dr \quad (1.23)$$

All the physicochemical parameters of the equations are known, allowing to calculate A_2 in a simple way.

The osmotic second virial coefficient can however also be measured by osmometry (Tombs & Peacocke, 1974), laser light scattering (Semenova, 1996), equilibrium sedimentation (Wills, Jacobsen, & Winzor, 1996) and chromatography (Dumetz, Chockla, Kaler, & Lenhoff, 2008) as it influences those colligative properties.

From this follows, that for a fixed volume fraction ϕ of colloidal spheres, the effect of addition of polymer molecules on A_2 can be calculated. At a certain polymer concentration, A_2 will equal to $-\frac{1}{2\phi}$, indicating the phase separation concentration for this specific volume fraction of the colloid. By repeating this procedure at various volume fractions, the phase diagram can be entirely predicted. This model has been shown to be valid to predict the phase behaviour of α -lactalbumin/pullulan (S. Wang, Van Dijk, Odijk, & Smit, 2001), gelatin/dextran (Edelman, Van der Linden, De Hoog, & Tromp, 2001) or β -lactoglobulin/k-carrageenan mixtures (S. Wang et al., 2001).

Similar to the case of the Flory-Huggins model, several approximations have been done in this case. The potential of mean force, does not depend only from the attractive depletion interactions $W_{dep}(r)$, but also from the attractive van der Waals potential $W_{VDW}(r)$, electrostatic repulsive potential $W_E(r)$ and lastly the steric repulsive potential $W_{steric}(r)$, which arises from the interaction between biopolymer adsorbed layers (Semenova & Dickinson, 2010):

$$W(r) = W_{VDW}(r) + W_E(r) + W_{dep}(r) + W_{steric}(r) \quad (1.24)$$

More complex models, such as the modified nonrandom two-liquid model (Wu, Lin, & Zhu, 1998) or the UNIQUAC model (C. H. Kang & Sandler, 1987) have been proposed, and most of those theories of phase diagram calculations have difficulties to coincide with experimental data. Furthermore, molecular weight is often ill-defined, due to the polydispersity of the samples and exact information about polymer-polymer or polymer-solvent interactions are difficult to obtain. Nevertheless, the models allow understanding how changes in polymeric or environmental parameters may qualitatively alter phase behaviour. Those effects on the phase behaviour are now discussed further details.

1.3.6 Effects of Physicochemical Parameters on Phase Behaviour in W/W Emulsions

Temperature:

Usually temperature decrease leads to a smaller region of miscibility, as the entropy of mixing is reduced. Thus for lower temperature, lower polymer concentrations are needed in order phase separation to occur (Figure 1.10).

However, the temperature dependence on other interaction parameters has to be taken into account. Most studies of phase behaviour have been performed at elevated temperatures, as cooling can cause, in many cases, one of the polymers to order, aggregate and form a network (N. Lorén et al., 2001; Lundin et al., 2000). Those temperature-induced enthalpic interactions between chains of the same species alter the macromolecular organisation in solution and affect phase behaviour (Figure 1.10). This effect is discussed in the section below.

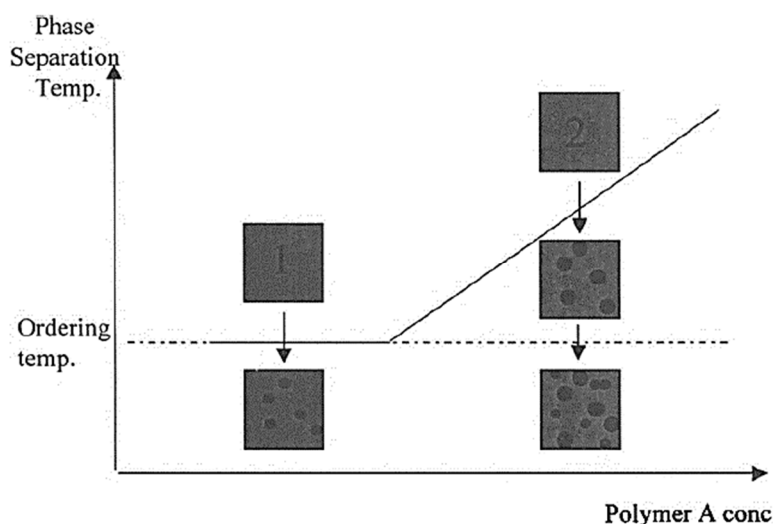


Figure 1.10. Model illustrating the phase separation temperature as a function of the concentration of polymer A, as constant concentration of the second polymer in solution. (Figure reproduced from (Lundin et al., 2000)). 1 and 2 are reference numbers of samples.

Molecular Weight:

The molecular weight plays a direct role on phase composition, as described in the thermodynamic models in the previous section. Increasing the molecular weight of the components reduces the number of species free to move independently and therefore reduces the mixing entropy of the system. As a consequence the phase boundary is moved towards regions of lower concentrations (Frith, 2010). Effect on molecular weight on phase behaviour has been studied in detail by Alevisopoulos et al. (Alevisopoulos & Kasapis, 1999).

Polymer polydispersity is thus a key factor that influences polymer-polymer interactions and phase behaviour. This can even lead to situations in which the high molecular weight portion of the polydisperse species will accumulate in one phase, and the low molecular weight portion of the polymer, in the other phase. This molecular weight fractionation of polydisperse samples has been studied for

the gelatin-dextran system (Edelman, Tromp, & van der Linden, 2003) and the agarose-maltodextrin system (Loret, Schumm, Pudney, Frith, & Fryer, 2005).

Ionic Strength:

The ionic strength of the solution strongly influences, phase behaviour, especially for charged polymers. In the case for mixtures of an uncharged and a charged polymer, phase separation is dominated by counterion entropy. At low ionic strengths, counterion entropy dominates, leading to formation of a homogeneous solution (entropic barrier for phase separation as number of counterions far higher than number of polymers, they have thus a higher entropic contribution to system). If salt is added to the system, thus the ionic strength increased, phase separation can be induced, as the imbalance in counterion concentration becomes less significant (Harding, 1997; Piculell & Lindman, 1992).

In the case of mixtures of two charged polymers, polyelectrolytes, it creates an analogous, but less pronounced barrier to phase separation and can similarly be offset by addition of salts (Morris, 2009). The barrier of counterion entropy for phase separation of charged polymers, is a reason why two uncharged polymers are more likely to segregate than ionic polymers.

pH:

pH will influence the charge density of biopolymers, thus also number of counterions associated with the polymers, which will in turn influence phase separation behaviour. The electrostatic interaction between the two polymers in solution also becomes altered, as it can be seen in Figure 1.11, for the case of β -lactoglobulin and pectin. If the pH lies below the isoelectric point (pI) the protein is positively charged and below a critical pH the anionic groups of pectin associate with the cationic groups of the protein, leading to complexation and phase separation. Depending on the pH difference from the pI, either coacervates or precipitates are formed, latter being packed more densely and thereby trapping less solvent. For pH above the isoelectric point both polymers are co-soluble or form soluble complexes, at which some cationic groups of the protein interact with pectin. As with temperature, pH changes may affect conformation or aggregation of the polymers and thus influence phase behaviour greatly.

Conformational Aggregation and Network Formation

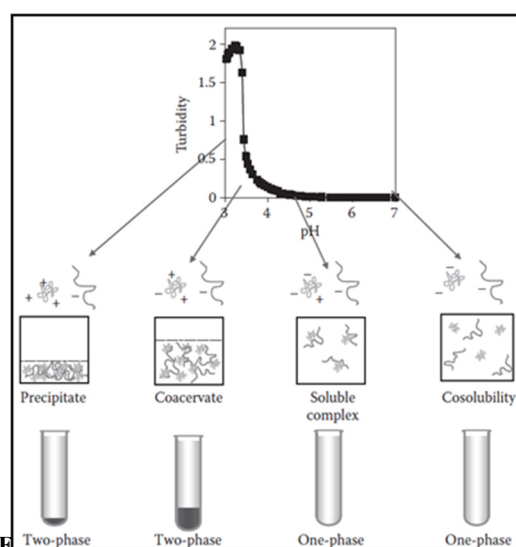


Figure 1.11. Influence of pH on phase behaviour of a biopolymer mixture of β -lactoglobulin and pectin. (Figure reproduced from (D. McClements, 2014)).

The onset of ordering, conformational changes in the polymer from disordered coiled to ordered helical structures, affects phase separation and can lead to aggregation of the polymers. Ordering occurs, when the energy gain offered by the ordered helical state, outweighs the entropic advantage in the disordered state. The stiffening of the chains and aggregation alters polymer interaction parameters and the effective molecular weight, which reduces miscibility, and drives the demixing process. In the gelatin/dextran system phase separation occurs at concentrations, as low as 1% of gelatin, for temperature below the gelation temperature of gelatin (25-30 °C). Whereas above this temperature, phase separation occurs only above 4% (Edelman et al., 2001). In the whey protein/pectin system, heating resulted into whey protein aggregation and gelation, which favoured phase separation (S. Wang et al., 2001).

Additionally, there is a competition between phase separation and network formation, which can lead to trapping of microstructures at various stages of separation or ripening (N. Lorén et al., 2001; Lundin et al., 2000). For example, Haug et al. (Haug, Williams, Lundin, Smidsrød, & Draget, 2003) obtained a multi-phase system upon cooling of a κ -carrageenan and fish gelatin mixture. The system was composed of an emulsion-like phase (associated fish gelatin–carrageenan) in a bi-continuous network. The formation of such microstructures was related to the gelling and ordering of carrageenan and was fully reversible.

Shear:

Applying shear to a mixed polymer system can affect the ripening kinetics and thus the phase morphology. Wolf and co-workers obtained shear induced anisotropic microstructures in phase-separated biopolymer mixtures, whose shape depended on the shear stress range (Wolf, Scirocco, Frith, & Norton, 2000b). Shear also can lead to phase inversion for sheared-cooled systems. It has been shown that for mixtures in which one of the components forms a gel during shear cooling, the other component will form the continuous phase (Foster, Brown, & Norton, 1996; Lundin et al., 2000)

Figure 1.12 summarises the influence of various parameters described, on phase behaviours of a binary polymer mixture.

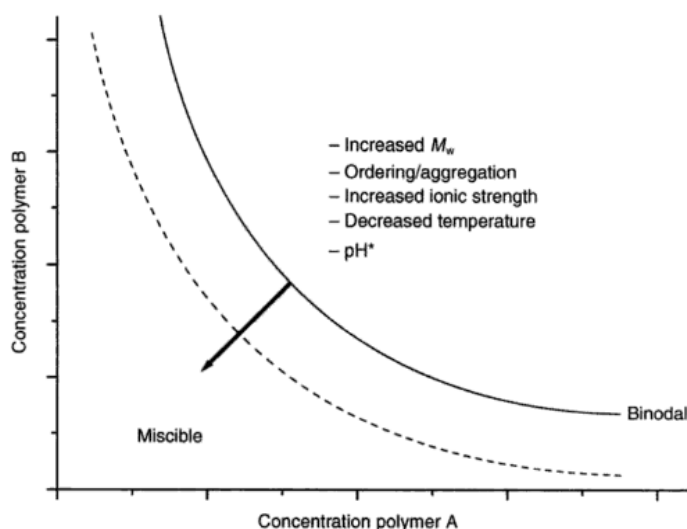


Figure 1.12. Schematic phase diagram showing the trend for increased immiscibility observed for biopolymer mixtures as certain polymer and physicochemical attributes are changed. (*pH can change the charge density of the polymer; see section on ‘Ionic strength’) (Figure reproduced from (Lundin et al., 2003)).

1.3.7 Phase Behaviour

As commented above, phase diagrams cannot be easily simulated in real practical systems, and are thus often obtained through experimental methods.

The axes of the ternary phase diagram indicate the concentration of the respective polymer or solvent in the system. As the solvent, which is normally water, constitutes often >80 % of the sample it is more common to present the phase diagram as x-y plots, rather than conventional triangular phase diagrams, shown in Figure 1.5.

To obtain data for the phase diagram, observations are made as to whether bulk phase separation has occurred, at a constant temperature, after equilibration of the sample or centrifugation.

Phase diagrams are divided into two areas by the binodal line: One area, where 2 phases coexist and the free energy of mixing is positive, and another miscible region of 1 phase, where the free energy of mixing is negative.

Systems within the 2 phase regions, with a composition X (as indicated in Figure 1.13 a) will separate into a phase with composition Y and another with the composition Z. The same happens with other compositions on the same tie line, but they will separate with another volume ratio. This figure shows how the two phases formed are not pure and that each phase is saturated with the second component. The tie-lines converge at the critical point, in which the composition difference between phases disappears. Beyond the critical point, the two immiscible phases vanish, forming one single phase.

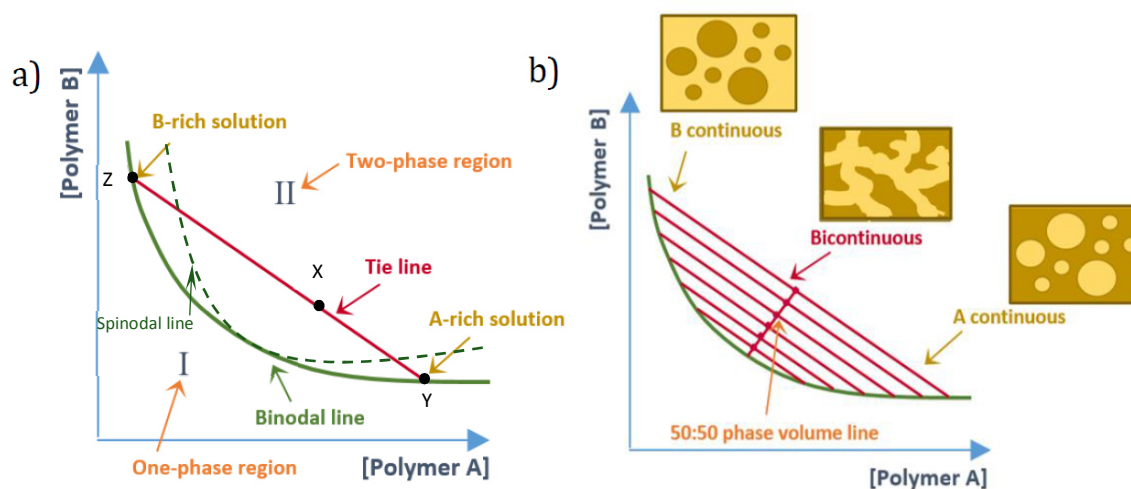


Figure 1.13. (a) Schematic phase diagram of an aqueous mixture of Polymer A and Polymer B. (b) Position in the phase diagram, and thus volume ratio of the solution, defines the microstructure of the mixture. Figure adapted from (Espigulé, 2016).

Volume ratio defines the microstructure of the mixture, thus which of the components will constitute the continuous phase, and which one the dispersed one. For example in a PEG:Dextran mixture with phase volumes of 75% PEG:25% Dextran, the emulsion will consist of dextran-rich droplets, dispersed in a PEG aqueous solution. In case both phase volumes are identical, bicontinuous structures will be observed (Figure 1.13 b).

Phase diagram and the microstructures are snap-shots relevant to a particular time. Structural and physical events are associated with the evolving conditions of phase separation. This process can be described by two mechanisms: nucleation and growth (NG) and spinodal decomposition (SD). The spinodal line divides in the phase diagram compositions which undergo NG and SD.

Solutions beyond the spinodal line, into the incompatible region, are unstable and phase separation undergoes spontaneously and rapidly by SD. Thereby, the two polymer phases start to cluster together into microscopic clusters, which are not necessarily spherical, rich in either of both polymers (Figure 1.14). These clusters then grow uniformly and coalesce. In SD phase volume is established immediately and the concentration of the phases evolve over time.

Systems lying between the binodal and spinodal line are metastable and separate via the NG mechanism. NG phase separation involves a high free energy barrier, thus the process is a slow one, in contrast to SD. Phase separation starts in this case at various nucleation sites (Figure 1.14). The droplets that form have a broad size distribution and form as a pure phase that grows with time. Phase volume changes continuously, while the equilibrium concentration of the two phases are established in the early stages.

The ripening of the mixtures, during which processes such as droplet coalescence, Oswald ripening, creaming and sedimentation occur, is in both cases dependent on various factors, such as the relative rheology of the different phases, molecular weight, the interfacial tension and the density difference between the two phases, or the amount of shear the system is subjected to (Buttler, 2002; E. Dickinson & Bergenstahl, 1997; Harding, 1997; Lundin et al., 2003). The ripening will end up in macroscopic phase separation, if the phase separation process is not arrested by e.g. gel formation, resulting in bicontinuous structures or gelled microparticles (Niklas Lorén & Hermansson, 2000; Turgeon, Beaulieu, Schmitt, & Sanchez, 2003) (Figure 1.14).

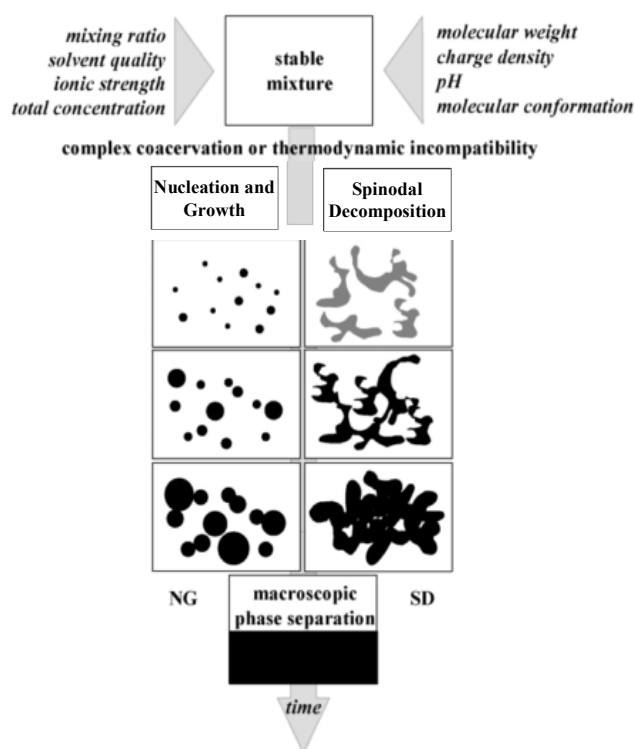


Figure 1.14. Factors affecting phase separation of polymer mixtures and the two mechanisms by which they phase separate: nucleation and growth (NG) and spinodal decomposition (SD) (Figure adapted from (Turgeon et al., 2003)).

1.3.8 Stabilisation of W/W Emulsions

W/W emulsions can be obtained by applying agitation in aqueous biphasic systems, simply by dispersing the phase with smaller volume fraction into the phase that has a larger volume fraction, forming thereby droplets. Those droplets are often poorly visible, as the refractive index of both aqueous phases are similar, making the emulsions therefore close to transparent. Peculiar to W/W emulsions is the co-solubility of the biopolymers in the coexisting phases, meaning they interact thus as well inside the separated phases with each other. Furthermore, the main component of both phases is the same solvent (water), which can freely diffuse across the interface.

W/W emulsions are governed by the same physical principles as W/O or O/W emulsions, including the rules for droplet break up and coalescence (Shewan & Stokes, 2013). The tension of this interface is far lower, in the order of 0.01 mN/m, than for a typical hydrocarbon(heptane)-water interface (50 mN/m) (Norton & Frith, 2001). In aqueous/aqueous two-phase systems it is mainly determined by measuring the deformation of droplets in a flow field at various shear rates (Ding et al., 2002; Wolf et al., 2000b). The low interfacial tension and the free flow of solvent between both phases has as a consequence than coalescence of the droplets is rather fast. In contrast, Ostwald ripening is slow, due to the low interfacial pressure, and sedimentation is slow as well, due to similar densities of both phases. The fast coalescence remains the biggest challenge for using W/W emulsion, as it conveys the system poor stability and rapid irreversible phase separation. Stabilisation of W/W emulsions is thus of the utmost technological importance, and finding new methods for the effective stabilization of emulsions is an important challenge for physical chemists.

In W/W emulsions, the interfaces between the two phases are usually thicker in comparison to oil-water interfaces. Their length scales are larger than the correlation length of the polymer solutions (Nguyen, Wang, Saunders, Benyahia, & Nicolai, 2015). Therefore, small hydrophilic molecules do not sense the interface when moving from one polymer phase to the other. As a consequence, small molecules do not adsorb on water-water interfaces. Experimental results showed, that bigger particles, had a greater ability to stabilise emulsions, considering that the energy of adsorption of a particle strongly depends on particle size (Aveyard, Binks, & Clint, 2003), as:

$$\Delta G = \pi R^2 \gamma (1 - \cos\theta)^2 \quad (1.25)$$

Where ΔG is the energy of adsorption, R is the radius of particles, γ is the interfacial tension and θ is the contact angle of adsorbed particles on the interface. Considering that the interfacial tension is very low in water-in-water emulsions, the energy of adsorption remains low except for large particles. Native proteins were not able to stabilize the emulsions because they were too small, but larger particles are able to successfully adsorb and stabilize. Preparation of this kind of Pickering emulsions for colloidal stability of W/W emulsion has first been reported in 2008 by Poortinga (Poortinga, 2008).

A list of various particles, used as W/W emulsion stabiliser is presented in Table 1.3, and Figure 1.15 illustrates two examples of them. For a deeper insight into particle stabilized W/W emulsions, Nicolai & Murray recently published an extensive review on the topic (Nicolai & Murray, 2017).

Table 1.3. Examples of different particles used, to stabilise all-aqueous emulsion systems

| Particle | W/W Emulsion System | Reference |
|---|----------------------------------|--|
| Silica nanoparticles | Waxy corn starch/Locust bean gum | (Murray & Phisarnchananan, 2014) |
| Nanorods (cellulose nanocrystals) | Dextran/PEG | (Peddireddy, Nicolai, Benyahia, & Capron, 2016) |
| Nanoplates (clay) | Gelatin/Dextran | (Vis et al., 2015) |
| Protein particles (β -lactoglobulin) | Dextran/PEG | (Nguyen, Nicolai, & Benyahia, 2013) |
| Microgels (whey protein) | Waxy corn starch/Locust bean gum | (Murray & Phisarnchananan, 2016) |
| Triblock-copolymers | Dextran/PEG | (Buzza, Fletcher, Georgiou, & Ghasdian, 2013) |
| Liposomes | Dextran/PEG | (Dewey, Strulson, Cacace, Bevilacqua, & Keating, 2014) |
| Latex Particles | Dextran/PEG | (Balakrishnan, Nicolai, Benyahia, & Durand, 2012) |

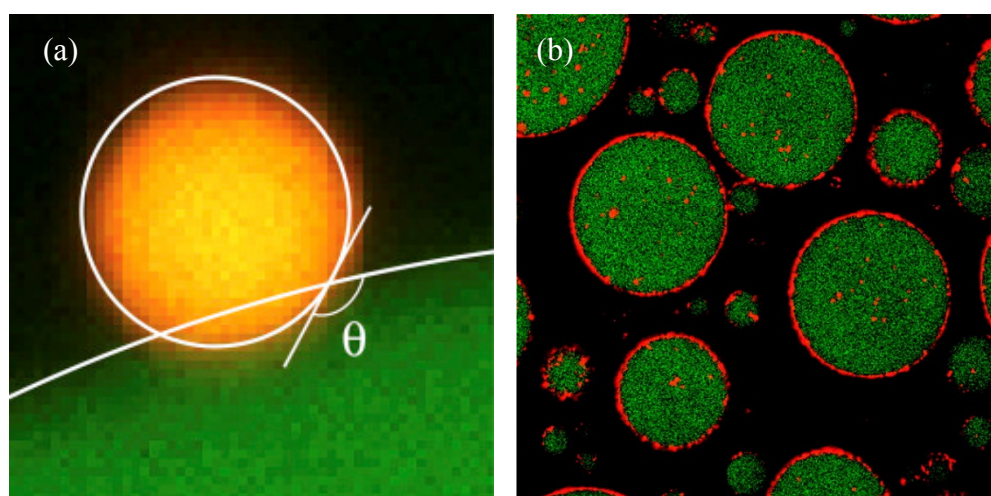


Figure 1.15. (a) Latex particle ($R=1\ \mu\text{m}$) at the interface between a large dextran drop and the continuous PEG phase (b) the same emulsion system, stabilised by β -lactoglobulin protein particles ($R=0.1\ \mu\text{m}$) Figures reproduced from (Balakrishnan et al., 2012)

Various authors have studied in detail the application of microfluidics on the formation of W/W emulsions (Song et al., 2013). Mechanically perturbing a stable W/W jet (Cheung Shum, Varnell, & Weitz, 2012) or a weak hydrostatic pressure difference of liquid-filled pipette tips introduced at the inlets of the continuous and dispersed phases (Abbasi, Navi, & Tsai, 2017; Moon, Abbasi, Jones, Hwang, & Tsai, 2016) allow W/W emulsions to be prepared in a controlled and reproducible fashion by microfluidics. Abbasi and coworkers combined microfluidic and pickering stabilisation techniques for the formation of dextran droplets stabilised by carboxylated particles. (Abbasi et al., 2017) (Figure 1.16).

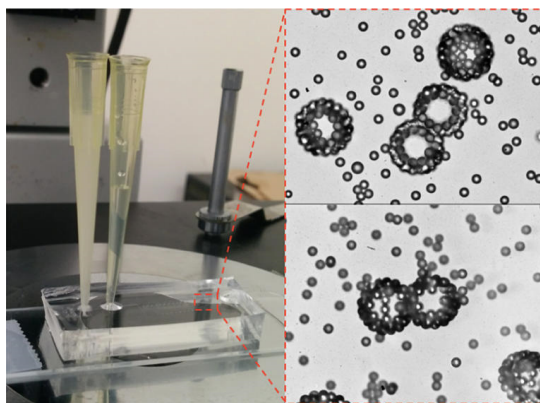


Figure 1.16. Carboxylated particles stabilising dextran droplets, prepared by emulsifying a dextran and a PEG solution by microfluidic techniques. Figure reproduced from (Abbasi et al., 2017)

1.3.9 Applications of W/W Emulsions

Aqueous polymer mixtures can be used in a great variety of applications. There are already various food products that are based on W/W emulsions, mainly containing mixtures of gelatin and polysaccharides (Eric Dickinson, 2015). As an example, sweet fruit gums contain modified starch, gelatin and gum arabic and have a phase separated microstructure (Lundin et al., 2003). They have also been used to create zero fat spreads, consisting of gelatin and maltodextrin (EP0574973, 1993), which was optimised to provide both acceptable spreading and in-mouth behaviour.

Moreover, W/W emulsions have been used as microreactors for the synthesis of various particles. They have the advantages that their interior maintains reaction-relevant microenvironments, while allowing entry/exit of substrates and products in mild conditions. Cacace et al. demonstrated the use of dextran/PEG emulsions droplets as microreactors for the enzymatic synthesis of CaCO_3 nanoparticles (Cacace, Rowland, Stapleton, Dewey, & Keating, 2015). Another example consists of a dextran/PEG system stabilized with liposomes, used to ribozyme cleavage reaction (Dewey et al., 2014). In both cases W/W emulsions droplets can be regarded as fully biomimetic microreactors, which allow the reproduction of biological reactions.

Another very important application of W/W emulsions is their use for the formulation of novel encapsulation and delivery systems. Using food-grade components a diverse range of biocompatible delivery systems suitable for encapsulating, protecting, and controlled delivery of active components have been developed (Matalanis, Jones, & McClements, 2011). These delivery systems can be prepared by simple methods, as e.g. mixing, homogenizing and thermal processing. The dynamics from encapsulation systems based on W/W emulsions has been reported by Sagis et al. (Sagis, 2008). So far, a big variety of ingredients have been encapsulated in all-aqueous emulsions, such as sugars (R. S. Khan, Nickerson, Paulson, & Rousseau, 2011), small molecules (Shivkumar V Ghugare, Mozetic, & Paradossi, 2009) or proteins (SV Ghugare, Chiessi, Fink, & Gerelli, 2011; Jin et al., 2008).

A major part of those delivery systems are microgels. Next section will give an introduction to microgels and be followed by an outline of existing work of W/W emulsion as templates for microgel production.

1.4 Microgels

Microgels are defined as particles of gel of any shape with an equivalent diameter of approximately 0.1 to 100 μm (Alemán et al., 2007), with in most cases the ability to swell in response to a change in the physicochemical environment (Figure 1.17). This enables them to incorporate and release molecules in a responsive manner, making them an interesting candidate as drug delivery vehicles.

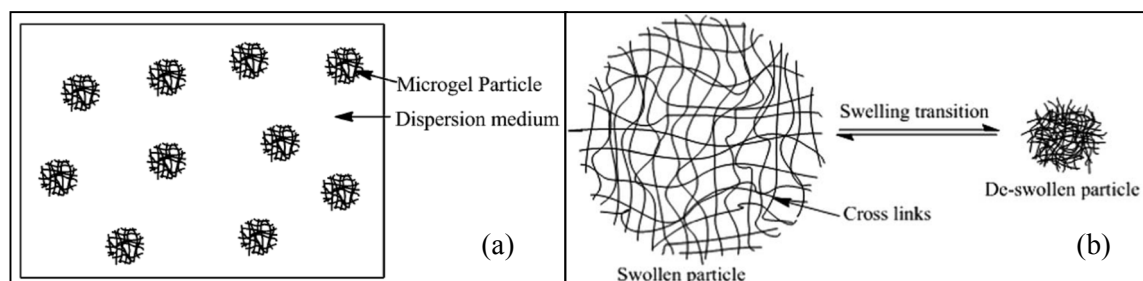


Figure 1.17. Microgels are cross-linked gel particles (a) and in most cases have the ability to swell in response to a change in the physicochemical environment. (Figure reproduced from (Bonham et al., 2014)).

Microgels should not be confused with microcapsules, which consist of a shell that encapsulates a core containing the drug. Microcapsules thus do not allow volume transitions as microgels, but drug release is more controlled by shell permeability (Bysell, Månsson, Hansson, & Malmsten, 2011).

The use of microgels as drug delivery vehicles is of interest as they combine the useful aspects of colloidal dispersions with the ones of conventional macrogels. This means they are free-flowing liquids with a high surface to volume ratio, which facilitates mass transport to and from the microgels, but also display controlled swelling, which makes them responsive delivery vehicles (Fernandez-Nieves, Wyss, Mattsson, & Weitz, 2011). Cross-link density, particle size, shape, surface properties, solvent quality and polymer type are all properties, which can be manipulated to adapt the system to the specific application.

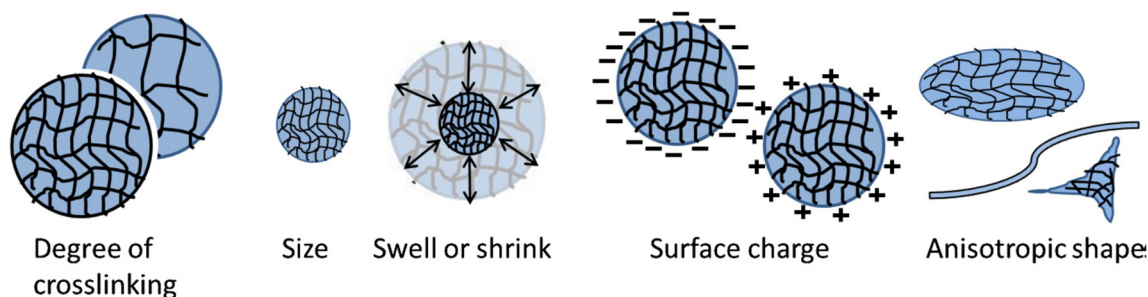


Figure 1.18. Many modifications of the microgels allow it to adapt it for specific applications. (Figure reproduced from (Shewan & Stokes, 2013)).

The last decade showed a surge of publications employing microgels as drug delivery vehicles (Fernandez-Nieves et al., 2011). However, microgels have already been used for many other applications before.

- Personal Care: E.g. carbopol microgels were used to form clear gels (Fernandez-Nieves et al., 2011).
- Coating Material: Use of microgels for coatings allow to remove harmful volatile organic compounds from paint formulations (Shewan & Stokes, 2013).
- Recovery of oil and gas: Xanthan or guar based microgels have already been used for recovery of oil and gas from porous rock formations (Fernandez-Nieves et al., 2011).

- Food Industry: Microgels can act as fat replacer. Microparticulated cross-linked whey protein, known under the product name Simplese™, was used in fat-free yoghurts and resulted in products which matched the textural characteristics and the sensory scores of full fat yoghurts (Ehren, Govindarajan, Morón, Minshull, & Khosla, 2008; Levett, 2011; 5171603, 1992).

1.4.1.1 Microgel preparation methods

Preparation of microgel particles consists of formation of droplets and their subsequent gelation. Polymers can be gelled by either physical or chemical bonds. Physical bonds consist of hydrogen bonds, hydrophobic bonds or ionic interactions, which all can be affected by counterions, pH or temperature (D. McClements, 2014; Shewan & Stokes, 2013). Chemical crosslinking creates covalent linkage between polymer functional groups and can be formed by either chemical agents, such as glutaraldehyde, formaldehyde and genipin, or by enzymes, such as transglutaminase and laccase (Jones & McClements, 2010; D. McClements, 2014; Shewan & Stokes, 2013). If the polymer has not been previously formed, polymerisation of the monomer has to be undertaken; the corresponding methods will not be discussed and can be found elsewhere (Bonham, Faers, & van Duijneveldt, 2014; Fernandez-Nieves et al., 2011).

The droplets can be formed in a big variety of methods, and some of them are presented next.

Atomisation

The preparation of microgels by atomisation relies on the principle of droplet formation in air and their subsequent gelation. Droplets are typically formed by breaking up a liquid stream using natural (Rayleigh) flow instabilities, ultrasonics or electrostatics (Shewan & Stokes, 2013). Spinning disk and spray nozzle atomisation are two methods to create droplets on an industrial scale.

The principle of spinning disk atomisation is that a liquid flows across a spinning disk leading to droplet break-up at the edge of the disk, due to Rayleigh instabilities (Figure 1.19). Concurrent flow of the active and encapsulating fluid across the disk can be used to encapsulate the active ingredient. Polydispersity of the particles is a drawback to be considered for this method (Shewan & Stokes, 2013).

Using a spray nozzle, droplets are formed by fluid jet instabilities of a liquid flowing concurrently with



Figure 1.19. Spinning disk showing jets and drop break up. (Figure reproduced from (Southwest Research Institute Website, 2015)).

air through a nozzle at a high flow rate. Caution must be taken when working with viscous fluids, which may block the spray nozzle (Shewan & Stokes, 2013).

Injection/Extrusion

This method involves the injection of a polymer into another solution, which promotes gelation. Formation of droplets before impacting the other solution can be done by above mentioned methods or by electrostatic generation, jet cutting or acoustic jet excitation, among other methods. Depending on the method of gelation, the second solution may contain a gelling agent (e.g. ions or enzymes) or be heated/chilled for heat-set or cold-set gelation (Figure 1.20).

The advantage of microgel preparation by extrusion is that it is a cheap and simple method, which allows them to be produced on an industrial scale (Matalanis et al., 2011; Shewan & Stokes, 2013)

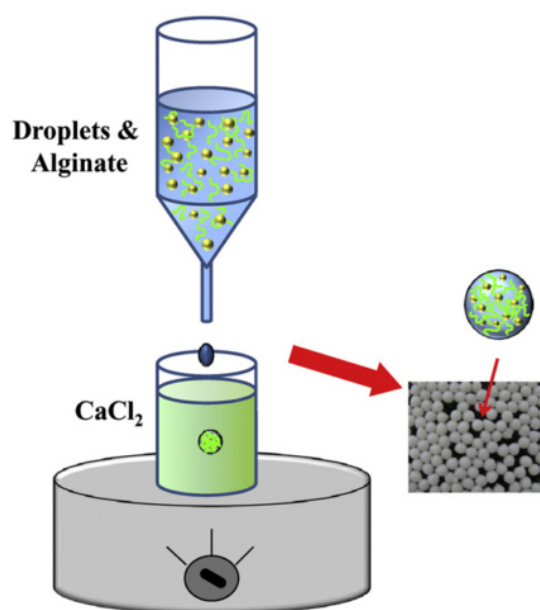


Figure 1.20. Injection of an O/W (aqueous containing Alginate) is dropped into a CaCl₂ solution which acts as a gelling agent for Alginate. (Figure reproduced from (Matalanis et al., 2011)).

Spray drying

Spray drying involves atomisation of solutions or suspensions of drugs, polymers, and particles to fine droplets. Microgels are formed by inducing quick evaporation of solvent from the droplets by means of a stream of hot air in the drying chamber. Even though the operation temperature is between 150 and 300°C, the actual temperature experienced by the material is considerably less due to the latent heat associated with liquid evaporation. Thermal damage is furthermore reduced due to the high surface-to-volume ratio of the drops, which allows for rapid drying.

As a consequence, this method is suitable for ingredients that are sensitive to heat such as proteins, flavour oils and lipid droplets. It has the advantage of forming a dry powder product with prolonged shelf life and low transport and storage costs. However, spray drying is not suitable for non-water soluble or high viscosity biopolymers. The potential breakdown of the porous particles during rehydration are mentionable drawbacks (Matalanis et al., 2011; Oh, Drumright, Siegwart, & Matyjaszewski, 2008; Shewan & Stokes, 2013).

Spray cooling

The opposite of spray drying is spray cooling, in which the liquid is atomized via a heated nozzle and cool air is used to solidify droplets into microgels. Encapsulation of hydrophilic ingredients such as mineral salts, enzymes, and flavours is routinely performed by this technology (Shewan & Stokes, 2013).

Emulsion-templating

Water in oil (W/O) emulsions can be used as a template for creating microgels. After obtaining the desired size of the water droplets by varying homogenization conditions, surfactant type or system composition, the aqueous phase is gelled. After separating the droplets from the organic phase and washing them, pure microgels dispersed in an aqueous solution can be obtained (Figure 1.21) (D. McClements, 2014; Shewan & Stokes, 2013).

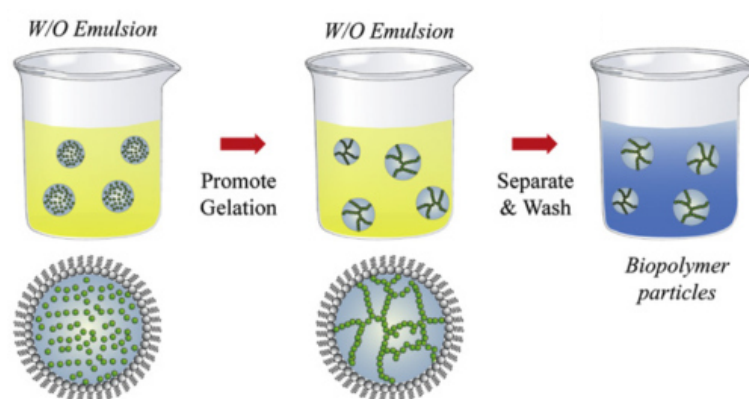


Figure 1.21. Gelation of the aqueous phase in a W/O emulsion and subsequent steps of separation and washing is a way to fabricate a microgel suspension. (Figure reproduced from (Matalanis et al., 2011)).

Microfluidics

Microfluidics is particularly interesting for basic research as a tight control of microgel characteristics is possible. Due to costs and problems in scale-up, it is less suitable for industrial use. Microgels are produced by flowing the polymer solution through an internal channel, while a solution of the gelling agent is made to flow in the external channel. Once the two liquids come into contact, emulsification/droplet formation is initiated and subsequent crosslinking results in microgels creation (Figure 1.22). Microfluidics is considered to be a reliable and reproducible method for preparing double emulsions with monodisperse included droplets. (D. McClements, 2014; Oh, Lee, & Park, 2009; Shewan & Stokes, 2013)

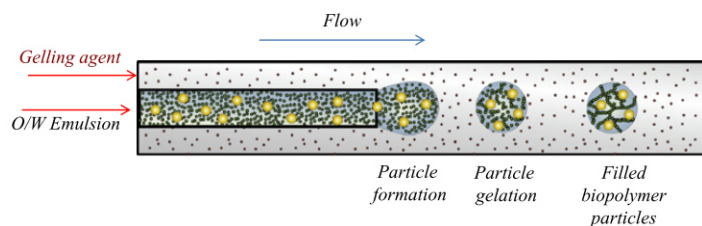


Figure 1.22. A co-axial microfluidic device, which contains an O/W emulsion in the inner channel and the gelling agent in aqueous solution in the exterior one. Once both liquids come into contact polymer particles are formed. (Figure reproduced from (Matalanis et al., 2011)).

Shear gels

Applying shear during gelation of polymers can prevent them of forming a network structure, but instead creating smaller polymer particles (Figure 1.23). This method is often used in W/W emulsions, as discussed below. Furthermore, applying shear to a preformed gel breaks it up into smaller gel particles. However these particles are polydisperse in size and highly irregular in shape (D. McClements, 2014; Shewan & Stokes, 2013).

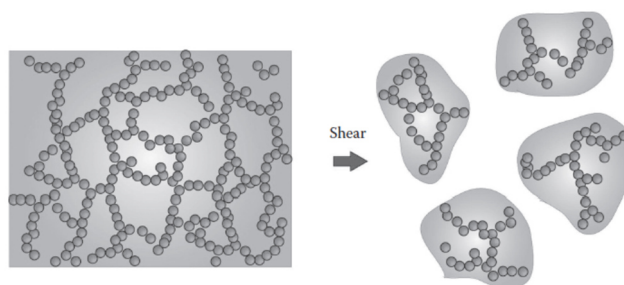


Figure 1.23 Applying shear to already formed or forming gels, allows to create microgels. (Figure reproduced from (D. McClements, 2014)).

1.4.1.2 Microgel formation from W/W emulsions

A big advantage of forming microgels from W/W emulsions is that no surfactants or organic solvents are needed. Adding a crosslinking agent or changing environmental conditions such as temperature, pH or solvent quality, allows gelling and thus stabilisation of the emulsion and formation of polymer particles. Most research work performed so far on the use of W/W emulsion for the production of microgels are based on the PEG/Dextran system, which is a well studied system. PEG can be crosslinked by for example coupling it to a UV photoinitiator. Recent developments can be found in Table 1.4. Gelatin-based microgels, can be found in Table 1.6.

Table 1.4. Examples of recent research works, in which microgels were produced by W/W emulsion

| Polymers | Crosslinker | Size | Application | Reference |
|--|--|---------------------------|---|--|
| PEG dithiol -4-arm PEG norbornene solution / Dextran. | UV Light | 10 µm | PEG microgels for VEGF release | (Impellitteri, Toepke, Lan Levensgood, & Murphy, 2012) |
| PEG- dithiothreitol polymer/Dextran | UV Light | 2-16 µm | Controlling degradation of PEG microgels by altering PEG MW, emulsion conditions etc. | (Parlato, Johnson, Hudalla, & Murphy, 2013) |
| Starch/PEG | Trisodium trimetaphosphate | 5-20 µm | Crosslinked starch microspheres were obtained from either W/W or W/O emulsion were compared | (B. Li, Wang, Li, Adhikari, & Mao, 2012) |
| Hydrolyzed cassava starch/PEG | - | 10-20 µm | Effect of molecular weight of starch on the properties of cassava starch microspheres prepared | (Xia, Li, & Gao, 2017) |
| PEG/Dextran and UV photoinitiator | UV Light | 200-800 nm | PEG nanospheres Testing release, biocompatibility of preglabin | (Aydin & Kizilel, 2017) |
| Dextran/PVA / NiPAAm and UV photoinitiator | UV Light | 500-800 nm | Thermoresponsive and biodegradable Dextran/poly-(methylmethacrylate-co-N-isopropyl acrylamide) microgels Prepared by emulsion polymerisation | (Shivkumar V. Ghugare et al., 2013) |
| Poly (vinyl alcohol)/ Poly (methacrylate-co-N-isopropyl acrylamide)/ Dextran and UV photoinitiator | UV Light | 1-5 µm | Temperature-Sensitive Poly (vinyl alcohol)/ Poly (methacrylate- co - N -isopropyl acrylamide) Microgels for Doxorubicin Delivery Prepared by emulsion polymerisation | (Shivkumar V Ghugare et al., 2009) |
| Methacrylated PVA/ dextran T40 and UV photoinitiator | UV Light | 1-5 µm | Methacrylated PVA microgels for doxorubicin delivery | (Cavaleri et al., 2008) |
| Whey protein isolate/ Low methoxyl pectin | CaCl ₂ | pH dependent (0.5-490 µm) | Hydrogel particles consisting of a protein-rich core and a pectin-rich shell. Formed by a two-step biopolymer phase separation method which relies on both segregative (pH 7) and aggregative (pH 5) phenomena. | (Duval, Chung, & McClements, 2015) |
| O/W/W emulsions Pectin/Casein | Transglutaminase | | Stability of microgels composed of adsorbed anionic pectin molecules around lipid-filled caseinate-rich particles | (Matalanis et al., 2010; Matalanis & McClements, 2012) |
| Methacrylated dextran/PEG | Polymerization of the methacryloyl groups attached to dextran. | 2.5-20 µm | Dextran microspheres | (Stenekes, Franssen, van Bommel, Crommelin, & Hennink, 1999) |

1.4.2 Controlled Release Properties

Microgels for encapsulation and delivery of active ingredients have been designed to react to different physicochemical stimuli, including temperature, pH, ionic strength, presence of specific metabolites or to external fields (not discussed here). The way it releases the active component can be through swelling, fragmentation or erosion of the microgel, or by diffusion of the component out of the vehicle (Figure 1.24).

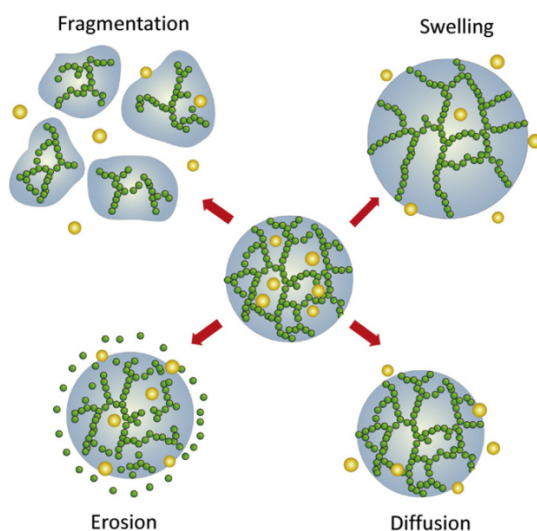


Figure 1.24. Four different mechanisms, by which the drug may be released from the microgel. (Figure reproduced from (Matalanis et al., 2011)).

1.4.2.1 Temperature-triggered Release

Change of temperature induces a change in solvency, consequently causing swelling or deswelling. Drug can then either be released by the “dissolving out” mechanism in which the drug is released in the swollen state, or the “squeezing out mechanism” in which the active ingredient is released at deswelling, similar to a sponge (Fernandez-Nieves et al., 2011; Kawaguchi, 2013).

Poly(N-isopropylacrylamide) (PNIPAm) microgels are among the most widely investigated thermoresponsive microgels. Due to reduced solvency, they deswell with increasing temperature. Insulin (Nolan, Gelbaum, & Lyon, 2006), magnetic nanoparticles (S. Bhattacharya, Eckert, Boyko, & Pich, 2007; Nayak, Lee, Chmielewski, & Lyon, 2004), ibuprofen (Vanessa Castro Lopez, Raghavan, & Snowden, 2004), doxorubicin (Shivkumar V Ghugare et al., 2009) or salicylamide (V Castro Lopez, Hadgraft, & Snowden, 2005) are only a few examples of materials that were loaded into PNIPAm composite microgels. PNIPAm has also been combined with biopolymers to give the microgels more biocompatible properties (Shivkumar V. Ghugare et al., 2012; A. Khan, Othman, Chang, & Akil, 2015). Composites of Poly(N-vinylcaprolactam) have a similar behaviour and have also been used to design thermosensitive microgels (Boyko et al., 2003; Peng & Wu, 2000).

1.4.2.2 Electrostatic-triggered Release

pH-controlled release is especially interesting if specific parts of the GI tract want to be targeted. Change of pH may lead to ionisation and thus swelling of the microgel network or to degradation of some bonds.

Polyacids, especially derivatives of polyacrylates, are particularly interesting for oral drug delivery. At low pH, which can be found in the stomach region, they are uncharged and thus collapsed, while at higher pH, as in the intestine, they get ionised and drug release occurs due to microgel swelling (Fernandez-Nieves et al., 2011). Babu et al. studied interpenetrating network microgels of sodium alginate-acrylic acid (Ramesh Babu et al., 2006) and Das et al. studied microgels containing PNIPAm and poly(N-isopropylacrylamide-co-acrylic acid) bioconjugated to tumor cell affine peptides (Das, Mardiyani, Chan, & Kumacheva, 2006). pH sensitive methacrylic acid–ethyl acrylate microgels were successfully designed by Tan and Tam. Those microgels progressively release procaine hydrochloride between pH 5 and 8 from the network (Figure 1.25) (Tan & Tam, 2007).

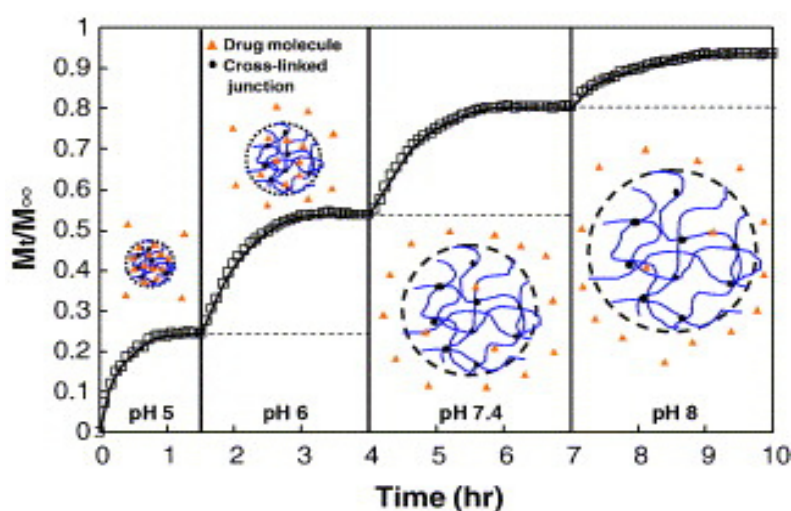


Figure 1.25. Release profile of procaine hydrochloride from methacrylic acid–ethyl acrylate microgels as a function of pH. (Figure reproduced from (Tan & Tam, 2007)).

Biopolymer-based microgels used for pH mediated delivery, were mainly based on chitosan. Chitosan with hydrolyzed poly(vinyl alcohol)-grafted-acrylamide matrices swelled at high pH, while microgels based on the chitosan derivative N-[(2-hydroxy- 3-trimethylammonium)propyl]chitosan chloride swelled at lower pH (Krishna Rao, Vijaya Kumar Naidu, Subha, Sairam, & Aminabhavi, 2006), making it interesting for stomach or cancer cell delivery (H. Zhang, Mardiyani, Chan, & Kumacheva, 2006).

Murthy *et al.* designed microgels containing acetal crosslinkers, which have a half-life of 24 h at pH 7.4 and only 5 min at pH 5.0. They applied this system to deliver proteins to phagosomes of antigen-presenting cells (Murthy et al., 2003).

1.4.2.3 Triggered Release by Specific Compounds

Drug release from microgels may be dependent on the presence of specific compounds.

For example the lectin concanavalin A (ConA) makes insulin containing microgels responsive to free glucose concentration. ConA acts as a crosslinker when mixed with dextran derivatives. If exposed to

increased glucose concentration, there is a competition for the ConA binding sites, rupturing the gel crosslinks and releasing hence insulin (Figure 1.26 a) (J. J. Kim & Park, 2001).

On a similar principle, antigens and antibodies were grafted to different polymers and a gel was formed when mixing them together. Addition of free antigen led to swelling, followed by dissolution of the gel due to binding competition to the antibody (Figure 1.26 b)(Miyata, Asami, & Uragami, 1999).

Other kind of sensitivity was obtained by adding glucose oxidase into a poly(acrylic acid)-grafted porous cellulose gel. Upon exposure to glucose, gluconic acid was generated, leading to reduced pH, which in turn promotes gel swelling and hence insulin release (Ito, Casolaro, Kono, & Imanishi, 1989).

Some groups also investigated swelling of gels due to conformational changes of proteins in response to specific compounds (Sui, King, & Murphy, 2007; Yuan, Yang, Kopecková, & Kopecek, 2008). Proteins of interest for such applications include those with hinge motion between sub-domains, shear-motion between domains and motor proteins (Bysell et al., 2011). Most mentioned studies have been performed in macrogels, but knowledge can easily be translated into the microgel field.

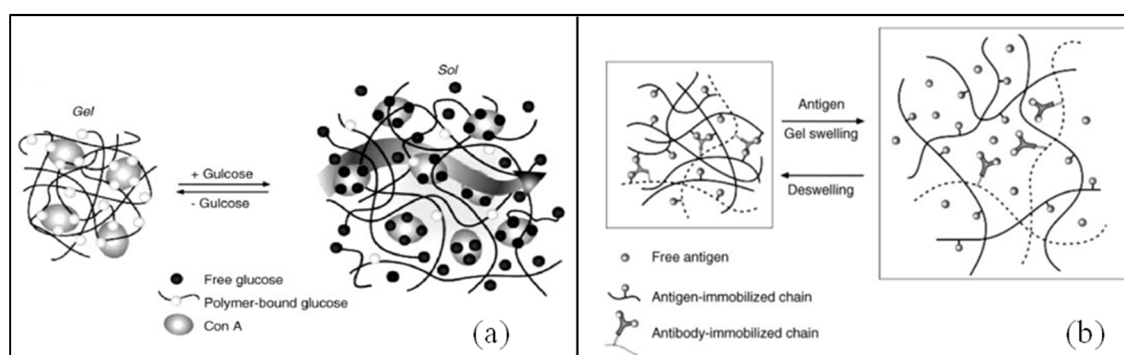


Figure 1.26. Swelling of microgel is dependent on glucose concentration due to use of ConA as a crosslinker (a) or dependent on antigen presence, as a consequence of antibody and antigen immobilised chains (b). (Figures reproduced from (J. J. Kim & Park, 2001) (a) and (Fernandez-Nieves et al., 2011) (b).

1.4.2.4 Triggered Release by Degradation

Microgels can be triggered to degrade by other mechanisms. Use of this mechanism was implemented in coating microgels with a shell impermeable to the drug. Kiser et al. coated microgels with lipids. Disruption of the shell by electroporation, membrane-active peptides or surfactants, led to swelling of the gel and thus drug release (Figure 1.27) (Kiser, Wilson, & Needham, 2000). De Geest et al. designed microgels surrounded by multilayers of polyelectrolytes. The inner dextran-based microgels swelled pH-dependently and at some point led to disruption of the membrane (De Geest et al., 2007).

Another possibility is to use microgels which are crosslinked with disulfide bonds. Chemical reduction of those bonds weakens polymer interactions and swelling follows (Bromberg, Temchenko, Alakhov, & Hatton, 2005; Oh, Siegwart, & Matyjaszewski, 2007).

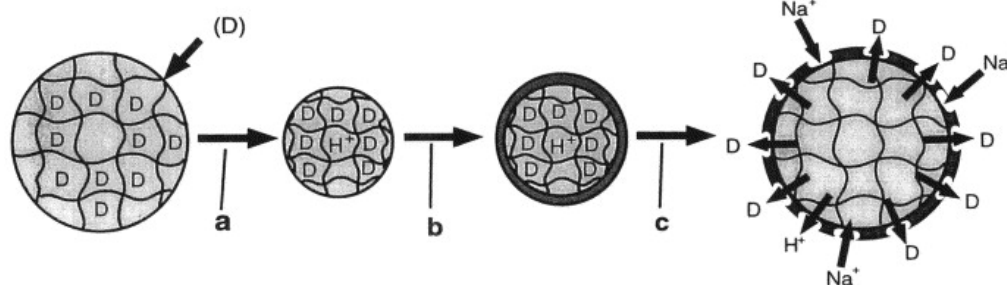


Figure 1.27. Loading of the microgel in the swollen state. In more acid conditions the microgel was condensed and coated with a lipid layer. Disruption of this layer, leads to swelling of the microgel and hence drug release. (Figure reproduced from (Kiser et al., 2000)).

1.5 Oral Delivery of Enzymes

Oral enzyme therapy aims at supplying the organism with enzymes which are either produced in insufficient amounts (lactose intolerance, exocrine pancreatic insufficiency etc.) or with the aim of degrading potentially harmful food components in situ (phenylketonuria, celiac disease etc.). The use of therapeutic proteins has increased in the last decades and revolutionized the pharmaceutical world. Nowadays there are more than 400 biopharmaceutical in advanced clinical trials and more than 40 protein drugs available on the market (Pawar et al., 2014). However, most therapeutic proteins are administered via the parenteral route (Gupta et al., 2013). Native enzyme delivery to the gastrointestinal (GI) tract has often proved very difficult, or only effective at high enzyme doses, due to enzyme inactivation on its delivery path (Fuhrmann & Leroux, 2014).

The first digestion point of the protein is in the stomach, where the acidic pH unfolds, and thus inactivates, the proteins and in addition to the hydrolysis produced by the presence of pepsin. Further down in the digestive track, in the small intestine, the therapeutic enzyme may be inactivated by pancreatic peptidases or intestinal bile salts.

Several reviews refer to the different manners of protecting orally administered enzymes (Fuhrmann & Leroux, 2014; Gupta et al., 2013; Pawar et al., 2014; Pereira de Sousa & Bernkop-Schnürch, 2014) and the main ones are summarised in Figure 1.28.

An approach to overcome those inactivations during passage through the GI tract may be to use enzymes which were bioengineered to resist those stress conditions. For the case of β -galactosidase O'Connell and Walsh isolated β -galactosidases from *Kluyveromyces marxianus* DSM 5418 (stable under neutral conditions) and from *Aspergillus niger* van Tiegh (stable under acidic conditions) to achieve a more effective hydrolysis of lactase in the GI tract (S O'Connell & Walsh, 2007; Shane O'Connell & Walsh, 2010).

Another option is to conjugate the enzymes to polymers in order to shield the enzyme from endogenous proteins and offer increased stability to the enzyme. Turner et al. modified β -galactosidase chemically with branched 40-kDa PEG, which created a zone of steric hindrance around the enzyme. The conjugate achieved higher stability at acidic pH and in simulated gastric fluids containing pepsin (K. M. Turner, Pasut, Veronese, Boyce, & Walsh, 2011). A third way of protecting the enzyme is to encapsulate it into gastro resistant polymers (enteric coating), which dissolve only in the higher pH environment of the small intestine or protect it by other mechanisms. Further details on those immobilisation techniques are detailed in the next section.

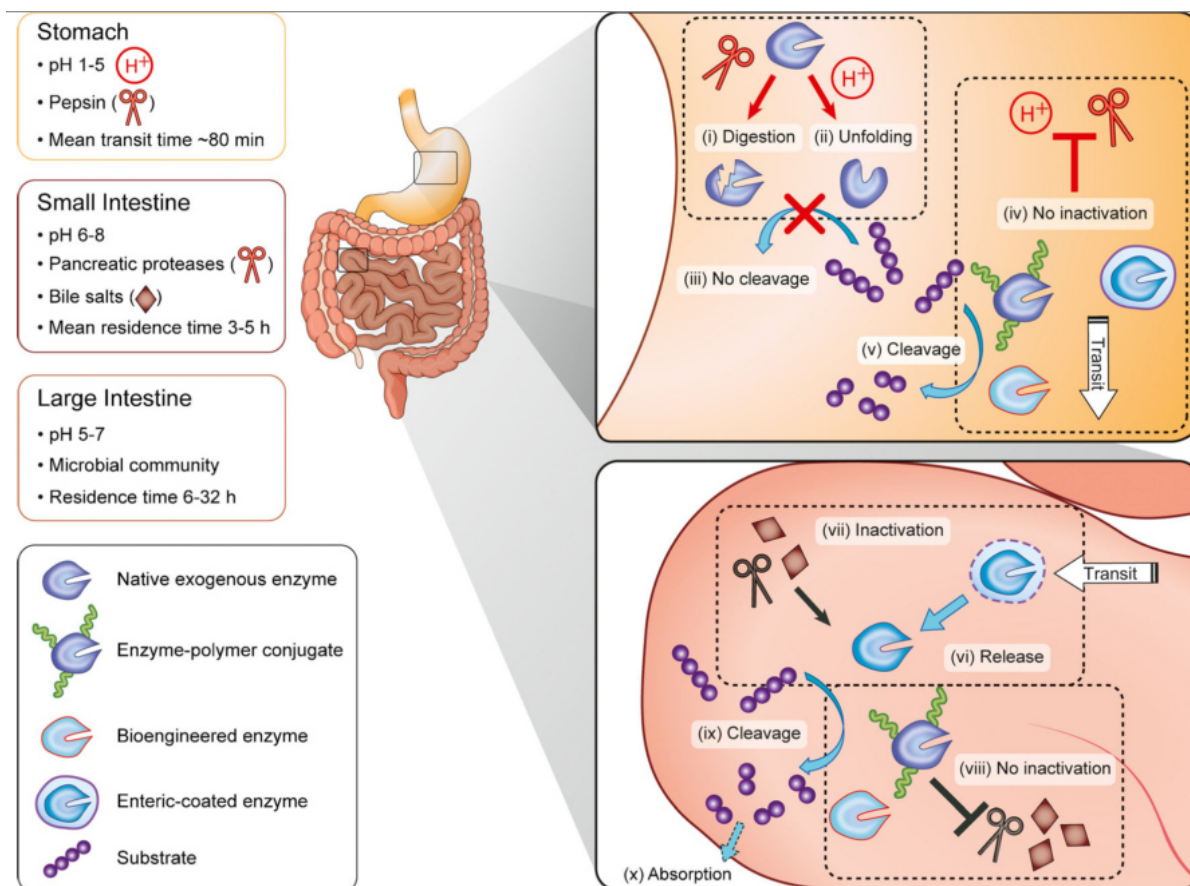


Figure 1.28. Fate of native or modified enzyme during path through GI tract. Enteric coated formulations provide enzyme protection only in the stomach, in contrast to bioengineered enzymes or enzyme-polymer conjugates. (Figure reproduced from (Fuhrmann & Leroux, 2014)).

1.6 Immobilisation of Enzymes

Enzymes can be immobilized into matrices over three different manners: adsorption, covalent attachment and entrapment (Husain, 2010).

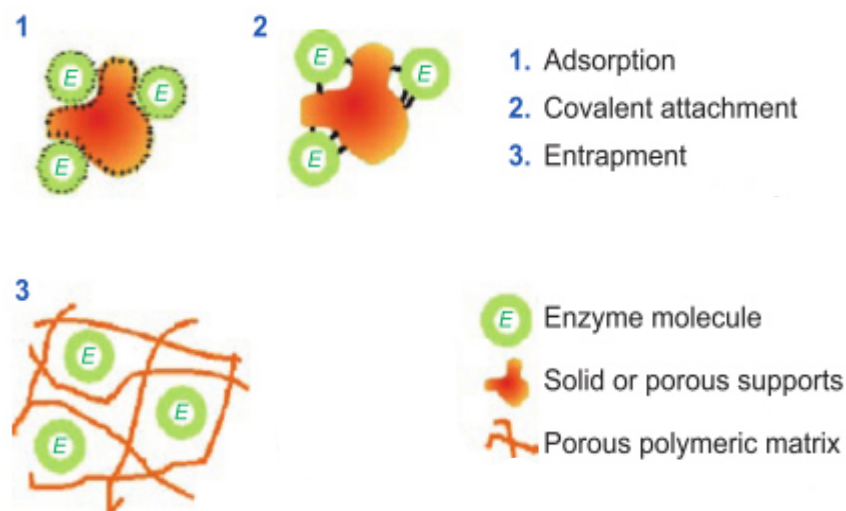


Figure 1.29. Methods of enzyme immobilisation (Figure adapted from (Husain, 2010))

Adsorption: This method is based on the physical adsorption of the enzyme through electrostatic or hydrophobic interactions on the surface of the carriers. The soft conditions, no reagents or activation steps are needed, lead to few or no conformational change of the enzyme nor to destruction of its active site. This method is simple and cheap, however desorption of the enzyme from the carrier may be easily induced by physicochemical changes, especially pH, ionic strength and temperature, in the environment. (Schachschal et al., 2011; Welsch, Becker, Dzubiella, & Ballauff, 2012).

Covalent attachment: Chemical bonding of enzymes to matrices is a permanent method of immobilization. The wide range of choice of carrier materials and methods, allows flexibility in tuning physical and chemical properties of the system. In contrast to enzyme adsorption this method is more expensive, and may lead to lower activity yields and modification of the enzyme active site.

Enzyme entrapment: Physical entrapment occurs if the enzyme is trapped into the lattices of a polymeric network or gel, by either forming a gel in the presence of the enzyme or by dispersing the enzyme in a gel solution. The former method may denature proteins due to impurities or exposure to air or organic solvents during gel formation. In the latter approach, enzymes may not enter the gel or only stay at the surface due to size exclusion (Jin et al., 2008; Y. Zhang, Zhu, Wang, & Ding, 2005).

Immobilisation of enzymes has the advantage of being able to reuse enzymes several times, which is of importance due to the high costs of those proteins. Furthermore, immobilization allows to protect the enzymes against various denaturing factors such as extreme pH, temperature, high ionic strength, chemical denaturants, proteases etc. and increase thus its activity.

1.6.1 Immobilisation of Enzymes into Microgels

Encapsulation of the enzymes into hydrogels or microgels is particularly attractive for application in the food and pharmaceutical industry, as the gels can be fabricated from food-grade material, are generally hydrophilic and the main component is water, which allows the enzymes to be incorporated with only moderate conformational changes and limited aggregation (Bysell et al., 2011; Fernandez-Nieves et al., 2011). The matrices are often designed to contain pores, allowing the substrates or products to move freely into and out of the matrix. For acid-sensitive enzymes (such as lactase), this however presents a problem. Protons can as well easily diffuse into the biopolymer network, thereby inducing enzyme deactivation. To improve acid-resistance of the hydrogel, a number of research groups have or reduced the pore size of the biopolymer network, coated the beads with biopolymer layers (Srivastava, Brown, Zhu, & McShane, 2005; Taqieddin & Amiji, 2004) or co-encapsulated the enzyme with a basic buffer to create an internal pH microenvironment (Z. Zhang, Zhang, & McClements, 2017).

Table 1.5 presents some examples of microgels into which enzymes have been encapsulated.

Table 1.5. Some examples of enzyme-loaded microgels, indicating the polymer, the encapsulated enzyme, the method of formation and applications.

| Polymers | Enzyme | Encapsulation | Release | Comments | Reference |
|---|------------------------|--|--|---|---------------------------------------|
| Copolymer of Pluronic F127 and lactic acid | Insulin | Incorporation into swollen microgel at 4°C (lyophilisation deswells the gel, keeps enzyme entrapped) | Biodegradation of microgel and diffusion of enzyme | Release over a period of some days | (Y. Zhang et al., 2005) |
| Oxidised Starch | Lysozyme | Dispersing enzyme into microgel solution | Triggered by changing pH (release at pH 8, none at pH 3) and salt concentration. Enzymatic degradation of the gel by α -amylase | Release within 20-30 min | (Y. Li et al., 2011) |
| Oxidised Starch covered by PLL/PGA complex layer | Lysozyme | Dispersing enzyme into microgel solution | Triggered by changing pH (release at pH 8, none at pH 3) and salt concentration | Release within more than 50 min | (Y. Li, Norde, & Kleijn, 2012) |
| PNIPAm | β -D-Glucosidase | Adsorption and penetration into network at swollen state. Hydrophobic interaction immobilize enzyme. | Substrate enters microgel and enzymatic activity takes place inside microgel | Activity of immobilized enzyme higher by a factor of 3 compared to free enzyme | (Welsch, Wittemann, & Ballauff, 2009) |
| Poly(N-isopropylacrylamide-co-acrylic acid) network | Lysozyme | Dispersing enzyme with microgels during 15 h and removing unbound enzyme through ultrafiltration | Substrate enters microgel and enzymatic activity takes place inside microgel | The activity in the bound state is enhanced and corresponds to the activity of lysozyme in the protonated state at its pH optimum | (Welsch et al., 2012) |
| PNIPAm /Acrylic acid Copolymer | β -Galactosidase | Enzyme entrapped during inverse suspension polymerization in W/O system | Substrate enters microgel and enzymatic activity takes place inside microgel | Enzyme activity can be modulated by swelling/deswelling of hydrogel beads at different temperatures | (Park & Hoffman, 1990) |
| PNIPAm | Laccase | Polymerisation of aqueous droplets (containing enzyme) in water/oil inverse emulsion | Substrate enters microgel and enzymatic activity takes place inside microgel | Deswelling between 30-40 °C | (Schachschal et al., 2011) |
| Copolymer of PNIPAm and N-vinylimidazole | Urease | Physical entrapping. Aqueous redox polymerization performed in presence of enzyme | Substrate enters microgel and enzymatic activity takes place inside microgel | Urease catalyses the hydrolysis of urea into ammonia and carbon dioxide, leading to pH change and subsequent swelling of microgel | (Ogawa, Wang, & Kokufuta, 2001) |

1.6.2 Immobilisation of Lactase for Oral Delivery

An in-depth overview of existing immobilisation methods for β -Gal can be found in following two reviews (Grosová, Rosenberg, & Rebroš, 2008; Husain, 2010). β -Gal were mostly immobilised in bigger matrices, such as large beads, fibers or bulk gels with the aim of application in food industry and industrial hydrolysis of lactose. Therefore a vast range of food-grade biopolymers, such as alginate (Fujikawa, Yokota, & Koga, 1988; Mai, Tran, & Le, 2013; Taqieddin & Amiji, 2004), chitosan (Klein et al., 2016; Taqieddin & Amiji, 2004), gelatin (Tanriseven & Doğan, 2002) or κ -carrageenan (Z. Zhang, Zhang, Chen, & McClements, 2016) were tested as matrices.

Only few studies focused on encapsulating lactase with the aim of using it as an oral delivery system. Thereby, researchers formulated either sustained release microparticles for the delivery of lactase, or tried to improve acid-resistance of the carrier.

Jin et al. formulated an interesting delivery system by encapsulating lactase into 1-2 μm dextran microparticles, which were produced by dextran-in-PEG water-in-water emulsions. Those microparticles were encapsulated into PLG microspheres (by formulating a solid-in-oil-in-water emulsion), which conveyed a sustained release of the enzyme. However the acid released during PLG degradation denatured the enzyme (Jin et al., 2008).

In another sustained release system, spray-dried PLGA particles functionalized with β -galactosidase, were studied for different types of spacers and coupling methods. This resulted in prolonged release and increased binding to artificial human intestinal epithelium, however acid-resistance was not tested in this work (Ratzinger, Wang, Wirth, & Gabor, 2010).

Silica was as well tested as matrix, by entrapping the enzyme into a silica gel. This preserved its biofunctionality and improved enzyme activity at pH 7.4 and 37°C, compared to the free enzyme. Nevertheless the enzyme became deactivated at acidic pH (Nichele, Signoretto, & Ghedini, 2011).

Another approach to use lactase in functional food was performed by Nussinovitch et al.. They produced 4 mm-sized chocolate coated agarose-lactase-containing carriers, which showed increased stability in gastrointestinal conditions. Lactase activity remained high, after 2 h in simulated gastric conditions (Nussinovitch, Chapnik, Gal, & Froy, 2012).

Recently, another group achieved similar resistance to gastric conditions, by fabricating carrageenan-based hydrogel beads (200 μm and 2 mm), which contained lactase and a buffer ($\text{Mg}(\text{OH})_2$). The buffer kept the pH inside the beads fairly constant (pH 7.2 to pH 6.6) after exposure to stomach conditions. As a consequence lactase remained active inside those beads after passage through simulated stomach and intestine conditions (Z. Zhang et al., 2017).

1.7 Polymers used and their Mixtures

In this study, microgels on the basis of two W/W emulsion systems will be formed: Sodium carboxymethylcellulose (NaCMC)/ bovine serum albumin (BSA) and gelatin/maltodextrin emulsions. The characteristics of those polymers and their gelling/crosslinking properties will be discussed next.

1.7.1 Sodium Carboxymethylcellulose

Cellulose is the most common organic polymer in nature, with one-third the world's vegetative material consisting of it. An issue is however its water insolubility, caused by partial hydrophobic properties and crystalline domains (Medronho, Romano, Miguel, Stigsson, & Lindman, 2012)

Therefore soluble derivatives have been developed, such as sodium carboxymethylcellulose (NaCMC). NaCMC, a semisynthetic polymer, is obtained from cellulose, by a carboxymethylation process. The polymer consist of linear chains containing β (1 \rightarrow 4)-linked glucopyranose residues (Figure 1.30).

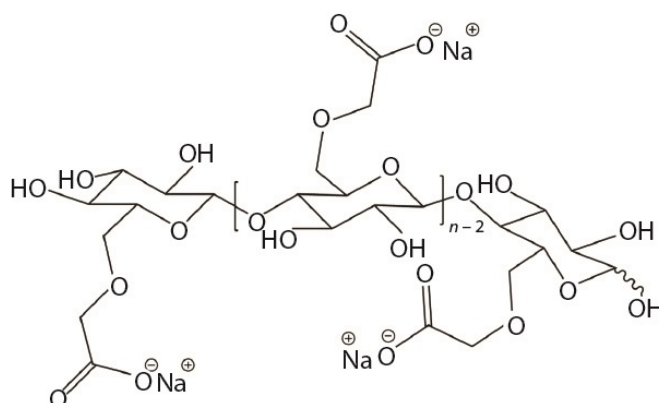


Figure 1.30. Molecular structure of Sodium Carboxymethylcellulose (NaCMC). Reproduced from (Frei-Rutishauser, Muehlenfeld, Watson, & Warnke, 2016),

Due to its high biocompatibility, biodegradability, and low immunogenicity it has found application in a big variety of food and pharmaceutical applications (C. Chang & Zhang, 2011; Qiu & Hu, 2013). Its carboxylic residues make it of interest for pH-sensitive drug delivery applications. NaCMC has a pKa of 4.3. This polymer thus shrinks at acidic pH and swells when exposed to neutral or basic pH, due to deprotonation of the carboxylic groups, leading to electrostatic repulsion within the polymer network (Agarwal et al., 2015; M. S. Kim, Park, Gu, & Kim, 2012; Y. Zhang et al., 2014). At low pH, the sodium in NaCMC is replaced with hydrogen, which promotes hydrogen bonding within the polymer. The hydrogen bonds induce a decrease of polymer solubility in water and result in the formation of an elastic hydrogel (Patil, Marapur, Gurav, & Banagar, 2015). Moreover, the carboxylic groups can interact with multivalent metal ions, to form ionotropic gels, which are stabilised by electrostatic interactions between the polymer and the ions (Figure 1.31). Those gels can be formed by crosslinking with for example ferric or aluminium salts, as shown in previous studies (S. S. Bhattacharya, Ghosh, Banerjee, Chattopadhyay, & Ghosh, 2012; M. S. Kim et al., 2012; Sungur, 1999; Xiao, Li, & Gao, 2009).

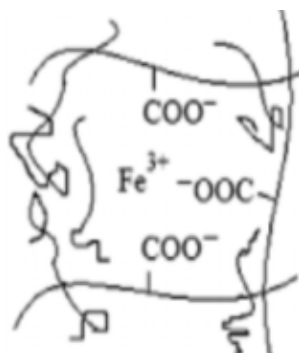


Figure 1.31. Crosslinking mechanism of NaCMC with trivalent ion, such as iron. Figure adapted from (Xiao et al., 2009).

Due to its pH sensitive properties NaCMC is of interest for oral delivery and has already been tested as delivery vehicle for enzymes. Mai et al. formulated lactase into combined alginate–carboxymethyl cellulose gel beads and showed increased protection of the enzyme under unfavourable pH conditions (Mai et al., 2013).

1.7.2 Bovine Serum Albumin

Albumin is the most abundant plasma protein in human blood (35–50 g/L human serum), and it serves as the primary carrier of solutes in the plasma. In the native state, BSA has three domains, each one formed by six helices, and its secondary structure is α -helical. The isoelectric point of the 66 kDa protein is around 5, while at pH = 7 BSA has around 10 effective negative charges per protein molecule (Navarra et al., 2009).

Bovine serum albumin is the serum albumin protein derived from cows, which can be readily purified from bovine blood. It is often used in biochemistry as protein standard in protein concentration assays, as nutrient in cell and microbial culture, or to prevent adhesion of enzymes to reaction tubes. Due to its low cost and easy determination of concentration, it is often used as model protein in drug delivery applications. However, it is less commonly used directly as a drug delivery vehicle in form of a gel. Albumin hydrogels can be formed by thermal denaturation, chemical crosslinking, polymer–albumin conjugates or by electrostatically triggered albumin self-assembly through pH changes or ions (Baler, Michael, Szleifer, & Ameer, 2014; Navarra et al., 2009; Oss-Ronen & Seliktar, 2010; Rubino, Kowalsky, & Swarbrick, 1993).

1.7.3 NaCMC/BSA Emulsions

The aim is to obtain NaCMC microgels, from a W/W emulsion template. Thus, a biopolymer was searched for, which shows incompatibility with NaCMC and thus allows to form emulsions. Grinberg et al. investigated close to 100 polysaccharide/protein mixtures and identified several proteins, which showed incompatibilities with NaCMC: soybean globulin, casein, edestin, zein, gliadin, gluten and

albumin (Grinberg & Tolstoguzov, 1997). The incompatibilities were shown to occur at basic pH, above pH 9. Under those pH conditions, the proteins have a negative charge, similar to NaCMC.

NaCMC has often been used as material for drug delivery vehicles (Kamel, Ali, Jahangir, Shah, & El-Gendy, 2008; Kamide & Kamide, 2005), however only one study was found, in which NaCMC was applied in a W/W emulsion. Singh et al. entrapped probiotic bacteria, *Lactobacillus rhamnosus* GG, into the NaCMC aqueous phase of NaCMC/gelatin emulsions (Singh, Medronho, Miguel, & Esquena, 2018). Most other studies formed interpenetrating networks or complexes between NaCMC and other polymers (Agarwal et al., 2015; Banerjee, Singh, Bhattacharya, & Chattopadhyay, 2013; S. S. Bhattacharya et al., 2012, 2013; M. S. Kim et al., 2012; Lohani, Singh, Bhattacharya, Rama Hegde, & Verma, 2016).

In this study we chose to test the formation of emulsions from NaCMC and BSA mixtures, due to its known properties and frequent use of BSA as a model protein in research.

1.7.4 Gelatin

Gelatin is derived from collagen, which is the primary constituent of all mammalian flesh and connective tissues (such as skin, muscle, bones, cartilage etc.). Collagen, usually derived from pigs, cows, fish and rats, but also insects (Mariod & Adam, 2013) exists in nature as a macromolecule of three polypeptide strands, 300 nm long. It has a triple helix conformation, and a molecular weight of around 100 kDa (Madeleine Djabourov, 1988). Two types of gelatin can be obtained, depending on the form of hydrolytic degradation of the collagen. Type A gelatin is isolated through an acid-based process, while Type B gelatin under alkaline conditions. The hydrolysis of collagen leads to separation of the triple helix into the three polypeptide strands that compose gelatin. Basic (lime) treatment leads to a lower pI, compared to Type A gelatin, produced by acid treatment. Moreover, hydrolysis time affects gelatin molecular weight, solution viscosity and gel viscoelastic response (bloom strength) (Mariod & Adam, 2013; P. A. Turner, Thiele, & Stegemann, 2017). One of the major physicochemical properties of gelatin is its ability to form a thermo-reversible gel in the concentration range of approximately 1-50 wt% (below 1 wt% there are not sufficient molecules in order to support a gel network) (Madeleine Djabourov, 1988). At high temperatures (> 50°C) gelatin prevails mainly as dispersed monomers. When cooling down, the monomers aggregate by hydrogen bonding into oligomers, which propagate through the liquid in a random coil conformation. Those disordered coils go over to ordered helices at lower temperatures, due to increased intra-oligomer hydrogen bonding. Finally, gelation occurs, induced by a crossover from single to triple helices. Over time, the helices reorganise themselves into a big interconnected macromolecular network, with triple helices forming the junctions that bind the gel network and provide its elasticity and strength (Parker & Povey, 2012) (Figure 1.32). As the entire sol-gel transition process is driven by weak interactions, the gelation is thermo-reversible.

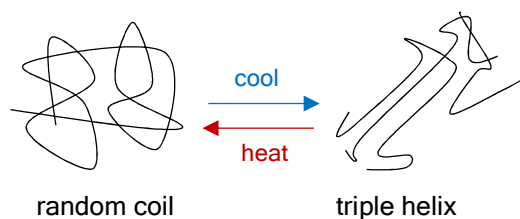


Figure 1.32. Coil to helix transition of gelatin during temperature changes.

Gelatin is mostly known for its use in food, where it acts amongst others as gel former, stabiliser (yoghurt), thickener (jam), whipping agent (marshmallows), texturizer or emulsifier (sauces) (Mariod & Adam, 2013). Gelatin is furthermore an ideal candidate for biomedical applications, as it is biocompatible, non-toxic, non-immunogenic, biodegradable and has cell-adhesive peptide sequences. Furthermore, it is cheap and readily available. Its first documented use in biomedicine dates back to 1945, as a hemostatic substance (Jenkins & Clarke, 1945). Since then, it has also been utilised for surgical glues, sealants, wound dressings and as drug delivery vehicle (Kirchmajer, Watson, Ranson, & Panhuis, 2013; P. A. Turner et al., 2017).

It has however to be noted, that unmodified gelatin hydrogels are water-soluble, turn liquid at body temperature and are mechanically weak. Therefore, generally, they are subject to some physical or chemical crosslinking processes.

The many functional groups in the amino acids of gelatin can be used as reaction points for chemical crosslinking. Examples of crosslinkers used are formaldehyde, glutaraldehyde, polyepoxy compounds, tannic acid, carbodiimides, diisocyanates and acyl azide (Apostolov, Boneva, Vassileva, Mark, & Fakirov, 2000; Bigi, Cojazzi, Panzavolta, Roveri, & Rubini, 2002; Olde Damink et al., 1995; Rault, Frei, Herbage, Abdul-Malak, & Huc, 1996). The most widely used crosslinker is glutaraldehyde, which is easily available, cheap and the crosslinking procedure is rapid and simple. However, this and all aforementioned chemical crosslinkers are relatively cytotoxic and bare thus risks in biomedical applications, which led to the search to new and less toxic compounds. Genipin, a naturally occurring crosslinking agent, first proposed as an alternative in 1999, demonstrated higher biocompatibility and 10,000 times lower toxicity than glutaraldehyde (Sung, Huang, Huang, & Tsai, 1999), while conveying to the material improved mechanical properties and resistance against enzymatic degradation.

Other methods for crosslinking gelatin include thermal treatment or exposure to gamma or ultraviolet radiation. Those methods have the advantage to not cause potential harm, however control of crosslinking amount is difficult (Yao, Liu, Chang, Hsu, & Chen, 2004).

Therefore, genipin is often used as a mild alternative to other methods for crosslinking gelatin. However, the properties and chemistry of genipin are not often well described, and next section is devoted to explain the use of genipin as a crosslinker.

1.7.5 Genipin

Genipin is obtained from geniposide, an iridiod glucoside, via enzymatic hydrolysis with β -glucosidase. Geniposide is mainly extracted from the fruits of *Gardenia jasminoides* Ellis, which can be found in South china, Taiwan, Vietnam and Japan. It can also be found in the fruits of genipap (*Genipa americana* Linnaeus), widely distributed in Central America and in the north of Brazil, *Castilleja tenuiflora*, *Bellardia trixago*, and *Eucommia ulmoides*, and as well in the leaves and stems of *Tocoyena formosa* and *Randia spinose* (Bellé et al., 2018).



Figure 1.33. Pictures of the *Gardenia jasminoides* Ellis flowers (a) and fruits (b). Geniposide (c) can be extracted from the plant and from it is produced its aglycone Genipin (d). Pictures from web (Itmonline.org, 2003; Logees.com, 2018).

Genipin has been widely used as an anti-inflammatory (Koo, Lim, Jung, & Park, 2006) and choleric (increase the volume of secretion of bile) (Akao, Kobashi, & Aburada, 1994) in herbal medicine. Moreover, the molecule can react with amino acids or proteins to form blue pigments, applied for example in the fabrication of food dyes (Touyama et al., 1994). It generates not only colour after the crosslinking reaction, but also fluorescence at 630 nm when excited at 590 nm (Almog, Cohen, Azoury, & Hahn, 2004). Additionally its capability to form crosslinked products, which are more stable against enzymatic degradation led to its use in bioadhesives (Sung, Huang, Chang, Huang, & Hsu, 1999), nerve guiding conduits (Chen et al., 2005), wound dressings (W.-H. Chang, Chang, Lai, & Sung, 2003), cartilage scaffolds (Lien, Li, & Huang, 2008) and in various drug delivery applications. It was mainly used to crosslink collagen, gelatin, proteins and chitosan. Table 1.6 summarises drug delivery applications of genipin-crosslinked gelatin microparticles and gelatin microparticles formed by W/W emulsions.

Table 1.6. Recent drug delivery applications of gelatin microgels/microspheres, either crosslinked with genipin or produced by water-in-water emulsion techniques.

| Preparation Method | Crosslinker | Size | Applications | Reference |
|---|---------------------------|--|---|--|
| W/W Emulsions | | | | |
| Gelatin/PEG | Glutaraldehyde | 25-45 μm | Influence of composition on size | (Kong, Li, Wang, & Adhikari, 2011) |
| Gelatin/Starch | - | “Fractal-type particle gel” | Analyse aggregation of microgel particles into fractal-type gel at cooling from 40-24°C | (Firoozmand, et al. 2007) |
| Gelatin/Poly(vinylpyrrolidone) and Gelatin/Dextran | - | 5-10 μm | Analysis of morphology First study reporting gel particle formation without surfactant/organic solvent | (Franssen & Hennink, 1998) |
| W/O Emulsions (Water Phase: Gelatin) | | | | |
| Oil: PDMS | Genipin | 15-60 μm | Local delivery of growth factors (VEGF/BMP2) | (P. A. Turner et al., 2017) |
| Oil: PDMS Surfactant: Pluronic L101 | Genipin | 2-6 μm | Local delivery of bone morphogenetic protein 2 to cells | (Solorio, Zwolinski, Lund, Farrell, & Jan, 2011) |
| Water: Phase-separated Maltodextrin-Gelatin mixture Oil: Canola Oil Surfactant: Span 85 | Genipin | 37-70 μm | Oral Delivery of Bifidobacterium adolescentis (Maltodextrin used as probiotic) | (Borza et al., 2010) |
| Oil: Sunflower seed oil | Genipin | 130- 580 μm | Microfluidic production of very uniformly sized, 5-FU-loaded, microcapsules | (Huang et al., 2009) |
| Oil: Corn Oil Surfactant: Span 85 | Genipin | 50-100 μm | Oral delivery of Bifidobacterium lactis Bb-12 | (Annan, Borza, Moreau, Allan-Wojtas, & Hansen, 2007) |
| Oil: Corn oil | Genipin or Glutaraldehyde | 20-100 μm | Physical, chemical and biological evaluation as intramuscular delivery vehicle. | (H.-C. Liang, Chang, Lin, & Sung, 2003) |
| Other | | | | |
| Porous CaCO ₃ template | Genipin | 5-10 μm | pH Sensitive release of Rhodamine B Doxorubicin | (A. Wang, Cui, Li, & Van Hest, 2012) |
| O/W/O Double Emulsion Oil: Ethyl acetate and edible oil | Genipin | 75-160 μm and 200-300 μm | Microcarrier of human fetal osteoblasts | (Lau, Wang, & Wang, 2010) |

1.7.6 Crosslinking Mechanism:

Two distinct mechanisms for reaction of genipin with biopolymers containing primary amine groups, such as gelatin, have been proposed (Michael F. Butler, Ng, & Pudney, 2003; F. Mi, Sung, & Shyu, 2000). In proteins, those amine groups are mainly originating from the lysine or arginine residues.

The first reaction, which takes place rapidly, is a nucleophilic attack of the genipin C3 carbon atom by a primary amine group to form an intermediate aldehyde group. Next, the secondary amine formed reacts with the aldehyde group to form a heterocyclic compound of genipin linked to the primary amine groups of the biopolymer (Figure 1.34 a).

The reaction taking place next, and which is slower, involves a S_N2 nucleophilic substitution that replaces the genipin ester by a secondary amide linkage with the biopolymer, releasing methanol into the solution (Figure 1.34 b).

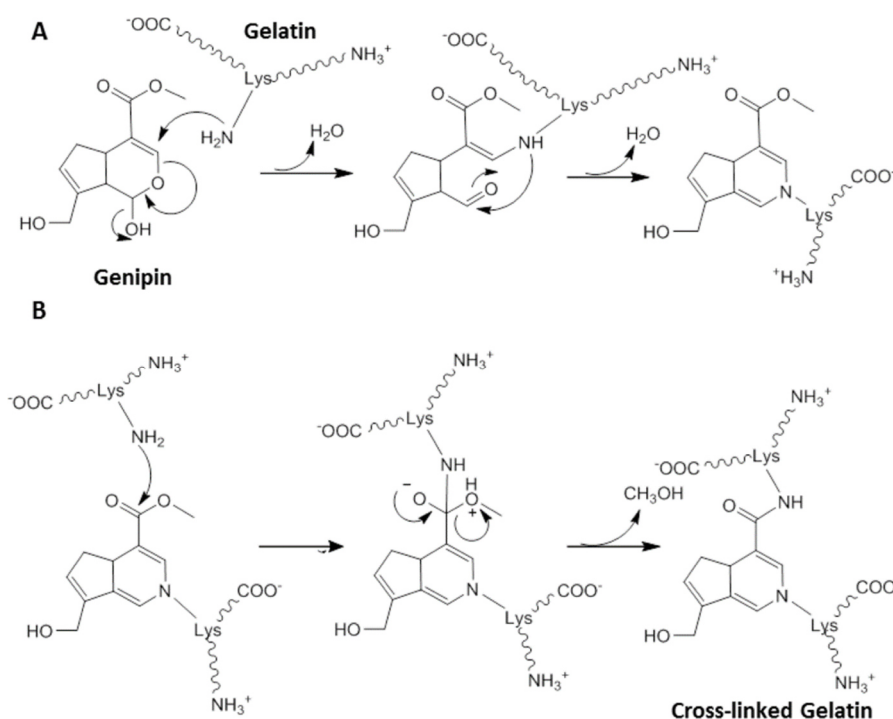


Figure 1.34. The crosslinking reaction of genipin is composed of two reactions: (A) First, there is a nucleophilic attack with a molecule containing a primary amine group (gelatin in this case). (B) Next, a S_N2 nucleophilic substitution takes place, between genipin and another primary amine group. Figure reproduced from (Rose et al., 2014)

More complex structures have been suggested in other studies, involving dimeric (F.-L. Mi, Shyu, & Peng, 2005; Sundararaghavan et al., 2008; L. Wang et al., 2013), trimeric (F.-L. Mi et al., 2005) and tetrameric (F.-L. Mi et al., 2005) genipin crosslinks. Those crosslinking structures are summarised in Figure 1.35.

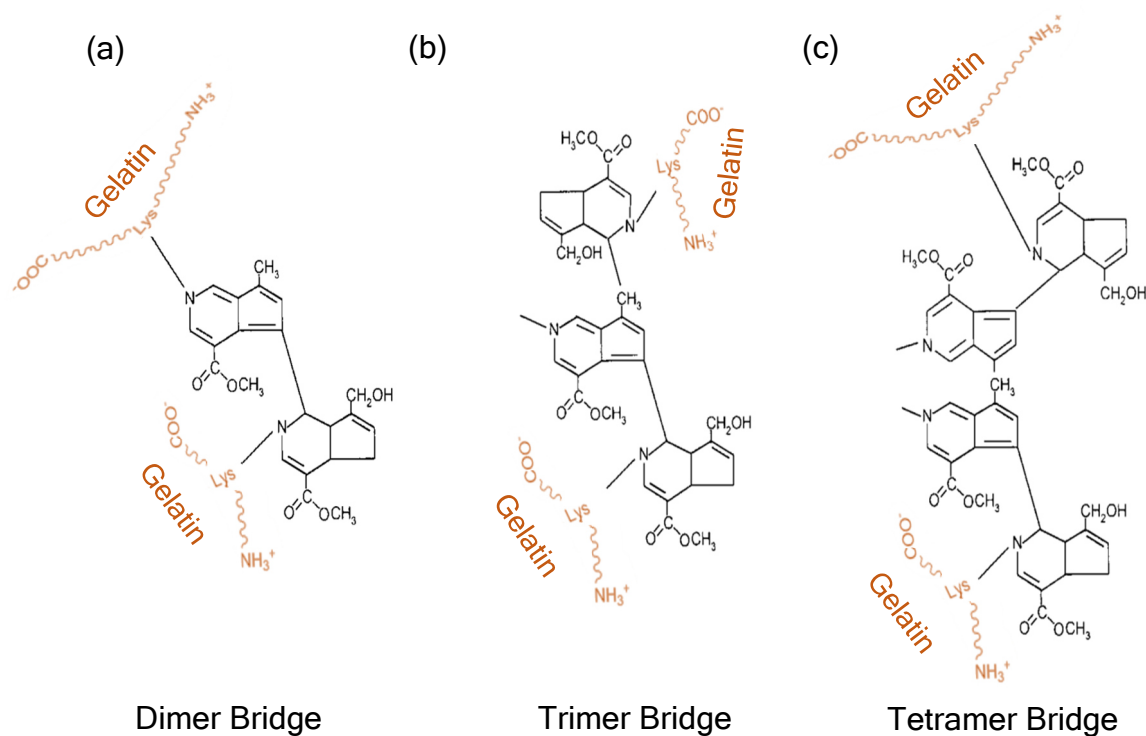


Figure 1.35 .Crosslinking mechanisms of gelatin by dimeric (a), trimeric (b) or tetrameric (c) genipin bridges. (adapted from (F. Mi et al., 2000))

Furthermore, a secondary reaction has been described, which leads to formation of blue colour, studied in details by Touyama and coworkers (Touyama et al., 1994). Its origin are the oxygen radical-induced polymerization of genipin and dehydrogenation of intermediate compounds, following the first crosslinking reaction (formation of the heterocyclic genipin compound). This hypothesis was supported by a study which observed, that the blue coloration was initially more pronounced at the gel-air interface of the samples, where more oxygen radicals are present, and then with time continuously moved down through the sample (Michael F. Butler et al., 2003). As the formation of blue pigment requires the nucleophilic attack of the amine on genipin to happen, the blue colour development in the sample is indicative for the crosslinking reaction to take place. Butler and coworkers followed the UV spectrum of chitosan (1.5 % (w/v)) crosslinked by 1 mM genipin at 20°C and observed the gradual increase of the peak at 605 nm, indicative for the blue colour, but also an increase of the peak at 240 nm (max. absorbance of genipin monomer) and 280 nm (Michael F. Butler et al., 2003) (Figure 1.36). The increase at 280 nm, also observed in other studies (Vilchez, Samitier, Porrás, Esquena, & Erra, 2009), was attributed to the formation of a heterocyclic amino compounds (F. Mi et al., 2000).

The reactivity of genipin has been shown to be pH dependent and undergoes spontaneous polymerization at basic pH (Kirchmajer et al., 2013; F.-L. Mi et al., 2005).

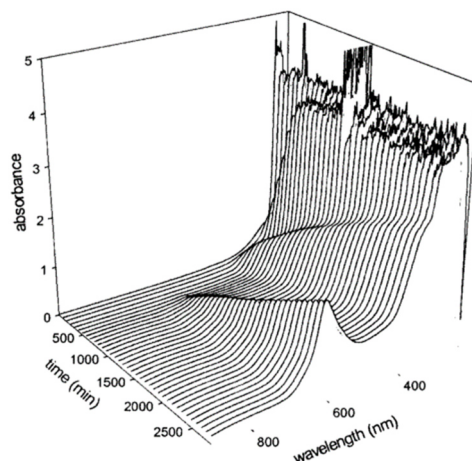


Figure 1.36. Evolution of the UV-vis spectrum of chitosan after mixing with genipin. Figure reproduced from (Michael F. Butler et al., 2003).

From the reaction mechanism it gets clear, that for molecules with secondary and tertiary structures, such as proteins, the amine groups (lysine or arginine residues), must be on the outside surface of the molecule, in order crosslinking can be effective. (Michael F. Butler et al., 2003). For more in-depth reading on physical, chemical and biological properties of genipin-crosslinked gelatin gels and the crosslinking process, a series of reviews and studies are recommended (Bigi et al., 2002; Michael F. Butler et al., 2003; Kirchmajer et al., 2013; Nickerson, Farnworth, et al., 2006; Nickerson, Patel, Heyd, Rousseau, & Paulson, 2006; Yao et al., 2004).

1.7.7 Maltodextrin

Maltodextrin, a neutral polysaccharide, can be obtained by hydrolysis of starch (originating from e.g. maize, oats, rice, tapioca, potato etc.) by means of heat and acid, specific enzymatic treatments or combined acid and enzyme hydrolysis. The hydrolysed products of starch mainly consist of D-glucose, maltose, and a series of oligo- and polysaccharides. Those hydrolysates are described in terms of their dextrose equivalent (DE) value, which is defined as the total number of reducing sugars relative to a glucose baseline of 100 and is expressed on a dry-weight basis. Hydrolysates with DE 100 are glucose (dextrose), between 20-100 are corn syrups, between 0-20 maltodextrins and 0 is starch. A DE of 5 corresponds to a polymeric species of 20 glucose molecules (degree of polymerisation of 20).

Maltodextrins contain linear amylose in a broad range of molecular weights and branched amylopectin degradation products (Figure 1.37). Amylose consists of individual α -D-glucopyranosyl residues, joined by α -(1 \rightarrow 4)-glycosidic linkages to give linear chains, and if they are branched by α -(1 \rightarrow 6)-linkages, they form amylopectin.

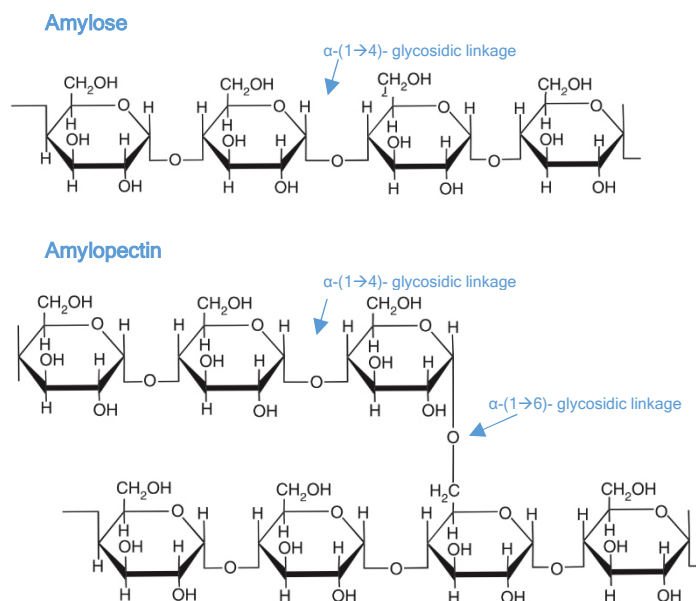


Figure 1.37. Molecular structures of amylose and amylopectin (Figure adapted from (Pich & Adler, 2007))

Maltodextrins have large amount of polymeric chains, which reduce solubility and promote gelation (Chronakis, 1998; Loret, Meunier, Frith, & Fryer, 2004). Gelation is explained by the high concentration of helical amylose segments, which aggregate with the branched and linear chains of amylopectin molecules, forming crystalline structures (Chronakis, 1998). The exact mechanism is explained elsewhere (Chronakis, 1998; Loret et al., 2004) and it has to be noted that not all maltodextrins gel, especially depending on the origin of the starch and the pattern of amylopectin branching within the sugar (Kasapis, Morris, Norton, & Clark, 1993a). Gelation happens especially at lower temperatures, and did not occur in the conditions of our experiments and with the maltodextrin (DE 4-7) we used.

Due to its gelation characteristics and biocompatibility, maltodextrin have been used since the 1980s frequently in the food industry, especially as a fat replacement, but also for bulking, crystallization prevention, promotion of dispersibility, freezing control, and binding (Chronakis, 1998). Furthermore it has been used as a prebiotic, as nutrient that stimulates the growth of bacteria, such as bifidobacteria (Borza et al., 2010).

A concern when using aqueous maltodextrin solutions is the precipitation. Lower dextrose equivalents and lower temperature favour precipitation of maltodextrin, while acidic pH (pH 3-3.5) provided a stabilisation effect of the polysaccharide in solution (Kennedy, Noy, Stead, & White, 1986). It was suggested that the precipitation of particles sized around 2 μm , arises through alignment of linear amylose molecules, via hydrogen bonding, leading to aggregates, which ultimately precipitate. Increased hydrolysis of maltodextrin by e.g. α -amylase (leading to higher DE products), reduces precipitation.

1.7.8 Gelatin/Maltodextrin Mixtures

Gelatin/Maltodextrin mixtures have been studied since 1993, when Kasapis and colleagues performed a systematic research work on the system (Kasapis, Morris, Norton, & Brown, 1993; Kasapis, Morris, Norton, & Gidley, 1993; Kasapis, Morris, Norton, & Clark, 1993a, 1993b). This polymer-polysaccharide mixture is thermodynamically incompatible and many parameters influence its phase behaviour. Using gelatin/maltodextrin emulsions as templates for microgel preparation have the great advantage that the gelatin phase, can be selectively gelled, forming thereby microgels, if it forms the dispersed phase. Cooling down and/or crosslinking amino groups, which are solely present in gelatin and not in maltodextrin, allows gelifying gelatin, while maltodextrin remains liquid.

In most past studies, polymer and solvent conditions were chosen, such that not only gelatin, but also maltodextrin gelled. Thus of great importance in this system is to analyse the competition of gel formation and phase separation kinetics, which has been the focus of a great number of works (Alevisopoulos & Kasapis, 1999; Alevisopoulos, Kasapis, & Abeysekera, 1996; Aymard, Williams, Clark, & Norton, 2000; Frith, 2010; Leisner, Blanco, & Quintela, 2002; N. Lorén et al., 2001; N Lorén, Langton, & Hermansson, 1999; Niklas Lorén & Hermansson, 2000; Lundin et al., 2000). In any case, one has to consider the gelation point of gelatin (approximately 30°C) and emulsions have to be formed above this temperature.

Cooling down a biopolymer mixture reduces the entropy of the system, and leads also to enthalpic interactions, namely ordering of the components. Those two factors shift the binodal line to lower concentrations, which was observed experimentally for a maltodextrin-in-gelatin emulsion (Figure 1.38). In the phase separation temperature versus maltodextrin concentration curve, at constant gelatin concentration, a clear change of slope appears at the gelatin gelation temperature T_{gel} (30 °C). At conditions above the gelation temperature, due to entropic reasons, increasing the temperature increases the minimum concentration needed to form two phases. Bulk phase separation is caused thereby by droplet coalescence. Droplet growth is modified and slowed if the temperature is quenched below T_{gel} , primarily due to restrictions imposed by the viscosity of the continuous phase (M. Williams, Fabri, & Hubbard, 2001). It was shown that maltodextrin droplet sizes decreased with increasing cooling rate (N Lorén et al., 1999; Niklas Lorén & Hermansson, 2000).

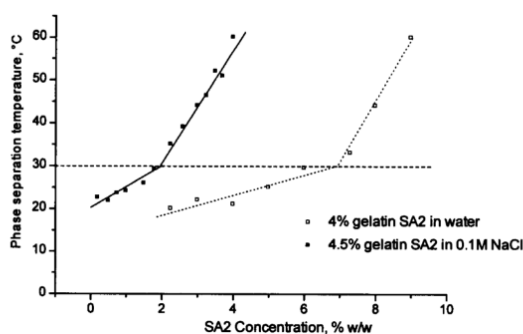


Figure 1.38. Phase separation temperature as a function of maltodextrin (SA2) concentration, for 4.5 % gelatin in 0.1 M NaCl and 4 % gelatin in water (Lundin et al., 2000)

At lower maltodextrin concentrations, for gelatin/maltodextrin mixtures, which initially were miscible, temperature decrease below T_{gel} induced phase separation, due to polymer ordering (M. Williams et al.,

2001). Droplets formed thereby, at phase separation temperatures below T_{gel} , were smaller, compared to aforementioned scenario (N. Lorén et al., 2001).

Cooling rate, not only influenced droplet size, but also influenced the kinetic competition between phase separation and gelling. Rapid cooling (quenching at 33°C/min) from 70 °C to 5 °C lead to gelation of the system, while cooling at a rate of 1°C/min gave sufficient time for phase separation to occur (Alevisopoulos & Kasapis, 1999; Alevisopoulos et al., 1996). The cooling rate was shown to influence the composition of the continuous phase of the gel: Quenching the mixture at a fixed gelatin concentration (5% Gelatin) required 15% maltodextrin for the formation of a maltodextrin continuous gel (Kasapis, Morris, Norton, & Clark, 1993b), while in contrast, if cooled down slowly, a gelatin-continuous phase was maintained up to 22 % maltodextrin (Alevisopoulos et al., 1996). The same research group found that the inversion point from a gelatin/maltodextrin emulsion to a maltodextrin/gelatin emulsion was influenced by the molecular weight of these polymers (Alevisopoulos & Kasapis, 1999).

Moreover, solvent conditions influence as well the phase diagram, as can be seen in Figure 1.38 (Lundin et al., 2000). Increasing ionic strength reduces the miscibility region of gelatin/maltodextrin mixtures and moves the binodal line to lower concentrations, due to counterion entropy. At low ionic strength, there is an entropic barrier to separate gelatin and maltodextrin in two distinct phases, as gelatin is associated to a great number of counterions, which is not the case for the uncharged maltodextrin. The imbalance of number of particles in both phases forms an entropic barrier for phase separation. At high ionic strengths there is a greater number of particles in the entire solution, outweighing the entropic contribution of gelatin-associated counterions to the free energy of mixing.

Finally, an important factor in determining the morphology of the dispersed phase is the shearing rate of the emulsion. The higher the shear rate, the smaller the radius of the droplets. As can be seen in Figure 1.39 droplet size bigger than 100 μm were obtained at shear rate of 1s^{-1} between two parallel plates (gap 500 μm), while the droplet size was reduced to less than 10 μm for shear rates of 100 s^{-1} (gap 100 μm) (Stokes, Wolf, & Frith, 2001).

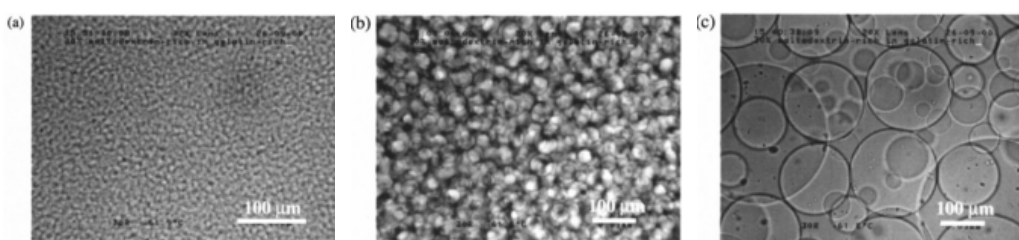


Figure 1.39. Morphology of 30% maltodextrin-rich phase maltodextrin-in-gelatin emulsion for preshear rates of (a) 100s^{-1} , (b) 10s^{-1} and (c) 1s^{-1} . Figure reproduced from (Stokes et al., 2001)

As in other biopolymer mixtures (Wolf et al., 2000b), applying shear upon de-mixing of the emulsion altered the rate of droplet elongation and break-up. At specific shear rates or by gelation of one of the components, stable anisotropic structures can be obtained, such as ellipsoids, threads, and/or gel composites with anisotropic inclusions (Michael F Butler & Heppenstall-Butler, 2003; Stokes et al., 2001).

Because of the many factors, which affect phase behaviour of the two polymers, phase diagrams of gelatin/maltodextrin mixtures do not coincide from study to study, as different conditions have been used for all of them. Figure 1.40 shows four different phase diagrams of gelatin/maltodextrin mixtures, reproduced from various authors, working at different conditions.

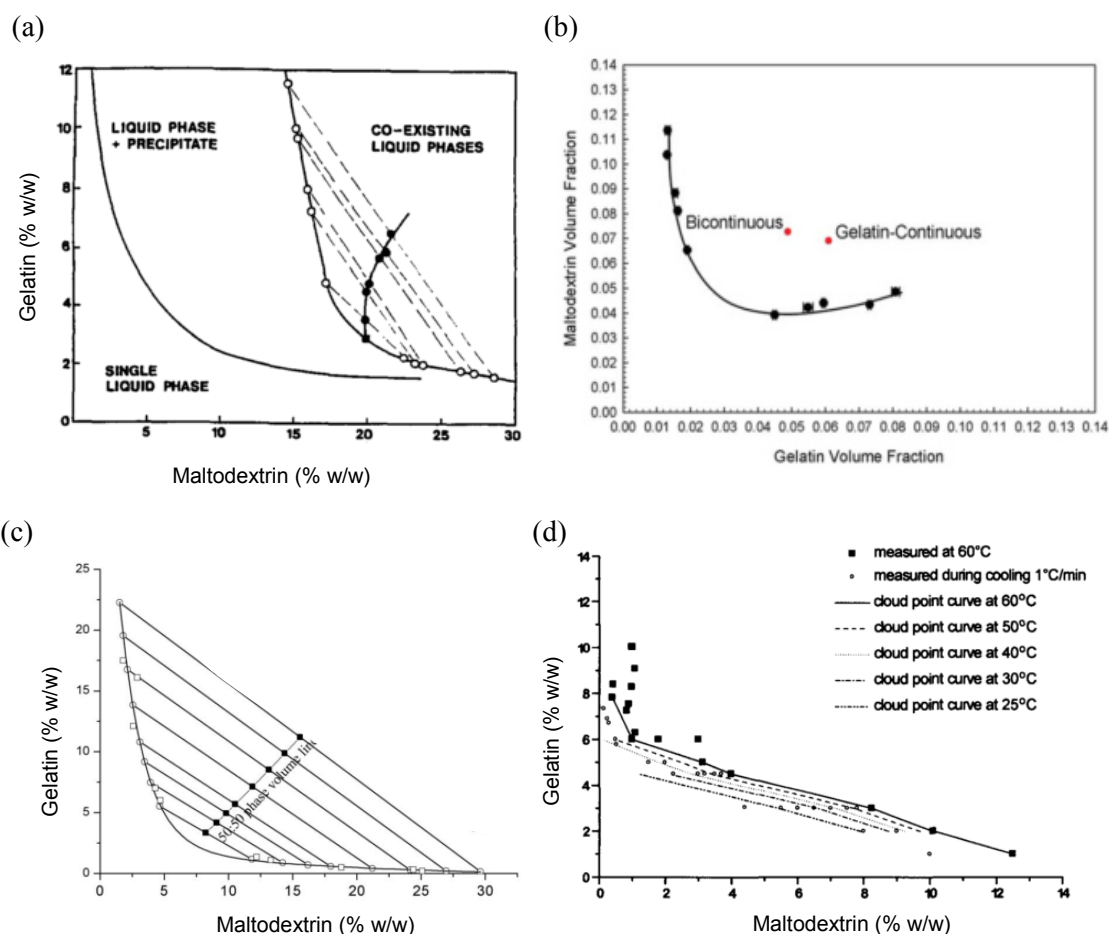


Figure 1.40. Phase diagrams of gelatin/maltodextrin mixtures obtained in different studies under following conditions. (a) Gelatin Type B, Maltodextrin (DE6) in water at 45 °C (Kasapis et al., 1993), (b) Gelatin Type A, Maltodextrin DE10 in water at 70 °C (R. S. Khan et al., 2011) (c) Gelatin Type B, Maltodextrin Type DE 2.5 in water at 60 °C (Norton & Frith, 2001), (d) Gelatin Type B, Maltodextrin DE 2.5, in 0.1 M NaCl (Lundin et al., 2000)

The binodal line, separating the one- from the two-phase region, does not coincide for the different studies, which is due to different types of polymers used, batch-to-batch variability of polymers, polydisperse molecular weight distribution and different physicochemical conditions under which those phase diagrams were obtained. Moreover, those phase diagrams were measured after few hours of equilibration or after centrifugation. In no case the samples were left to equilibrate for more than 1 day.

Interestingly, few researchers observed precipitation of maltodextrin in the gelatin/maltodextrin mixtures (Kasapis et al., 1993). The packed precipitate made up in some cases more than 80% of the total sample volume and occurred above a certain polymer concentration, as shown in the phase diagram in Figure 1.40 (a). The amount of the maltodextrin precipitate (M) was found to be proportional to the concentration of gelatin and to the square of its own initial concentration: $M = k \cdot [\text{maltodextrin}]^2 \cdot [\text{gelatin}]$. Still, they found that few gelatin was also present in the precipitate.

It was proposed that gelatin drives a two-coil to double helix transition of maltodextrin, which ultimately leads to self-association and aggregation of the polysaccharide (Hoey, Ryan, Fitzsimons, & Morris,

2016; Kasapis et al., 1993). The more compact uncharged helical conformation grows then by addition of branched species until the ordered core gets screened from the disordered outer part. Kasapis et al. showed that the precipitated maltodextrin is higher in molecular weight and degree of branching than the remaining polymer in solution.

Many of the studies focussed on basic physicochemical properties of the system and did not use the system for specific applications. Few applications of gelatin/maltodextrin mixtures as templates to produce gels exist so far. Most of the studies focussed on maltodextrin-in-gelatin emulsions.

- Nickerson et al. formed maltodextrin-in-gelatin gels at different pH conditions (pH 3, 5, 7) and using different crosslinker molecules (genipin, glutaraldehyde and sodium tripolyphosphate). They found that the pH influenced firstly phase separation and thus also morphology of the gel. Low pH hindered phase separation, leading to a homogenous gel network, while higher pH lead to phase separation and thus gelatin networks with maltodextrin inclusions. pH also influenced crosslinking capacity of the different crosslinkers and thus the elastic modulus of the gels (Nickerson, Paulson, et al., 2006).
- Khan et al. formed genipin-crosslinked gelatin-continuous or bicontinuous microstructures and studied the swelling and release behaviour of four fluorescent markers of varying molecular weights (A. Khan et al., 2015). Reduced marker size, pH below gelatin pI, and reduced crosslinking all tended to increase the release rate.
- Firoozmand et al. studied how the yeast *Saccharomyces cerevisiae*, the bacteria *Lactobacillus delbrueckii* subsp. *bulgaricus* or the microalgae spirulina adsorbed to the protein-polysaccharide interface of maltodextrin-in-gelatin emulsions. The microbes acted as structure-modifiers and their presence in the gels resulted in food-grade bijels that remained kinetically stable for months (Firoozmand & Rousseau, 2015).

Chapter 2

MAIN OBJECTIVES
AND WORKING PLAN

2 Main Objectives and Working Plan

The final aim is to formulate microgels as vehicles for oral delivery, which would encapsulate an enzyme and deliver it to the intestine. The use of biocompatible materials, for enzymes non-harmful but also cheap and simple preparation methods are thus important factors to consider. Most existing microgels are based on synthetic polymers which offer the advantage of fine-tunable degradation kinetics, mechanical properties etc. However, they often involve toxic degradation products. Focus will thus be laid on trying to obtain microgels made of biocompatible polymers, such as polysaccharides and proteins. Another very important objective is to study the use of W/W emulsions as reaction media for the preparation of the microgels. Many studies have been performed to analyse the physicochemical behaviour of W/W emulsions based on biopolymer mixtures, but only few have isolated microgels and used it as a drug delivery vehicle (Jin et al., 2008; J. Kang et al., 2014; R. S. Khan et al., 2011; B. Li et al., 2012; D. Liang, Fu, Liao, Yuan, & Su, 2013; Stenekes et al., 1999). Two examples of very well studied biopolymer-based systems are the dextran-PEG and gelatin/maltodextrin mixtures.

In a first step a pH responsive, biocompatible polymer, whose gels are less soluble under acidic conditions was selected as the main component of the microgels. Sodium carboxymethylcellulose (NaCMC) was chosen, which has shown to form W/W emulsions with the protein bovine serum albumin (BSA) under basic conditions (Grinberg & Tolstoguzov, 1997).

Next, the gelatin/maltodextrin system was selected, as it is a previously described biopolymer mixture, able to form W/W emulsions, at neutral pH conditions. Moreover, gelatin has interesting gelation properties, which can be explored for the preparation of microgels.

The study will thus be divided into two parts:

NaCMC/BSA System

- Understanding the phase behaviour of the biopolymer mixture
- Formation of NaCMC/BSA emulsions and their characterisation
- Evaluation of possibilities to gel and crosslink the biopolymers in the mixture with multivalent ions
- Study the stability of the crosslinked beads under acidic and neutral pH conditions
- Study the possibilities for immobilising enzymes into the microgels

Gelatin/Maltodextrin System

- Study the parameters which influence the crosslinking rate of gelatin by genipin
- Investigation of the gelling and swelling characteristics of crosslinked gelatin macrogels
- Evaluate the most adequate methods to quantify and identify gelatin and maltodextrin in their mixtures
- Study the phase behaviour of gelatin/maltodextrin/water ternary mixtures
- Formation and characterisation of gelatin/maltodextrin emulsions

- Preparation of crosslinked gelatin microgels from gelatin/maltodextrin emulsion templates
- Study of the parameters which influence microgel size
- Evaluate the swelling properties and the stability of gelatin microgels under varying physicochemical conditions
- Immobilisation of the enzyme lactase into the microgels and optimisation of encapsulation yield and activity recovery

Chapter 3

MATERIAL AND METHODS

3 Material and Methods

3.1 Material

This section is divided into four subsections: biopolymers, crosslinkers, enzyme and its related reagents, and other products used.

Biopolymers

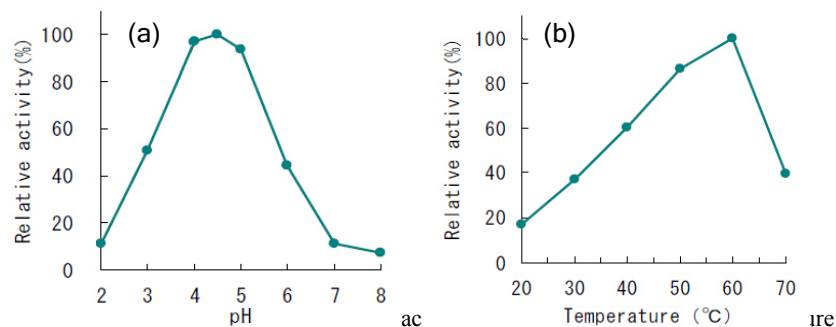
- **Gelatin:** Protein from bovine skin. Gel strength ~225 g Bloom, Type B, molecular mass: 50-100 kDa (Sigma-Aldrich, CAS 9000-70-8)
- **Maltodextrin:** Polysaccharide, composed by D-glucose units connected in chains with $\alpha(1\rightarrow4)$ glycosidic bonds (Figure 1.37). Dextrose equivalent 4.0-7.0, molecular mass: 3.6 kDa (Sigma-Aldrich, CAS 9050-36-6)
- **Bovine Serum Albumin:** A serum albumin protein derived from cows. Molecular mass 67 kDa (BSA, Sigma-Aldrich, CAS: 9048-46-8)
- **Sodium Carboxymethylcellulose:** Polysaccharide, which is a cellulose derivative with carboxymethyl groups to some of the hydroxyl groups of the glucose monomers (Figure 1.30), molecular mass 250 kDa (NaCMC, Sigma-Aldrich, CAS: 9004-32-4)

Crosslinkers

- **Genipin:** Molecule extracted from gardenia fruits. (>98 %, Challenge Bioproducts Co., LTD., CAS 6902-77-8) (Figure 1.33 d)
- **Iron (III) chloride anhydrous:** FeCl_3 (>97%, Sigma-Aldrich, CAS: 7705-08-0)
- **Aluminum sulfate hydrate:** $\text{Al}_2(\text{SO}_4)_3 \cdot \text{H}_2\text{O}$ (>99.99 %, Sigma, CAS: 17927-65-0)
- **Aluminum potassium sulfate:** $\text{AlK}(\text{SO}_4)_2$ (>98 %, Sigma, CAS: 10043-67-1)
- **Calcium chloride:** CaCl_2 (> 98 %, Merck, CAS: 10043-52-4)

Enzyme and Enzyme Activity/Quantity Measurements

- **Enzyme lactase, β -galactosidase** (denoted as β -Gal):
 - **Lactase F “Amano”** extracted from *Aspergillus oryzae*, EC 3.2.1.23, was provided from Amano Enzyme Europe (United Kingdom) in powder form. Activity profile of the enzyme at different pH and temperature conditions are presented in Figure 3.1.



activity profile of Lactase F “Amano” at pH 4.5. (data and graphs from manufacturer, AMANO ENZYME).

- **Ha-Lactase 5200**, extracted from *K. lactis*, EC 3.2.1.23, was provided by Chr. Hansen (Denmark) with activity of 5200 NLU/g (= 113 μ kat/g) in a concentration of 25 mg of protein/mL of PEM buffer solution (details of buffer below) and glycerol (1:1 w/w). The hydrodynamic diameter of the tetrameric lactase was ~14 nm and its molecular weight 470 kDa. Activity profile of the enzyme at different pH and temperature conditions are presented in Figure 3.2.

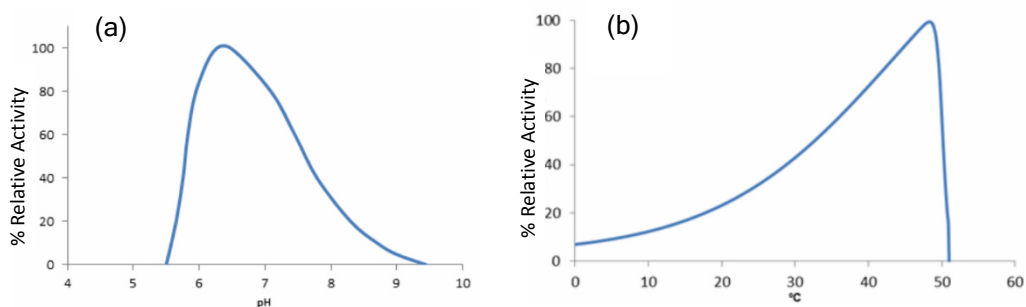


Figure 3.2. (a) pH activity profile of Ha-Lactase 5200 (at 40 °C). (b) Temperature activity profile of Ha-Lactase 5200 at pH 6.5. (data and graphs from manufacturer, Chr. Hansen)

- **Phosphate-EDTA-Magnesium (PEM) buffer solution (pH 6.5):**

Preparation detailed in Table 3.1. Buffer contains:

- Potassium dihydrogen phosphate (KH_2PO_4 , >99 %, Merck, CAS: 7778-77-0)
- DiPotassiumhydrogenphosphate $3\text{H}_2\text{O}$ ($\text{K}_2\text{HPO}_4 \cdot 3\text{H}_2\text{O}$, >99.5 %, CalbioChem, CAS: 16788-57-1)
- Magnesium sulphate ($\text{MgSO}_4 \cdot 7\text{H}_2\text{O}$, >99.5 % Sigma-Aldrich, CAS: 10034-99-8)
- EDTA ($\text{C}_{10}\text{H}_{14}\text{N}_2\text{Na}_2\text{O}_8, 2\text{H}_2\text{O}$, >99 %, Sigma-Aldrich, CAS: 60-00-4)

Table 3.1. Preparation and composition of PEM Buffer (pH 6.5)

| Chemical | 1 litre |
|--|--------------------|
| Potassium dihydrogen phosphate (KH_2PO_4) | 8.8 g (65 mM) |
| Di-potassium hydrogenphosphate $3 \cdot \text{H}_2\text{O}$ ($\text{K}_2\text{HPO}_4 \cdot 3\text{H}_2\text{O}$) | 8.0 g (35 mM) |
| Magnesium solution (2.47 g/100 mL in water) | 10.00 ml (1 mM) |
| EDTA solution (0.186 g/100mL in water) | 10.00 ml (0.05 mM) |
| Water | up to 1000 ml |

- **0.1 M Citric Acid Buffer (pH 4.5):**

- 0.1 M Citric Acid ($\text{C}_6\text{H}_8\text{O}_7$, >99%, Merck, CAS: 77-92-9)
- 0.1 M Trisodium citrate ($\text{Na}_3\text{C}_6\text{H}_5\text{O}_7 \cdot 2\text{H}_2\text{O}$, Merck, CAS: 6132-04-3)

- **Sodium carbonate solution:** Preparation detailed in section 3.3.6.1. Contains:

- Sodium carbonate (Na_2CO_3 , > 99.8 %, Sigma-Aldrich, CAS: 144-55-8)
- EDTA ($\text{C}_{10}\text{H}_{14}\text{N}_2\text{Na}_2\text{O}_8, 2\text{H}_2\text{O}$, >99.5 %, Sigma-Aldrich, CAS: 60-00-4)

- **ONPG solution:** Preparation detailed in section 1.3.6.1. Contains:

- o-Nitrophenyl b-D-galactopyranoside (ONPG, Carbosynth, CAS: 369-07-3)

- **Bradford Assay:**

- Protein Assay Dye Reagent Concentrate (Bio-Rad, 5000006)

- **Simulated Gastric Fluid (pH 1.2):**

0.11 M NaCl and 0.71 M HCl (after dilution in 6 L water) (01651 Sigma-Aldrich)

- **Simulated Gastric Fluid (pH 3)** (standard protocol adapted from literature (Minekus et al., 2014), exact composition detailed in Table 3.2)

- Potassium dihydrogen phosphate (KH_2PO_4 , >99 %, Merck, CAS: 7778-77-0)
- Calcium chloride (CaCl_2 , > 98 %, Merck, CAS: 10043-52-4)
- Magnesium chloride (MgCl_2 , Sigma, CAS: 7786-30-3)
- Ammonium carbonate ($(\text{NH}_4)_2\text{CO}_3$, Sigma-Aldrich, CAS: 506-87-6)
- Potassium chloride (KCl, >99 %, Sigma-Aldrich, CAS : 77-86-1)
- Sodium Hydrogen Carbonate (NaHCO_3 , >99.7 %, Panreac, CAS:144-55-8)
- Sodium chloride (NaCl, >99 %, Sigma-Aldrich, CAS: 7647-14-5)
- Hydrochloric acid fuming 37% (HCl, Merck, CAS: 7647-01-0)

Table 3.2. Composition of Simulated Gastric Fluid (pH 3)

| Chemical | Concentration |
|---|--------------------------------|
| Potassium dihydrogen phosphate (KH_2PO_4) | 0.5 M |
| Calcium chloride (CaCl_2) | 0.3 M |
| Magnesium chloride (MgCl_2) | 0.15 M |
| Ammonium carbonate ($(\text{NH}_4)_2\text{CO}_3$) | 0.5 M |
| Potassium Chloride (KCl) | 0.5 M |
| Sodium Hydrogen Carbonate (NaHCO_3) | 1 M |
| Sodium Chloride (NaCl) | 1 M |
| 6 M Hydrochloric Acid (HCl) | Add to adjust solution to pH 3 |

Other products

- **Water:** If not otherwise mentioned deionised water filtered by the water purification system Millipore model Synergy Smart UV (resistivity at 25°C: 18.2 MΩ·cm; conductivity 0.056 μS/cm, water quality: type I, ion concentration < 1μg/L) was used.
- **Rhodamine B:** Sigma Aldrich, CAS: 81-88-9
- **Fluorescein isothiocyanate isomer I (≥90%) (FITC):** Sigma-Aldrich, CAS: 3326-32-7
- **Rhodamine B isothiocyanate mixed isomers (RITC):** Sigma-Aldrich, CAS: 36877-69-7
- **Ortho-Nitrophenol:** ONP, Sigma-Aldrich, CAS: 88-75-5
- **Davies buffer solution:** Details of preparation in Table 3.3. Buffer contains:
 - Citric acid ($\text{C}_6\text{H}_8\text{O}_7$, >99 %, Merck, CAS: 77-92-9)
 - Potassium dihydrogen phosphate (KH_2PO_4 , > 99%, Merck, CAS: 7778-77-0)
 - Sodium tetraborate ($\text{Na}_2\text{B}_4\text{O}_7$, >99 %, Sigma, CAS: 1330-43-4)
 - Tris(hydroxymethyl)aminomethane (TRIS, >99.8 %, Fluka, CAS: 77-86-1)
 - Potassium chloride (KCl, >99 %, Sigma-Aldrich, CAS : 77-86-1)

3.2 Instruments

- **Balance**
Analytical Balance Mettler Toledo AB204-S/FACT with a precision of $\pm 10^{-4}$ g
Digital Lab Balance Sartorius CPA3202-S with a precision of $\pm 10^{-2}$ g.
- **Centrifuge**
Eppendorf model 5804R, maximal velocity 5000 rpm with a maximal working temperature of 40°C
- **Confocal Scanning Laser Microscope**
LEICA model TCS SPX AOBS. Fluorescence emissions were recorded within an Airy disk confocal pinhole setting (Airy 1). This instrument belonged to the imaging core facility (PTIBC IBISA Nancy) from the FR3209 CNRS - BMCT based at the Biopole of Université de Lorraine.
- **Chromatography Column**
PD-10 Desalting Columns contain Sephadex G-25 resin (GE Healthcare, Life Sciences)
- **Densimeter**
DMA4500M (Anton Paar), with accuracy of density measurement of ± 0.00005 g/cm³ and temperature regulation of ± 0.03 °C.
- **Dialysis Tubing**
Purification of microgel suspensions:
 - Cellulose membrane, Nominal MWCO: 12 kDa, Wall Thickness: 28 μ m, Width: 25 mm (CelluSep, T3-25-15)Labelling of Polymers:
 - Standard Grade Regenerated Cellulose membrane, Nominal MWCO: 3.5 kDa, (Spectrum Labs, Spectra/Por[®] 3)
 - Cellulose Esther membrane, Nominal MWCO: 8-10 kDa, (Spectrum Labs, Float-A-Lyzer G2)
- **Electrospraying Device**
The in-house assembled electrospraying device possesses a variable high-voltage with a 0-30 kV power supply. A sterile plastic syringe is connected to a stainless steel sterile needle (23G, BD) over a plastic tube. The anode is connected to the needle and the ground electrode to the aluminium plate holding the collector dish. This instrument belonged to the University of Lorraine, at which a research stay was performed.
- **Extruder**
An extruder (Avanti Polar Lipids, Inc., 610000-1EA) made for filters with size 13 mm was used. The filters used were polycarbonate filters with pore size 0.8 μ m (Merck Millipore, ATTP01300) and 10 μ m (Merck Millipore, TCTP01300). The setup was as follows: The solution passed from the syringe into the extruder over the membrane through a stainless steel sieve out of the extruder.
- **Freeze-dryer**

Christ Alpha 2-4 LD Plus with a working pressure and temperature of ~ 0.03 mbar and -85 °C.

- **Heating and magnetic stirring plate**
IKA RCT basic with integrated temperature control (PT 1000 temperature sensor (PT 1000.60)) and external electronic contact thermometer (IKA ETS-DG). Mixing speed range: 50 - 1500 rpm.
- **Light diffraction particle size analyser**
Mastersizer 2000 light diffraction particle size analyzer (Malvern Instruments), equipped with a dispersion unit Hydro 2000G. The instrument uses red (640 nm) and blue (466 nm) lasers and has a measuring range of 0.1-1000 μm .
- **Optical Microscope**
Olympus model BX51TRF-6, coupled to a digital camera Olympus DP73, controlled over an image/video capture software Stream Essential of Olympus.
- **pH meter**
Mettler Toledo, model Seven Easy
- **Polarimeter**
PerkinElmer Inc.-Model 341 Polarimeter, connected to a thermoregulatory water bath to control the temperature inside the quartz sample holders
- **Refractometer**
ATAGO NAR-3T Abbe Refractometer with a Scale Range of 1.30000 to 1.71000 and accuracy of ± 0.0001 .
- **Raman microscope**
Micro-Raman (Jobin-Yvon LabRam HR 800), coupled to an optical microscope (Olympus BXFM). The micro-Raman was equipped with a Laser Diode (TEC-120 de Sacher Lasertechnik) emitting at $\lambda = 785$ nm. This instrument was located in the scientific technical services of the University of Barcelona.
- **Scanning Electron Microscope (SEM)**
HitachiTM-1000 Tabletop Microscope, operating at 5 kV
- **Sonicator**
Sonoplus Ultrasonic homogenizer HD3200 (Bandelin)
- **Thermostated Bath**
A 15 L water bath of methacrylate was used, whose temperature was controlled by the thermostat HAAKE DC10.
- **Ultra-Turrax®**
Janke+Kunkel, IKA-Labortechnik Stauten, model T25, dispersing element S25N-10G
- **UV Spectrometer**

Variant Cary 300 UV-Vis. Measurements done in Quartz sample holders.

3.3 Methods

3.3.1 *NaCMC/BSA Emulsions as Template for Microgel Formation*

3.3.1.1 *Stock Solutions of Polymers*

A 3 wt% CMC stock solution was prepared by dispersing CMC into solvent and stirring during 4 h at 25 °C. The 25 wt% BSA stock solution was prepared by dispersing BSA into solvent and stirring during 1 h at 25 °C. The solvent was normally 0.1 M NaOH, if not otherwise mentioned. In some cases Milli-Q water was used.

3.3.1.2 *Study of Phase Behaviour of NaCMC/BSA Mixtures*

Mixtures of NaCMC and BSA at different concentrations were prepared in order to determine their phase behaviour. Two distinct cases were investigated: Phase behaviour with 0.1 M NaOH as solvent (pH 13) and in water. NaCMC concentrations ranging from 0 - 2.5 wt% and BSA concentrations from 2 - 8 wt% were examined. The samples were prepared in 5 mL glass vials and filled up to a total weight of 4 g, by adding first solvent, then NaCMC and finally BSA stock solutions. After vortexing the samples during 10 seconds, the samples were placed into a thermostated bath at 25 °C constant temperature, for a period of 2 days.

Phase behaviour was consequently determined by carefully taking the sample out of the water bath and visual observation served to identify whether the two liquid phases could be distinguished. As BSA has a more yellowish and turbid colour, probably due to impurities in the product, it could be distinguished from the more transparent and colourless NaCMC phase. Emulsions were consequently formed for different mixtures by stirring them for 10 min at 500 rpm at 25 °C and observing them subsequently under the microscope. The emulsions were kept at 4 °C in the fridge and observed again after a period of up to 20 days.

3.3.1.3 *Formation of Capsules with Multivalent Ions*

Solutions of 3 wt% NaCMC, 15 wt% BSA and emulsions of both components (0.5% NaCMC / 4.5 % BSA and 2.5% NaCMC / 2.6 % BSA), all prepared in 0.1 M NaOH, were dropped with the help of a pasteur pipette into 10 mL salt solutions containing multivalent cationic ions. The following salt solutions, prepared in MiliQ water, were tested: 1, 2 and 8 wt% FeCl₃, 10 wt% Al₂(SO₄)₃, 10 wt% AlK(SO₄)₂ and 2 and 8 wt% CaCl₂. Pictures were taken after 5 min of crosslinking with those multivalent ions. For the NaCMC sample in FeCl₃ (2 wt%), the samples were left for 5 min and 45 min, before removal from the crosslinker solution. The beads were consequently freeze-dried and observed by the SEM.

3.3.1.4 Electro spraying the NaCMC/BSA Emulsion

To reduce droplet size of the emulsion dropped into the crosslinking medium, the electro spraying method was used (experiments performed at Université de Lorraine).

The principles of electro spraying are based on the ability of an electric field to deform the interface of a liquid drop. If an electrified field is applied to a droplet, the electric charge generates an electrostatic force inside the droplet, known as the Coulomb force, which is in competition with the cohesive force inside the droplet. If the applied electrostatic force overcomes the cohesive force, defined by the surface tension, the droplet will break up into smaller droplets. This phenomenon begins often by shrinkage of the unstable, charged macro-droplet into a cone, referred to as the Taylor Cone, from which smaller charged droplets will be ejected as soon as the Coulomb force overcomes the surface tension (Bock, Woodruff, Hutmacher, & Dargaville, 2011).

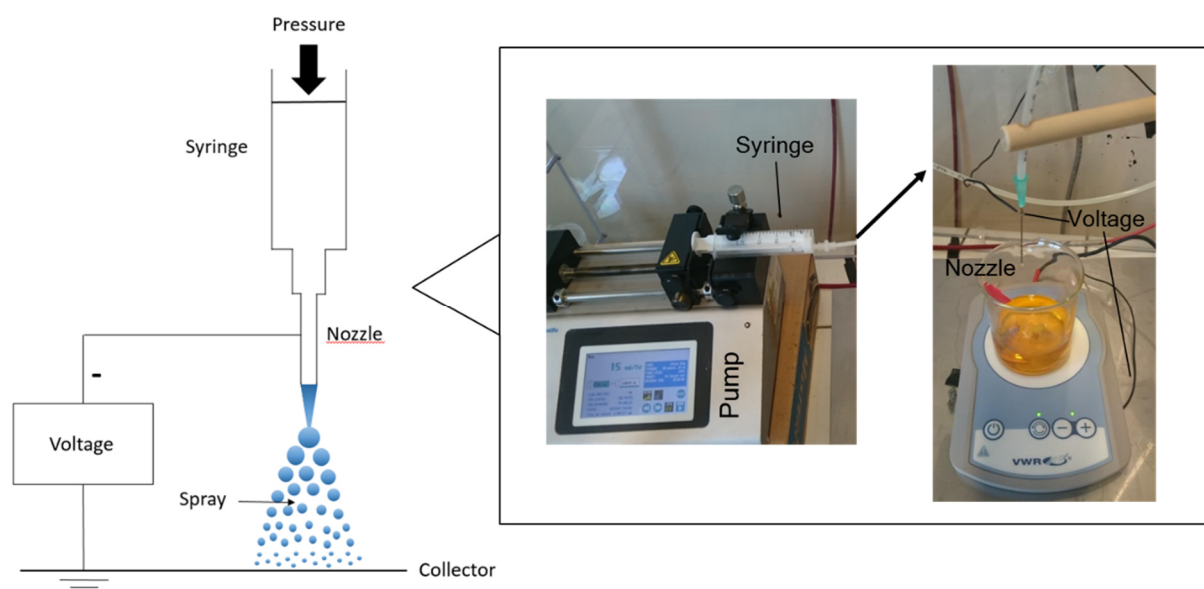


Figure 3.3. Experimental setup of electro spraying unit, with its different components. Left a sketch of the setup (adapted with permission from F. Haffner), right pictures of it.

Figure 3.3 shows our experimental setup. A 0.5% NaCMC / 4.5 % BSA emulsion was introduced into a plastic syringe connected over a plastic tube to a stainless steel sterile needle (23G, BD). The anode was connected to the needle and the ground electrode to the aluminium plate holding the glass beaker with a 2 wt% FeCl_3 crosslinking solution. Negative voltage is applied to the needle, while the aluminium plate and the glass beaker were connected to the ground. A challenge, when electro spraying, is finding experimental settings, which allow the solutions to be sprayed. If not adequate settings are used, the solution can get out of the nozzle as normal sized drops, or in form of a long fiber (of interest in electro spinning). We adapted thus voltage, flow rate and the tip-to-collector distance, till spraying of the emulsion was achieved. Optimal conditions for spraying were obtained with 10 kV, 15 mL/h flow rate and 12 cm tip-to collector distance.

The electro sprayed encapsulated emulsions were kept for 30 min in the 2 wt% FeCl_3 solution, then transferred into water and analyzed under the optical microscope.

3.3.1.5 Evaluation of pH-Stability of Capsules

To simulate pH conditions during oral delivery across the stomach and finally to the intestine, the stability of crosslinked capsules under those conditions was tested. Therefore, 3wt% NaCMC and 0.5% NaCMC / 4.5 % BSA emulsions were dropped into 10 wt% $\text{Al}_2(\text{SO}_4)_3$ and 10 wt% $\text{AlK}(\text{SO}_4)_2$ solutions, kept there for 30 min and then immersed into either a pH 6.5 PEM buffer solution or a pH 1.2 SGF solution. After 2 h at 25 °C the beads were transferred into the other pH solution: the beads at pH 6.5 were added for 2 h into pH 1.2 and those from pH 1.2 were transferred for 2 h to pH 6.5. A final switch between pH solutions was done, in case the beads remained stable. The pH sensitivity of the beads was analyzed by observing whether swelling occurred and whether they remain stable or not.

3.3.1.6 Immobilisation of Enzymes into NaCMC/BSA Emulsion Beads

Two different methods were evaluated to immobilise the enzyme into NaCMC/BSA emulsion beads. In the first method, the enzyme was added to the crosslinker solution. To test whether the enzyme remains active inside the $\text{Al}_2(\text{SO}_4)_3$ solution, the enzyme (in citric acid buffer), with a final concentration of 12.5 µg/mL, was mixed with:

- 10 wt% $\text{Al}_2(\text{SO}_4)_3$ solution (pH 2.8)
- 8.33 wt % $\text{Al}_2(\text{SO}_4)_3$ solution at pH 3.7 (pH risen by addition of 0.1 M NaOH)

The activity of the enzyme was measured during 24 h, using the ONPG assay (details in section 3.3.6.1. PEM buffer was replaced by Citric Acid Buffer).

For the second method, the aim was to add the enzyme into a NaCMC/BSA emulsion, before crosslinking it. Formation of NaCMC/BSA emulsions at different pH conditions, more favourable to the enzyme was tested and details can be found in (Corvo, 2017).

3.3.2 Properties of Gelatin, Maltodextrin and Genipin

3.3.2.1 Reaction of Genipin with Water, Maltodextrin and Gelatin

Genipin is known to develop dark blue pigments by spontaneous reaction with amino acid groups (Touyama et al., 1994). To investigate the color development upon reaction with the different polymers, water, gelatin (5 and 10 wt %) and maltodextrin (10 and 15 wt%) solutions were prepared and mixed with a 0.5 wt % genipin solution to obtain a final genipin concentration of 4 mM. After agitating the sample by vortex, the samples were incubated for 16 h at 45 °C. After incubation, the samples were observed visually.

3.3.2.2 Influence of Temperature and Time on Crosslinking of Genipin

The crosslinking reaction of gelatin microgels was followed colorimetrically at different temperatures (25, 45 or 60 °C) and different crosslinking concentrations (0.1, 1 or 10 mM Genipin). Therefore a 4.5

% Gel/ 13 % MD emulsion was prepared in water, homogenised for 1 min at 9500 rpm, using an Ultra-Turrax® homogenizer and then continuously stirred at 500 rpm at constant temperature. At various time points the UV spectra of the samples was measured to observe the colour development of the genipin reaction. Measurements were terminated after maximum 4 days or when the microgels crosslinked between each other to form a single bulk macrogel separated from the continuous medium.

The microgels had a maximum absorption at 605 nm, which corresponds to the blue colour observed by eye. The highest absorption measured, just before intercrosslinks between microgels occurred, was defined as $Abs_{max}(\lambda_{605nm})$.

3.3.2.3 Gelatin Sol-Gel Transition Temperature

For determining the temperature of gelation of gelatin, samples (5 g in glass vial) of different concentrations were placed into a water bath heated to 45 °C. Every 10 min the temperature was decreased by 1 °C. Once 21 °C was reached, the temperature was raised again 1 °C every 10 min. Whether the solution gelified or not was determined by the tube inversion method, at which the vial was inverted and it was observed whether the sample flows or remains immobile.

For the measurement of gelation, when crosslinked with genipin, the samples were kept at room temperature (22 °C) at which they were gelified. For 46 h, at specific time points they were put into the thermostated bath, which was continuously heated (~1 °C/min) till they became a fluid liquid (measured by the tube inversion method).

3.3.2.4 Measurement of Swelling of Gelatin-Genipin Macrogels

100-200 mg of gel were cut into cubes and immersed into 6 mL of either a citric acid/sodium phosphate buffer of pH 7 or a HCl solution of pH 2.5. After determined time periods the gel was taken out of the solution and blotted dry with a tissue and weighed. As soon the sample could not be removed from the solution anymore, as it was too liquid or broke if in contact with the spatula, the experiment was terminated for the respective sample.

Swelling ratio (SR) was calculated as follows:

$$SR = \frac{m(t) - m_0}{m_0} \cdot 100\% \quad (3.1)$$

where $m(t)$ is the weight of a gel at a specific time point and m_0 the initial gel weight.

3.3.2.5 Density of Gelatin and Maltodextrin

Density at 50 °C of gelatin (4 wt% and 12 wt%) and maltodextrin (5 wt% and 20 wt%) solutions, dispersed in water was measured. Therefore, the 50 °C solution were carefully introduced with the help

of a syringe into the density meter, preheated to 50 °C. It was verified that no bubbles entered the measurement cell, as this would affect the experimental outcome. The measurements were done in triplicate and in between them the cell was washed with water and ethanol and finally dried.

3.3.2.6 Measurement of UV Spectra of Gelatin, Genipin and Maltodextrin

The UV spectra of various solutions of gelatin, genipin and maltodextrin, prepared in water was measured between 200 and 800 nm with the UV Spectrometer Variant Cary 300. The UV spectra of water served as baseline.

3.3.2.7 Concentration Measurement of Maltodextrin and Gelatin by Optical Rotation

Several studies (Kasapis et al., 1993; Scholten, Visser, Sagis, & van der Linden, 2004) have used optical rotation to obtain the concentration of the different polymers inside a mixture of unknown polymer concentration.

Therefore in the first step, a calibration curve of different concentrations of gelatin (0-4 wt%) and maltodextrin (0-20 wt%) solutions in water were prepared and introduced into a quartz sample cuvette. Measurements were performed at 45 °C and calibration curves for 4 different wavelengths $\lambda = 365, 405, 546$ nm (Hg lamp) and 589 nm (Na/Hal lamp) were obtained. The optical rotation of water at 365 nm was defined as zero. All measurements were performed at 45 °C and 10 measurement points were recorded per sample to obtain an average value for the optical rotation $\alpha(\lambda)$.

The variation of optical rotation with wavelength can be described by the Drude expression (Drude, 1900):

$$\alpha(\lambda) = \frac{A}{\lambda^2 - \lambda_0^2} \quad (3.2)$$

thus,

$$\frac{1}{\alpha(\lambda)} = \frac{1}{A} \lambda^2 - \frac{\lambda_0^2}{A} \quad (3.3)$$

where A is called the rotation constant and λ_0 the dispersion constant. To check the reliability of the calibration curves, Drude plots were constructed, in which $1/\alpha$ is plotted against λ^2 . Linearity of the plots indicates the reliability of the calibration curve (Kasapis et al., 1993).

To calculate the polymer concentration of mixtures of polymer 1 and polymer 2, the overall optical rotation $\alpha(\lambda)$ of the mixed solution was determined. The analysis was based on the principle that the measured optical rotation is the linear sum of the optical rotation contributions of the individual components, which will in turn be directly proportional to their concentration:

$$\alpha(\lambda) = c_1 \alpha_1(\lambda) + c_2 \alpha_2(\lambda) \quad (3.4)$$

with c_1 and c_2 being the concentrations of the two polymers and $\alpha_1(\lambda)$ and $\alpha_2(\lambda)$ stand for the specific optical rotation per unit concentration at wavelength λ . By measuring the optical rotation at two distinct wavelengths, the equation could be solved to obtain the concentrations of the individual polymers in the polymer mixture.

3.3.2.8 Labelling Polymers

Different approaches to label either gelatin or maltodextrin were tested. The fluorescence emission of the signals was then observed, if not otherwise mentioned, by the Olympus BX51 microscope by light reflection and use of fluorescence filter cubes. Two fluorescent dyes with distinct emissions were used: Fluorescein isothiocyanate (FITC) and Rhodamine B isothiocyanate (RITC). Moreover, the crosslinker genipin has also fluorescent properties.

For the samples labeled with FITC (excitation/emission spectra in Figure 3.4 a), the U-MWB2 Wide Band Blue Fluorescence Filter was used, which excites the sample at 460-490 nm and emitted light passes through a 520 Long Pass filter, which lets light over 520 nm through (Figure 3.4 a).

For Rhodamine B, RITC (excitation/emission spectra in Figure 3.4 b) and Genipin (excitation maximum at 590 nm and emission maximum at 630 nm (Almog et al., 2004) the U-MWG2 Wide Band Green Fluorescence Filter was used, which excites the sample at 510-550 nm and emitted light passes through a 590 Long Pass filter, which lets light over 590 nm through (Figure 3.4 b).

Labelling with Fluorescent Dyes

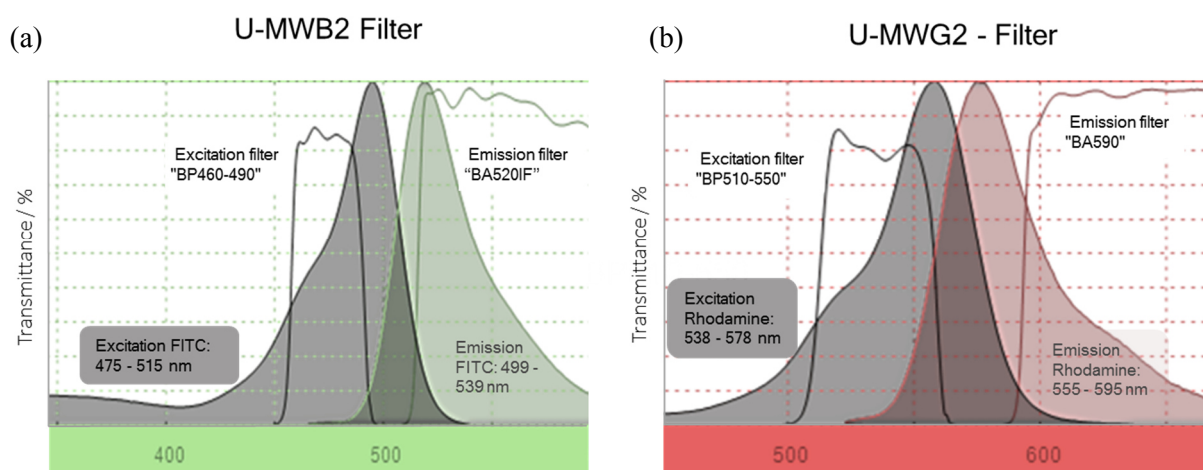


Figure 3.4. Spectra of light passing through emission and excitation filters of the UMWB2-Filter, used to observe FITC-labelled samples, and U-MWG2-Filter, used to observe Rhodamine B/Genipin-labelled samples. The figure shows also the excitation and emission spectra of FITC and Rhodamine B. (Figures adapted from <http://webtools.olympus.eu/micro/fluorophore/en-GB/Cube>)

3.3.2.8.1 Adding Rhodamine B to Emulsion

0.01 % (w/w) Rhodamine B was added into samples of 10% Gel / 6% MD and 10% Gel / 18% MD. After vortexing the sample during 10 s, the sample was put onto a glass slide and observed under the

microscope in the contrast phase and in the fluorescence mode. Assumption was taken that Rhodamine B would have a higher affinity for gelatin, as the dye is positively charged and gelatin is the only charged polymer in solution, with negative charges.

3.3.2.8.2 Covalent Labelling of Maltodextrin and Gelatin with either RITC or FITC

The protocol for labelling of maltodextrin and gelatin with RITC has been adapted from (Mladenovska et al., 2007) and (Lamprecht, Schäfer, & Lehr, 2000). Covalent labelling of the protein or polysaccharide by fluorescence dyes with an isothiocyanates group (e.g. RITC or FITC) is based on an attack of the nucleophile amino or hydroxyl groups on the central, electrophilic carbon of the isothiocyanate group (Figure 3.5). The resulting electron shift creates a thiourea linkage between the dye and the protein (after reaction with the amino group of the protein) or an isothiocarbamate linkage for the case of the polysaccharide (after reaction with the amino group of the protein). Maltodextrin was dissolved in one case in water and in another one in DMSO to diminish possible side reactions with the hydroxyl groups of water.

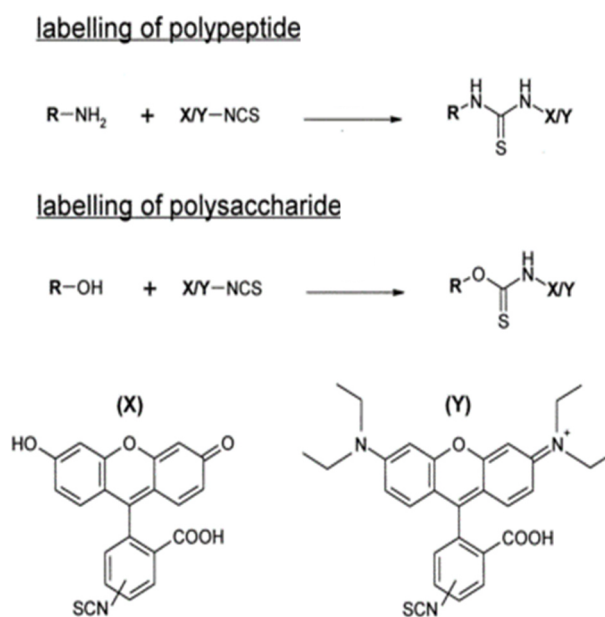


Figure 3.5. Reaction schemes for labelling procedure of the polypeptides (gelatin in our case) and polysaccharide (maltodextrin) with the two fluorescence markers. X, FITC and Y, RITC (Figure reproduced from (Lamprecht et al., 2000))

In our procedure, polymer stock solutions were mixed, protected from light, with 4 mL of 0.1 % w/v RITC (in DMSO) during 1.5 h at 40 °C:

- a) 10 g of a 4 wt % gelatin solution (in water), adjusted to pH 8 by a 0.1 % w/v NaOH solution.
- b) 2 g of a 5 wt% maltodextrin solution (in water), adjusted to pH 8 by a 0.1 % w/v NaOH solution.
- c) 10 g of a 30 wt% maltodextrin solution (in DMSO)

The choice of the polymer concentrations was a compromise between molar balance between polymer and dye, solubility of polymers and amount of product needed. The reaction was stopped with 1 mL

ethanolamine (equivalent to twice the concentration of RITC in the mixture). Ethanolamine reacts rapidly with free RITC, due to its high nucleophilicity, and removes free RITC.

For purification and extraction of unbound RITC, the labeled polymer solutions were next inserted into a dialysis bag (pore size 8-10 kDa for dialysis of gelatin, 3.5 kDa for maltodextrin) and dialysed in 1 L purified water at 30 °C till most unbound RITC was removed. This corresponded to 48 h for gelatin and maltodextrin solutions in water, The solution outside the dialysis bag was replaced once, after 16h. For maltodextrin in DMSO dialysis was performed during 4 days (dialysis solvent replaced with fresh one after first 4 h and then all 24h).

The concentration of RITC remaining in the dialysis bag, thus bound to the polymer, was determined by UV absorbance measurement at 551 nm. A calibration curve of RITC concentration at its absorption maxima of 551 nm was done previously. It was also verified that maltodextrin and gelatin do not absorb at 551 nm. For the maltodextrin in water sample, the polymer precipitated in the dialysis bag solution, thus RITC-concentration was calculated by subtracting the free RITC in the dialyzing solution from the initially added amount of dye.

Finally, the polymer solution, which remained in the dialysis bag, was freeze-dried.

Labeling efficiency was determined as the ratio of the mass of RITC which remained on the polymer in the dialyzing tube, m_{RITC} , to the mass of RITC added initially $m_{RITC,0}$.

$$\text{Labelling efficiency [\%]} = 100 \cdot \frac{m_{RITC}}{m_{RITC,0}} \quad (3.5)$$

The degree of labelling was determined as the mole RITC (n_{RITC}) per mole polymer (n_{Pol}). Molar weights of 3600 kDa for maltodextrin, 50,000 kDa for gelatin were used for the calculations.

$$\text{Degree of labelling} = \frac{n_{RITC}}{n_{Pol}} \quad (3.6)$$

To observe whether labeling was successful, five different 3% Gel / 20% MD emulsion were prepared in water:

- Gelatin-labeled: 3% Gel-RITC / 20% MD
- Maltodextrin-labeled (in water): 3% Gel / 20% MD-RITC (Water)
- Maltodextrin-labeled (in DMSO): 3% Gel / 20% MD-RITC (DMSO)
- Addition of free RITC: 3% Gel / 20% MD + 50 mg of a 0.1 % w/v RITC (in DMSO) solution in 2.5 g emulsion
- Control (no RITC) 3% Gel / 20% MD

For the cases when labeled polymers were used, only a small proportion of the polymer consisted of labeled polymer chains, as fluorescence was very intense and a small fraction of labelled molecules can be used. Samples were mixed and observed under the confocal laser scanning microscope (CLSM).

Confocal observations of samples were carried out with a LEICA TCS SPX AOBS CLSM. First channel detection were set from 565 to 681 nm with a 555 nm excitation laser line. Second channel detection were set in transmission mode with a 488 nm excitation laser line. The imaging of the sample was done in collaboration with Sébastien Hupont from the imaging core facility (PTIBC IBISA Nancy) from the FR3209 CNRS - BMCT based at the Biopole of Université de Lorraine.

3.3.2.8.3 Gelatin-labelling with RITC/FITC

The final chosen protocol for gelatin labelling with isothiocyanate dyes (RITC or FITC) was adding a FITC (or RITC) solution (2 % w/v in DMSO) directly to a 25 wt% gelatin solution, in a final concentration of 0.1 wt %, and stirring during 2 h at 40 °C.

3.3.2.8.4 Fluorescence Emission of Genipin-Crosslinked Emulsions

A 8% Gel/ 20% MD (5 mM Genipin) and a 10% Gel / 8% MD (5 mM Genipin) solution was prepared, with the former having maltodextrin, the latter gelatin as continuous phase. The emulsions were mixed for 20 min at 60 °C allowing crosslinking to occur. After 10 s of vortexing the samples were observed under the microscope in both phase contrast and fluorescence mode with the U-MWG2 Filter (Figure 3.4).

3.3.3 Phase Behaviour of Water/Gelatin/Maltodextrin System

3.3.3.1 Determination of Phase Diagram

Mixtures of gelatin and maltodextrin at different concentrations were prepared in order to study their phase behaviour. The 25 wt% gelatin stock solutions were prepared by dispersing gelatin into cold water and then stirred continuously at 60 °C during 30 min. For the 30 wt% maltodextrin stock solutions, maltodextrin was dispersed into cold water and stirred continuously at 95 °C during 30 min. The gelatin and maltodextrin stock solutions at 50 °C were mixed together with water, to obtain samples of gelatin concentrations ranging between 0-12 wt% and maltodextrin of 0-22 % wt. The samples were prepared in 5 mL glass vials and filled up to a total weight of 4 g, by adding first water, then maltodextrin and finally gelatin.

After vortexing the samples during 10 seconds, the samples were placed into a thermostated bath at 50 °C constant temperature, for a period of 5 days. Phase separation of the two liquid phases was determined by carefully taking the sample out of the water bath and observing visually if two liquid phases could be distinguished. As gelatin has a more yellowish and turbid colour, probably due to impurities in the product, it could be distinguished from the more colourless maltodextrin phase. By slightly tilting the sample it could be analysed whether the samples contained a solid precipitate at the bottom. For some samples the white precipitate did not accumulate at the bottom of the sample, but was located at the interphase between the two liquid phases.

3.3.3.2 Study of Influence of Temperature on Phase Behaviour

The influence of temperature on the position of the binodal line was investigated. Presence of a solid precipitate was not taken into account in this study, but focus was laid on whether the mixture was composed of one or two liquid phases. Therefore, the samples, prepared as mentioned above, were vortexed during 10 seconds and then put into the thermostated bath at 60 °C. As soon the samples equilibrated (at least 5 h), phase behaviour was observed. Then temperature of the water bath was changed to 52.5 °C, the samples vortexed again and the sample was equilibrated again for 5 h. The procedure was repeated for 45 °C.

3.3.3.3 Turbidity Study of Gelatin/Maltodextrin Mixtures

The stability of some gelatin/maltodextrin emulsions was assessed from multiple light scattering measurements by means of a Turbiscan™ Lab Expert (Formulation) at constant temperature (50 °C) and $\lambda = 880$ nm. For this purpose 18 g of sample were introduced in a glass measurement cell tightly stoppered to avoid solvent evaporation. The sample was thoroughly shaken by hand and introduced into the measuring instrument. Transmission and backscattering data were acquired for a period of 5 days.

3.3.3.4 Raman Spectroscopy of Maltodextrin/Gelatin Mixtures

Raman spectra were obtained at room temperature using a confocal micro-Raman (Jobin-Yvon LabRam HR 800), coupled to an optical microscope (Olympus BXM). The micro-Raman was equipped with a Laser Diode (TEC-120 de Sacher Lasertechnik) emitting at $\lambda = 785$ nm. Radiation power was 6 mW.

Gelatin and maltodextrin samples, in solid powder form, and the precipitate of several gelatin/maltodextrin emulsions, were analysed. The precipitate was obtained from emulsions by the following preparation procedure:

The 25 wt% gelatin stock solutions were prepared at 50 °C and maltodextrin stock solutions were prepared at 30 wt% at 95 °C. Both solutions were stirred during 0.5-1h and prepared in tightly sealed glass vial to avoid water evaporation. The gelatin and maltodextrin stock solutions at 50 °C were mixed together with milliQ water to obtain samples of gelatin concentrations ranging between 3 and 12 wt% and maltodextrin of 5 and 20 wt%. The final solutions were mixed with a magnetic stirrer during 5 min at 50 °C and then placed into a thermostated bath at 50 °C constant temperature, for a period of 5 days. The precipitate formed after 5 days was recovered with a pipette and dried in an oven at 50 °C overnight to determine its chemical composition by Raman spectroscopy.

3.3.3.5 Observation of Emulsions by Optical Microscopy

Gelatin-Maltodextrin mixtures of various concentrations and parts of the phase diagram were prepared and their morphology observed under the microscope. For microscopy images, the sample were stirred for 5 min at 500 rpm at 50 °C and observed under the microscope.

3.3.4 Gelatin Microgel Preparation

3.3.4.1 Microgel Preparation

The 25 wt% gelatin stock solutions were prepared by dispersing gelatin into cold water and then stirred continuously at 60 °C during 30 min. For the 30 wt% maltodextrin stock solutions, maltodextrin was dispersed into cold water and stirred continuously at 95 °C during 30 min. Genipin stock solutions were prepared at varying concentrations, lower than 8 mg/ mL in order to assure total solubility of genipin in the solution. Those solutions were mixed together at 50 °C with water in a glass vial, in the following order: First water, maltodextrin solution, genipin solution and finally the gelatin solution. Proportions of each solution were adapted to get the final concentration of choice. The mixture was then mixed by homogenisation using an Ultra-Turrax® homogenizer. Then, the dispersions were continuously stirred at ~500 rpm with a magnet stirrer, in order to allow gelatin-genipin crosslinking reactions to occur. Conditions of mixing varied, according the experiment, and will therefore be specified in the concerned sections.

Finally, the sample vials were immersed for 1 min at 0 °C and then samples were diluted by adding 0 °C cold water (twice the sample volume) to the mixture. Figure 3.6 summarises the preparation method of the microgels.

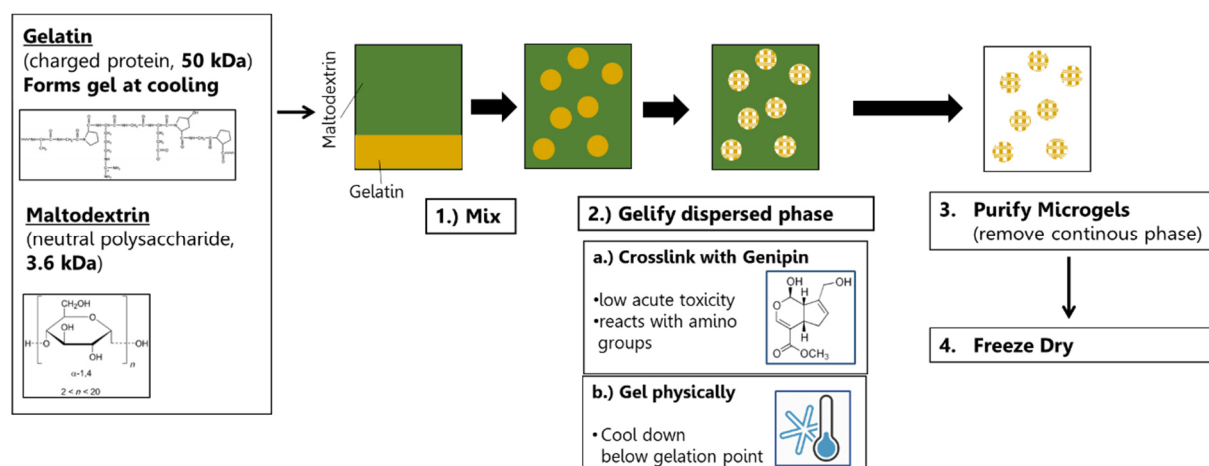


Figure 3.6. Preparation method for obtaining a stable microgel suspension from a gelatin-maltodextrin emulsion, crosslinked with genipin.

3.3.4.2 Purification Methods of Microgels

After obtaining a stable microgel suspension, the continuous phase was intended to be removed by three distinct methods. For those purification experiments, microgels of 4.5% Gel / 13% MD (1 mM Genipin) were used. After preparation of the mixtures they were homogenised for 1 min at 9,500 rpm, then continuously stirred with a magnet stirrer at 60 °C for 20 min, in order genipin has time to form some initial crosslinks in the droplets. Then, the sample was cooled down in an ice bath during 1 min and finally diluted by adding 0 °C cold water (twice the sample volume) to the mixture.

After vortexing the samples the purification experiments were started.

Filtration:

Around 1 mL of the sample was taken with a syringe and passed through a polycarbonate filter, with the help of a mini-extruder (Avanti Polar Lipids Inc., Alabaster, AL). A filter pore size of 10 µm was

used. Assuming the microgels remained on the filter, the filter was immersed into water at room temperature (23 °C) and stirred during 4 h to remove mechanically the microgels from the filter surface. The solution was kept for analysis or freeze-drying.

Dialysis:

Around 5 mL of the sample was put into the dialysing tube (Nominal MWCO: 12 kDa, (CelluSep, T3-25-15)). Using this pore size, maltodextrin (3.6 kDa), which is supposed to be in the continuous phase, is able pass the membrane, while bigger-sized gelatin (50 kDa) and microgels will remain inside the dialysing tube. The tube was immersed for 4 h into ~800 mL of water (25 °C) which was continuously stirred. The water was then exchanged with fresh one and the dialysis continued for 22 h. The solution remaining inside the dialysis tube was removed and kept for analysis or freeze-drying.

Centrifugation:

Microgels were purified by a simple centrifugation-resuspension method. First, gelatin microgel suspensions were sedimented by centrifugation at soft conditions (if not otherwise noted: 10 min, 2000 rpm, 5 °C) and the supernatant, rich in maltodextrin, was extracted. Then, the same volume of purified milliQ water was added to replace the previous supernatant. The microgels were then redispersed again by gentle agitation. This purification procedure was repeated once more.

3.3.4.3 Freeze-Drying of Microgels

To freeze-dry the samples, liquid samples were frozen in a carbon-ice/acetone mixture, if not mentioned otherwise. In one experiment the samples were frozen in liquid nitrogen and compared with the freezing method using a carbon-ice/acetone mixture. The vials were agitated inside the freezing medium till the entire sample was frozen. The lid was removed, replaced by a perforated plastic paraffin film and consequently introduced into the freeze-dryer (Christ Alpha 2-4 LD Plus). Samples were kept there till they were totally dried.

3.3.4.4 Observation of Freeze-Dried microgels under SEM

Dried samples were put onto a carbon conductive adhesive tape and introduced into the SEM microscope. The sample chamber was vacuumed and then imaging initiated by turning the electron beam on. Structure and morphology of the microgels were characterised.

3.3.4.5 Resuspension of Freeze-Dried Microgels

To observe the morphology of microgels after resuspension, dried samples were suspended by manual shaking in some mL of water and subsequently observed under the microscope.

3.3.5 Characterisation of Microgel Particles

3.3.5.1 Study of Influence of time between emulsification and cooling down

To analyse whether the time between emulsion mixing and cooling down, to achieve droplet gelation, had an effect on final sample morphology or droplet size, 3 % Gel/ 20 % MD emulsions were prepared and mixed at 500 rpm for 30 min at 30 °C. Stirring of the samples was stopped and 0, 0.5, 1 or 5 min was waited till the samples were transferred to an ice bath. They were kept there for 1 min and then diluted with twice the sample volume of 0 °C water. Finally, microscopic analysis of the microgels was performed.

3.3.5.2 Size Determination of Emulsion Droplets / Microgels by Microscope

Particle size was determined by using an optical microscope (Olympus model BX51TRF-6, coupled to a digital camera Olympus DP73) fitted with a calibrated micrometer scale. Image analysis of the micrographs was performed using Image J software and size distribution was obtained from measuring a minimum of 300 particles.

3.3.5.3 Size Determination of Microgels by Light Diffraction Particle Size Analyser

Microgel droplet size distribution was measured by light diffraction, with the help of the light diffraction particle size analyser (Mastersizer 2000). This technique is based on the analysis of the backscattered and diffraction intensity of monochromatic light (red light, $\lambda=640$ nm and blue light $\lambda=466$ nm were used in our case) inciting onto the sample. The bigger the diffraction angle is, the smaller the particle size (de Boer, de Weerd, Thoenes, & Goossens, 1987). Calculations to obtain the particle size distribution from the diffraction pattern are based on the Mie theory (Mie, 1908), which considers that all particles are spherical. For the measurements, several optical properties have to be known: the refractive index and absorption of the particles and the refractive index of the medium, into which they are dispersed.

Based on the particle volume distribution for the different particle diameters, the volume mean diameter (de Brouckere mean diameter), $D[4,3]$, and the polydispersity *Span* are calculated and defined as:

$$D[4,3] = \frac{\sum d^4}{\sum d^3} \quad (3.7)$$

where d is the diameter of the drop.

$$Span = \frac{d(0,9) - d(0,1)}{d(0,5)} \quad (3.8)$$

where $d(0,1)$, $d(0,5)$ and $d(0,9)$ are the droplet diameters at 10, 50 and 90 %, respectively, of the total accumulated volume distribution.

For the measurements, microgels based on 3 % Gel / 20 % MD (1 mM Genipin) emulsions were prepared. The emulsion was therefore homogenised by Ultra-Turrax® for 1 min at 9500 rpm, then mixed

at 500 rpm for 20 min at 60 °C. The rest of the procedure and purification method was performed as usual.

The refractive index (RI) of the microgels was determined (after removal of the suspension medium after centrifuging) by a refractometer and corresponded to 1.341. The absorption index was defined as 0.1, in agreement with various studies (Kong et al., 2011), and it was the absorption index which gave the best residual (measure of fit between calculated and measured scattering profile of sample). The refractive index used for the continuous phase, water, was 1.33.

The microgel suspension was introduced into the dispersing unit, which contained water, and was stirred at 10,000 rpm. Volume particle size distribution, $D[4,3]$ and *Span* were obtained from the laser diffraction measurements at 0h, 24 h, 1 week and after 1 month.

Besides light diffraction measurements, microscopic images of the samples were taken and the size distribution of microgels obtained from over 500 particles. To obtain their volume distribution, the number particle size distribution was transformed into a volume distribution by calculating the volume (assuming spherical microgels) at each particle size interval. Furthermore, using equation (3.7) and (3.8), the volume mean diameter $D[4,3]$ and *Span* were calculated, based on the microgel size measurements under the microscope.

3.3.5.4 Study of the Influence of Preparation Parameters on Microgel Size

3.3.5.4.1 Influence of Emulsion composition on microgel size

Microgels, were prepared from various gelatin/maltodextrin emulsions and compared. Emulsions with 3, 4.5 or 6 wt% of gelatin, mixed with 13, 16 or 20 wt% maltodextrin were used. The crosslinker concentration was 1 mM genipin. After mixing the emulsions with the Ultra-Turrax® homogenizer for 1 min at 9500 rpm, they were stirred for 20 min at 500 rpm at 60°C. Finally, they were cooled down to obtain microgels.

The size and morphology of the samples was analyzed and compared by microscopy observations.

3.3.5.4.2 Influence of Ultra-Turrax® Speed on Droplet Size

8% Gel / 20% MD samples were prepared at 50 °C and then homogenised for 1 min at 7,500 rpm or 9,500 rpm and for 30 s (not 1 min due to foaming of sample) at 13,500 or 19,500 rpm. Samples were directly cooled for 1 min in an ice bath and then diluted with twice the sample volume of water. Finally, their size distribution was determined.

3.3.5.4.3 Influence of Emulsification Temperature on Droplet Size

To analyse whether mixing temperature had an effect on emulsion droplet size and morphology, 3 % Gel/ 20 % MD emulsions were prepared and mixed at 500 rpm for 30 min at three different temperature conditions: 30, 45 or 60 °C. The samples were directly cooled for 1 min in an ice bath and then diluted with twice the sample volume of water. Finally microscopic analysis of the microgels was performed and their size distribution determined.

3.3.5.4.4 Comparison of the two media (PEM and Water)

Emulsions with as solvent PEM buffer, instead of water, were prepared. Stock solutions of gelatin and maltodextrin were thus also prepared in PEM buffer at pH 6.5. A 3% Gel/ 20% MD emulsion was prepared, stirred for 30 min at 500 rpm, at 30, 40 or 60 °C. The emulsion was then cooled down in ice for 1 min and finally diluted by adding 0 °C cold PEM buffer (twice the sample volume) to the mixture. The size and morphology of the microgels were analysed by microscope and compared to samples prepared by the same way, but in water, instead of PEM buffer.

3.3.5.4.5 Crosslinker Concentration

First, crosslinking at milder temperature conditions was investigated in this experiment. 4.5% Gel/ 13% MD mixtures were prepared with different concentration of Genipin (0.1, 1 and 10 mM Genipin). The samples were stirred at 9500 rpm by homogenisation using an Ultra-Turrax® homogenizer, then the dispersions were continuously stirred at 500 rpm with a magnet stirrer for 24 h at 25 °C. After 24 h, their morphology was observed under the microscope.

Second, 3 % Gel/ 20 % Mal emulsions were prepared in PEM buffer with 0, 0.1, 1 or 5 mM Genipin. The samples (40 °C) were stirred 1 min at 9,500 rpm, and then mixed for 30 min at 40 °C (500 rpm) to promote crosslinking. After rapid cooling down in ice and dilution with PEM buffer (twice sample volume), the microgels were purified by centrifugation. The microgel solutions were kept in the fridge (4 °C) and their size followed, by microscopy observations, over a period of 1 month.

3.3.5.4.6 Long Term Stability of Microgels

A 4.5% Gel/ 13% MD (1 mM Genipin) emulsion was stirred by Ultra-Turrax® homogenizer (1 min, 9500 rpm) and crosslinked during 20 min at 60 °C (mixing at 500 rpm) and kept for 500 days in the fridge (4 °C) and analysed at various time points microscopically.

3.3.5.5 *Study of the Influence of Physicochemical Parameters on microgel size/morphology*

3.3.5.5.1 Influence of pH on Microgel size

The aim was to investigate the influence of pH on the swelling behavior of the microgels. The pH was adjusted by using an universal pH Buffer, the Davies buffer (Davies, 1959), which was prepared as follows:

Davies Stock Solution

In water:

0.1 M Citric Acid ($C_6H_8O_7$)

0.1 M Potassium dihydrogen orthophosphate (KH_2PO_4)

0.05 M Sodium tetraborate ($Na_2B_4O_2$)

0.1 M Tris(hydroxymethyl)aminomethane (TRIS)

0.1M Potassium Chloride (KCl)

Solutions for pH adjustment

0.4 M NaOH and 0.4 M HCl solutions in water.

Final solutions were prepared as detailed in Table 3.3.

Table 3.3. Preparation of Davies Buffer of different pH.

| pH | Davies Stock solution [mL] | 0.4 M HCl [mL] | 0.4 M NaOH [mL] | Water [ml] | Ionic Strength [M] | Osmolarity [osmol/L] |
|-------|----------------------------|----------------|-----------------|------------|--------------------|----------------------|
| pH 2 | 25 | 17.4 | - | 57.6 | 0.17 | 0.33 |
| pH 3 | 25 | 9.8 | - | 65.2 | 0.15 | 0.27 |
| pH 4 | 25 | 5 | - | 70 | 0.13 | 0.23 |
| pH 5 | 25 | - | 0.2 | 74.8 | 0.12 | 0.19 |
| pH 8 | 25 | - | 16.6 | 58.4 | 0.27 | 0.32 |
| pH 11 | 25 | - | 32.8 | 42.2 | 0.3 | 0.40 |

The microgels were prepared as usual from a 3% Gel / 20% MD (1 mM Genipin) emulsion. The emulsion was homogenised for 1 min at 9500 rpm, using an Ultra-Turrax® homogenizer and then stirred for 20 min at 500 rpm at 60 °C. The solutions were cooled down for 1min at 0°C and diluted with 3 times the sample volume of ice-cold water. The microgel suspensions were centrifuged at 2000 rpm (10 min at 10 °C), the supernatant removed, replaced with fresh water, and centrifuged a second time in same conditions. The supernatant was then replaced with the Davies Buffer, prepared as described in Table 3.3, or water (for the control sample) and consequently stored for 2 weeks at 4 °C.

At various time points, particle size was determined by measuring the diameter using an optical microscope fitted with a calibrated micrometer scale. Image analysis of the micrographs was performed using Image J software and size distribution was obtained from a minimum of 300 measurements.

3.3.5.5.2 Influence of Salt Concentration on Microgel swelling

The aim was to investigate if swelling at different pH was caused due to the pH or by the difference in osmotic pressure and ionic strengths of the different pH solutions. Therefore, NaCl solutions of different

osmolarities and ionic strength were prepared. Microgels, based on 3% Gel/ 20% MD (1 mM Genipin) emulsions, were prepared, in the same way as in the assays to test influence of pH onto microgel swelling. After the second purification by centrifugation the supernatant was replaced by following solutions (Table 3.4):

Table 3.4. Solutions of different osmotic pressures used to test influence of osmolarity/ionic strength on microgel swelling

| Solution | Osmolarity [osmol/L] | Ionic Strength [M] |
|-----------------|---------------------------------|-------------------------------|
| Water | 0 | 0 |
| 0.1 M NaCl | 0.2 | 0.1 |
| 0.2 M NaCl | 0.4 | 0.2 |

At various time points, particle size was determined by measuring the diameter using an optical microscope.

3.3.5.5.3 Stability of Microgels at 37 °C and in Simulated Gastric Fluid

Microgels were prepared in water from a 3 % Gel / 20 % MD emulsion with 0, 1 or 5 mM Genipin and stirred during 90 min at 30 °C to allow crosslinking to occur. After purification, the microgels were redispersed or in water or in simulated gastric fluid (SGF). The composition of the SGF can be found in Table 3.2, and was adapted from a standard protocol (Minekus et al., 2014). The solutions containing microgels were stirred during 2 h at 500 rpm at 37 °C and consequently observed under the microscope.

3.3.6 Encapsulation of Enzymes into the Gelatin Microgels

3.3.6.1 Measurement of Enzyme Activity

β -Gal enzyme was in most cases dissolved into a Phosphate-EDTA-Magnesium (PEM) buffer, which offers favorable conditions for the enzyme. It consists of a phosphate buffer, magnesium, which serves as a cofactor to the enzyme and EDTA which binds traces of ions strongly competing with binding of magnesium. The exact composition of the PEM buffer (pH 6.5) can be found in Table 3.1.

β -Gal activity was determined with the ONPG assay. Ortho-Nitrophenyl- β -galactoside (ONPG) has a similar molecular structure as lactose and can be hydrolysed by lactase (β -Gal). β -Gal usually hydrolyses the disaccharide lactose to its monosaccharide components glucose and galactose. If using ONPG, instead of lactose, β -Gal catalyses the cleavage of ONPG into glucose and ortho-nitrophenol (ONP), which can be determined spectrophotometrically, by measuring its absorbance at $\lambda=420\text{nm}$ (Figure 3.7).

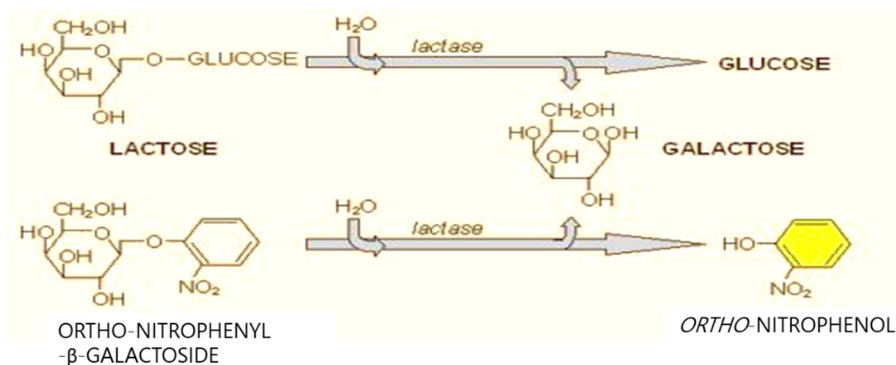


Figure 3.7. Hydrolysis of ortho-nitrophenyl- β -galactoside by lactase forms galactose and ortho-nitrophenol, which gives a yellow colour and can be detected and quantified by UV-Spectroscopy ($\lambda=420$ nm).

Therefore, 0.5 mL of enzyme-containing sample was reacted with 2.5 mL of a 40 mM ONPG solution (in PEM buffer) at 30 °C. The reaction took place inside a sample tube, under constant stirring (500 rpm) till absorption was in the range between 0.2-1. Samples were diluted accordingly, in order those absorption values were reached between 5 and 25 min. When reaching these absorption conditions, the reaction was stopped with a 1 mL of a sodium carbonate pH 11 solution containing 0.5 M Na_2CO_3 and 0.13 M EDTA. The activity was determined as the formation rate of the product ONP, by using Lambert-Beers law and dividing by the reaction time:

$$\text{Enzyme Activity [kat]} = \frac{\Delta_{\text{abs}} \cdot 8 \cdot V}{\varepsilon \cdot t \cdot d} \quad (3.9)$$

$$\text{Specific Enzyme Activity [kat/g]} = \frac{\Delta_{\text{abs}} \cdot 8 \cdot DF}{\varepsilon \cdot t \cdot d} \quad (3.10)$$

- Δ_{abs} is the absorbance of the sample after subtracting the background.
- V is the volume of the sample
- DF is the dilution factor of the enzyme in the sample measured.
- The factor 8 is the dilution of the sample with the reaction solutions (ONPG and sodium carbonate solution)
- ε is the extinction coefficient of ONP. Found by recording standard curve of ONP (see below)
- t is the time of the reaction in seconds
- d is the cuvettes diameter in centimeter

Enzyme activity is described either in the SI unit katal (1 kat = 1 mol s⁻¹), or as this unit is very large, the enzyme unit (U), which corresponds to 16.67 nanokatals. We will stick to the SI unit.

The extinction coefficient of ONP was determined by forming a calibration curve of the product ONP at different concentrations. The determined extinction coefficient of ONP $4.33258 \cdot 10^6 \text{ M}^{-1}\text{cm}^{-1}$ (see Figure 8.1 in the annex).

As a blank sample, 0.5 mL of the sample was mixed with 1 mL of a sodium carbonate pH 11 solution, to deactivate the enzyme. Then 2.5 mL of ONPG solution was added to the mixture and mixed.

3.3.6.2 Measurement of Enzyme Concentration

Enzyme concentration was determined by two different methods. First, by measurement of UV-absorption at the, for protein typical, wavelength around 280 nm, and second, using the Bradford assay.

3.3.6.2.1 Protein Absorption at 280 nm

Enzyme quantity was determined by measuring the UV-Absorption of the enzyme β -Gal at different concentrations (dilution in PEM buffer). A calibration curve at the absorption maximum of 280 nm was determined to estimate if this method is valid as a quantification assay of the enzyme.

Next, a 3 % Gel / 20 % MD emulsion in PEM buffer, containing enzyme with a total concentration of 0.36 mg/mL (70-fold dilution of stock solution), was prepared (mixing 5 min at 30 °C). The emulsion was cooled down and diluted to obtain microgels. The microgel suspension was purified by centrifugation and the supernatant kept. The UV-VIS absorption of the enzyme solution added to the emulsion, and the supernatant of the microgels was taken, to determine enzyme quantity inside them.

3.3.6.2.2 Bradford Protein Assay

The Bradford Protein Assay (Bradford, 1976), a standard protein quantification assay, was used in another approach to measure enzyme quantity. The assay is based on the shift of the absorbance maximum of Coomassie Brilliant Blue G-250 from 465 nm to 595 nm when binding to protein occurs. Thereby 100 μ L of sample is mixed during 5 min with 5 mL of filtered Bradford reagent at room temperature. Within 30 min after mixing the absorption at 595 nm was measured. As a blank sample 100 μ L of solvent, free from protein, was mixed with the Bradford reagent.

A calibration curve of Bovine Serum Albumin (BSA), used as a model protein, and β -Gal, was performed under three different conditions, for concentrations between 0 and 1 mg/mL:

- a.) Protein in PEM buffer
- b.) Protein in a 3 wt% Gelatin (in PEM buffer) solution
- c.) Protein in the supernatant of a microgel suspension, produced from a 3% Gel / 20% MD emulsion, after its first purification step by centrifugation

3.3.6.2.3 Fluorescent Labelling of Enzyme with FITC

For labelling of the enzyme, the β -Gal solution was diluted tenfold in a 0.1 M sodium carbonate buffer (pH 10), consisting of 1:1 mixture of ratio 1:1 of 0.1 M NaHCO_3 and Na_2CO_3 . A FITC solution (0.2% w/v in DMSO) was added to the enzyme solution with a final concentration of 5 vol% and the mixture stirred during 2h at 20°C. Excess free fluorescent dye was removed by passing the mixture through a Sephadex G-25 size-exclusion chromatography column and washing with PEM buffer. To determine the degree of labelling, the absorbance of the labelled enzyme was measured.

First, the enzyme concentration was calculated:

$$\text{Enzyme concentration [M]} = \frac{[A_{280} - (0.3 \cdot A_{494})] \cdot DF}{\epsilon_{enzyme}} \quad (3.11)$$

Where A_{280} and A_{494} are the absorbance of the labelled enzyme at 280 and 494 nm and ϵ_{enzyme} is the extinction coefficient of the enzyme at 280 nm, which corresponds to 185355 $\text{M}^{-1}\text{cm}^{-1}$ (data from manufacturer). 0.3 is a correction factor included to compensate for absorption of FITC at 280 nm. DF is the dilution factor.

And the degree of labelling was calculated as follows:

$$\text{Dye per enzyme molecule} = \frac{A_{494} \cdot DF}{\epsilon_{FITC} \cdot \text{enzyme concentration}} = \frac{\epsilon_{enzyme} \cdot A_{494}}{\epsilon_{FITC} \cdot [A_{280} - (0.3 \cdot A_{494})]} \quad (3.12)$$

Where ϵ_{FITC} corresponds to the extinction coefficient of FITC at 494 nm, and corresponds to 68000 M⁻¹cm⁻¹ (data from manufacturer).

3.3.6.3 Study Enzyme Compatibility of Crosslinker and Microgels

3.3.6.3.1 Enzyme Activity in Presence of Genipin and Gelatin

The enzyme was added to a PEM buffer solution containing 0, 5 or 10 wt% gelatin and 0, 1 or 10 mM genipin, with a final enzyme stock solution concentration of 31 µg/mL. The solutions were mixed during a period of 30 min at 37 °C. 0.5 g of each solution was taken and placed into a vial, which was stored during 3 h at 4 °C. The specific activity of the solutions were tested with the ONPG assay.

3.3.6.3.2 Enzyme Activity in Suspension of Crosslinked Microgels

Microgels with 0 and 10 mM genipin were prepared from 3% Gel / 20% MD emulsions (crosslinking by stirring 20 min at 40 °C). After purification of the microgels, they were redispersed in PEM buffer and mixed with an enzyme solution in PEM buffer, with a final enzyme stock solution concentration of 31 µg/mL. The samples were mixed, kept at the fridge at 4 °C and their activity determined with ONPG assay, at 3 h, 2 days and 2 weeks.

3.3.6.4 Different Encapsulation Methods

For the purpose of introducing the enzyme lactase into the microgel particles, 3% Gel / 20% MD emulsions in PEM buffer were used and homogenised by stirring at 500 rpm. The temperatures of treatment were selected, taking into account the temperature sensitiveness of gelatin gelation and enzyme activity. For this reason, solutions of gelatin and enzyme were mixed at 35°C, emulsions were treated with genipin at 30°C, and gelatin microgels were treated at 25°C. The rest of the preparation procedure (gelation of gelatin droplets and purification of microgel suspension) was the same, as detailed above.

Three different methods (summarised in Table 3.5 and Figure 3.8) were tested to incorporate enzymes into the microgels, with the main objective to maximise encapsulation yield and minimising activity loss of enzyme. The differences between the methods are the moment at which the enzymes or genipin was added.

Table 3.5. Preparation methods of enzyme-loaded microgels. Details in the text.

| | Method Gen(E)/Enz(M) | Method Gen(E)/Enz(E) | Method Gen(M)/Enz(E) |
|-----------------------------|---------------------------------|---------------------------------|---------------------------------|
| Addition to Emulsion | Genipin | Genipin + Enzyme | Enzyme |
| Addition to Microgel | Enzyme | - | Genipin |

- *Addition of enzyme after microgel formation (Method Gen(E)/Enz(M)):*
First, microgels were prepared by mixing the emulsion during 90 min at 30 °C and then cooling it down.
 - a) *Adding enzymes to a microgel suspension:*
Enzyme was added to the 0°C cold PEM buffer, in the last step of microgel production, the dilution of cooled-down emulsions. The solution was consequently stirred with a magnet during 3h at 25 °C.
 - b) *Rehydrating freeze-dried microgels with an enzyme solution*
Microgels were purified and freeze-dried. 40 mg of freeze-dried microgels were mixed with the enzyme solution in PEM buffer for 2 h at 0 °C.

- *Addition of enzyme before microgel formation:*
 - *Crosslinking during emulsification (Gen(E)/Enz(E))*
The enzyme was stirred together with the gelatin stock solution during 3h at 35°C. After addition of both maltodextrin and genipin solutions, at 30°C, the 3% Gel / 20% MD emulsion was formed and microgels were prepared as detailed above.

 - *Crosslinking after microgel formation (Method Gen(M)/Enz(E)):*
Enzyme-loaded microgels were crosslinked after their formation, by adding genipin to the 0°C cold PEM buffer, in the last step of microgel production. Afterwards, the mixture was stirred with a magnet during 3h at 25 °C.

Finally, the free enzyme remaining in the continuous medium was removed by centrifugation, removing of the supernatant (kept for further analysis) and resuspension of the microgels into fresh PEM buffer.

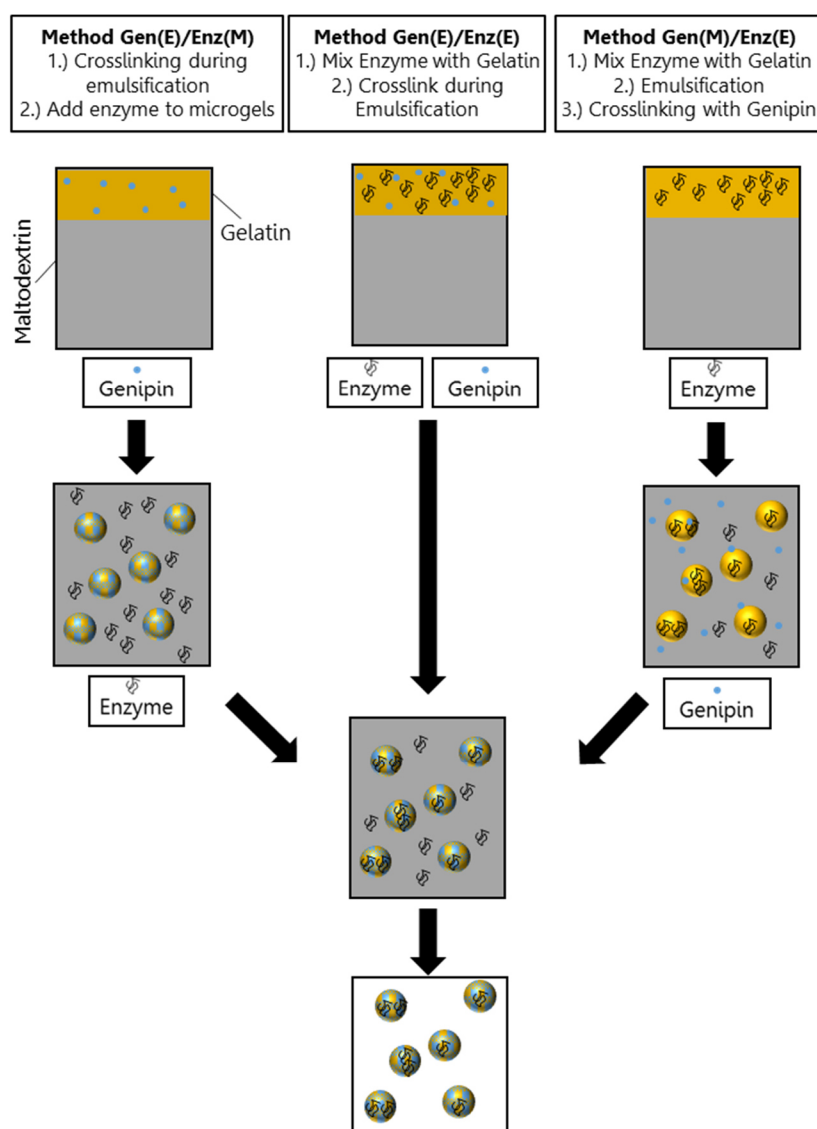


Figure 3.8. Illustration of the three different preparation methods of enzyme-loaded microgels.

To analyse enzyme encapsulation efficiency, the enzymes were fluorescently labelled and their concentration or their activity determined.

Additional details of above-mentioned preparation methods are explained below:

Encapsulation efficiency determined by enzyme activity:

In all cases the final enzyme concentration in the microgel suspension corresponded to approximately 1610x dilution of the enzyme stock solution, which results in an enzyme activity of 70 nkat/g.

Only exception was the Method Gen(E)/Enz(M), with freeze-dried microgels: enzyme activity in the microgel suspension corresponded to 8 nkat/g (enzyme stock solution was diluted 14430 times).

Enzyme activity with the ONPG-assay after encapsulation was determined in the supernatants remaining from the washing steps and in the microgels.

Encapsulation efficiency determined by Bradford assay:

Only Method Gen(E)/Enz(M) was tested. Microgels were prepared by mixing during 20 min at 60 °C. First, samples were purified twice by centrifugation and redispersion into PEM buffer. PEM buffer was removed and replaced with 3 mL 0.7 mg/mL enzyme solution in PEM buffer (36x dilution of enzyme stock solution). After 2 h stirring at 0 °C, the suspensions were twice purified by centrifugation and redispersion into 3 mL PEM buffer.

Enzyme quantity was determined by the Bradford assay in the enzyme solution added to the microgels, and in the supernatants remaining from the washing steps and in the microgels.

Encapsulation efficiency determined by fluorescently labelled enzymes:

Final concentration of Lactase-FITC in microgel suspension was 0.48 mg/mL (200 μ l of lactase-FITC inside total volume of 2 mL of microgel/emulsion). Location of the fluorescently-labelled was observed under the microscope, using the U-MWB2 Wide Band Blue Fluorescence Filter (excitation filter 460-490 nm, emission filter >520 nm) (Figure 3.4 a).

3.3.6.5 Determination of Enzyme Encapsulation Efficiency

Figure 3.9 illustrates the distribution of active and inactive enzyme in microgel solution, on basis of which the percentage of active enzyme, the encapsulation yield and the activity recovery were calculated. The definitions of these parameters were adapted from literature (Sheldon & van Pelt, 2013).

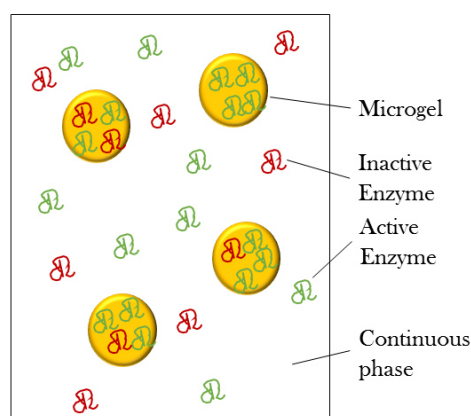


Figure 3.9. Illustration of a microgel solution, before purification, containing active and inactive enzymes within the microgels and the continuous phase (=supernatant, when purifying by centrifugation).

- Percentage of active enzyme was calculated as the ratio of the total enzyme activity (A_{tot}) in the sample containing the crosslinker genipin, with respect to the total enzyme activity in the control sample (without genipin) ($A_{tot}(control)$).

$$\text{Percentage of active enzyme (\%)} = \frac{A_{tot}}{A_{tot(control)}} \cdot 100 \quad (3.13)$$

- Encapsulation yield of the enzyme was determined by calculating the ratio of the enzyme activity within the microgel dispersions A_{mg} in respect to the total enzyme activity A_{tot} (calculated as the sum of the activities of supernatants A_{sn} and microgel particles A_{mg}). This calculation assumes that the ratio of active/inactive enzyme is the same inside and outside the microgel particles.

$$\text{Encapsulation yield (\%)} = \frac{A_{mg}}{A_{sn} + A_{mg}} \cdot 100 = \frac{A_{mg}}{A_{tot}} \cdot 100 \quad (3.14)$$

- Activity recovery of encapsulated enzyme was calculated as the product of encapsulation yield and percentage of active enzyme.

$$\text{Activity recovery (\%)} = \frac{A_{mg}}{A_{tot}} \cdot \frac{A_{tot}}{A_{tot(control)}} \cdot 100 = \frac{A_{mg(sample)}}{A_{tot(control)}} \cdot 100 \quad (3.15)$$

3.3.6.6 Enzyme Long-Term Stability in Microgels

Enzyme-loaded microgels produced with method Gen(E)/Enz(E) (with genipin concentration of 5 mM Genipin, 30 and 90 min crosslinking) were stored during a period of 30 days in the fridge at 4°C. The activity of the microgel suspension was tested at 0, 7 and 30 days.

To quantify the amount of enzyme which remained inside the microgels, and determine how much was released from them during storage, the microgel suspension was centrifuged after 7 days storage and enzyme activity was determined in the supernatant and inside the microgels.

3.3.6.7 Freeze-Drying of Enzyme-Loaded Microgels

Enzyme-loaded microgels were produced with method Gen(E)/Enz(E) (with genipin concentration of 0 and 10 mM Genipin, 90 min crosslinking). Their activity was measured before freeze-drying and subsequently the particles were freeze-dried. To freeze-dry the samples, liquid samples were frozen in a carbon-ice/acetone mixture. The vials were agitated inside the freezing medium till the entire sample was frozen. The lid was removed, replaced by a perforated plastic paraffin film and consequently introduced into the freeze-dryer (Christ Alpha 2-4 LD Plus). To determine the effect of the drying process, the microgel powder was redispersed into the same amount of PEM buffer and the activity of the suspension determined with the ONPG assay.

3.3.6.8 Study of Enzyme stability under simulated gastric pH and body temperature conditions

Enzyme-loaded microgels were prepared with method Gen(E)/Enz(E) , with various concentrations of genipin. Either water or PEM buffer was used as solvent for the entire preparation process. After purification, they were immersed at a ratio 1:10 into SGF, which had a pH 3 (Table 3.2). This mixture was then stirred for 2 h at 37 °C and activity was determined as a function of time with the ONPG assay.

Chapter 4

RESULTS AND DISCUSSION

4 Results and Discussion

The goal of this work is to form crosslinked microgels, as a delivery vehicle for enzymes. For a number of advantages, detailed in the introduction, water-in-water (W/W) emulsions have been used as templates to prepare the microgels. Sodiumcarboxymethyl cellulose (NaCMC) /bovine serum albumin (BSA) and gelatin/maltodextrin emulsions will be used therefore.

As a first step, preliminary studies will be done with the W/W emulsion system consisting of NaCMC and BSA. This system will be evaluated for its use as template of enzyme-loaded crosslinked NaCMC microgels.

Next, for the gelatin/maltodextrin system our aim will be to first characterise the properties of the individual polymers, test methods to identify or quantify them, and evaluate how the crosslinking mechanism of genipin functions. After that, the phase behaviour of the polymer mixture will be investigated, and methods to prepare microgels from the emulsions and the properties of those will be studied. Finally, the immobilisation methods of the enzyme and its stability will be tested.

4.1 NaCMC/BSA Emulsions as Template for Microgel Formation

Sodium carboxymethylcellulose (NaCMC) has been chosen as a pH-sensitive biopolymer, which remains stable under acidic pH conditions found in the gastric environment. Its carboxylic groups remain protonated under acidic conditions, reducing its solubility, and making it able to form gels. Under more neutral conditions, found in food or the intestine, NaCMC gels remain stable if crosslinked with multivalent cations, creating bridges between the negatively charged carboxylic groups. Therefore, W/W emulsion with NaCMC in the dispersed phase was formed by mixing with Bovine Serum Albumin (BSA) and in a second step, the NaCMC droplets were crosslinked to obtain NaCMC microgels. Those NaCMC microgels could be potentially used as oral delivery vehicle for enzymes, targeting the intestinal region.

4.1.1 Phase Behaviour of the NaCMC/BSA/Water System

Analysing the phase behaviour of NaCMC/BSA mixtures in water, close to neutral pH, no liquid-liquid phase separation was observed, but rather the formation of a coacervate. The polymers are closer to their isoelectric point ($pI= 5$ for BSA, $pK_a=4.3$ for NaCMC) when dissolved in water. Positive charged functional groups of BSA may interact with the negative charged carboxyl groups of CMC to form an ionic complex. As in our study, we are interested in getting segregative phase separation, to form emulsions, the phase behaviour of NaCMC and BSA in water was not studied in further details.

Therefore, similar to a study from 1976 in which phase separation between NaCMC and BSA was observed (Antonov, Grinberg, & Tolstoguzov, 1976), the mixtures were prepared in 0.1 M NaOH (pH 13) and their phase behaviour studied in detail (Figure 4.1). Under those conditions, a region in the phase diagram, in which phase separation into two liquid phases occurs, could clearly be observed. Most results in this section were obtained from the research of undergraduate student Cristina Miquel, under the supervision of Yoran Beldengrün (Espigulé, 2016).

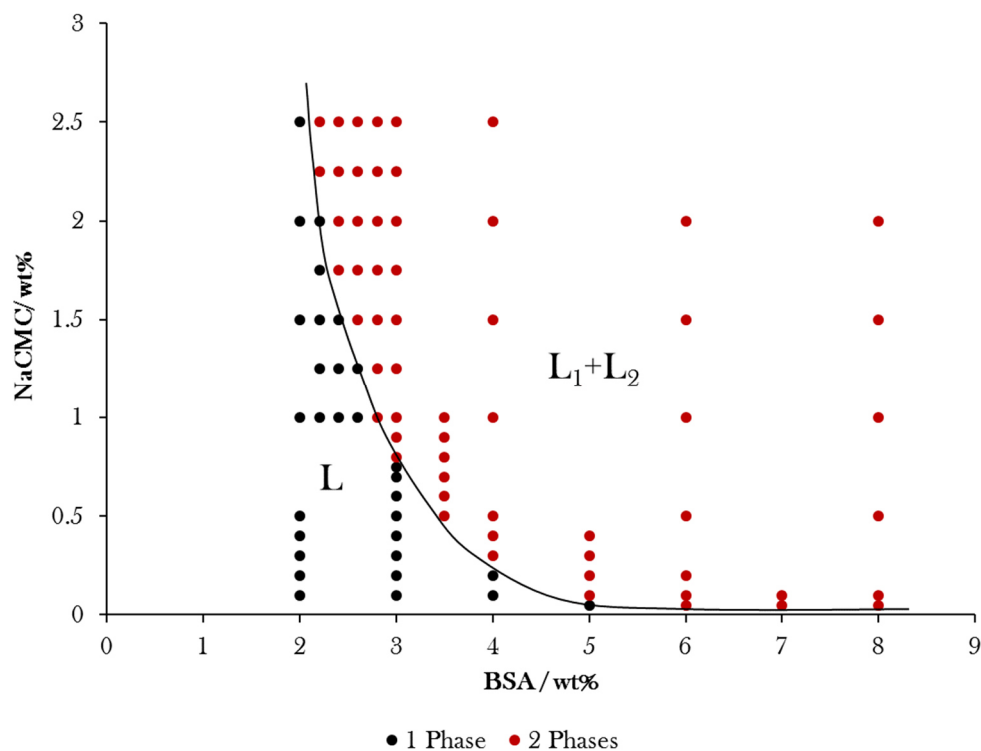


Figure 4.1. Phase Diagram after 2 days of NaCMC/BSA mixtures in 0.1 M NaOH at pH 13 and 25 °C. At low concentrations both biopolymers are miscible (L), while at increased concentrations phase separation occurs into two liquid phases (L_1+L_2).

Figure 4.1 shows that at low polymer concentrations only one liquid phase (L) was formed, meaning that both polymers are miscible under those conditions. At increased polymer concentrations phase separation into two liquid phases (L_1+L_2) could be observed. Figure 4.2 shows an example of a NaCMC/BSA mixture in which this phase separation is visible.

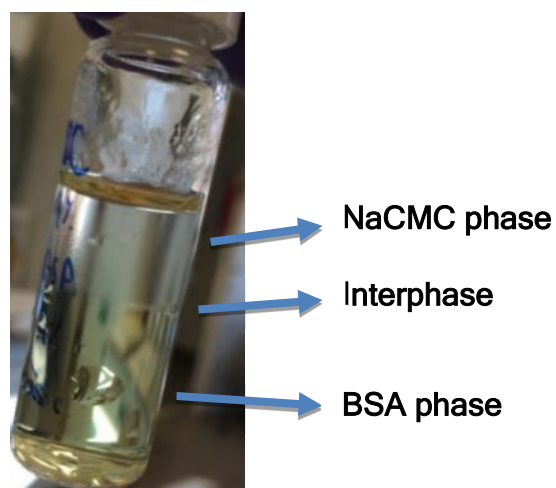


Figure 4.2. Phase separation in 1% NaCMC/ 4% BSA mixture. The transparent upper part consists majorly of NaCMC. The lower more turbid part corresponds to BSA-rich solution. Image reproduced from (Espigulé, 2016).

Interesting in the phase diagram is that at higher BSA concentrations ($> 5\text{wt}\%$) NaCMC seems to be extremely insoluble in the protein phase and phase separation occurs already at very low NaCMC concentrations ($<0.1\text{ wt}\%$). In contrast, up to $2\text{ wt}\%$ BSA was miscible with high concentrations ($2.5\text{ wt}\%$) of NaCMC.

The radius of gyration of NaCMC is 40 nm in water (Zhivkov, 2013) and the hydrodynamic radius of BSA is significantly lower, namely 3 nm (González Flecha & Levi, 2003). Due to entropic reasons NaCMC will phase separate already at low concentrations. This could explain the asymmetric solubility of one component into the other and thus the asymmetric binodal line.

It has to be noted, that the higher the BSA concentration, the more viscous was the mixture, until reaching a point at which the mixture did not have any fluency and formed a gel. This is illustrated in Figure 4.3, for mixtures of $2\text{ wt}\%$ NaCMC with $2\text{--}8\text{ wt}\%$ of BSA. In addition, the gelation was so rapid that the system did not have enough time to phase separate, which made it complicated to observe phase separation on highly viscous samples. Under those conditions, because of the turbidity and their concentrations lying within the two-liquid phase region, it was assumed that those consisted of two phases.

The individual polymers at those high concentrations are liquid, however their mixture became highly viscous/gelled. This may have occurred because of denaturation of BSA and/or conformational changes in the presence of NaCMC. Conformational changes of BSA, from a N-form to F-form (upon pH change from $\text{pH } 7.4$ to 3.5), have previously shown to induce its gelation (Baler et al., 2014). The conformational change leads to exposure of core hydrophobic regions, consequently to protein–protein aggregation and eventually to hydrogel formation. Also an interpenetrating network between BSA and CMC may have been formed at higher polymer concentrations.

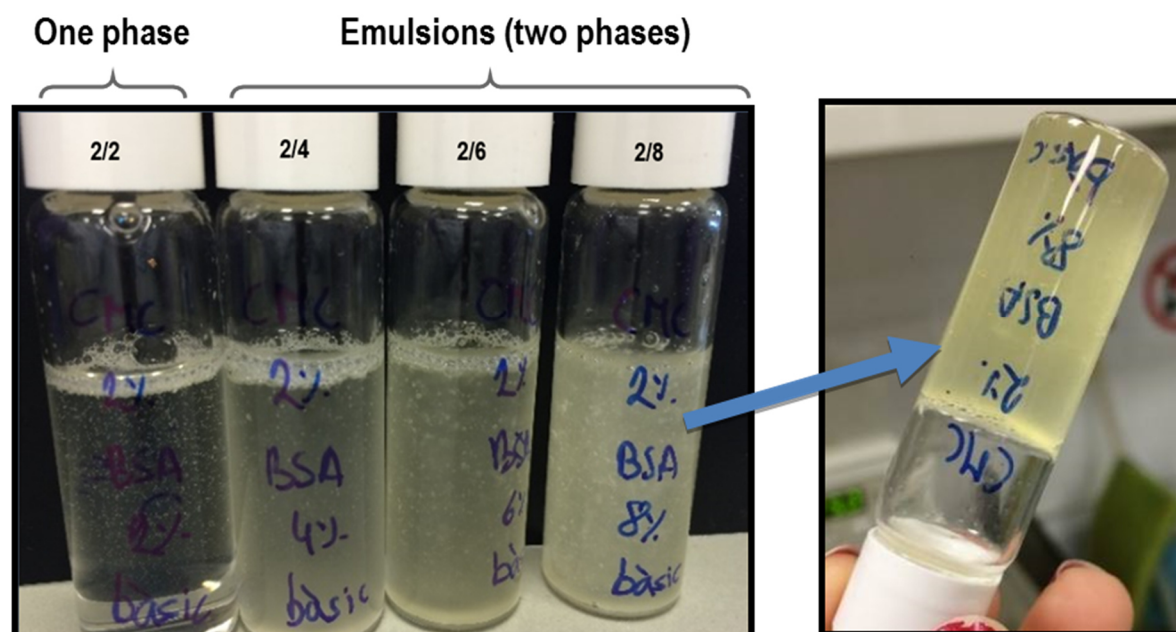


Figure 4.3. Representation of the increase in viscosity due to the BSA concentration rise in solution (picture on the left). At high BSA concentrations the solution converts into a gel (picture on the right). The compositions (CMC/BSA concentration ratios) are indicated. Image reproduced from (Espigulé, 2016).

4.1.2 Formation of Emulsions

NaCMC/BSA emulsions with, as dispersed phase NaCMC, were formed. As in this case the polymer were not marked fluorescently, it was assumed that the polymer with the smaller phase volume forms the dispersed phase, while the other polymer with the larger volume fraction, constitutes the continuous phase, as it is usual in W/W emulsions (Esquena, 2016). After stirring, the morphology of the emulsions were observed under the microscope. Figure 4.4 shows the morphology of several emulsions, containing NaCMC droplets. Figure 4.7 shows examples of emulsions of other compositions. The droplet size was in average 5-20 μm . Smallest droplet size of around 5 μm were obtained for 2.5 % NaCMC / 2.6 % BSA (Figure 4.7). Interestingly, the NaCMC/BSA emulsions were rather stable over prolonged period of time without mixing, or even after centrifugation. As an example are shown a 0.5% NaCMC/ 4% BSA emulsion and a 1% NaCMC/ 4% BSA emulsion just after homogenising (Figure 4.4 a,c) and after 10 or 20 days (Figure 4.4 b,d) storing without mixing at 4 °C in the fridge. It can be seen that over this time period droplets remained stable, without phase separation. The even higher viscosity of the mixture at low temperatures (phase diagram in Figure 4.1 was obtained at 25 °C) seemed to lower the rate of coalescence and keep the droplets stable. We also observed that the droplets remained stable after lowering the pH of an 2.5 % NaCMC/ 2.8 % BSA emulsion to pH 12 and centrifugation for 10 min at 4000 rpm. Details can be found in the Final Degree Thesis of C. Miquel (Espigulé, 2016).

In order to isolate those NaCMC droplets in form of NaCMC microgels, it was tried to find the

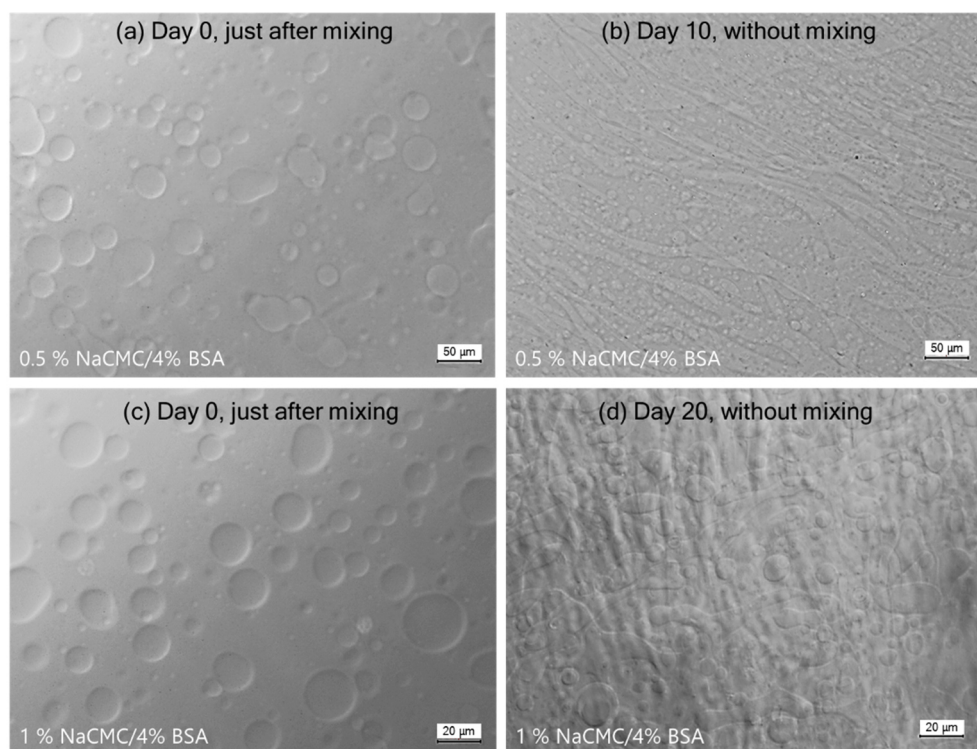


Figure 4.4. 0.5 % NaCMC / 4% BSA and 1 % NaCMC / 4% BSA emulsions at $\text{pH}\approx 13$, just after mixing (a and c) and 10 (b) or 20 (d) days later, without mixing, by keeping samples in the fridge at 4°C.

appropriate crosslinker and crosslinking conditions to crosslink selectively NaCMC.

4.1.3 Formation of Capsules with Multivalent Ions

A simple method to achieve crosslinking of NaCMC is by using multivalent cations, which can strengthen the polymer network by physical crosslinking due to ionic complexation between the cations with the negatively charged carboxyl groups of NaCMC (Figure 1.31). Several multivalent ions were first tested, to verify their crosslinking capabilities on NaCMC and for comparison, a control on BSA. Also a 0.5% NaCMC / 4.5% BSA emulsion was tested. The ions Fe^{3+} , Al^{3+} and Ca^{2+} , which are commonly used for crosslinking of NaCMC (S. S. Bhattacharya et al., 2012; M. S. Kim et al., 2012; Reddy & Tammishetti, 2002; Sungur, 1999; Xiao et al., 2009) were investigated. Table 4.1 summarises the results.

Table 4.1. Crosslinking capability of various di- and trivalent salts on NaCMC, BSA and an emulsion of both polymers. (+) crosslinking occurred, (-) no-crosslinking

| | FeCl_3 | $\text{Al}_2(\text{SO}_4)_3$ | $\text{AlK}(\text{SO}_4)_2$ | CaCl_2 |
|-----------------------------------|-----------------|------------------------------|-----------------------------|-----------------|
| 3wt% NaCMC | + | + | + | + |
| 15wt% BSA | + | + | + | - |
| 0.5% NaCMC / 4.5% BSA Emulsion | + | + | + | - |

FeCl_3 (tested between 1 and 8 wt%), $\text{Al}_2(\text{SO}_4)_3$ (10 wt%) and $\text{AlK}(\text{SO}_4)_2$ (10 wt%) crosslinked NaCMC, BSA and also the emulsion. Those salts crosslinked the zwitterionic protein BSA (Figure 4.5). Consequently, both phases of the emulsion were crosslinked: not only the dispersed, but also the continuous phase, leading to formation of encapsulated emulsions, instead of crosslinked NaCMC microgels. BSA gelation in presence of the trivalent ions may have been caused by the shielding of the ions against the charges present on the protein surface, leading to possible conformational changes and protein gelation (Baler et al., 2014). The cations may have also acted as bridges, coordinating several oligomeric structures of BSA, which was observed earlier (Navarra et al., 2009).

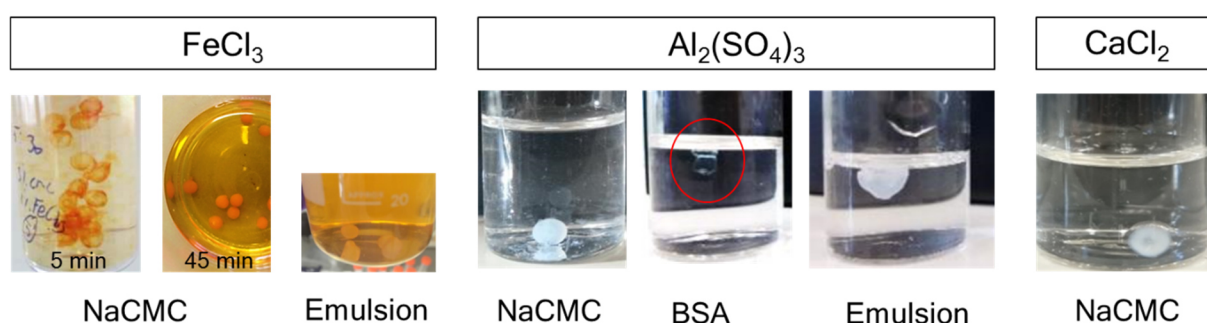


Figure 4.5. Formation of capsules by ionic complexation of NaCMC, BSA and their emulsions by different types of multivalent salts solutions (2 wt% FeCl_3 , 10 wt% $\text{Al}_2(\text{SO}_4)_3$, 2 wt% CaCl_2). Pictures were taken after 5 min crosslinking, in the case of FeCl_3 additionally after 45 min. The emulsion crosslinked by FeCl_3 is an 2.5 % NaCMC / 2.6% BSA emulsion, the one crosslinked by $\text{Al}_2(\text{SO}_4)_3$ a 0.5 % NaCMC / 4.5 % BSA emulsion

Crosslinking time influenced the characteristics of the crosslinked NaCMC droplets, as illustrated with the crosslinker FeCl_3 , which is orange in water (Figure 4.5). At short crosslinking times (5 min in FeCl_3 , Figure 4.5) capsules were obtained, which consist of a crosslinked, gelled surface and a liquid core. The cations diffuse only slowly into the interior of the NaCMC, thus after 5 min only the shell of the capsules

was crosslinked, keeping the interior liquid. This was observed by the orange outer layer in Figure 4.5. Allowing for longer crosslinking times (45 min in FeCl_3 , Figure 4.5), beads were also crosslinked and gelled in the interior, as the ion had time to diffuse into the interior of the NaCMC droplets. Both, capsules and beads, were freeze-dried and observed under the SEM (Figure 4.6). In the dried form, the shell of the capsule was dense, with a porous interior. The beads, in contrast, had a similar morphology outside and inside. Cutting it carefully open, separated the very brittle bead in two pieces, while for the capsules, the shell could be separated easily. Controlling crosslinking time is therefore a simple manner, to either obtain capsules or beads, which makes it interesting in design of delivery vehicles with respective properties.

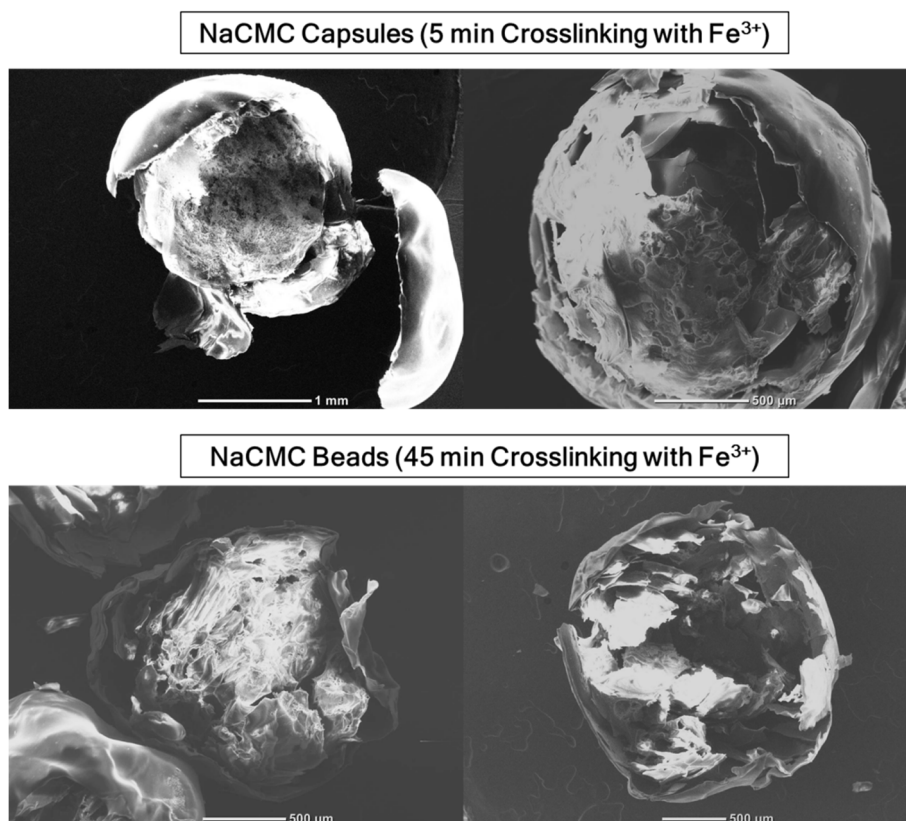


Figure 4.6. SEM images of freeze-dried NaCMC Capsules and Beads

CaCl_2 in contrast to the other salts, did only crosslink NaCMC and not BSA (Table 4.1). Concentrations of up to 8 wt% CaCl_2 were tested. Divalent ions are thus not strong enough to achieve gelation of the protein BSA. This makes it interesting as a crosslinker to selectively obtain crosslinked NaCMC droplets, while keeping BSA liquid. Crosslinking of Ca^{2+} ions occurred however slower, compared to the trivalent ions Fe^{3+} and Al^{3+} . This is known, and has already been observed in a similar study with carboxymethyl guar gum (Reddy & Tammishetti, 2002). The divalent calcium cation bonds NaCMC in a planar two-dimensional manner, while the trivalent cations of iron and aluminium form a stronger three-dimensional bonding structure (M. S. Kim et al., 2012).

CaCl_2 will thus be tested as a potential crosslinker for formation of NaCMC microgels, from NaCMC/BSA emulsions.

4.1.4 *Crosslink NaCMC/BSA Emulsion with Ca²⁺ to obtain NaCMC Microgels*

The potential of forming NaCMC microgels by crosslinking NaCMC/BSA emulsions with CaCl₂ was tested. Details can be found in the Final Degree thesis (Corvo, 2017). In brief, first an emulsion of NaCMC/BSA was formed by mixing NaCMC and BSA stock solutions (both in 0.1 M NaOH) together with a CaCl₂ solution to obtain final concentrations of 0.5 % NaCMC / 4.5 % BSA. The resulting emulsions, containing NaCMC droplets, probably crosslinked with Ca²⁺, were consequently tried to be isolated by centrifugation, filtration or dialysis. None of these methods was successful, because the droplets did either not remain stable and may have dissolved during the purification process, or BSA was not successfully separated and removed.

Alternatively, a 0.5 % NaCMC / 4.5 % BSA emulsion was introduced into a dialysing tube, with as external medium a 2 wt% CaCl₂ solution. After 24 h the entire mixture in the dialysis tube gelified (Corvo, 2017). Probably phase separation occurred and Ca²⁺ crosslinked the NaCMC-rich phase.

Further experimentations are thus needed to try isolate Ca²⁺ crosslinked microgels. Moreover, the crosslinking potential of the trivalent ions will be studied in further detail.

4.1.5 *Crosslinking of NaCMC/BSA Emulsions with Trivalent Ions*

As observed in Table 4.1, the trivalent ions Al³⁺ and Fe³⁺, are capable to crosslink both phases of NaCMC/BSA emulsions. Dropping thus NaCMC-in-BSA emulsions into a crosslinking solution, allows to gel the emulsion droplets and introduces the emulsions into beads, which will be called “encapsulated emulsions”. Such a delivery system may be interesting due to its double protection capabilities, by the two polymers: One forming the continuous phase, in this case BSA, and the other, in this case NaCMC, the droplets. Of interest would be to encapsulate the active component into the NaCMC droplets. Such a delivery system can be compared to a multiple emulsion in a gelled state.

Encapsulated emulsions were formed by two methods. First, by a simple method, dropping the emulsion directly after mixing, with the help of a Pasteur pipette into a crosslinking solution of FeCl₃. This method is appropriate for initial studies, but results in large beads in the range of 2 mm. Next, droplet size was intended to be reduced by electrospraying the emulsion into the crosslinker solution.

As can be seen in Figure 4.5, the 0.5 % NaCMC / 4.5 % BSA emulsion floated in the ion (Al₂(SO₄)₃) solution, while the 2.5 % NaCMC / 2.6% BSA sedimented to the ground in the FeCl₃ solution. Depending on the emulsion compositions, the emulsion density was lower or higher than the ion solution. This affected the morphology of the bead, as only total immersion of the droplet into ion solution, allows formation of a spherical bead. At lower densities, the droplet floats on the surface, and disk shaped or half-spherical beads were obtained. To obtain more spherical particles, the emulsion were dropped into ion solutions that were constantly stirred with a magnet bar. This allowed, for most cases, to form beads with shapes closer to spheres.

The emulsions were dropped with the Pasteur pipette into the 2 % FeCl_3 solutions, kept there for 30 min and the 2 mm large beads were subsequently freeze-dried and observed by SEM (Figure 4.7). The encapsulated emulsions, in the dried state, resulted in beads with pores with very similar size than those of the emulsion droplets: $\sim 20 \mu\text{m}$ for the 0.5 % NaCMC / 4.5 % BSA emulsion and $\sim 5 \mu\text{m}$ for the 2.5 % NaCMC / 2.6% BSA emulsion. Consequently, the emulsion droplets template the formation of pores of the beads.

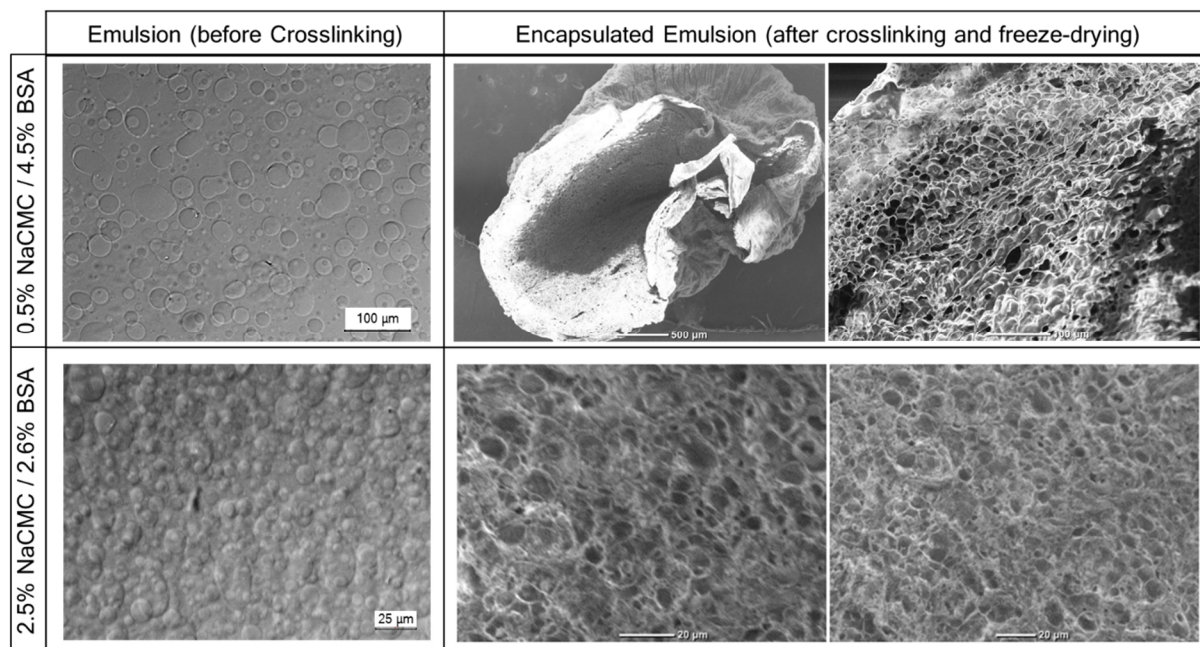


Figure 4.7. Formation of encapsulated emulsions. Morphology of emulsion just after mixing (left) and SEM images of encapsulated emulsion formed by crosslinking with Fe^{3+} and consequent freeze-drying (right).

This method is thus a simple strategy to control pore size of beads. Of interest would be to analyse the composition of the freeze-dried porous beads. The interior of the droplets were not only composed of water, but also NaCMC, which is not removed after freeze-drying. Thus it may be that during freeze-drying NaCMC diffused to the interphase, forming a shell around the surface of droplets. Consequently, the pore walls in the dried state might consist of NaCMC. BSA which made up the continuous phase of the emulsion, may connect those pores, which are basically hollow CMC capsules, inside a BSA network.

With the aim to reduce droplet size, the emulsion was electrosprayed into a FeCl_3 solution (experiments performed at the Université de Lorraine, in the group of Andreea Pasc). A challenge, when electrospraying, is finding optimal experimental settings. If not adequate settings are used, the solution can get out of the nozzle as normal sized drops, or in form of a long fiber. The voltage, flow rate and the tip-to-collector distance have to be adapted accordingly, till spraying of the solution of interest is achieved. As the 2.5 % NaCMC / 2.6% BSA emulsion was too viscous to be successfully electrosprayed (too high voltages would have been needed to allow spraying), only the 0.5 % NaCMC / 4.5% BSA was tested.

Optimal conditions for spraying were obtained with 10 kV, 15 mL/h flow rate and 12 cm tip-to collector distance. The emulsions was thus introduced into the syringe and sprayed into a 2 wt% FeCl_3 solution lying below the nozzle (Figure 3.3). The obtained encapsulated emulsions had sizes between 600–800 μm (Figure 4.8). This is in a similar size range as for 500 μm alginate beads obtained by spray drying

with the same instrument (Haffner, Van de Wiele, & Pasc, 2017). Other studies, using other polymer solutions got droplets in sizes down to 10 μm (Bock et al., 2011). Further optimisation of the electrospaying experimental parameters may allow to reduce the size of our sprayed emulsions.

The microscopic images of the spray dried encapsulated emulsions in Figure 4.8 show very clearly that the emulsion droplets remained stable inside the bead. Emulsion droplet size was in the range of 20 μm , which corresponded to the size before electrospaying. In conclusion, the emulsion remained stable during all the spraying process.

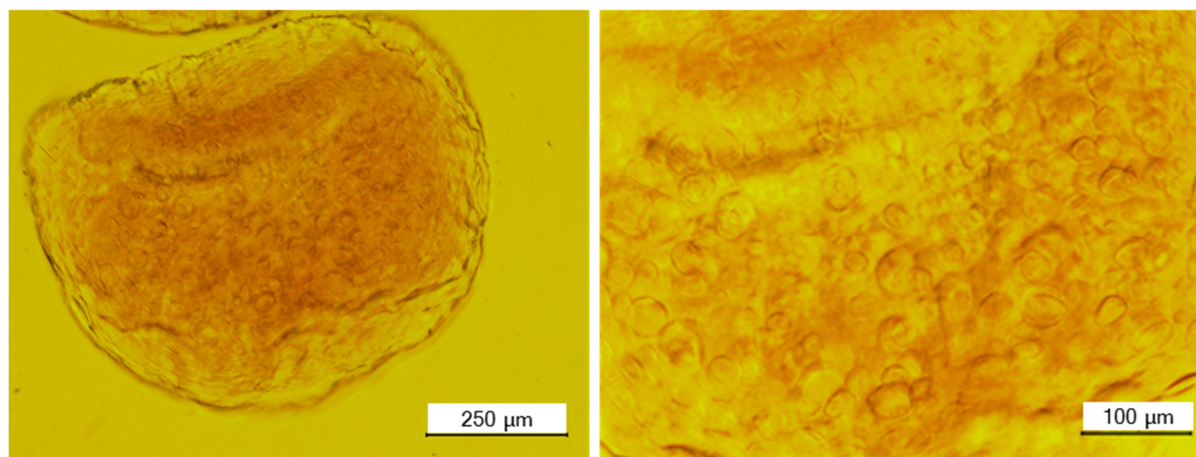


Figure 4.8. Electrospayed NaCMC/BSA emulsions crosslinked in a 2 % FeCl_3 solution.

The encapsulated emulsions could thus be an interesting delivery vehicle for active components, such as enzymes, which need protection from environmental factors. Therefore, the stability of the encapsulated emulsions under different pH conditions was tested.

4.1.6 Stability of Crosslinked Emulsions and Beads at pH 1.2 and 6.5

Stability of crosslinked NaCMC beads and encapsulated emulsions at pH 1.2 and pH 6.5 was tested. As the final aim is to use the encapsulated emulsions in applications in food and pharmaceutical industry, the salts of $\text{Al}_2(\text{SO}_4)_3$ and $\text{AlK}(\text{SO}_4)_2$ were used for further studies. Despite FeCl_3 being generally regarded as safe (GRAS) by the Food and Drug Administration (FDA), FeCl_3 has been reported to bare health risks with toxic effects on the body and being corrosive (PubChem: Open Chemistry Database., 2004). The aluminium salts are regarded as less toxic and even being used in food (PubChem: Open Chemistry Database., 2018a, 2018b).

Most results of this section were obtained from work by the undergraduate student Laura Corvo (Corvo, 2017) under the supervision of Yoran Beldengrün. The samples were added to a pH 6.5 solution, simulating neutral pH environments, found for example in food or drinks, in which the beads might be kept. Then, they were immersed for 2h into pH 1.2, simulating gastric pH conditions, and finally, if remaining stable, they were transferred for 2h to a pH 6.5 solution, simulating intestinal pH conditions. In another experiment, the beads were transferred directly from the crosslinking solution, into pH 1.2 for 2h, and then for 2h at pH 1.2.

It was expected, that in neutral pH conditions, the carboxylic groups of NaCMC are negatively charged, allowing them to be crosslinked by the Al^{3+} salts and thus the beads would remain stable (Figure 4.9).

When switching to acidic gastric conditions (pH 1.2), the carboxylic groups become protonated, releasing the trivalent ions. NaCMC with protonated carboxylic groups, is less soluble than in neutral pH conditions, as hydrogen bonds between the carboxylic groups and absence of electrostatic repulsion may strengthen the NaCMC network. Adding non-crosslinked solutions again to pH 6.5, simulating intestinal conditions, may finally lead to increased swelling of the bead, due to repulsion of the negatively charged carboxylic groups. This could eventually lead to the release of the encapsulated component.

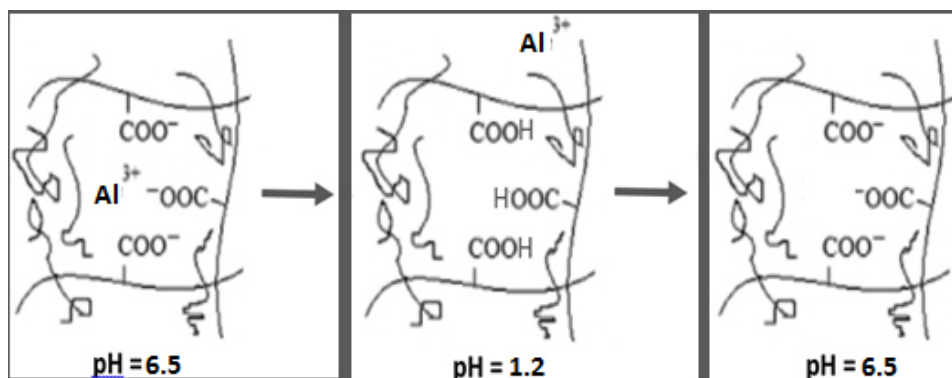


Figure 4.9. Scheme of possible states of Al^{3+} -crosslinked NaCMC under different pH conditions (Figure adapted from(Xiao et al., 2009)).

The stability of the beads was analysed, and results were the same for both Al^{3+} salts (Table 4.2). The Al^{3+} -crosslinked NaCMC beads remained stable if added for 2 h into either pH 1.2 or pH 6.5. At pH 6.5 they swelled (Figure 4.10 a), at pH 1.2 they shrank (Figure 4.10 b). Transferring those beads to the opposite pH conditions, thus from pH 6.5 to pH 1.2 and vice versa, lead to them getting dissolved. The possible reasons will be explained next.

Table 4.2. Stability at different pH conditions of NaCMC beads or 0.5% NaCMC / 4.5% BSA emulsions crosslinked with 10 wt% $\text{Al}_2(\text{SO}_4)_3$ or $\text{AlK}(\text{SO}_4)_2$. They were mixed with media of pH values indicated in the table. After 2 h they were removed and placed into the 2nd medium. Finally, after further 2 h the beads were changed to the 3rd medium. Stable beads are indicated by green colour, while red indicates dissolution.

| Sample | | 1 st Medium (2h) | 2 nd Medium (2h) | 3 rd Medium (2h) |
|------------------------------|----------|--------------------------------|--------------------------------|--------------------------------|
| $\text{Al}_2(\text{SO}_4)_3$ | NaCMC | pH 6.5 | pH 1.2 | |
| | | pH 1.2 | pH 6.5 | |
| | Emulsion | pH 6.5 | pH 1.2 | pH 6.5 |
| $\text{AlK}(\text{SO}_4)_2$ | NaCMC | pH 6.5 | pH 1.2 | |
| | | pH 1.2 | pH 6.5 | |
| | Emulsion | pH 6.5 | pH 1.2 | pH 6.5 |

NaCMC crosslinked with 10wt% $Al_2(SO_4)_3$

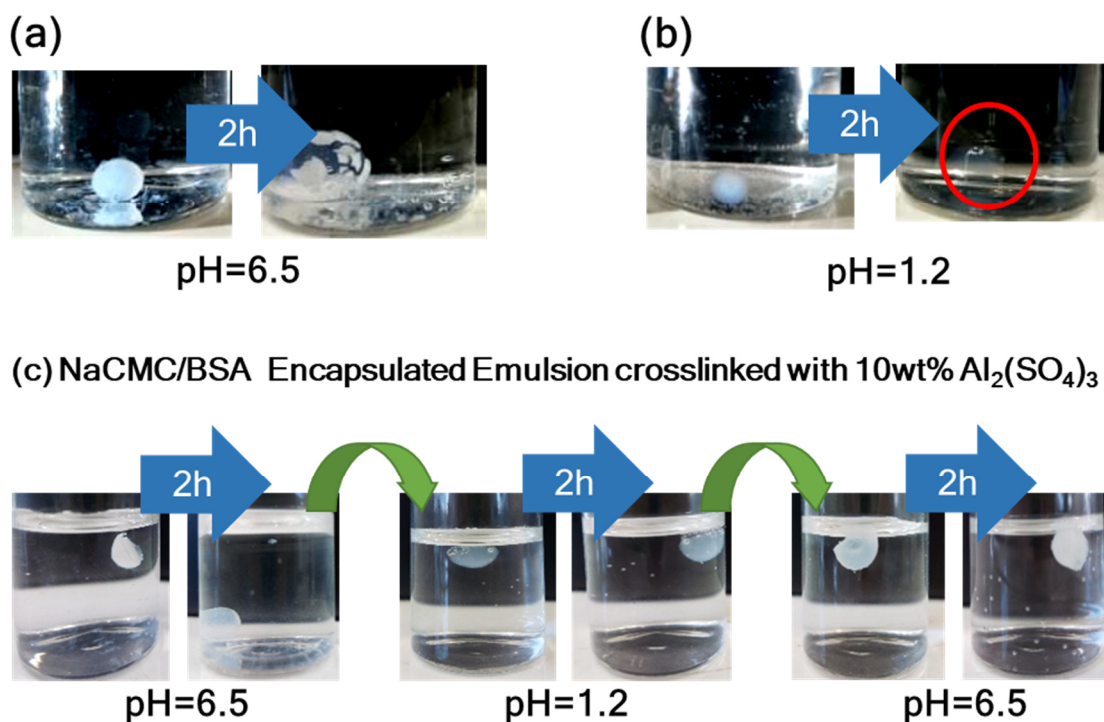
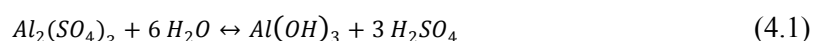


Figure 4.10. Stability of with $Al_2(SO_4)_3$ – crosslinked (a+b) 3 wt% NaCMC and (b) 0.5% NaCMC / 4.5% BSA emulsion beads at pH 1.2 and pH 6.5.

Increased swelling in the buffer at pH 6.5 (Figure 4.10 a) was probably caused by dissociation of the Al^{3+} ions from the NaCMC network, keeping the polymer non-crosslinked and thus leading to its swelling, due to repulsion of the negatively charged carboxylic groups. A possible explanation can be found from the turbidity in the beads, also observed in Figure 4.10 a. $Al_2(SO_4)_3$ solutions are usually transparent and acidic, with a pH 2.8 for a 10 wt% solution (Corvo, 2017). In water $Al_2(SO_4)_3$ reacts to $Al(OH)_3$ and H_2SO_4 by following reaction:



$Al(OH)_3$ has a very low solubility in water (0.1 mg/100 mL) and precipitates as white particles. Raising the pH of the $Al_2(SO_4)_3$ solution, by adding it to the pH 6.5 PEM buffer, will favour the formation of $Al(OH)_3$ particles. This was also observed in a separate experiment when adding NaOH to a $Al_2(SO_4)_3$ solution (Corvo, 2017). As a consequence, less Al^{3+} is available to crosslink NaCMC, which leads to swelling of the NaCMC at neutral pH.

Moreover, swelling is not promoted only by electrostatic repulsion of the negatively charged carboxylic groups, but also by the increase of counter ion concentration inside the polymeric network, when the carboxylic groups are deprotonated. As a consequence, osmotic pressure difference between the internal and external solutions of the beads, leads to increased influx of solvent into the beads and therefore to its swelling (S. S. Bhattacharya et al., 2012). The increased swelling of NaCMC beads crosslinked with trivalent ions at neutral pH conditions was already observed earlier (S. S. Bhattacharya et al., 2012; M. S. Kim et al., 2012). The beads did not dissolve probably due to some remaining Al^{3+} keeping the network crosslinked.

Once those swelled beads were added to pH 1.2, the carboxylic groups in the NaCMC become protonated, the remaining Al^{3+} probably desorbed. As the beads were already in a swelled state, the distance between the carboxylic groups was probably too big, in order to keep the NaCMC bead stable, over hydrogen bonding, leading to the dissolution of the bead (Table 4.2).

In the case of adding the NaCMC first into pH 1.2 (Figure 4.10 b), the bead remained stable and deswelled. It can be seen that it turned more transparent, indicating that most Al^{3+} and $\text{Al}(\text{OH})_3$ was removed from the bead, and mainly hydrogen bonding might have kept the bead stable. It deswelled as probably the osmotic pressure reduced inside the bead due to protonation of the carboxylic groups and dissociation of Al^{3+} into the surrounding solution. After 2 h at pH 1.2, the beads were placed into pH 6.5. This led to the dissolution of the beads (Table 4.2), as deprotonation of the carboxylic groups made NaCMC more soluble.

However, interestingly the NaCMC/BSA encapsulated emulsions remained stable, in the simulation of the passage from food, over gastric to intestinal pH conditions (Table 4.2 and Figure 4.10 c). It is supposed, that besides the interactions between the solvent, the trivalent ion crosslinker and NaCMC there is also the interaction between NaCMC and the zwitterionic BSA, which contributes to the stability of the encapsulated emulsion. Non-covalent interaction between both biopolymers, might have kept the bead stable, despite eventual deprotonation of the NaCMC carboxylic groups or release of the crosslinker Al^{3+} . This makes NaCMC/BSA encapsulated emulsions promising delivery vehicles in oral delivery applications.

Initial studies of the encapsulation of the enzyme into the encapsulated emulsions have been performed by the undergraduate student Laura Corvo (Corvo, 2017) under the supervision of Yoran Beldengrün, and the challenges encountered in achieving encapsulation of the enzymes and maintaining them active inside the bead will be explained in the next section.

4.1.7 Immobilisation of Enzymes into NaCMC/BSA Emulsion Beads

Two different methods for encapsulating the enzyme into the Al^{3+} crosslinked NaCMC/BSA emulsion beads are proposed (Figure 4.12). The difference is the moment during the preparation at which the enzymes are added, thus also the pH. Two different lactase enzymes will be tested: The Ha Lactase 5200, which has a pH optimum at pH 6.5, and the more acid stable Lactase F “Amano”, which has a pH optimum at pH 4.5. Their pH activity profiles can be found in Figure 4.12 a.

(a) Adding the enzyme into the crosslinker $\text{Al}_2(\text{SO}_4)_3$ solution

The enzyme could be added to the crosslinker solution and would get encapsulated into the emulsion after dropping the emulsion into the enzyme-containing crosslinker solution (Figure 4.12 b). A challenge is the low acidic pH of the $\text{Al}_2(\text{SO}_4)_3$ solution. A 10 wt% $\text{Al}_2(\text{SO}_4)_3$ solution has a pH of 2.8. Diluting it down to 0.5 wt% raises its pH up to 3.5. Enzyme activity was measured, and the results shown that lactase F “Amano” become rapidly inactivated at pH 2.8. At pH 3.5, in which they remained active, the emulsion components did not get crosslinked as the concentration of Al^{3+} (0.5 wt%) was too low (Corvo, 2017). As an alternative, the pH of a 10 wt% $\text{Al}_2(\text{SO}_4)_3$ solution was risen by adding NaOH, up to pH

3.7. At this pH, the enzyme remained active over a period of at least 24 h, however activity decreased in this time period (Figure 4.11).

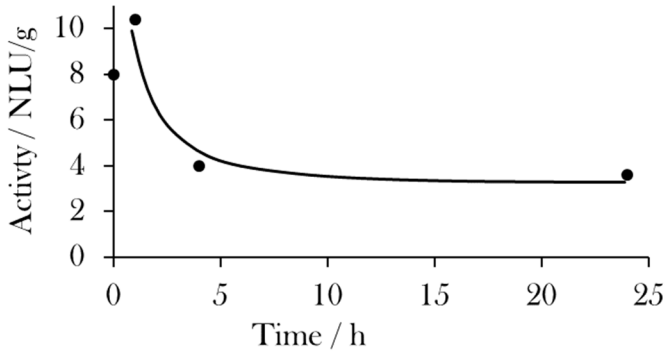


Figure 4.11. Enzyme activity of Lactase F “Amano” kept for 24 h in a 10 wt% $Al_2(SO_4)_3$ solution at pH 3.7 and 25 °C.

When much more NaOH was added, a large amount of $Al(OH)_3$ precipitated, leading to reduction of Al^{3+} available to crosslink the components emulsion. This method can be promising for incorporation of the enzyme into the beads. However, a major challenge is that the free Lactase F “Amano” enzyme is not stable under intestinal pH conditions, the environment in which it is supposed to remain active.

(b) Adding the enzyme into the emulsion

The highest encapsulation yield would be achieved probably, by adding the enzyme directly into the emulsion, before crosslinking it and forming encapsulated emulsion (Figure 4.12 c). The drawback of this method is however, that NaCMC/BSA emulsions are stable only between pH 11-13. We showed that no emulsions of those biopolymers can be formed at pH lower than 11 (Corvo, 2017). Under pH conditions above pH 11 the enzyme would get directly deactivated.

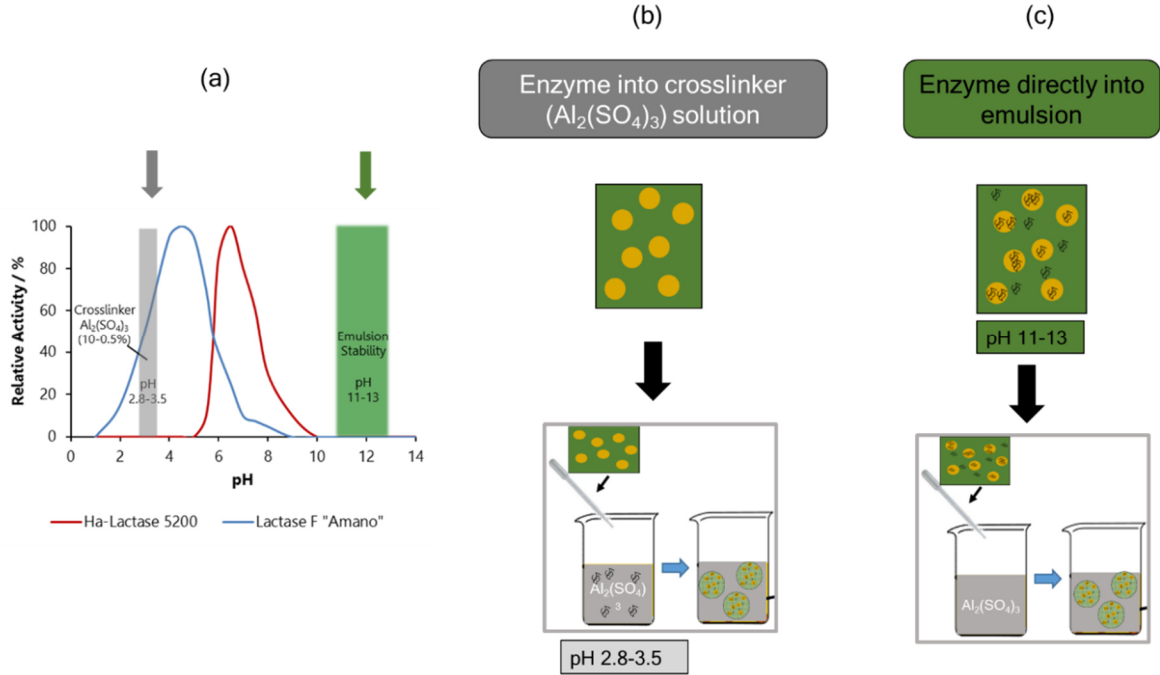


Figure 4.12. (a) pH activity profiles of Lactase F “Amano” and Ha-Lactase 5200 (data supplied by the manufacturer). Illustration of two different immobilisation methods of the enzyme into the encapsulated emulsions: (b) adding enzyme into the crosslinker solution or (c) adding the enzyme directly into the emulsion.

4.2 Using Gelatin/Maltodextrin Emulsions as Templates for Crosslinked Gelatin Microgel Formation

4.2.1 Crosslinking Reaction of Genipin

4.2.1.1 Reaction of Genipin with Water, Maltodextrin and Gelatin

The visual aspect of the reaction of genipin with gelatin was investigated in solutions of water, maltodextrin and gelatin. According to the theory, the solutions should only turn blue, if the sample contains primary amine groups and crosslinking reaction takes place. The origin are the oxygen radical-induced polymerization of genipin and dehydrogenation of intermediate compounds, following the first crosslinking reaction (formation of the heterocyclic genipin compound) (Michael F. Butler et al., 2003; Touyama et al., 1994). After 16 h at 45 °C, the gelatin samples gelled and became dark blue, while the water sample remained transparent and liquid (Figure 4.13). The maltodextrin liquid solutions, unexpectedly turned slightly blue, which might origin from reaction with some impurities in the maltodextrin biopolymer powder. Biopolymers are extracted from natural products and contain thus often traces of impurities. In this case those impurities seemed to contain some primary amines which reacted with genipin. No gel formation was however observed in the maltodextrin solutions, which thus makes genipin still a selective crosslinker for gelatin in a gelatin/maltodextrin emulsion.

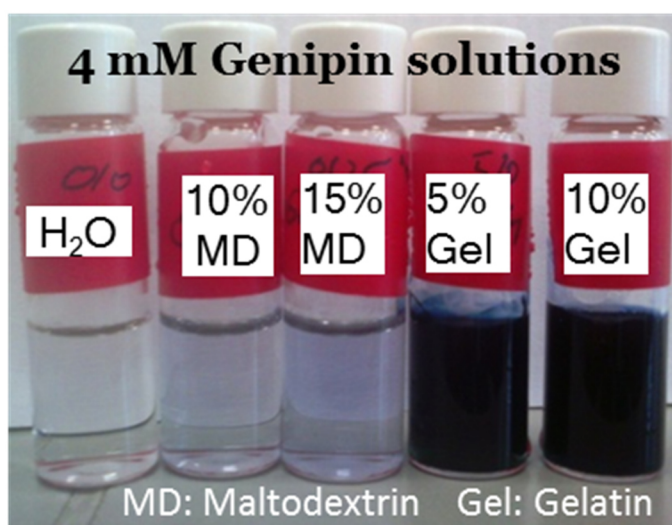


Figure 4.13. Colour development of solutions of water, maltodextrin (MD) and Gelatin (Gel) containing 4 mM Genipin.

4.2.1.2 Study Influence of Temperature and Time on Crosslinking of Genipin

The crosslinking process of gelatin microgels (prepared from a 4.5 % Gel/ 13 % MD emulsion) was investigated by following the UV spectrum of the samples over time, using a method previously described (Michael F. Butler et al., 2003). The influence of temperature and genipin concentration on crosslinking kinetics was investigated, by performing the experiments at three distinct temperatures (25, 45 and 60 °C) and crosslinker concentrations (0.1, 1 and 10 mM Genipin). At specific time points UV spectra were recorded and the absorption at 605 nm over time was plotted. This wavelength corresponds to the blue colour generated as side reaction to the crosslinking reaction of genipin with the primary amine groups of gelatin (Michael F. Butler et al., 2003; Touyama et al., 1994). This method is an indirect method to measure crosslinking efficacy, as compared to other methods such as the ninhydrin assay which determines the amount of free amino groups of each test sample. The ninhydrin assay allows to give an exact value of the crosslinking index (percentage of free amino groups remaining), however is a destructive method, which implies heating the sample with a ninhydrin solution for 20 min at above 100 °C. Furthermore some authors reported complications using this method for crosslinking determination of gelatin-genipin gels, due to genipin self-polymerisation (Nickerson, Farnworth, et al., 2006). Measuring the absorbance at 605 nm is a simple online, non-destructive method to follow qualitatively the crosslinking reaction. It does not allow however to determine the exact percentage of polymer, which became crosslinked. Previous studies followed the gradual increase of the peak at 605 nm (Rangel-Rodríguez et al., 2014), but also an increase of the peak at 240 nm and 280 nm (Michael F. Butler et al., 2003; Vílchez et al., 2009) (Figure 1.36). Interestingly, neither the strong peak between 200-260 nm of the genipin molecule of a 1 mM genipin solution in water (Figure 4.14), nor the absorption maximum peak 241 nm (for lower concentrations of genipin), was observed in the spectra of the gelatin microgels crosslinked with genipin (Figure 4.15). As commented in section 4.2.3.1, gelatin absorbs mainly in the spectral region between 200-300 nm (Figure 4.22) and thus masked probably those regions of the spectrum. This study focussed thus on the peak, originating of the blue colour at 605 nm, as there is less background signal in this region of the UV-VIS spectrum of gelatin-genipin mixtures. The evolution of the entire spectra of the gelatin-genipin mixture, can be observed in Figure 4.15.

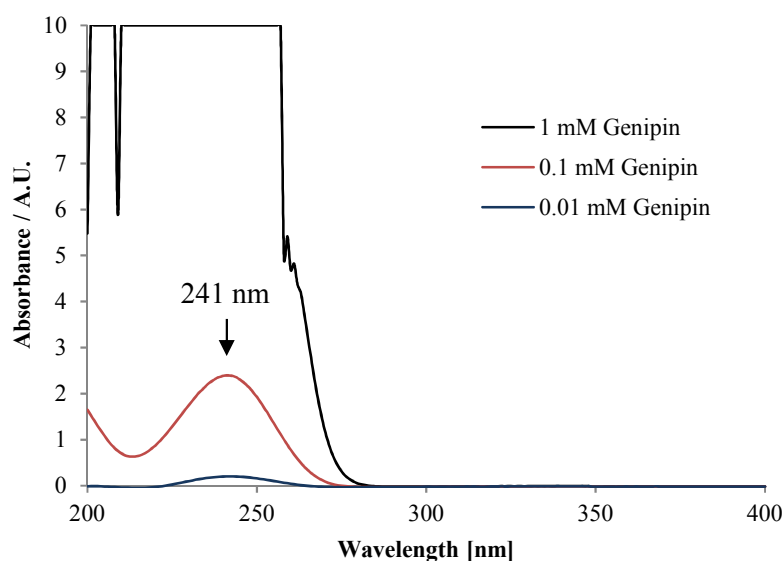


Figure 4.14. UV-Spectra of genipin solutions in water at various concentrations.

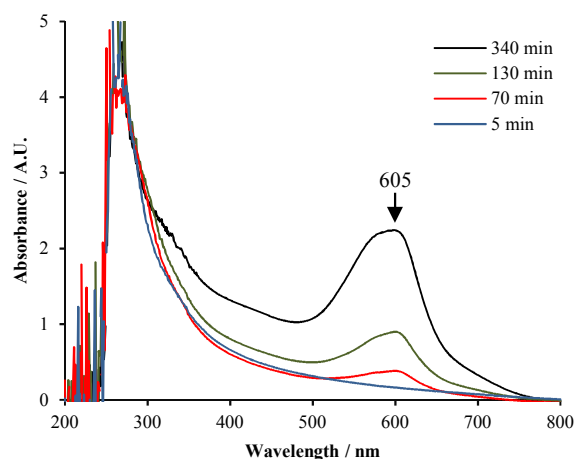


Figure 4.15. Evolution of UV-VIS spectra of gelatin microgel suspension crosslinked at 45 °C with 1 mM Genipin.

Crosslinking was followed for a maximum period of 4 days or was interrupted when the individual microgels in suspension, aggregated and formed one single macrogel surrounded by continuous medium. This process can be probably explained by the fact that genipin at a critical crosslinking concentration does not only crosslink gelatin within the microgels, but forms as well bridges between microgel particles, leading to formation of one continuous macrogel.

Results indicated that crosslinking increased, as expected, with increasing crosslinker concentration (Figure 4.16 (a)) and temperature (Figure 4.16 (b)). For samples with 1 mM genipin maximum crosslinking, before turning from a microgel suspension to a single macrogel, was attained in approximately 2 h (60 °C) or ~5.5 h (45 °C) and not within the measured time period for 25 °C (Figure 4.16 (b)). For samples being crosslinked at 45 °C critical crosslinking was attained in ~1 h (10 mM genipin) or ~5.5 h (1 mM genipin) and not within the measured time period for 0.1 mM genipin (Figure 4.16 (a)).

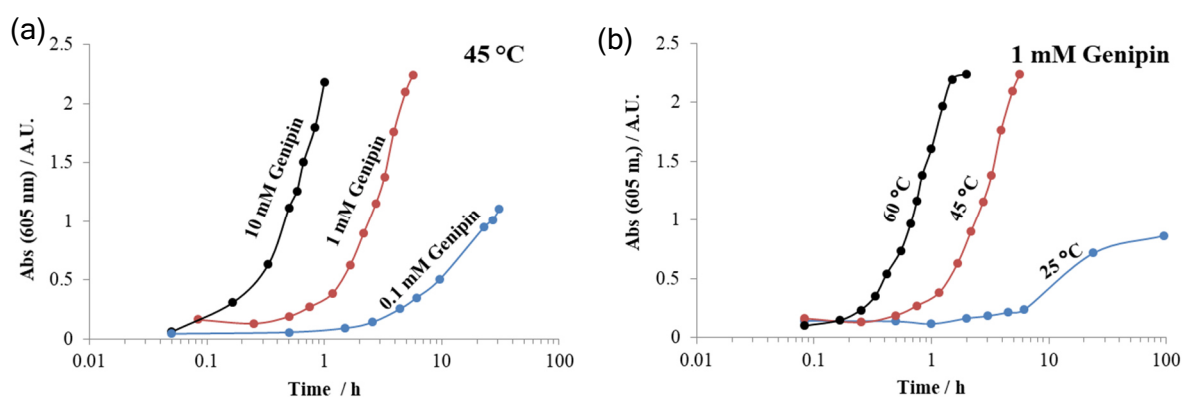


Figure 4.16. (a) Crosslinking kinetics of gelatin microgels at different genipin concentrations at 45 °C. (b) Crosslinking kinetics of gelatin microgels at different temperatures at 1 mM Genipin.

Table 4.3 summarises the results, by comparing the times at which the samples reached half of the maximal absorbance.

Table 4.3. Time at which samples attained 50% of maximal absorbance ($t_{50\%}$), for different temperatures and genipin concentrations

| | 0.1 mM Genipin | 1 mM Genipin | 10 mM Genipin |
|-------|----------------|--------------|---------------|
| 25 °C | - | > 96 h | - |
| 45 °C | 31 h | 2.70 h | 0.50 h |
| 60 °C | 27 h | 0.75 h | 0.13 h |

Other similar studies, which followed the crosslinking of gelatin by genipin over time, focussed on the extent of crosslinking after 24 h at room temperature (Bigi et al., 2002; Kirchmajer et al., 2013; Yao et al., 2004). With the ninhydrin assay they could determine the extent of crosslinking, by the percentage of free amino groups lost during the reaction. Concentrations worked with were usually in the range of up to 2 wt % genipin (88 mM Genipin), which are very high concentrations, not normally used in crosslinking of gelatin microparticles (H.-C. Liang et al., 2003; Solorio et al., 2011; P. A. Turner et al., 2017). The studies concluded that crosslinking increased with increasing crosslinker concentration and maximal extent of crosslinking was 84%–90% for all concentrations of gelatin examined. Genipin is unable to attain 100% of crosslinking of a gelatin macrogel, due to the tertiary structure of gelled gelatin, which shields some of the lysine residues and prevents them thus from reacting with genipin. Glutaraldehyde, which is smaller and more flexible than genipin, has been reported to attain a maximum extent crosslinking of 100% (Bigi, Cojazzi, Panzavolta, Rubini, & Roveri, 2001).

Besides crosslinker concentration, we conclude that temperature is also very important in determination of the extent of crosslinking of gelatin microgel. At higher temperatures gelatin is more probable to be in a random coil structure, which increases accessibility of amine groups to genipin. Furthermore, the crosslinking reaction is endothermic and thus favoured by higher temperatures.

4.2.2 Study of Gelatin MacroGel Gelling and Swelling

4.2.2.1 Determination of Gelatin Sol-Gel Transition Temperature

The determination of gelling temperature was done in order to determine the temperature ranges where the gelatin polymers, which we were working, are expected to be in a gelled state and in which conditions they are supposed to flow like a liquid. Therefore, we used a qualitative method, based on tube inversion and visual inspection to determine the sol-gel transition temperature. Deeper insights into the gelation of gelatin were obtained in previous studies by techniques such as calorimetry (sensitive to heat-induced structural changes within the polymer) (Godard, Biebuyck, Daumerie, Naveau, & Mercier, 1978), optical rotation measurements (allows to track the degree of helical conformation) (Madeleine Djabourov, 1988) and rheometry (to determine viscoelastic properties) (Djabourov et al. 1985). Gelation of gelatin depends on many physicochemical factors, we focussed on concentration, temperature and extent of crosslinking.

As expected, when heated (1 °C up every 10 min) the gelatin solutions liquefied, cooling down (1 °C down every 10 min) the samples gelled. Increasing gelatin concentrations led to increasing gel-sol transition temperatures (Figure 4.17).

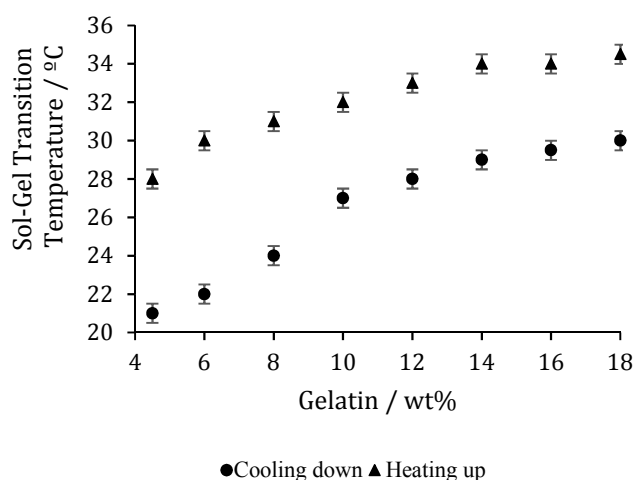


Figure 4.17. Increasing gelatin concentration leads to increasing sol-gel transition temperature. This temperature is dependent of the direction of temperature change (1 °C every 10 min).

Sol-gel transition temperatures experienced a hysteresis of up to 7°C, in this experimental setup, depending on direction of temperature change. Gelation temperatures ranged between 21 and 30 °C and liquefaction temperature 28 and 35 °C for this concentration range. Thermal history of the sample influenced thus the sol-gel transition temperature: When heating, gelatin remained up to higher temperatures a gel, compared to cooling the solutions, where gelatin regained its gel form only at lower temperatures. The reasons can be found on molecular level. As explained in the introduction, thermo-reversible gelation of gelatin occurs over a transition from random coil conformation, over single helices to triple helix formation, which organise themselves to an infinite interconnected molecular network (Parker & Povey, 2012). Ordering and structuring in sol-gel transition demand energy and time, which explains the hysteresis observed. Experimental conditions, such as equilibration time between each temperature change, are thus very important for the determination of sol-gel transition temperature of a system (Madeline Djabourov et al., 1985). Kinetics of gelation is very crucial, which was already discussed in many other studies (Alevisopoulos et al., 1996; Madeline Djabourov et al., 1985; Niklas Lorén & Hermansson, 2000; Tromp, Rennie, & Jones, 1995).

It can be concluded from our conditions tested, that, if not crosslinked, gelatin remains as a gel at room temperature and becomes a liquid at body temperature (37 °C). Thus influence of crosslinking on gelation was investigated.

4.2.2.2 Study of Gelation of Genipin-Crosslinked Gelatin

Gelatin samples at three different concentrations (4, 8 and 12 wt%), containing four different genipin concentrations (0, 0.1, 1 and 10 mM) were prepared and kept at 25 °C. Their liquefaction temperature ($T_{gel \rightarrow sol}$) was determined by continuous heating at 1°C/min till the samples turned liquid. Those measurements were performed at various times and the results after 1.5 h and 48 h are summarised in

Figure 4.18. It can be seen that the gel-sol transition temperature increased over time, as crosslinking was still ongoing in the samples (minimal time for completing crosslinking reaction, under similar conditions, was 24h (Yao et al., 2004)).

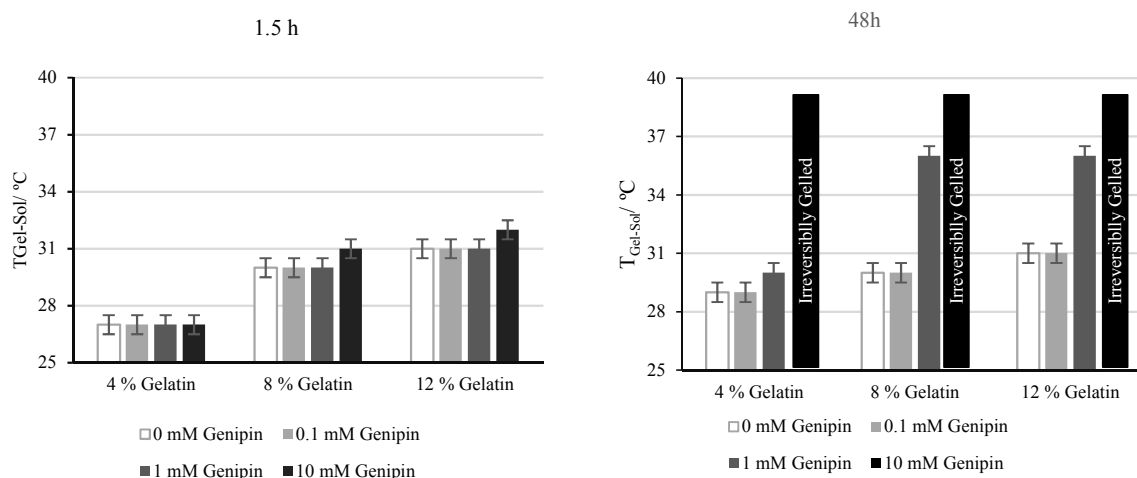


Figure 4.18. Gel-Sol transition temperatures of genipin-crosslinked gelatin gels after 1.5 h (left) and 48 h (right) of crosslinking at 25 °C.

The temperature of the gel-sol transition became constant after 3 h of crosslinking for the samples with 0 and 0.1 mM Genipin, whereas for samples with 1 and 10 mM genipin, the kinetics of the crosslinking reaction had a measurable effect on $T_{gel \rightarrow sol}$ over a prolonged time.

Low genipin concentrations (0.1 mM Genipin) have little influence on gel-sol transition temperature, with similar values as non-crosslinked gels. Samples with 1 mM genipin remain up to higher temperatures in the state of a gel: 30 °C (4 wt% gelatin), 36 °C (8 and 12 wt% gelatin). In this case gelatin network was probably only partly crosslinked (~15 % according to similar studies, which tested crosslinking with the ninhydrin assay (Bigi et al., 2002)) and thus not sufficient enough to create a covalently crosslinked infinite gel network. In contrast, samples with 10 mM genipin remained irreversibly as a gel, in the temperature ranges measured (till 60 °C), as extent of crosslinking of the gelatin network was ~70 % (Bigi et al., 2002; Yao et al., 2004). It can be concluded that crosslinking conveys greater thermal stability to gelatin gels.

Previous studies demonstrated that the time of gelling of genipin-gelatin mixtures at constant temperatures (we did inverse: kept time constant (1°C/min) and measured liquefaction temperatures) increased with increasing temperatures, but at a critical temperature declined again. The reason is that there is a competition between physical and chemical crosslinking and thus gel formation. Low temperatures favour coil-to-helix transformations, while higher temperature favour chemical crosslinking, due to accelerated reaction rates of genipin at higher temperatures (Nickerson, Patel, et al., 2006). This further leads to the conclusion that the temperature, at which crosslinking of gelatin is performed, influences whether the polymer network is chemically crosslinked in its random coil or its ordered triple helix molecular structure.

4.2.2.3 Study of Swelling of Gelatin-Genipin Macrogels

The influence of pH (pH 2.5 and 7), gelatin concentration (4, 8 and 12 wt%) and genipin concentration (0, 0.1, 1 and 10 mM) were tested on the swelling behaviour of bulk hydrogels. Therefore, small pieces (100-200 mg) of crosslinked gelatin gels were introduced into solutions (Figure 4.19) and weighed at specific time points. Furthermore, the gels were observed visually for a period of 7 days to see whether they did not disrupt or dissolve.



Figure 4.19. 8wt % Gelatin gels, crosslinked with different amounts of Genipin, inside a citrate/phosphate buffer solution of pH 7.

The gelatin gels were crosslinked during 72 hours at 22 °C and introduced into a solution of pH 2.5 (adjusted with HCl) or pH 7 (citrate/phosphate buffer) at 22 °C.

At pH 2.5, all gels, except the ones crosslinked with 10 mM genipin, dissolved after a period of 6 h to 3 days (no observations were done in between). The ones crosslinked with 10 mM genipin remained stable over a period of more than 7 days. The 4 wt% gelatin samples of 0 and 0.1 mM genipin swelled very fast and dissolved before 6h. At pH 7 all of them remained stable at least during 3 days.

Most samples (except 4wt% gelatin 0/0.1 mM genipin at pH 2.5) remained stable at 6 h thus their swelling were compared for this time point. The swelling was calculated by measuring the weight ratio in respect to the initial weight.

Influence of pH:

Gels had a major swelling at acidic pH compared to neutral pH (Figure 4.20). Differences were 5- to 9-fold. As an example, while at pH 7 the 8 wt% Gelatin gels swelled between 15 % (10 mM Genipin) and 67 % (0.1 mM Genipin), at pH 2.5 they swelled 138 % (10 mM Genipin) and 340 % (1 mM Genipin). The reason for the difference in swelling at the different pH environments is that, as gelatin has pH sensitive ionisable groups, it swells in a greater extent in an environment that causes ionisation, increasing repulsion of biopolymer chains and thus obtaining greater mesh sizes. The greater solvent uptake was notable at pH 2.5, as the pI of the used gelatin is 4.7-5.2 (supplier's data). Additionally the increased swelling at acidic conditions could be ascribed to the hydrolysis of amide linkage of the crosslinked gelatin network by acid, as reported elsewhere (F. Mi et al., 2000).

Gelatin concentration:

At both pH levels higher gelatin concentrations led to a higher swelling ratio. This can be explained by the fact that gels with higher polymer content are able to incorporate more water than gels with lower polymer content, due to different osmotic pressures.

Crosslinking concentration:

Samples with 10 mM genipin had the lowest swelling compared to the samples with less crosslinker. Crosslinking of gelatin leads to lesser flexibility of the polymer network, smaller mesh sizes and thus fewer solvent uptake. However no direct correlation between genipin concentration and swelling could be found, as gels with 0.1 and 1 mM genipin had in most cases a higher swelling than uncrosslinked gelatin gels. The reason why the gels without genipin had an apparent lower swelling, than the gels with 0.1 and 1 mM genipin could be explained with the fact that erosion/dissolution of superficial, unbound gelatin may have occurred. This was also observed in other studies and confirmed by protein quantification assays of the solution (Bigi et al., 2002; Kirchmayer et al., 2013; Yao et al., 2004). As the swelling ratio is measured by the mass of the bulk gel, the mass of the eroded part is not taken into consideration, in our calculations.

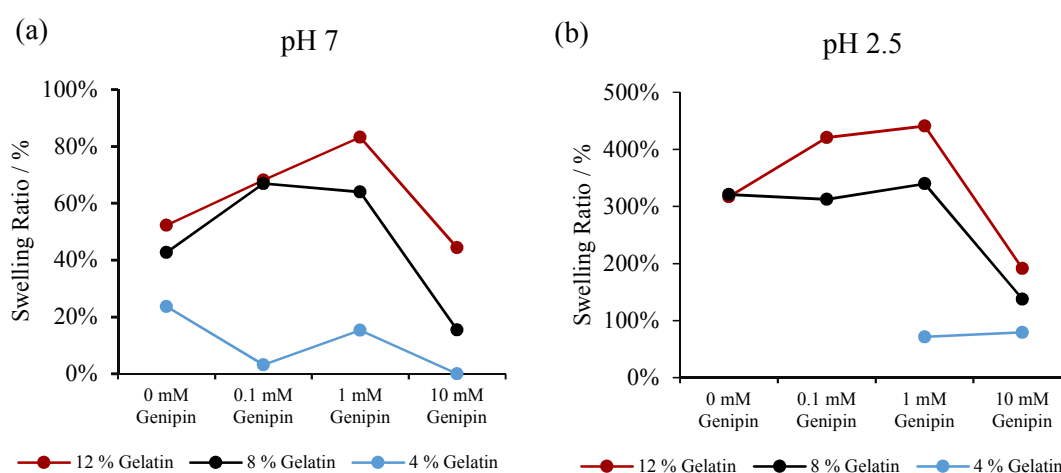


Figure 4.20. Swelling ratio of gelatin gels, crosslinked with genipin at pH 7 (a) and pH 2.5 (b). Swelling ratio was measured after 6 h at 25 °C.

4.2.3 Identification and Quantification of Gelatin and Maltodextrin

4.2.3.1 Density of Gelatin and Maltodextrin solutions

The density of gelatin and maltodextrin solutions in water was measured at 50 °C with a densiometer (Figure 4.21). Aim was to obtain exact values of density, needed to transform weight percentages of the solutions into volume fractions. This was necessary in the numerical evaluation of phase diagram of water-gelatin-maltodextrin described with the Flory-Huggins theory, which was done in collaboration with the research group of J. Bonet of the Universitat Rovira i Virgili (details of this study will not be presented in this thesis, but will be published elsewhere). The knowledge of density is also of interest for separation of gelatin microgels from a maltodextrin-rich solution, by sedimentation/centrifugation.

As can be seen from the results (Figure 4.21), densities of the different polymer solutions are very close to each other, but maltodextrin solutions of similar concentrations than gelatin solutions have higher densities. This can be observed in phase separated gelatin/maltodextrin mixtures, at which the maltodextrin-rich phase constitutes the bottom phase (Figure 4.34). Thus, if gelatin microgels are to be sedimented in the centrifugation process of gelatin/maltodextrin mixtures, maltodextrin solutions must be diluted, in order to have a lower density than gelatin and allow sedimentation of gelatin to occur (Figure 4.55).

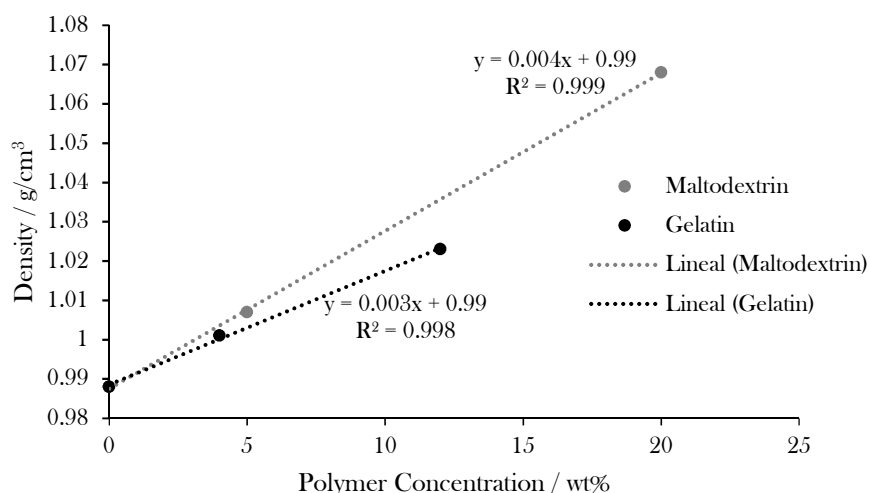


Figure 4.21. Density of maltodextrin and gelatin solutions in water at 50 °C.

4.2.3.2 UV Spectra of Gelatin and Maltodextrin

The UV spectra of the various components with which the microgels were prepared, have been obtained to evaluate the use of UV-VIS techniques for quantification and identification of the components in a mixture.

Maltodextrin has an absorption maxima at 262 nm and 204 nm, similar to the ones observed in its monomer glucose (265 nm and 210 nm, according to (Kaijanen, Paakkunainen, Pietarinen, Jernström, & Reinikainen, 2015)). Gelatin has a peak at 277 nm, originating from amino acids with aromatic rings within the protein. The individual polymers can be quantified by UV, as shown by calibration curves of gelatin at 277 nm and maltodextrin at 262 nm, however the spectra of their mixture overlap in the characteristic regions of both polymers, making it impossible to quantify gelatin/maltodextrin mixtures by UV spectroscopy. Other methods to identify/quantify the polymers are thus needed.

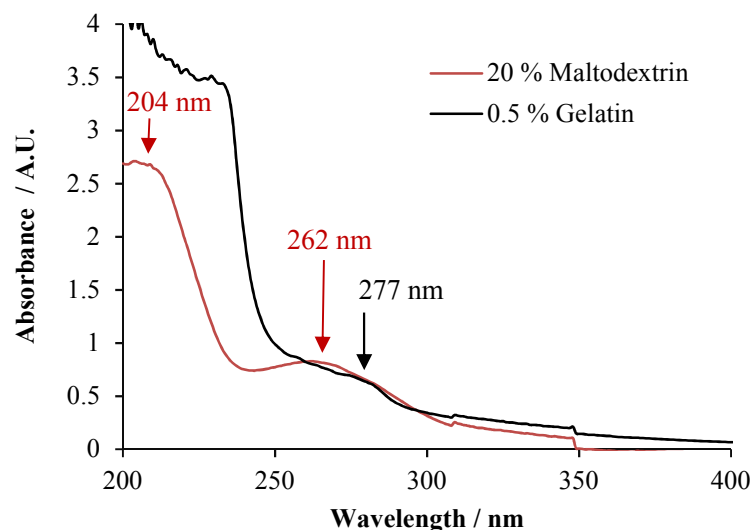


Figure 4.22. UV Absorption Spectra of Gelatin and Maltodextrin

4.2.3.3 Measure Concentration of Maltodextrin and Gelatin by Optical Rotation

The optical rotation of gelatin and maltodextrin solutions were measured at various wavelengths and concentrations. Optical rotation is dependent on concentration of the components and the wavelength (Drude expression), allowing to predict the composition of the individual components in a mixture of two optically active molecules, such as a gelatin/maltodextrin mixture. This method has been previously used to quantify gelatin and maltodextrin/dextran in polymer mixtures (Edelman et al., 2001; Kasapis et al., 1993; Scholten et al., 2004).

As a first step, calibration curves of gelatin and maltodextrin were obtained (Figure 4.23 and Figure 4.24). The polarimeter measured the intensity of the light, which reached the detector, after passing through the sample. For most samples the intensity was below the recommendation of the manufacturer and for some conditions, especially at higher wavelengths (589 nm) or at too high gelatin concentrations, no measurement data was obtained, as the intensity reaching the detector was too low. Gelatin solutions are turbid, probably due to impurities inside the protein raw product, and therefore only solutions of maximum 2 wt% could be measured.

Figure 4.23 and Figure 4.24 show the calibration curves of gelatin and maltodextrin at 365, 405 and 546 nm. The optical rotation of the solvent, water, at 365 nm was defined as 0°. Gelatin has a low negative optical rotation (Figure 4.23), in the measured domain (0-2 wt %) and had the drawback, that at higher concentrations no measurement were possible, as not enough light reached the detector. In the case of maltodextrin (0-20 wt%) optical rotation was positive and the polymer reached optical rotations of up to 90° (Figure 4.24). The calibration curves showed close to linear behaviour, allowing to predict the concentrations of the individual components, inside this concentration range, by optical rotation.

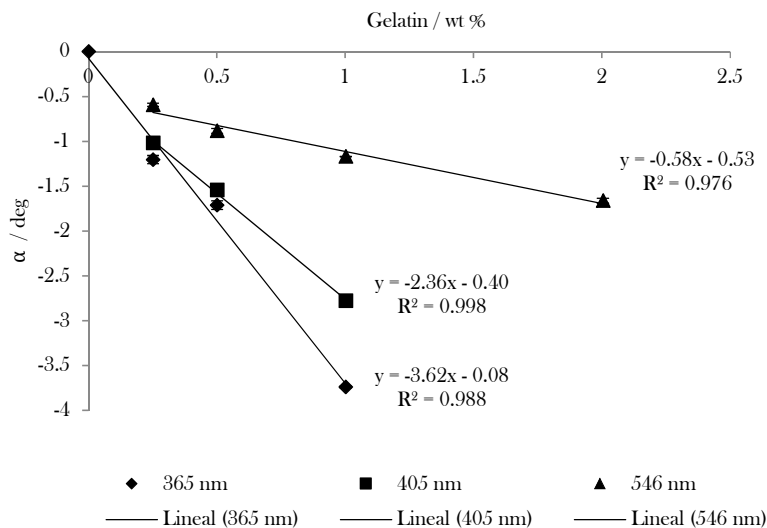


Figure 4.23. Calibration curve of the concentration-dependent optical rotation of gelatin, measured at three distinct wavelengths ($T=45\text{ }^{\circ}\text{C}$).

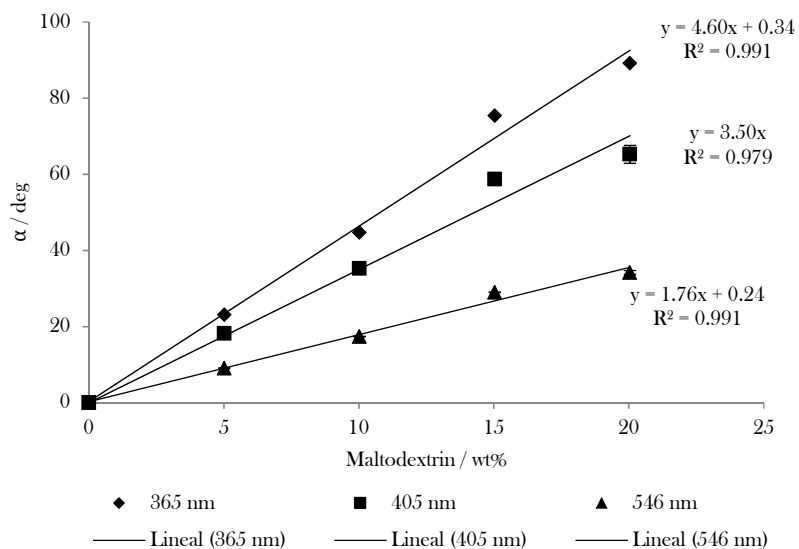


Figure 4.24. Calibration curve of the concentration-dependent optical rotation of maltodextrin, measured at three distinct wavelengths.

The reliability of the calibration values at the different concentrations of both polymers was furthermore checked by constructing Drude plots of $1/\alpha$ versus λ^2 (see equation 3.3). The standard of linearity was achieved and is illustrated in Figure 4.25 and Figure 4.26.

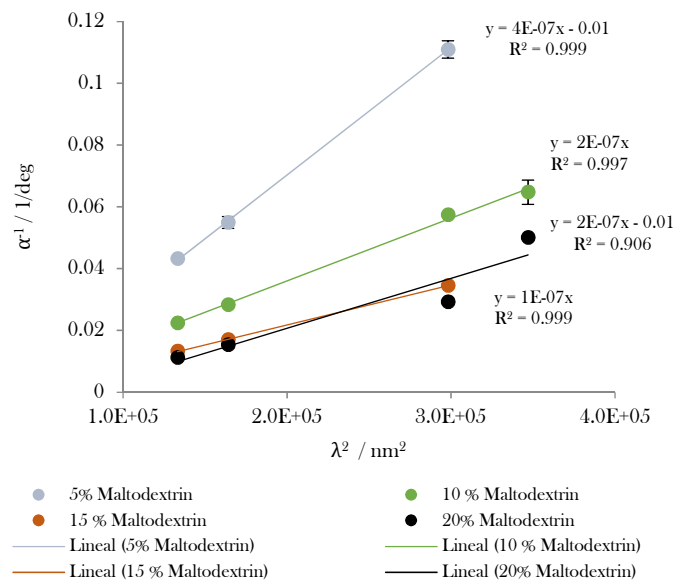


Figure 4.26. Drude plots for solutions of maltodextrin at 45°C, measured at wavelengths of 365, 405, 546 and (for 10 and 20 wt % maltodextrin) 589 nm

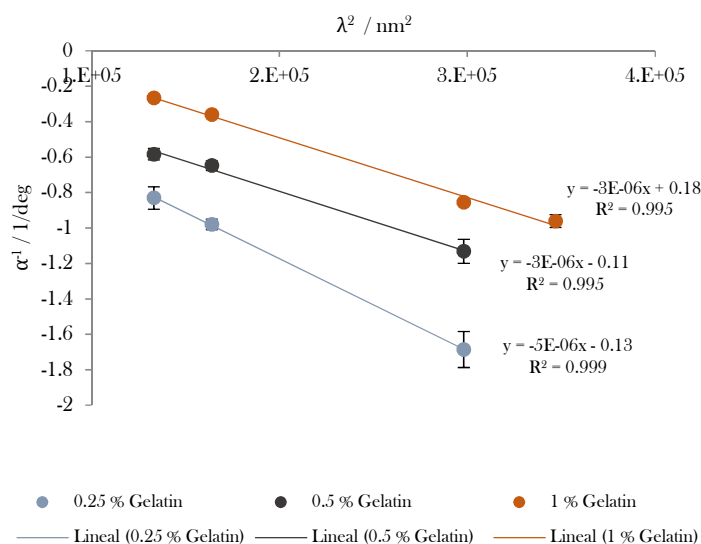


Figure 4.25. Drude plots for solutions of gelatin at 45°C, measured at wavelengths of 365, 405, 546 and (for 1 wt % gelatin) 589 nm

From the calibration curves, it was seen that most reliable results, and up to higher concentrations, were obtained for both polymers at 365 nm and 546 nm. Therefore, those wavelengths were selected to measure concentrations of the individual components inside polymer mixtures. This can be done by solving a system of equations, taking as an assumption that the total optical rotation in a sample is the simple addition of the contribution of each polymer. The optical rotation of each polymer can be obtained from the calibration curves in Figure 4.23 and Figure 4.24.

$$\alpha(c_{MD}, c_{Gel}, \lambda = 365 \text{ nm}) = (4.6 c_{MD} + 0.34) + (-3.62 c_{Gel} - 0.08) = 4.6 c_{MD} - 3.62 c_{Gel} + 0.26 \quad (4.2)$$

$$\alpha(c_{MD}, c_{Gel}, \lambda = 546 \text{ nm}) = (1.76 c_{MD} + 0.24) + (-0.58 c_{Gel} - 0.53) = 1.76 c_{MD} - 0.58 c_{Gel} - 0.29 \quad (4.3)$$

Solving the system of equations for concentrations of maltodextrin (c_{MD}) and gelatin (c_{Gel}), following relation is obtained:

$$c_{MD}(\alpha) = 0.98 \alpha(\lambda = 546 \text{ nm}) - 0.16 \alpha(\lambda = 365 \text{ nm}) + 0.32 \quad (4.4)$$

$$c_{Gel}(\alpha) = 1.24 \alpha(\lambda = 546 \text{ nm}) - 0.48 \alpha(\lambda = 365 \text{ nm}) + 0.48 \quad (4.5)$$

From those equations the concentration of both polymers can be determined, by measuring the optical rotation of the sample at two different wavelengths (365 and 546 nm).

To verify the simple additivity of optical rotation contributions, for each wavelength, the optical rotations of two mixtures of gelatin and maltodextrin was measured and compared to the calculated value (Table 4.4). Furthermore, based on the optical rotation of the samples, the theoretical sample composition was calculated (Table 4.4).

Table 4.4. Measured optical rotation of two gelatin/maltodextrin mixtures at 365 nm and 546 nm, at 45 °C, compared with the calculated optical rotations. ¹Theoretical composition of sample calculated from measured optical rotations at 365 nm and 546 nm.

| Samples | Measured $\alpha(\lambda=365 \text{ nm})$ | Calculated $\alpha(\lambda=365 \text{ nm})$ | Measured $\alpha(\lambda=546 \text{ nm})$ | Calculated $\alpha(\lambda=546 \text{ nm})$ | Calculated sample composition ¹ |
|-------------------------|---|---|---|---|--|
| 1% Gel / 2% MD | 0.06 ° | 5.84 ° | 0.67 ° | 2.65 ° | 1.28% Gel / 0.97% MD |
| 0.25% Gel / 3.75% MD | 12.4 ° | 16.61 ° | 6 ° | 6.17 ° | 1.97% Gel / 4.22% MD |

As can be seen in Table 4.4, the measured and calculated values of the optical rotation do not coincide. As a consequence, neither the correct sample composition could be calculated, based on the optical rotation measurements. Despite previous groups showing that the linear additivity of the optical rotations of gelatin and maltodextrin can be applied for this system (Kasapis et al., 1993), it does not seem to hold under our measurement conditions. The linear relation between the individual optical rotation must hold true, if the system is considered ideal and no interactions between the polymers is taking place. Gelatin and maltodextrin have physicochemical interaction and this may be one of the reasons why the concentration of the individual polymers could not be calculated over this method.

Optical rotation, in our experimental conditions, could thus not be considered as valuable measurement method to determine the composition of gelatin/maltodextrin mixtures. It will however be used to qualitatively determine presence of polymers in solution, during purification of microgel suspensions (see section of purification of microgels by centrifugation).

4.2.3.4 Labelling of Polymers

In order to identify the nature of the emulsion (gelatin-in-maltodextrin or maltodextrin-in-gelatin) fluorescently labeled molecules were used.

Different approaches were tried, adapting protocols from the literature.

4.2.3.4.1 Adding Rhodamine B to the W/W emulsion

As an initial study, Rhodamine B was added to a 10% gelatin / 18% maltodextrin emulsion in a concentration of 0.01 wt%, adapting the protocol from (M. F. Butler & Heppenstall-Butler, 2001) who labeled in this manner gelatin. In the composition tested, the gelatin-rich phase was the continuous phase. Rhodamine B is positively charged and may interact selectively with the charged negative residues of gelatin. Maltodextrin has no charges and would remain thus unlabeled.

As can be seen in Figure 4.27 the gelatin-rich continuous phase was labeled by this method. However no strong contrast between both phases was observed, which can be attributed to the fact that Rhodamine B was not covalently anchored to any of the polymers. Therefore, further methods of labeling were tested, to achieve higher contrast in the images.

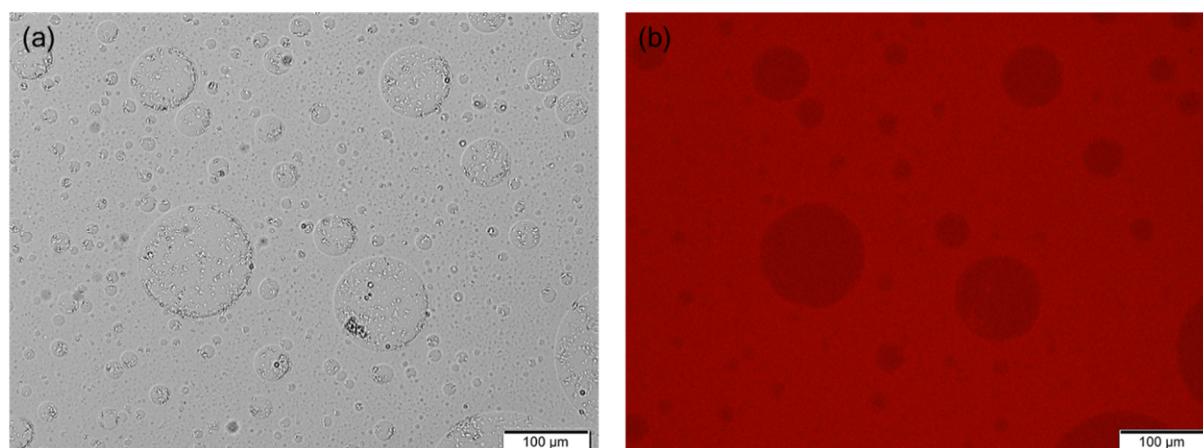


Figure 4.27. 10% gelatin / 18% maltodextrin emulsion, in which the continuous phase, rich in gelatin, was successfully labelled with Rhodamine B. (a) shows the sample in the light transmission mode, (b) in the light reflexion mode, with fluorescence filters adapted to excitation/emission spectrum of Rhodamine B.

4.2.3.4.2 Covalently labelling gelatin and maltodextrin with Rhodamine B isothiocyanate

Next, a protocol for covalent protein and polysaccharide labeling has been adapted from (Mladenovska et al., 2007) and (Lamprecht et al., 2000). It is based on the formation of a thiourea linkage between Rhodamine B isothiocyanate (RITC) and the protein or an isothiocarbamate linkage for the case of the polysaccharide (Figure 3.5). The polymer solutions were labelled and the free dye was removed by dialysis, as described in the experimental section.

Labelling efficiency was measured by quantifying the amount of RITC, which remained in the dialysis tube. Previously for this purpose, a calibration curve of RITC concentration at its absorption maxima of 551 nm was done. Results (Table 4.5) show that labeling efficiency was highest for gelatin (19 %), followed by maltodextrin in DMSO (7 %) and lastly maltodextrin in water (2 %). This followed our expectations, as the amino groups of gelatin are more reactive with isothiocyanates than the hydroxyl groups of maltodextrin. Dissolving in maltodextrin in DMSO increased labeling efficiency as the hydroxyl group of the polysaccharide did not compete with the ones of water.

Table 4.5. Amount of RITC bound to polymer after labelling reaction and removal of free dye by dialysis. Labelling efficiency and degree of labelling calculated with equations 3.5 and 3.6

| | Gelatin (in water) | | Maltodextrin (in water) | | Maltodextrin (in DMSO) | |
|---|--------------------|-----------------|-------------------------|-----------------|------------------------|-----------------|
| | mg | μmol | mg | μmol | mg | μmol |
| RITC before dialysis | 2.48 | 4.7 | 3.9 | 7.1 | 4 | 7.5 |
| RITC after dialysis | 0.47 | 0.88 | 0.06 | 0.19 | 0.27 | 0.52 |
| Polymer before dialysis | 251 | 5 | 95 | 28 | 3000 | 833 |
| Polymer after dialysis | 184 | 3.68 | 55 | 15 | 1250 | 347 |
| Labelling efficiency [%] | 19 | | 2 | | 7 | |
| Degree of Labelling ($n_{\text{dye}}/n_{\text{pol}}$) | 0.24 | | 0.01 | | 0.001 | |

The degree of labelling was calculated from the known molar concentrations of the polymers and RITC in the dialysis bag. For gelatin 0.24 mol of RITC was labelled per mole of gelatin. In the case of maltodextrin in water 0.01 mol of RITC and for maltodextrin in DMSO 0.001 mol per mole of polysaccharide was labelled. The degree of labelling depends on the labelling efficiency and the initial concentration of polymer and dye. Higher degrees of labelling could have been obtained by varying the initial concentrations of the molecules, but other factors, such as solubility and yield of polymer in the product were more important. RITC can be detected at very low concentrations. It has also to be noted that some polymer chains might have passed through the dialysis membrane, as the mass of them before and after dialysis was not the same in the dialysis bag (Table 4.5). Labelled polymer may have escaped from the bag, and this was not taken into account in the calculations.

Above values are based on the amount of RITC, which remained in the dialysis bag, thus should have been associated to the polymers. To assure labelling was effective gelatin-in-maltodextrin emulsions were prepared with the labelled polymers (Figure 4.28).

Considering that the microgels are made of gelatin, if gelatin-RITC is used, the dispersed phase should be labeled, while if Maltodextrin-RITC is used, the continuous phase should be marked by the fluorescent dye. Figure 4.28 (a-c) shows that in all cases the gelatin droplets were labelled. Using Gelatin-RITC resulted in clearly marked gelatin droplets, indicating that gelatin labelling has been successful, confirming the results from Table 4.5 Maltodextrin-rich continuous phase was however not labeled in Figure 4.28 b and c. Instead, the gelatin droplets were marked. This indicates that maltodextrin was not labelled and either gelatin showed some autofluorescence or RITC in the sample associated to gelatin.

To verify whether the fluorescence from the gelatin droplets does not origin from gelatin autofluorescence, a control samples was prepared without RITC. 3% Gel / 20% MD emulsions, free from fluorescent dye, did not show any fluorescence signal (Figure 4.28 d), which signifies that none of the polymers present autofluorescence under given excitation (555 nm) and emission (565 to 681 nm) conditions.

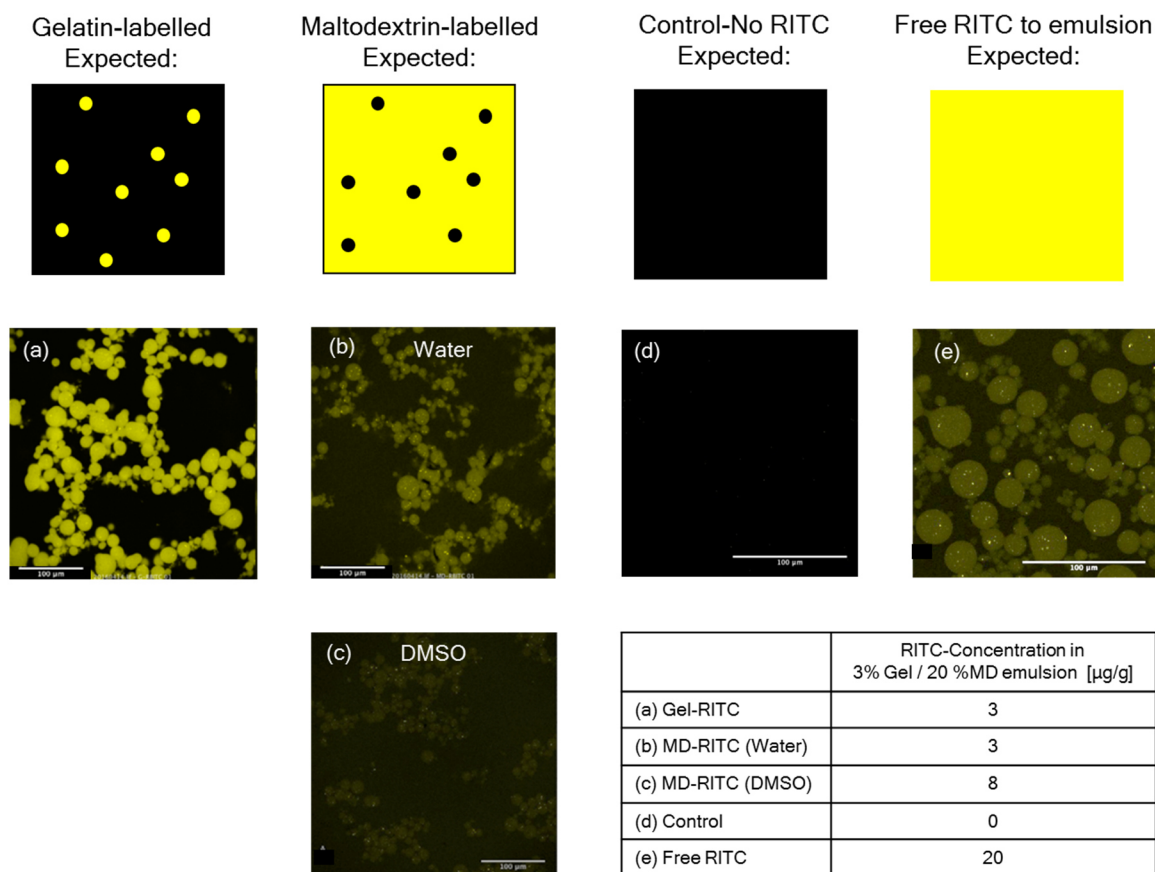


Figure 4.28. CLSM micrographs of 3% Gel / 20% MD emulsions, prepared with (a) Gel-RITC, (b) MD-RITC (labeled in water), (c) MD-RITC (labeled in DMSO), (d) without RITC, (e) addition of free RITC to emulsion. The illustrations above the micrographs illustrate the expected outcome, in case labelling of the polymers was successful. The table indicates the total concentration of RITC, bound to the polymers or free, which has been added to each sample.

The explanation for the fluorescence of gelatin droplets in the samples with maltodextrin-RITC, was that maltodextrin was not labelled covalently with RITC and only associated to free RITC, which has not been washed away during the dialysis process. Free RITC dye might have diffused towards gelatin and remain associated to it. To confirm this hypothesis free RITC was added to a non-labelled emulsion and observed under the CLSM. Effectively, free RITC did not distribute equally in the entire sample, as would have been expected, but was mostly associated with gelatin (Figure 4.28 e).

This brings us to the conclusion, that this labelling protocol is not adequate for maltodextrin-labeling. What remained together with maltodextrin in the dialysis bag may have been either free RITC, which was not washed away during dialysis or RITC associated to maltodextrin by non-covalent bonds.

On the other hand, it is clear that gelatin was successfully labelled by this method and that simple addition of free RITC does also label gelatin, by ionic interactions between the charged dye and gelatin and maybe also covalent thiourea linkages, formed under non-basic conditions. Therefore, for future experiments, gelatin will be labelled by mixing the stock solution with a fluorescent dye during 2 h at 40 °C. Results of this labelling procedure can be found further below, in Figure 4.41.

4.2.3.4.3 Fluorescence emission of genipin-crosslinked emulsions

We could further show, that crosslinking gelatin with genipin, within gelatin/maltodextrin emulsions, allowed to detect the genipin-rich, thus the gelatin-rich phase, by fluorescence microscopy. Genipin has a emission maximum at 630 nm, when excited at 590 nm (Almog et al., 2004). This is likely due to the formation of the pyridine-like structures after reaction of genipin with gelatin. Our microscope did not have filters allowing excitation/emission exactly at those wavelengths, but using the U-MWG2 filter (Figure 3.4) with excitation of the sample at 510-550 nm and emission of light with wavelengths over 590 nm, allowed to detect the fluorescence of genipin (Figure 4.29). A 8 % Gel / 20 % MD emulsion with a dispersed phase of gelatin, and a 10 % Gel / 8% MD emulsion, with a continuous phase of gelatin were prepared, in both cases crosslinked with 5 mM genipin. Thus, besides its crosslinking capabilities, genipin can be used to label gelatin.

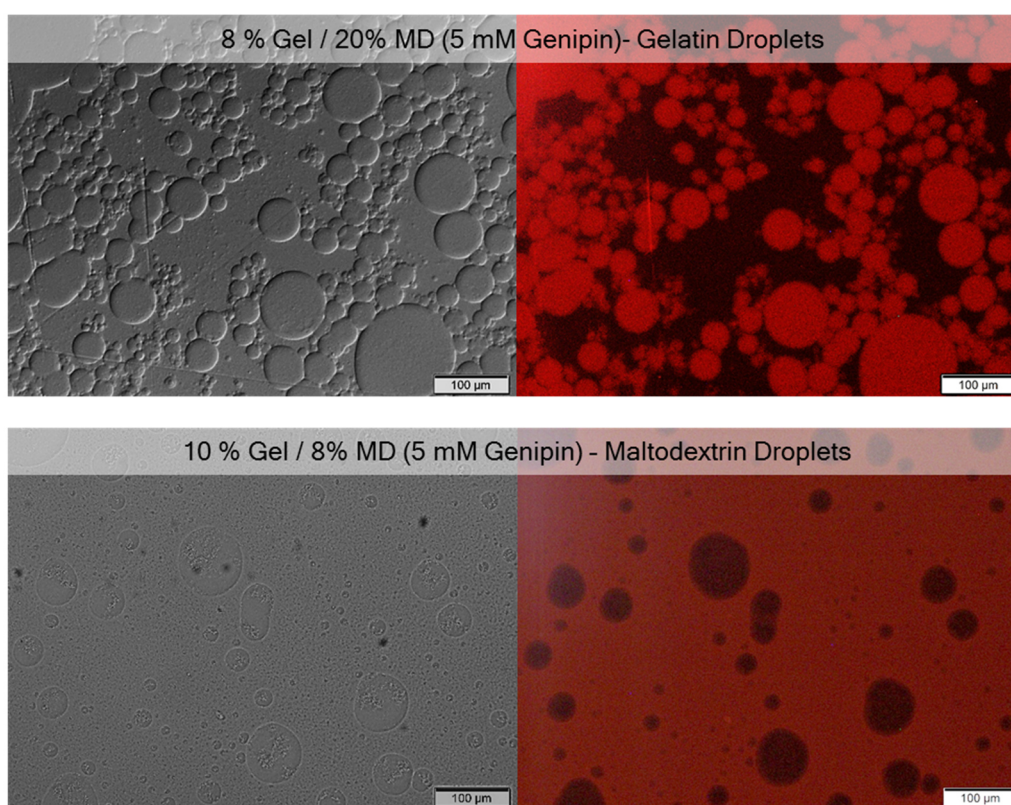


Figure 4.29. Genipin-crosslinked emulsions, in absence of fluorescent dyes, with gelatin in the dispersed phase (8 % Gel / 20% MD) or gelatin continuous emulsions (10 % Gel / 8% MD) allowed identifying the gelatin-rich phase under fluorescence microscopy, due to the fluorescence properties of the crosslinker genipin.

4.2.4 Phase Behaviour of Water/Gelatin/Maltodextrin System

The phase behaviour of gelatin and maltodextrin mixtures in water was evaluated at constant temperatures and different concentrations. As pure gelatin solutions gel below 30 °C and pure maltodextrin solutions precipitate at low temperatures, phase behaviour was studied 50 °C to assure that all polymers are soluble and form liquid solutions.

The stock solutions of gelatin and maltodextrin were mixed with water and the vials placed in the thermostated water bath, for a period of 5 days at 50 °C. Close to 150 samples with concentrations between 0-12.5 wt% Gelatin and 0-21 wt% Maltodextrin were analysed.

Figure 4.30 shows pictures of several gelatin/maltodextrin mixtures just after preparation and after 5 days at 50 °C. The yellowish liquid phase is attributed to the gelatin polymer and the more transparent liquid phase is maltodextrin-rich. Gelatin solutions have a lower density and, in case of phase separation it forms the upper liquid phase. While the solid phase at the liquid-liquid interphase is not easily observable in those images, the sedimented precipitate can be clearly observed for the samples 8% Gel / 10% MD, 12% Gel / 6% MD and 12% Gel / 12% MD. Furthermore, it can be seen how the 6% Gel / 9% MD samples turns from two liquid phases to one liquid phase, after 5 days, due to below-mentioned reduction of effective polymer concentration in solution.






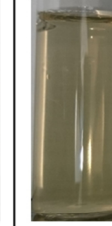







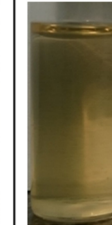

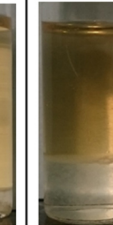
| | 1% Gel / 3% MD | 3% Gel/ 20% MD | 6% Gel/ 3% MD | 6% Gel/ 9% MD | 8% Gel/ 10% MD | 12% Gel/ 3% MD | 12% Gel/ 6% MD | 12% Gel/ 12% MD |
|-------|---|---|---|---|---|--|---|---|
| Day 0 |  |  |  |  |  |  |  |  |
| Day 5 |  |  |  |  |  |  |  |  |

Figure 4.30. Pictures of gelatin/maltodextrin samples just after preparation (day 0) and after 5 days at 50 °C (day 5).

After two and five days, phase behaviour of those samples was determined (Figure 4.31). Parameters taken into account were number of liquid phases, whether a solid phase coexisted with the liquid phases and where this solid was located within the sample.

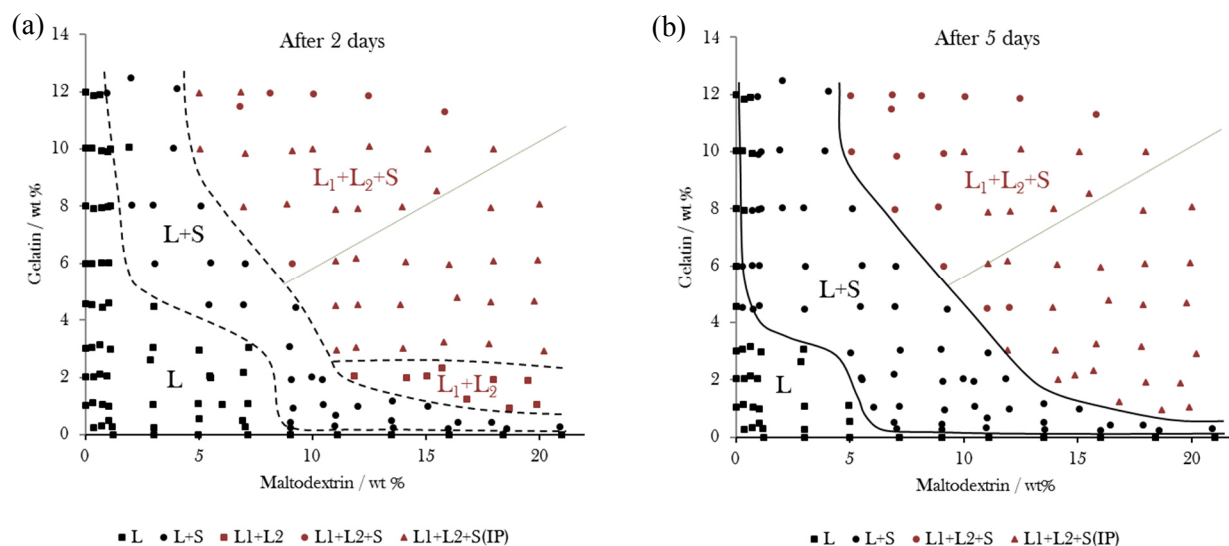


Figure 4.31. Phase behaviour of binary mixtures of maltodextrin and gelatin in water, observed after (a) 2 and (b) 5 days at 50 °C. The diagrams indicate whether one or two liquid phases is present and if and where a solid precipitate can be found in the sample. The green dotted line is the 50:50 phase volume line. L: One liquid phase, L+S: One liquid and a solid phase, L₁+L₂: Two liquid phases, L₁+L₂+S: Two liquid phases coexisting with a solid phase at the bottom of the sample, L₁+L₂+S (IP): Two liquid phases coexisting with a solid phase at the interphase between both liquid phases

After two days at 50 °C, probably still far from real equilibrium, gelatin/maltodextrin mixtures experiences four different types of phase behaviour, depending on their concentration. At low concentrations of gelatin and maltodextrin only one liquid phase was observed, both polymers were perfectly miscible. At increased concentrations, the mixture still consisted of one liquid phase, but a solid white precipitate was present at the bottom of the sample.

Immiscibility of the two liquid phases occurred at higher concentrations and those regions are separated by the binodal line from the one-liquid phase region. Within the region of two liquid phases, at low gelatin concentrations, no precipitate was observed, while at higher concentrations, this one was located at the interphase between the gelatin-rich and maltodextrin-rich liquid phases (L₁+L₂+S (IP)). For samples above 12 % gelatin and 10 % maltodextrin, the precipitate was found as a sediment at the bottom (L₁+L₂+S) (Figure 4.31 a).

After five days, closer to real thermodynamic equilibrium, the one liquid phase (L) region was observed to be smaller, consequently samples contained precipitation in the one liquid phase region (L+S) already at lower concentrations (Figure 4.31 b). The L₁+L₂ region vanished completely, with all samples in the two liquid phase region containing a solid phase. It was observed that the solid phase sediment to the bottom at higher concentrations of both biopolymers, while at lower concentrations the solid phase was localised at the liquid-liquid interphase.

Moreover, the binodal line shifted slightly to higher concentrations, as few samples which contained two liquid phases after two days turned into to L+S at five days (Figure 4.32). The sample 6% Gel / 9% MD in Figure 4.30 showed this type of behaviour. This can be explained by the fact that as parts of the polymers in solution precipitate, the effective concentration of the polymers in solution get reduced and thus is not high enough to phase separate into two liquid phases. The reduction in effective polymer concentration can also affect the phase volumes of both liquid phases and consequently the properties of the resulting emulsions. The green dotted line in Figure 4.31 is the 50:50 phase volume line, meaning that along this line samples have two liquid phases of equal volume.

The overlay of the phase boundary lines at day two and day five in Figure 4.32 demonstrate the changes in this period.

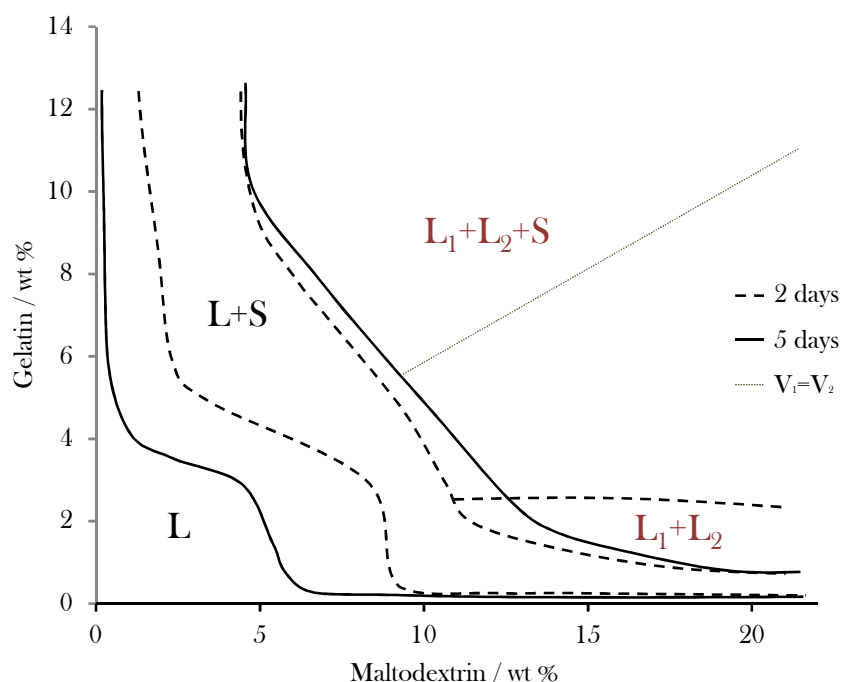


Figure 4.32. The evolution of gelatin/maltodextrin mixtures in water at 50 °C after 2 days (dotted line) and 5 days (solid line). The green dotted line indicates compositions where L_1 and L_2 have equal volumes.

Comparing the obtained phase diagram with other previously described in the literature (Figure 1.40) the tendency of the binodal line is similar, but depending on the reports, the curve is shifted from higher concentrations to lower concentrations (Aymard et al., 2000; R. S. Khan et al., 2011; Norton & Frith, 2001) or vice versa (Kasapis et al., 1993). Furthermore only few studies (Hoey et al., 2016; Kasapis et al., 1993) have reported about the existence of the third solid phase in this biopolymer mixture. In contrast to our study, Kasapis et al. observed the precipitation of the biopolymers already after centrifugation of the freshly prepared sample at 45 °C (Kasapis et al., 1993). The differences originate from the fact that different studies use different sources of gelatin and maltodextrin polymers and physicochemical properties might differ on sources and from batch to batch, and moreover, the temperature at which the phase diagram was studied was also different.

As already discussed, the formation of the solid phase is rather slow, being observed that its precipitation occurs, in many samples, after the separation of L_1 and L_2 phases. The time evolution of samples is evaluated in more details in the next section.

4.2.4.1 Kinetics of Phase Separation in Gelatin-Maltodextrin Mixtures

4.2.4.1.1 Separation of L₁ and L₂ Phases

The phase separation into two liquid phases happened for most gelatin-maltodextrin emulsions within 1.5 hours after mixing (Figure 4.33 a). This was measured by light transmission at the liquid-liquid interface from multiple light scattering measurements, using the Turbiscan apparatus, at constant temperature (50 °C) and $\lambda = 880$ nm. The phase separation process was considered completed, once the light transmission at the region of the liquid-liquid interphase remained stable for a prolonged period of time. Initial destabilisation mechanisms of the emulsion induced variation of light transmission due to droplets coalescing to bigger ones up to complete bulk phase separation.

Figure 4.33 b shows the light transmission profile through a vial containing a 8 % Gel / 10 % MD emulsion (filled up to 35 cm of the vial) just after mixing, at 45 min, 1 h and 2 h later. It can be seen how gradually the two phases separated, with the phase-separating interphase having lowest light transmission. No detailed study on dependency of phase separation time on different factors was performed, but those results serve as an indication for how long samples need in order to become totally phase separated, which is important to know in the practical application of emulsions.

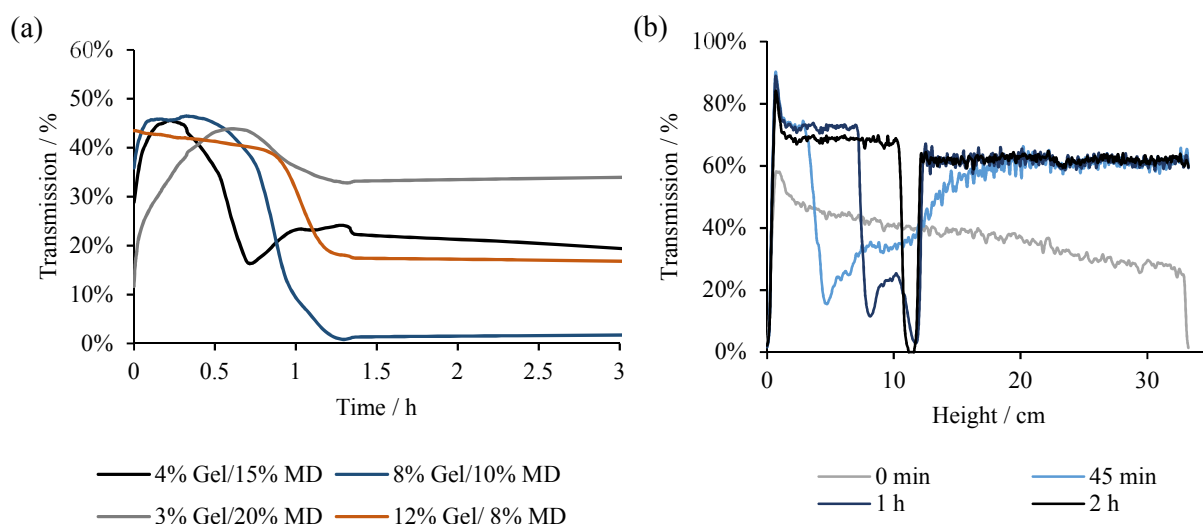


Figure 4.33. (a) Light transmission measurement at the liquid-liquid interphase of four different gelatin-maltodextrin emulsions, measured by the Turbiscan apparatus. (b) Evolution of light transmission data throughout the vial containing a 8 % Gel / 10 % MD emulsion (height indicates the height in the vial. 0 cm is the bottom, 35 cm the top of the vial).

4.2.4.1.2 Formation of the Solid Phase

The first conclusion from the phase diagrams is that formation of the precipitate underlies a kinetic process and is a function of concentration of both maltodextrin and gelatin concentration. At higher concentrations, in the one- and two-liquid phase regions, the precipitate was observed already after 2 days, while most mixtures with lower biopolymer concentration contained a solid phase after five days. In the region close to the axes in the phase diagram no precipitate was observed after 5 days, however it is to be supposed that over longer periods, biopolymer mixtures in those regions would also start to form a solid phase.

In the phase diagram in Figure 4.31 an unexpected behaviour can be seen for low maltodextrin concentrations (0.5 wt % maltodextrin). No solid phase is formed (L) for samples between 0 - 4.5 wt % gelatin, solid can be found (L+S) in between 4.5 - 8 wt% gelatin and finally above 8 wt % gelatin the samples seem to be free from solid particles (L) again. It makes no physicochemical sense that increasing the polymer concentration (in this case gelatin) the sample gets suddenly free again from solid precipitate. An explanation for having observed this phenomenon, may very probably come from an experimental error. Those results rely on observations by naked eye of the sample. The higher the gelatin concentration, the more yellow and turbid the sample gets. This may explain that at higher gelatin concentrations the small solid particles could not be identified by eye anymore and samples may therefore have been consequently wrongly characterised as L instead of L+S. Therefore, the boundary line between L and L+S, drawn in Figure 4.31 (day 5), takes into consideration this possible experimental error, and follows a more logical path.

Next, it can be concluded, from the presence and position of the solid phase in the two-liquid phase region at day two and five, that the solid precipitate seems to form at the interphase between the gelatin and maltodextrin-rich phases and then continuously over time sediments to the bottom of the vial. This can be seen from samples which did not contain solid precipitate after two days at 50 °C, but three days later a solid phase started being formed at the liquid-liquid interphase. For samples, at which the solid precipitate was already present at the interphase at two days, after five days many of those solid particles sedimented. A reason why the precipitate may be formed at the interphase of the lower maltodextrin-rich phase with the upper gelatin-rich phase, is that in this region of the emulsion highest concentrations of both polymers are in physical contact. As found in previous studies the self-association and aggregation of maltodextrin, and thus its precipitation, is promoted by gelatin, which drives a two-coil to double helix transition of maltodextrin (Hoey et al., 2016; Kasapis et al., 1993). As this process is proportional to the concentrations of maltodextrin and gelatin (Kasapis et al., 1993), it makes sense that precipitation is enhanced in regions where the two polymers are in contact at higher concentrations, thus at the interphase.

Over time the solid phase starts to sediment to the bottom of the sample. This may have been caused by increased concentrations of the solid phase, the particles may have compacted and overcome interfacial and buoyancy forces, which maintained them at the liquid-liquid interphase. Figure 4.34 illustrated this situation at which the solid phase sedimented to the bottom of the gelatin/maltodextrin emulsion.

The process of solid formation at the interphase and consequent sedimentation to the bottom had

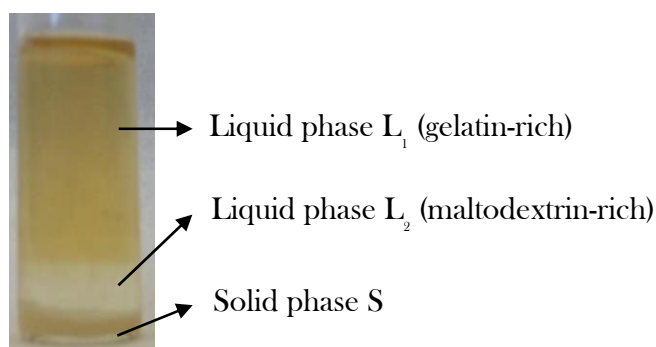


Figure 4.34. Close-up look of a 10% Gel / 8% MD emulsion, in which the two liquid L_1 and L_2 phases and the solid phase, which sedimented, are clearly observable. Picture reproduced from (Aragon Artigas, 2016).

different kinetics, depending on the initial concentrations of the biopolymer mixtures. To get a more detailed follow-up of this process, the transmission data of some samples were acquired for a period of

5 days from multiple light scattering measurements, with the Turbiscan apparatus, at constant temperature (50 °C) and $\lambda = 880$ nm. Transmission was followed at the liquid-liquid interphase of the emulsions and at the bottom of the samples.

The four samples analysed were 8% Gel / 10% MD and 12% Gel / 8% MD, in which the gelatin-rich phase had a bigger volume, and 3% Gel / 20% MD and 4% Gel / 15% MD, with a bigger phase volume for the maltodextrin-rich phase (Figure 4.35).

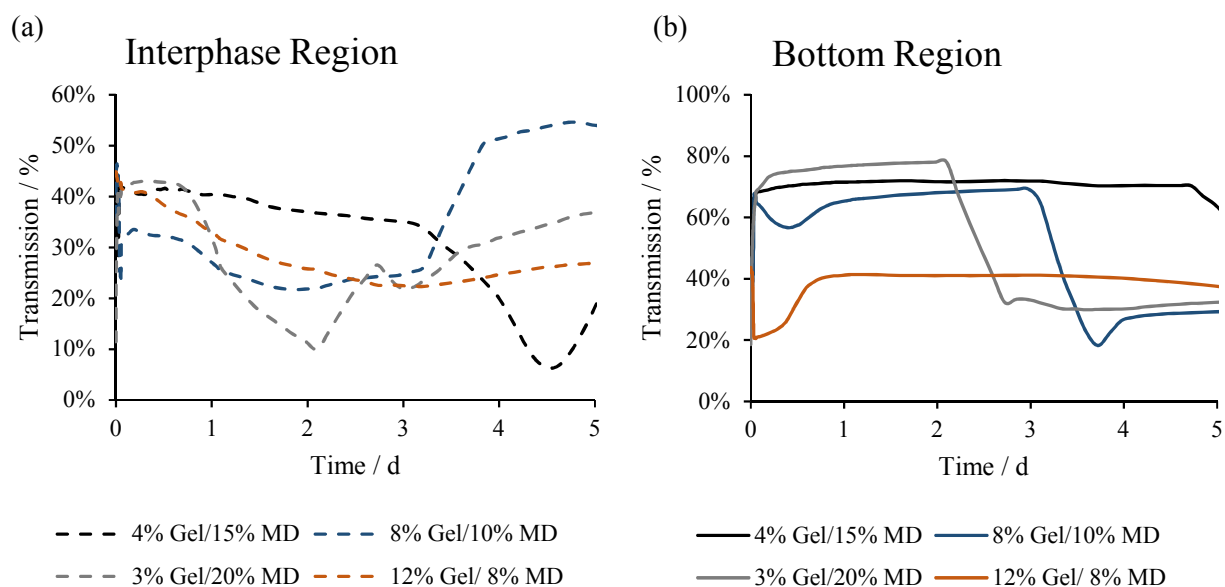


Figure 4.35. Light transmission, measured by using the Turbiscan apparatus, through sample changes due to formation of solid particles inside the four different gelatin/maltodextrin mixtures, which phase separate into two liquid phases. (a) shows transmission of the sample at the liquid-liquid interphase, (b) transmission at the bottom of the sample.

Following the light transmission at the liquid-liquid interphase, it can be seen that transmission starts to decrease fastest for the 12% Gel / 8% MD sample (4 h) and slowest for the 4% Gel / 15% MD sample (3 d). This decrease in transmission may be attributed to formation of solid particles, which reduce light transmission through this part of the sample. The transmission goes down in all samples up to a moment, at which there is an abrupt increase of transmission again (Table 4.6 and Figure 4.35). The reason for this abrupt increase in transmission is the detachment of solid particles from the liquid-liquid interphase, as shown, by analysing the transmission at the bottom of the sample.

Table 4.6. Summary of moments at which light transmission changes in gelatin/maltodextrin samples.

| | Transmission starts to lower at interphase | Transmission rises again at interphase | Transmission lowers at bottom of sample |
|------------------------|--|--|---|
| 12% Gel / 8% MD | 4 h | 3.5 d | 4 d |
| 8% Gel / 10% MD | 10 h | 3.5 d | 3.5 d |
| 3% Gel / 20% MD | 20 h | 2 d | 2 d |
| 4% Gel / 15% MD | 3 d | 4.5 d | 4.7 d |

The light transmission was for most samples quite high at the bottom of the mixtures, where the maltodextrin-rich transparent phase is located. The only exception formed the gelatin-rich 12% Gel / 8% MD sample, which after 20 h had already reduced transmission. In this case the precipitate seemed to appear rapidly at the bottom of the sample, after less than 1 day. In the first 20 h transmission was lower in this region of the sample possibly due to the presence of emulsion droplets, up to its migration into the upper liquid phase, at complete phase separation.

In the three other samples transmission lowered strongly at the bottom, in the moment, that transmission raised at the liquid-liquid interphase of the emulsions (Figure 4.35). This is an indication that solid particles detached from the liquid-liquid interphase and sedimented to the ground. Would the solid have been formed directly in the lower maltodextrin-rich liquid phase, a gradual decrease of transmission would have been observed, which is not the case.

As a control, light transmission through blank samples of maltodextrin and gelatin were recorded, which showed that under the same conditions (5 days at 50 °C) no precipitate was formed (Figure 4.36). The light transmission remained constant throughout the period of five days at the bottom of the sample for maltodextrin, and was the same for upper parts of the sample. At gelatin there was a slight decrease in light transmission after 15 h, which was however the case not only at the bottom, but throughout the entire sample. Thus the decrease in light transmission is not caused by formation of precipitate, as this one would have sedimented (or creamed) over time, leading to a gradual change in light transmission at the bottom or top of the sample. The change might have thus occurred due to a conformational change of the protein structure at prolonged time at higher temperatures.

Our study is incomplete and only four samples were analysed in details. No relationship between sample composition and solid formation kinetics was calculated.

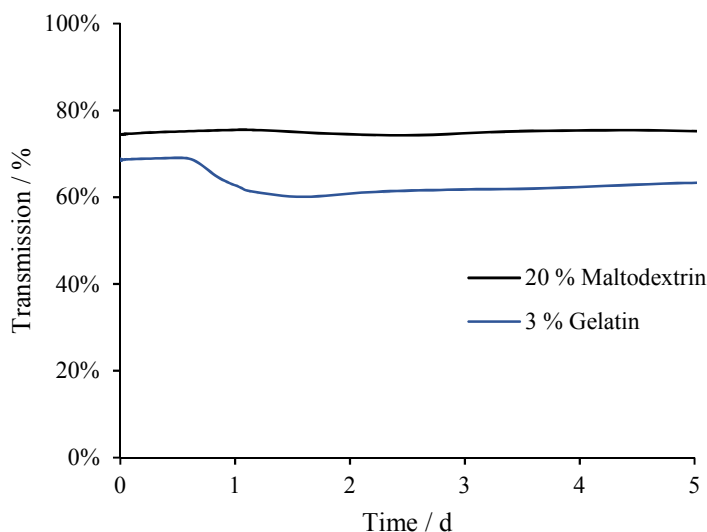


Figure 4.36. Light transmission development during five days of 20 wt% maltodextrin and 3 wt% gelatin kept at 50 °C. The graph shows the transmission for the bottom of the sample, however throughout the sample the light transmission was the same.

4.2.4.2 Identification of Solid Phase in Gelatin/Maltodextrin Mixtures

The solid particles formed in the mixtures were analysed by Raman spectroscopy and observed under the microscope.

First, the reference Raman spectra of gelatin and maltodextrin were obtained (Figure 4.37). The bands in the spectra are assigned to characteristic vibrational modes as shown in Figure 4.37. The Raman spectrum of maltodextrin (De Veij, Vandenabeele, De Beer, Remon, & Moens, 2009) has a characteristic sharp band around 485 cm^{-1} , which can be assigned to the $\nu(\text{C-C})$ backbone stretch modes of pyranose rings (De Gussem, Vandenabeele, Verbeke, & Moens, 2005). The glycosidic stretching modes, $\nu(\text{C-O-C})$ and $\nu(\text{C-C})$, appear in the region $850\text{--}1200\text{ cm}^{-1}$; and the $\delta(\text{CH}_2)$ and $\delta(\text{C-OH})$ deformations region is from 1200 to 1500 cm^{-1} (Hecht, Blanch, Bell, & Day, 1999; Pereira, Sousa, Coelho, Amado, & Ribeiro-Claro, 2003). The Raman spectrum of gelatin had main bands at 1240 cm^{-1} , 1440 cm^{-1} and 1656 cm^{-1} , corresponding to the Amide III ($\delta(\text{NH})$, $\nu(\text{CN})$), Amide II ($\delta(\text{NH})$, $\nu(\text{CN})$) and Amide I ($\nu(\text{C=O})$) bands, respectively. Those are typical assignments for protein backbone vibrations (Schrader, 1995). The spectrum is also in agreement with the previously reported for gelatin (De Veij et al., 2009). Raman bands between 800 and 950 cm^{-1} could correspond to $\nu(\text{C-O-C})$ stretching vibrations, while the Raman bands in the range of 1000 to 1100 cm^{-1} can be corresponded to the deformation $\delta(\text{CH}_2)$, and stretching vibrations of $\nu(\text{C-C})$ and $\nu(\text{C-O})$.

What allows distinguishing the two spectra is the strong peak at 485 cm^{-1} and the ones between $1000\text{--}1200\text{ cm}^{-1}$ for maltodextrin and the Amide I band at 1656 cm^{-1} for gelatin. Other characteristic bands of the spectra overlap each other in both spectra and are therefore not suitable to distinguish both polymers from each other.

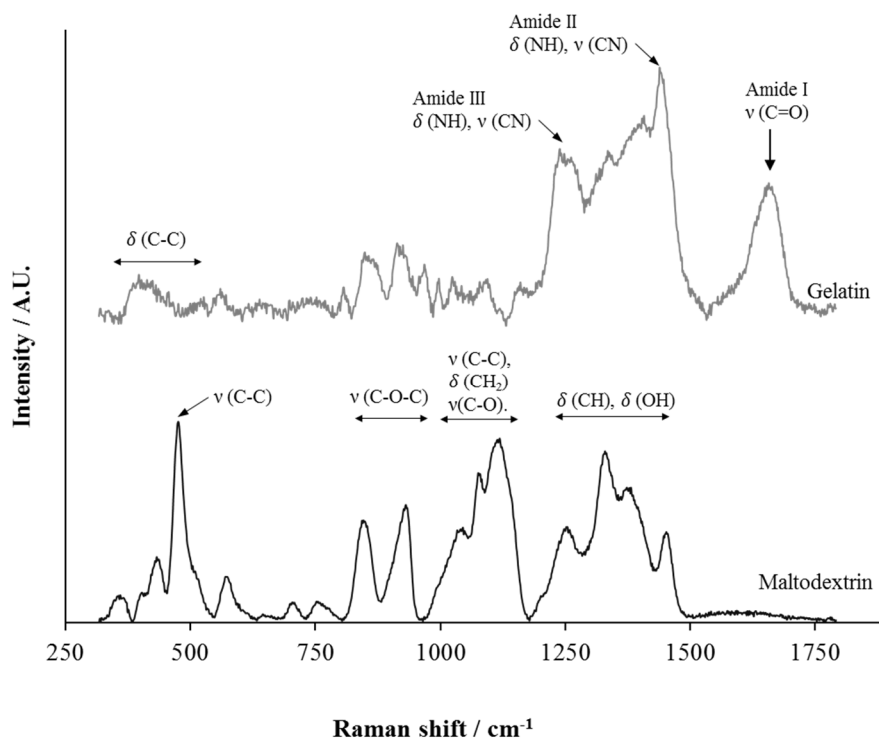


Figure 4.37. Confocal micro-Raman spectra of gelatin and maltodextrin polymers. (unpublished results produced by J. Miras)

Kasapis et al. analysed the precipitate by optical rotation and indicated that it is mainly composed of maltodextrin (Kasapis et al., 1993). Optical rotation measurements were not successful in our case (mentioned in the section above) therefore, it was replaced by the qualitative method of Raman spectroscopy.

Thus, the composition of the solid phase of four different gelatin/maltodextrin emulsions were analysed. The precipitate formed after 5 days was recovered with a pipette, dried in an oven at 50 °C overnight and its chemical composition determined by Raman spectroscopy.

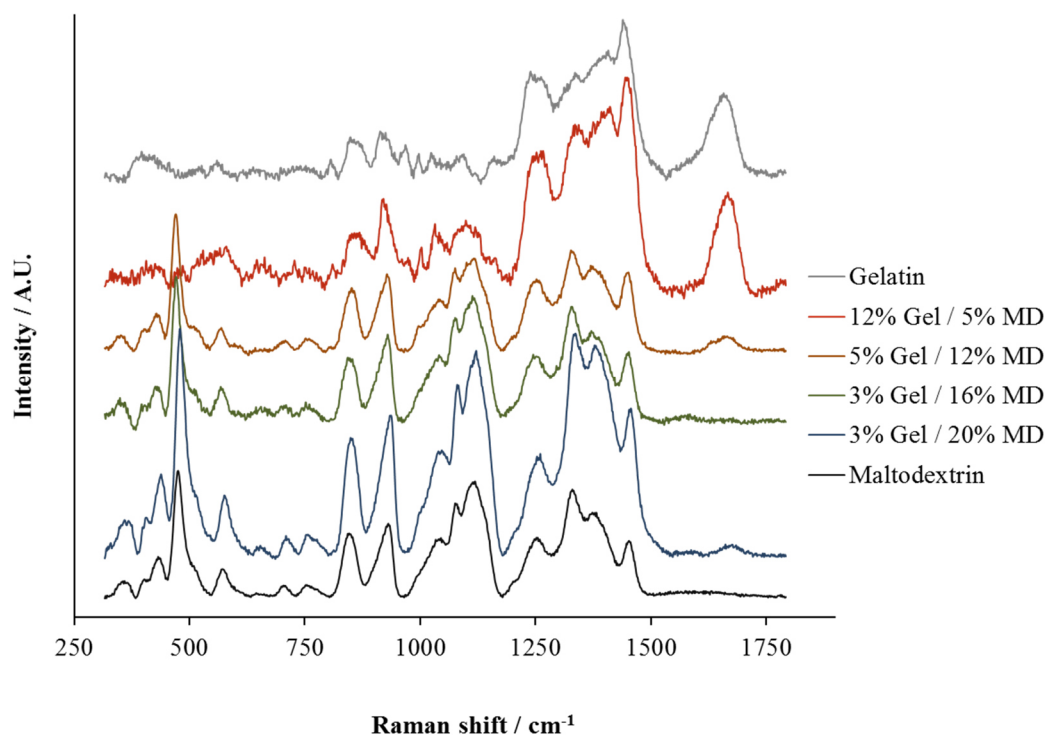


Figure 4.38. Confocal micro-Raman spectra of gelatin and maltodextrin polymers and the solid phase found in four of their respective emulsions after 5 days at 50 °C (unpublished results produced by J. Miras)

Figure 4.38 compares the obtained Raman spectra to the ones of pure gelatin or maltodextrin. The analyzed samples are 3% Gel / 20% MD, 3% Gel / 16% MD, 5% Gel / 12% MD and 12% Gel / 5% MD, in an increasing Gel:MD ratio. From the spectra it can be seen that the emulsions with a Gel:MD ratio < 1 , have a Raman spectrum which closely resembles the one of maltodextrin. Amongst those, the solid phases of 3% Gel / 20% MD, and 5% Gel / 12% MD have a very weak band around the region of the Amide I band (1656 cm^{-1}). This indicates that for those emulsions the solid phase is mainly composed by maltodextrin, even though traces of gelatin seem as well to be present in them. In the case of the 12% Gel / 5% MD emulsion the solid phase closely resembled the spectrum of gelatin, with a an Amide I band and a missing $\nu(\text{C-C})$ backbone stretch peak at around 485 cm^{-1} . Furthermore, the spectrum was not as smooth, as compared to the one as maltodextrin. This is another fingerprint for a protein, as it its amino acids contain a big number of functional groups, which all give a different signal in the Raman spectrum upon irradiation. Actually, most other spectra of the solid phases of the emulsion were not smooth either, indicating that they are not purely composed of maltodextrin.

Those results indicate that, against previous studies (Kasapis et al., 1993), that not all precipitates of gelatin/maltodextrin emulsions consist mainly of maltodextrin, but that its main component depends on the composition of the mixture. Moreover, the solid phase never had a Raman spectrum fully resembling

the ones of the pure components, indicating that precipitates were mixtures of both biopolymers, enriched by one of them. One of the reason for presence of both polymers in the precipitate is cross contamination, which happened when isolating the solid phase, as parts of the liquid phase may have remained associated to it.

Besides this, and more important, we propose following reasons for precipitation of both biopolymers in the gelatin/maltodextrin mixture:

Maltodextrin precipitation:

The reason for precipitation of maltodextrin has been outlined above, and is proposed to origin from segregative interactions of maltodextrin with disordered gelatin leading to conformational ordering of maltodextrin from 2 coils to double helix (Hoey et al., 2016; Kasapis et al., 1993). This leads to hydrophobic interactions and aggregation of the uncharged helices forming an insoluble precipitate.

Pure maltodextrin precipitation was also observed in our experiments and was analysed separately. Solutions up to 15 % (w/w) did not precipitate if left during 60 h at 25 °C. Concentrations between 15 and 30 % remained soluble at 50 °C (5 days), but precipitated if left at room temperature for 60 h. This known phenomena (Chronakis, 1998; Kennedy et al., 1986; Sibel & Jones, 1996) of maltodextrin precipitation originates amongst others from short chains of amylose which retrograde, aggregate and precipitate out of solution. This insolubility of maltodextrin occurs at low temperatures and it was not our case at 50 °C.

Gelatin precipitation:

Gelatin, in this system, may precipitate due to reduction of the solvation layer around the protein, when in solution with maltodextrin. This is usually one of the reasons for segregative phase separation, at increased concentrations. However, the competition for water molecules continues to happen at the liquid-liquid interphase, of the phase-separated gelatin/maltodextrin emulsions. In this region of the emulsion, instead of phase separation, which already occurred, the reduced solvation layer around the protein increases protein-protein interactions and local protein concentration. This leads to reduced solubility of the protein, and thus could finally lead to its precipitation.

Not here, but in other processes, it is of interest, to get protein precipitation: especially in concentrating and purification of proteins. Dextrans and aqueous-two phase systems have been used therefore in the past (Asenjo & Andrews, 2011).

Conclusion:

We propose following model of polymer precipitation in the gelatin/maltodextrin system.

One-liquid phase:

Precipitate mainly formed by maltodextrin.

- Precipitation is favoured by conformational ordering of maltodextrin, caused by gelatin, leading to formation of an insoluble precipitate of maltodextrin.
- Gelatin remains soluble, without precipitation, as maltodextrin concentration too low to induce phase separation or precipitation, due to reduction of solvation layer of gelatin.

Two-liquid phases:

The main component of precipitate dependent on biopolymer concentrations.

- At low gelatin/maltodextrin ratios:

- Precipitate mainly formed by maltodextrin. Precipitation favoured at liquid-liquid interface as concentration of polymers highest in this region.
- Solubility limit of gelatin is not reached and/or proportion of gelatin precipitate in relation to entire precipitate is very low, due to overall low concentration of gelatin in mixture.
- At high gelatin/maltodextrin ratios:
 - Precipitate is mainly composed by gelatin, which is formed at the liquid-liquid interface. Proportion of gelatin is higher in solid phase, as initial gelatin concentration is closer to solubility limit and total proportion of gelatin in biopolymer mixture is higher than the one of maltodextrin.
 - Maltodextrin, in low amounts, forms also part of precipitate, due to its precipitation in presence of gelatin.

To confirm this hypothesis more samples, especially in the one-liquid phase region, will have to be analysed.

Our theory does not contradict the previous theory from Kasapis et al., which argued that the precipitate is mainly formed by maltodextrin and that mass of precipitate is proportional to the gelatin concentration and to the square of maltodextrin concentration (Kasapis et al., 1993). In their case, they analysed only the solid phase of the one-liquid phase region, and do not mention of any solid phase in the two-liquid phase region. We confirm their theory, by proposing that the precipitate in the one-liquid phase region of the gelatin/maltodextrin aqueous mixture is mainly composed by maltodextrin.

The composition of the solid phase in the two-liquid phase region was not analysed by them. They obtained the precipitate from the bottom of the sample, after centrifugation. Furthermore, they quantified and analysed the precipitate directly and did not wait 5 days, as in our case.

Thus, here we propose a new model to explain precipitation of both biopolymers in the gelatin/maltodextrin mixture. This model is based on two different modes of polymer precipitation, depending on the region in the phase diagram, and quantitative prediction of the precipitation cannot be calculated as straightforward, as commented by Kasapis et al.

4.2.4.3 Morphology of Solid Precipitate

The solid particles of gelatin/maltodextrin mixtures were observed under the microscope. As can be seen in Figure 4.39 the solid particles after five days at 50 °C had sizes of few micrometers with few aggregates ranging up to 200 μm . Those aggregates were bigger in size with increasing gelatin concentrations, which confirms previous studies from Kasapis et al. (Kasapis et al., 1993), who observed precipitates between 50 μm (4% Gel / 10 % MD) and 80 μm (12% Gel / 10% MD). The first reason for the bigger size of aggregates in the 12 % Gel / 12 % MD sample, in our experiments, is that precipitates are formed at a higher rate in those samples and thus also have time to grow by day 5. Furthermore, according to our theory, they are mainly composed of gelatin and thus have a different morphology, than the precipitate of the 3 % Gel / 8% MD sample, whose precipitate is mainly composed by maltodextrin (Figure 4.39). Maltodextrin precipitate may thus be more spherical shaped, while gelatin precipitate has a lamellar morphology.

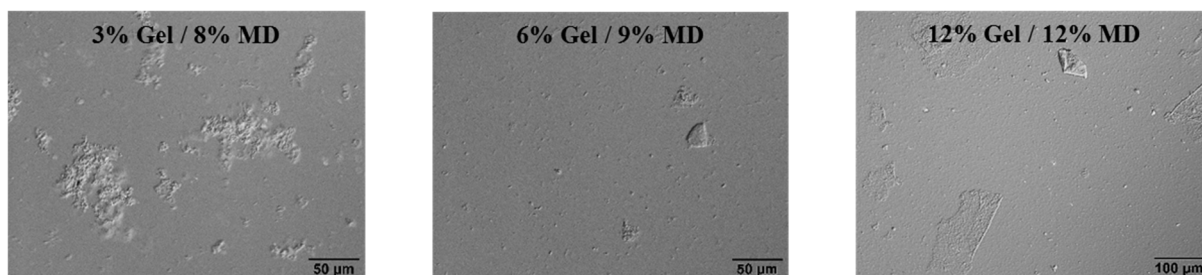


Figure 4.39. Morphology of solid particles present in gelatin-maltodextrin mixtures

4.2.4.4 Influence of Temperature on Phase Diagram

The influence of temperature on phase behaviour of gelatin-maltodextrin mixtures has been extensively studied in the past (Alevissopoulos et al., 1996; Niklas Lorén & Hermansson, 2000; Lundin et al., 2000; M. Williams et al., 2001) and phase diagram compared at different temperatures (Lundin et al., 2000), as highlighted in the introduction. These authors described that the binodal line of the phase diagram moves slightly to higher polymer concentrations, indicating a small increase in miscibility at higher temperatures.

In preliminary studies of this work, phase behaviour of gelatin and maltodextrin mixtures at 45, 52.5 and 60 °C were analysed, without taking into account the solid phase in the sample. Those temperatures were chosen to assure a temperature high enough (above 30 °C), allowing gelatin to be in a liquid state, but not too high (< 60°C) which could favour denaturation of gelatin. Furthermore, maltodextrin is more soluble at higher temperatures, thus temperatures between 45 °C and 60 °C were chosen, to assure that all polymers form liquid solutions.

Only the presence of one or two liquid phases were determined and samples were thus equilibrated during 5 h, enough time, for the separation of two liquid phases. In the phase diagram in Figure 4.40 it can be observed how the binodal line shifts to lower concentrations at 45 °C, compared to the lines at 52.5 °C and 60 °C, which have a similar trend. This result agrees with previous studies (Lundin et al., 2000). The shift of the binodal line may be explained by the decrease in mixing entropy at lower temperatures and consequent increased free energy of mixing. Consequently, mixtures start to be incompatible already at lower concentrations and phase separate.

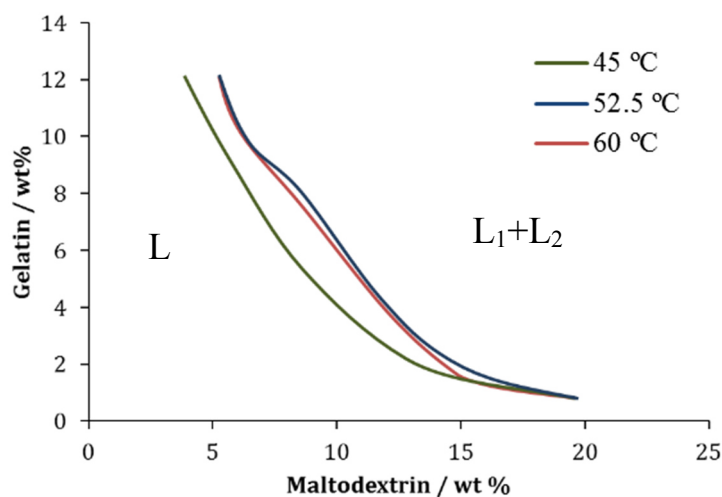


Figure 4.40. Influence of temperature on position of binodal line in gelatin-maltodextrin phase diagram

Thus precipitation of polymers over time and temperature rise, can lead under our conditions (gelatin-maltodextrin-water mixture) to transform a phase-separated emulsion into a one-phase system. As in our research work we are interested to work with emulsions, it will be of importance to take this into account and work with mixtures with a certain distance from the binodal line.

4.2.5 Properties of Gelatin-Maltodextrin Emulsion

After determination of the phase diagram of gelatin/maltodextrin aqueous mixtures, various compositions from the two-liquid phase region were observed under the microscope, after mixing. The aim was to understand the different types of emulsion morphologies, which can be obtained depending on the region in the phase diagram.

In the phase diagram (Figure 4.31) the two-liquid phase region is separated into two regions. One region with a bigger phase volume of the gelatin-rich phase, and another region in which the maltodextrin-rich phase makes up a bigger fraction of the sample volume. Compositions lying close to the 50:50 phase volume line have phases of similar volumes for both polymers.

In absence of an emulsifier, whose HLB value would, according to Bancrofts Rule (Bancroft, 1912), determine which of the two phases (in a W/O or O/W emulsion) will be the continuous phase, the phase with the bigger phase volume makes up the continuous phase.

As maltodextrin and gelatin solutions have very similar refractive indexes, their emulsions have less optical contrast than conventional W/O (or O/W) emulsions, making it more difficult to distinguish both phases under the microscope. Gelatin was labelled with a fluorescent dye (Fluorescein isothiocyanate, FITC) to be able to distinguish the polymers from each other and clearly identify which one makes up the continuous and which the dispersed phase. Samples of different compositions were observed under the microscope, after agitation (Figure 4.41).

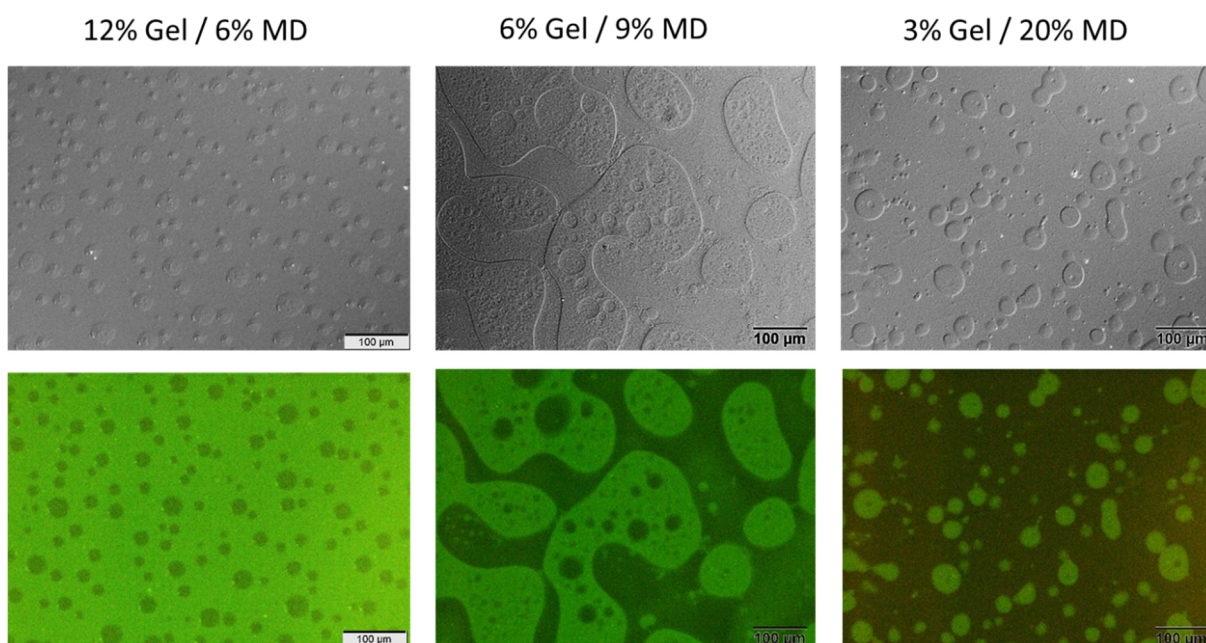


Figure 4.41. Depending on the concentrations of the different biopolymers gelatin-in-maltodextrin (3% Gel / 20% MD), bicontinuous (6% Gel / 9% MD) or maltodextrin-in-gelatin (12% Gel / 6% MD) microstructures can be obtained, as shown by the micrographs. The upper row shows the sample observed by light transmission, the lower row shows the same samples observed by fluorescence microscopy. (Green: FITC-labelled gelatin).

Figure 4.41 shows that either maltodextrin-rich droplets, for samples with a greater phase volume of gelatin (e.g. 12% Gel / 6% MD) or gelatin-rich droplets, for samples with a greater phase volume of maltodextrin (e.g. 3% Gel / 20% MD) can be obtained. If the phase volumes are similar, bicontinuous structures can be observed (e.g. 6% Gel / 9% MD). The microscopic images show moreover, that it is not easy to distinguish whether a droplet is enriched in gelatin or in maltodextrin, if not labelled. A further way to distinguish the two types of droplets is that maltodextrin droplets are enriched in solid particles, which form rapidly, if observed under room temperature (25 °C) under the microscopic slide (Figure 4.42). Those particles can be observed in maltodextrin droplets, however not in gelatin droplets. Furthermore gelatin droplets, if gelled, are observed with higher contrast under the microscope.

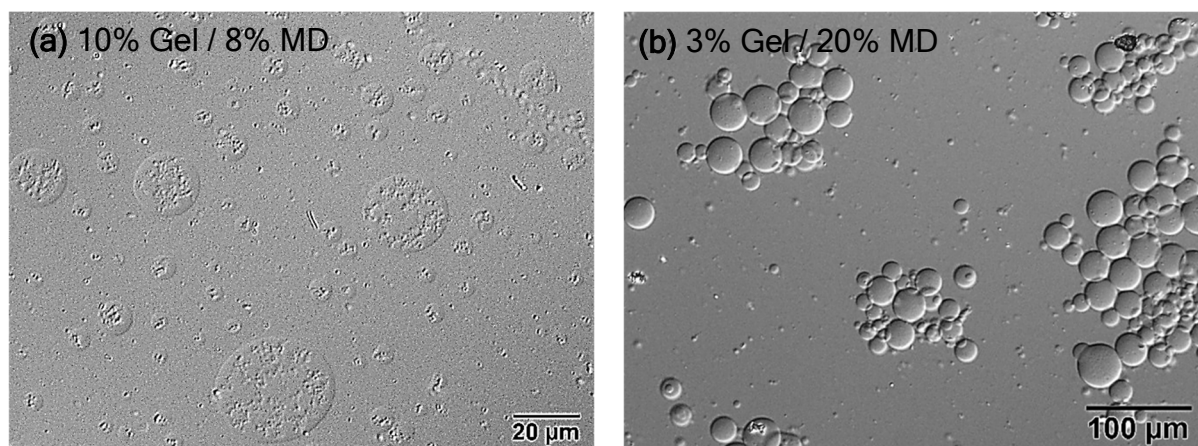


Figure 4.42. (a) Maltodextrin droplets contain solid particles of maltodextrin precipitate, whose formation is promoted by higher maltodextrin concentrations and cooler temperatures. (b) Gelatin droplets can be seen with a high contrast under the microscope.

The microscopic images show that the emulsion droplets, if mixed by gentle agitation by hand are highly polydisperse. More in-depth studies on the influence of various parameters on droplet size have been performed and are highlighted in section 4.2.8.4 .

Interestingly, in various compositions droplets within droplets structures have been observed (multiple emulsions). No special preparation method was applied to those types of emulsions, and the secondary structure formed spontaneously. Such structures have already been observed elsewhere for gelatin/maltodextrin mixtures (Foster et al., 1996). To understand this phenomenon it is important to note, that droplets are never purely composed of only one polymer, but are always mixtures of both polymers. Their composition can be determined, if the tie line of a phase diagram is known. It corresponds to the end points of the tie line on the binodal line.

It is supposed that the multiple emulsions are formed by secondary phase separation within the already formed droplets. The initially formed droplets behave thus like an isolated phase, creating a microenvironment which allows secondary phase separation. This phase separation was induced when decreasing the temperature of the sample from 50 °C, the temperature at which the emulsion was mixed, to lower temperatures. Lowering the temperature leads to increased incompatibility between the two polymers, due to entropic reasons, shifting the binodal line to lower concentrations (Figure 4.40 and Figure 1.10). In the case of gelatin droplets, gelatin gelling induces a conformational change of the molecule, which favours phase separation (N. Lorén et al., 2001; Lundin et al., 2000). Partial gelation of the droplet may also change the effective concentration within the rest of the droplet, by raising maltodextrin concentration, which is not included in the gelatin polymer network. This increase of maltodextrin concentration can lead to an internal droplet polymer composition, which lies within the

two-liquid phase region of the gelatin/maltodextrin phase diagram. The energy cost of having different curvatures in this double emulsion is far lower than in ordinary O/W emulsions due to the lower interfacial tension between the two phases in biopolymer mixtures (Norton & Frith, 2001).

We found three different factors influencing this secondary droplet formation:

1. Secondary droplet formation found only in gelatin-in-maltodextrin mixtures

In maltodextrin-in-gelatin emulsion droplets this phenomenon was not observed, probably due to two reasons. The first one is that precipitation of maltodextrin during cool down, because of reduced maltodextrin solubility at lower temperatures, decreased maltodextrin effective concentration in the droplets. Reducing maltodextrin concentration moves the composition further into the one-liquid phase region of the phase diagram, in which no phase separation, and thus droplet formation, occurs. Secondly, in contrast to gelatin droplets, no gelation happened, which could have created a barrier to its surroundings, allowing to treat maltodextrin droplets as isolated phase. Diffusion between the dispersed and continuous phase could have established a new balance and avoid secondary phase separation.

2. Temperature

As mentioned above, it was observed that cooling down could produce the formation of multiple emulsions. The quicker the sample was cooled to the final temperature, at which the gelatin droplets gel, the smaller were the internal droplets (Figure 4.43). This can be attributed to slower coalescence at lower temperatures, once the normal droplets are gelled. Droplets within the droplets might be formed by nucleation and growth, and thus, internal droplets grew over time. Figure 4.43 shows a 4.5% Gel / 13% MD emulsion directly introduced into an ice bath, after mixing at 50 °C (cooling was faster, at ~2 °C/s) compared to the same emulsion cooled down at 0.3 °C/s (20 °C/min, controlled by placing sample on a microscope thermal stage) from 50°C to 10°C. It can be seen that droplets formed at slower cooling contained bigger internal droplets, than the once quenched immediately to 0 °C.

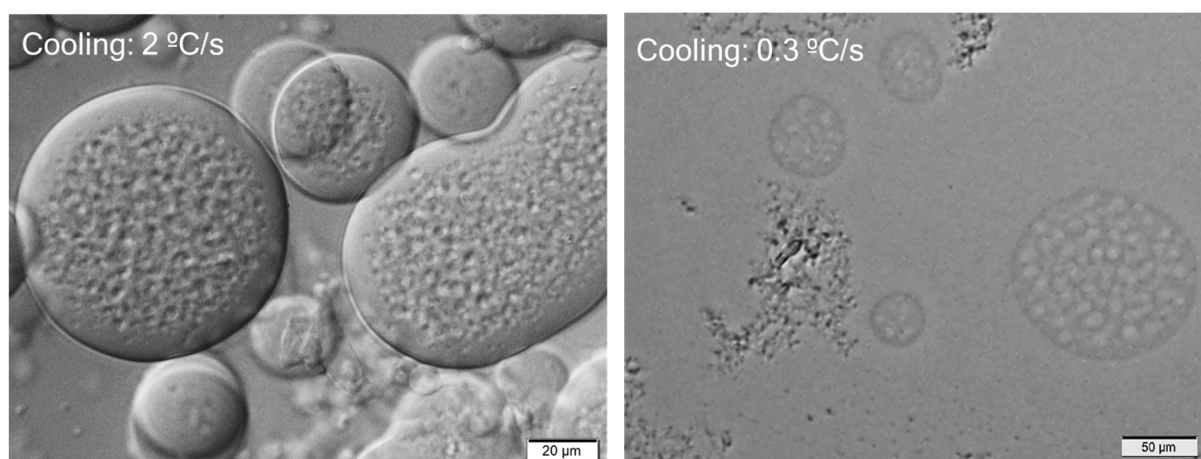


Figure 4.43. Multiple emulsions formation is controlled by cooling rate. The images show multiple emulsions obtained from 4.5% Gel / 13% MD, with two different cooling velocities (~2°C/s and 0.3°C/s). Faster cooling rate leads to smaller internal droplets within the gelatin droplets.

3. Distance to binodal line

Internal droplet formation was more strongly observed at compositions close to the binodal line of the phase diagram, than at compositions further from it (Figure 4.44). The overall composition inside the external droplets is determined by the intersection of the tie line, with the binodal line. Emulsions with compositions lying further away from the tie line, have thus continuous and dispersed phases with higher gelatin or maltodextrin concentrations. As an example, a 4.5 % Gel / 11% MD emulsion might have a dispersed phase of ~10% Gel / 5%MD and a continuous phase of ~2% Gel / 14% MD, while a 4.5 % Gel / 20% MD emulsion could have a dispersed phase of ~20% Gel / 5%MD and a continuous phase of ~0.5% Gel / 25% MD. At those high concentrations, temperature change may have a lower effect on phase behaviour, while in the other case a temperature change induces a shift of the binodal line and thus promotes formation of internal droplets.

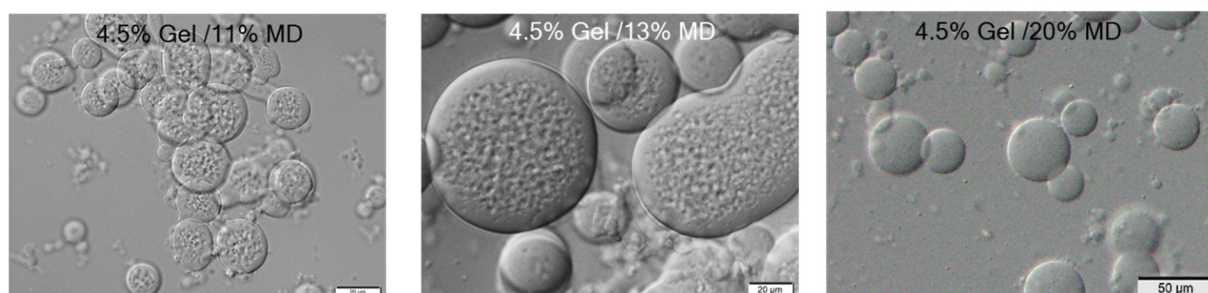


Figure 4.44. Internal secondary droplets are highly abundant at emulsion compositions close to the binodal line (4.5/11), while merely absent at high concentration of maltodextrin, far away from the binodal line (4.5/20).

In conclusion, our results demonstrated that multiple emulsions can be obtained by a very simple method, by preparing emulsions at compositions close to the binodal line, and by decreasing temperature.

4.2.6 Obtaining Microgels from Gelatin/Maltodextrin Emulsion

Once a protocol was established to obtain droplets of gelatin from gelatin/maltodextrin emulsions, the aim was to obtain gelled, crosslinked gelatin microgels, dispersed in the solvent, free from maltodextrin. Therefore, on one hand the gelatin droplets were to be gellified, and on the other hand the continuous phase of the emulsion removed.

Therefore, in the first preliminary study the emulsion was cooled down to selectively gel gelatin droplets.

In the second preliminary study, maltodextrin was intended to be removed from the emulsion, containing crosslinked gelatin droplets.

Finally, from lessons learned in the preliminary studies, a protocol was established to successfully isolate gelatin microgels from a gelatin/maltodextrin emulsion.

4.2.6.1 Preliminary study 1: Gelation of Gelatin Droplets

In contrast to maltodextrin, gelatin gelfies by cooling below approximately 35 °C. Therefore, it was assumed that by cooling the entire emulsion, gelled gelatin droplets could be isolated from the mixture. For this purpose, gelatin/maltodextrin emulsions were prepared and then placed for 10 min into an ice-bath. Unfortunately, as seen in for a 8% Gel / 20% MD (10 mM Genipin) sample, not only did the gelatin droplets gelify, but also maltodextrin solution precipitated. The white turbid part of the solution in Figure 4.45 (a) is maltodextrin, which precipitated due to its decreased solubility at low temperatures. This was also seen by observing under the microscope the sample, which was cooled down just after homogenisation by Ultra-Turrax® (Figure 4.45 (b)). Gelatin microgels were clearly observed under the microscope, as shown in Figure 4.45 .

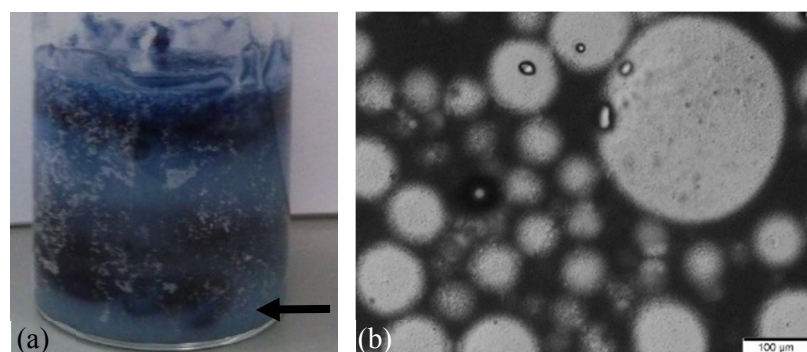


Figure 4.45. (a) Picture of 8% Gel / 20% MD (10 mM Genipin) emulsion after 10 min in an ice-bath. The arrow indicates the precipitate which probably consist of maltodextrin (b) Microscopic images of cooled down samples indicate a lot of precipitate (black parts of microscopic image) in the continuous phase of the emulsion.

4.2.6.2 Preliminary Study 2: Remove Maltodextrin, before Gelling Gelatin

As cooling down of the emulsion in ice during some minutes, led to precipitation of the continuous maltodextrin phase, the continuous maltodextrin phase was tried to be removed, before cooling down the gelatin droplets. Three different approaches were tested: Filtration, dialysis and centrifugation of the emulsions.

4.2.6.2.1 Filtration

A 4.5% Gel / 13% MD (1 mM Genipin) emulsions was prepared, homogenised at 9500 rpm with the Ultra-Turrax® and then stirred for 20 min at 60 °C. The emulsion was then directly pressed through a polycarbonate filter of 0.8 µm, with the help of an extruder. Aim was that the 10-50 µm big gelatin droplets remain inside the filter, while the continuous phase is pushed through. Furthermore, droplets should remain stable during the process of filtration.

After initial tries, at which the membranes of the filters broke due to too high pressure needed to press the polymer solution through to them, the emulsion was passed through two filters, which remained stable during the process. The filter was removed, immersed into cold water to wash off the gelatin droplets, which were supposed to have remained attached to it.

This solution was analysed, however no droplets were observed under the microscope, which means, that the gelatin droplets passed through the membrane, together with the continuous phase, as they were still in a liquid flexible state. Or, the droplets remained on the membrane, but coalesced there to one liquid phase.

4.2.6.2.2 Dialysis

A 8% Gel / 20% MD emulsion was prepared, kept at 45 °C and after homogenisation at 9500 rpm with the Ultra-Turrax®, 5 mL of the sample was introduced into dialysis tubing with a 12 kDa cut-off. Dialysis was performed inside a 500 mL water bath of 40 °C. Aim was that maltodextrin (3.6 kDa) passes through the dialysis membrane, while gelatin (50 kDa) would have stayed within the membrane. The drawback of this technique was however rapidly recognised, as phase separation in the emulsion was quicker than diffusion of maltodextrin from the sample to the water outside the dialysis tubing. As can be seen in Figure 4.46 the emulsion phase separated after 30 min and part of the maltodextrin phase started to get turbid, thus precipitate.

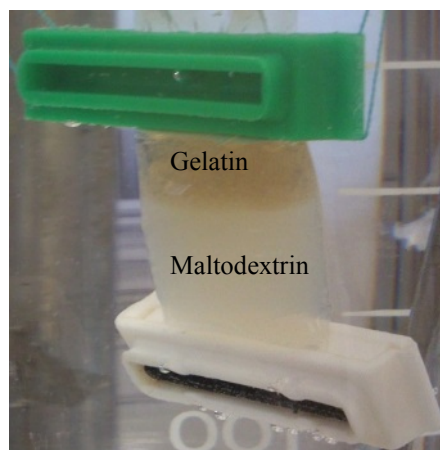


Figure 4.46. 8% Gel / 20% emulsion phase separates inside the dialysis tubing after 30 min in the water solution (40 °C).

4.2.6.2.3 Centrifugation

In a first try a 4.5% Gel / 13% MD (10 mM Genipin) emulsion was homogenised by Ultra-Turrax® at 9500 rpm and then centrifuged immediately for 10 min at 3000 rpm at 10°C. By centrifuging the sample at 10°C it was hoped that the gelatin droplets gelify and sediment. What was obtained was a gradient of crosslinked gelatin in the centrifuge tube (Figure 4.47). As gelatin has a lower density than maltodextrin, it remained in the upper layer, and compacted there to a solid gel. Centrifugation thus accelerated the coalescence of the droplets to one phase. From the blue gradient in the tube it can be concluded that the concentration of gelatin diminished towards the bottom, where mainly maltodextrin was supposed to sediment. Few microgels could be observed under the microscope in the middle fraction of the sample, however no complete isolation of the microgels was achieved.

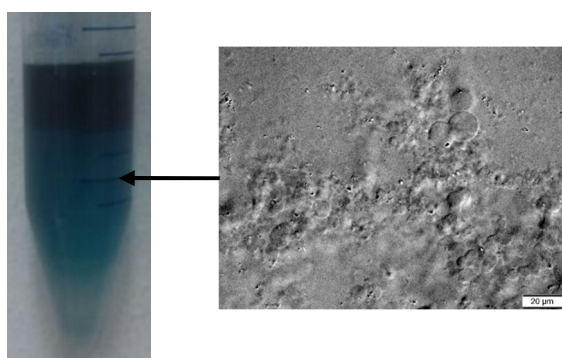


Figure 4.47. Centrifugation of a 4.5% Gel / 13% MD (10 mM Genipin) emulsion for 10 min at 10 °C lead to phase separation of the emulsion and the blue gradient indicates the presence of some gelatin droplets in the lower maltodextrin phase.

Therefore, in another experiment, a 4.5% Gel / 13% MD (1 mM Genipin) emulsion was homogenised by Ultra-Turrax® at 9500 rpm (left part of Figure 4.48) and then placed 10 min into an ice bath, in order to gelify the gelatin droplets and promote the precipitation of maltodextrin. It was expected that centrifugation would separate the precipitated maltodextrin from a dispersion of gelatin microgels in water. After centrifugation for 10 min at 3000 rpm at 10 °C the different layers of the centrifuged tube were observed under the microscope (Figure 4.48).

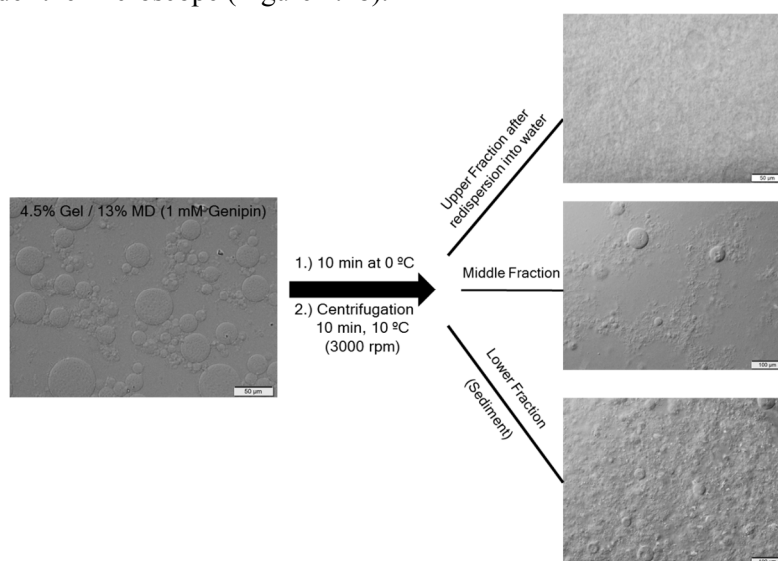


Figure 4.48. Centrifugation of a 4.5% Gel / 13% MD (1 mM Genipin) emulsion, which was cooled during 10 min to induce maltodextrin precipitation and gelatin gelation. The emulsion morphology before centrifugation and microscopic images from different layers of the centrifuged tube are shown.

The upper fraction was observed, after redispersion in water. It consisted of a compact gel with some dispersed gelatin droplets in it. In the middle and lower (sediment) fractions of the centrifuge tube gelatin droplets inside a dispersion of maltodextrin precipitate in water were observed. The amount of precipitate increased towards the bottom of the tube. This method of centrifugation was thus not adequate to be able to isolate gelatin droplets from the continuous maltodextrin phase.

4.2.6.3 Final Protocol: Gelation of Gelatin Droplets and Purification of Microgel Suspension

From the first two preliminary studies it got clear that gelatin has to be gelled before maltodextrin removed, in order to avoid coalescence of the droplets and phase separation during the purification process. The drawback of the cooling was however, that at those high maltodextrin concentrations, maltodextrin rapidly precipitates at low temperatures.

Thus, a compromise was found and the following protocol to obtain gelatin microgels was established:

After mixing the gelatin/maltodextrin emulsion in order to obtain gelatin microgels, the emulsion was further mixed during 20 min at 60 °C to crosslink the gelatin droplets with genipin. The sample was then introduced directly, to avoid coalescence of the droplets, for 1 min in an ice-water bath. Short enough to obtain gelation of the gelatin droplets, but not long enough to induce maltodextrin precipitation. At low temperatures, gelation of gelatin and precipitation of maltodextrin both occur. However, precipitation of maltodextrin does not happen at low concentrations. The sample was consequently diluted with twice the sample volume of 0 °C cold water. The gelatin microgels thereby remained stable. Whereas the concentration of maltodextrin in the continuous phase was low, and thus, precipitation of maltodextrin was prevented. Figure 4.49 shows that this method allows to keep the gelatin droplets, gelled as microgels, inside the continuous dilute maltodextrin phase, over prolonged period of time in the fridge.

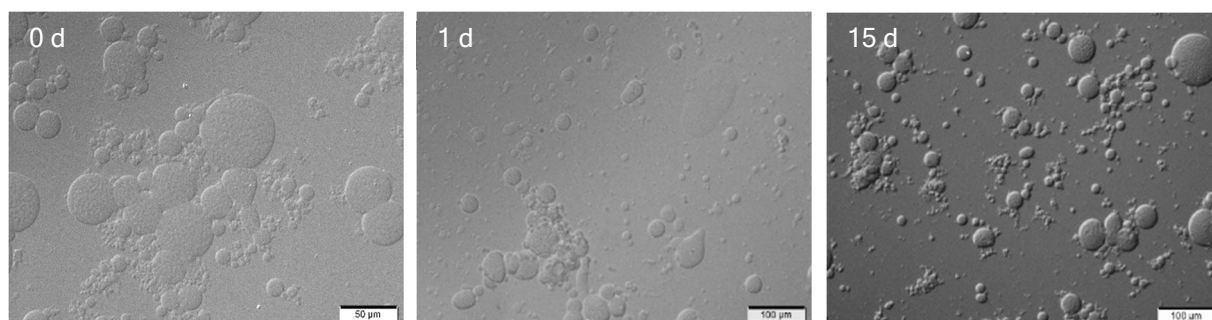


Figure 4.49. Gelatin droplets (here from a 4.5% Gel / 13% MD (1 mM Genipin) emulsion) remained stable during at least 15 d (stored at 4 °C in the fridge) after cooling and dilution with cold water. No/few maltodextrin precipitation was formed in this time period in the samples.

No phase separation or major coalescence of the droplets was observed, as they were in a gelled state, forming microgels. Thus, under those conditions, the microgel dispersion could be purified to replace the continuous phase, which was supposed to be a suspension rich in maltodextrin and with a low concentration of dissolved gelatin, with pure water. The samples were moreover, freeze-dried, in order to observe if the continuous phase contained polymers or was free of it. In case the continuous phase

consists only of water, all of it would be evaporated and only microgels would remain in the dried microgel suspension powder. The freeze-dried sample, originating from a non-purified 4.5% Gel / 13% MD (1 mM Genipin) emulsion, was thus observed under the scanning electron microscope (SEM) (Figure 4.50). Besides porous microgel particles, much unstructured solid material was observed, which is attributed to the remaining polymers in the continuous phase of the microgels, before purification. Those images serve as reference, to compare with freeze dried samples after purification.

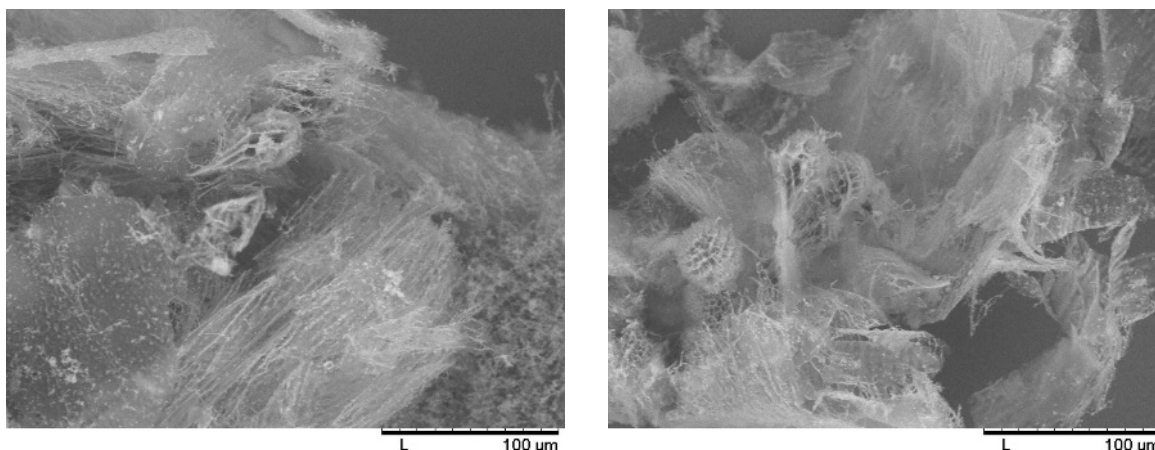


Figure 4.50. SEM images of freeze-dried gelatin microgels, obtained from a 4.5% Gel / 13% MD (1 mM Genipin) emulsion, after cooling and dilution in cold water. The porous particles are surrounded by unstructured solid material, which is attributed to the polymers that remain in the continuous phase of the microgels, before purification.

Various approaches to purify the suspensions were evaluated, taking into consideration that the gelatin microgels of the 4.5% Gel / 13% MD (1 mM Genipin) samples (used to compare different purification methods) had a diameter of 10-50 μm . Another important factor to know for the purification of the samples, is the molecular weight of the polymers: Gelatin polymer had a molecular weight of 50 kDa, maltodextrin of 3.6 kDa. As above, three different purification methods were evaluated: Elimination of the continuous phase by filtration, dialysis and centrifugation. Those purification methods will be tested and the samples observed before and after purification, by microscopy and, after freeze-drying, by SEM imaging. We will not go into the details of the microgel morphology after freeze-drying in this section, this will be done further below in section 4.2.7.1.

4.2.6.4 Filtration

The most simple method to separate the microgels from the surrounding continuous medium could be filtration. What would remain in the filter were the microgels, while the continuous phase could pass through.

The microgel suspension was pushed through a polycarbonate filter with pore size 10 μm . Pore size of 10 μm was chosen, as lower pore size would lead to rapid obstruction of the pores in the membrane and make filtration of the sample impossible or only possible under very high pressures. After filtration of the sample, the filter was agitated in a vial of water and the microgels, which remained on the filter membrane, were observed under the microscope. Optical microscopy images were taken of both sample fractions. Analysis of the pass-through portion of the suspension contained not only the continuous

phase, but also microgels and particles bigger than 10 μm (Figure 4.51 b). This can occur since the microgels could have squeezed themselves through the pores due to their high elasticity. On the other hand, the portion remaining in the filter contained many particles smaller than 10 μm , but also bigger than average microgels of 50-120 μm (Figure 4.51 c). This is probably a consequence of some microgels remained aggregated or adhered on the pores and thus blocking the pass through the filter. Under the high pressure, to which the microgels were subject during filtration, many of them become deformed or strongly aggregated, as can be seen in Figure 4.51 c and Figure 4.57.

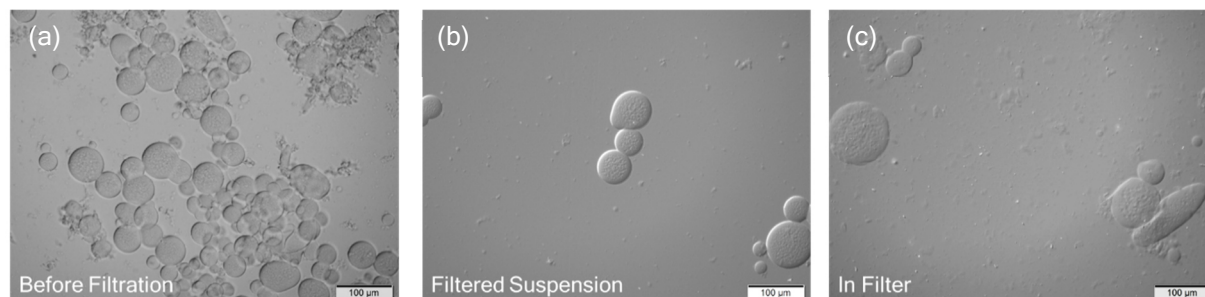


Figure 4.51 . Filtration of gelatin microgels, in a maltodextrin-rich continuous phase, through a 10 μm filter. Images show the microgel suspension before filtration and after filtration (what passed through the filter and what remained on it).

Lyophilisation of the fraction that did not pass across the filter and observation under the SEM reveal some porous spherical/elliptical structures within a flocculate of unordered structures, which could be remains of polymers (Figure 4.52).

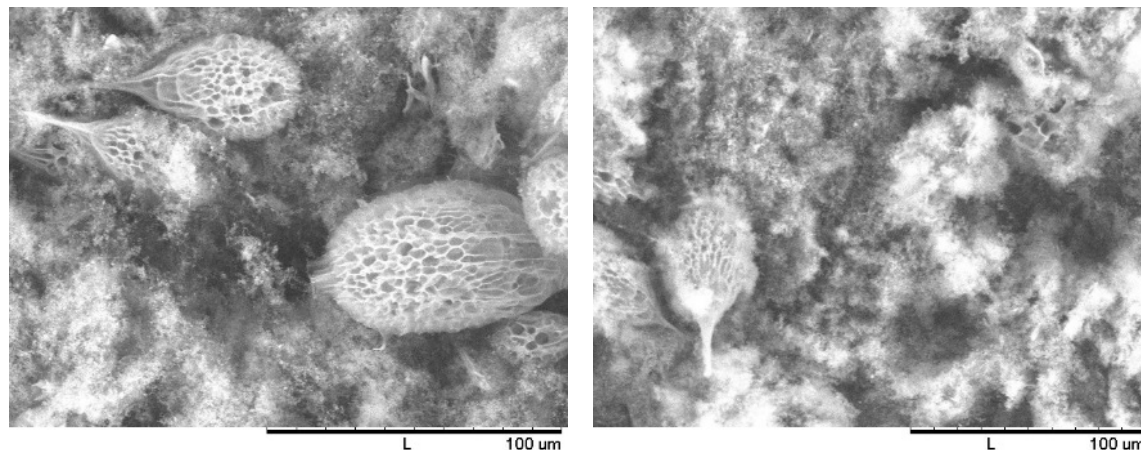


Figure 4.52. SEM images of freeze-dried gelatin microgels after purification by filtration. Porous microgel particles are surrounded by unstructured material. The two images were observed in the same sample.

Due to the ineffective purification and the limitation of purifying 1 mL of sample per filter, due to blocking of the filter, this method was not selected for further studies.

4.2.6.5 Dialysis

Microgel suspension purification by dialysis was performed in former studies especially for nanometer-sized microgels (Ogawa et al., 2001; Tan & Tam, 2007). The microgel suspension were therefore

introduced into dialysis tubing with a pore size of 12 kDa, which lets pass maltodextrin polymers (3.4 kDa) and retains the 10-50 μm sized microgels and remaining gelatin in solution. The dialysis was performed in water at 25 $^{\circ}\text{C}$. As the microgels were crosslinked, they remained solid-like. After 4h, the water was replaced and dialysis continued for further 22h.

The samples were then observed under the microscope and SEM (after freeze-drying). The microscopic images of the sample indicated a very clear continuous phase with few particles of suspended material (Figure 4.53 b). The microgels remained in their original size and shape.

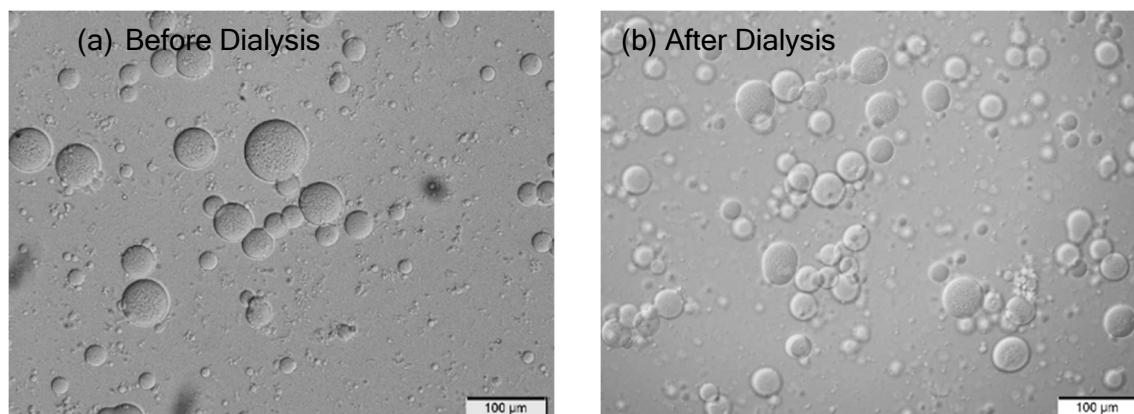


Figure 4.53. Microscopic images of the microgel suspension before and after dialysis shows that the suspension remained stable after 26 h of dialysis and the continuous phase seemed purer than before dialysis.

Furthermore, microgels obtained by this dialysis method were less aggregated than by using filtration.

The lyophilised sample (Figure 4.54) showed besides the dried microgels more dispersed filaments than expected from the optical microscope images. The dried microgels had a similar shape than the other purified samples. This method takes place under soft conditions, which prevents deformation and aggregation of the microgel particles. It takes however long time (> 24 h) and can be only performed with a small sample volume.

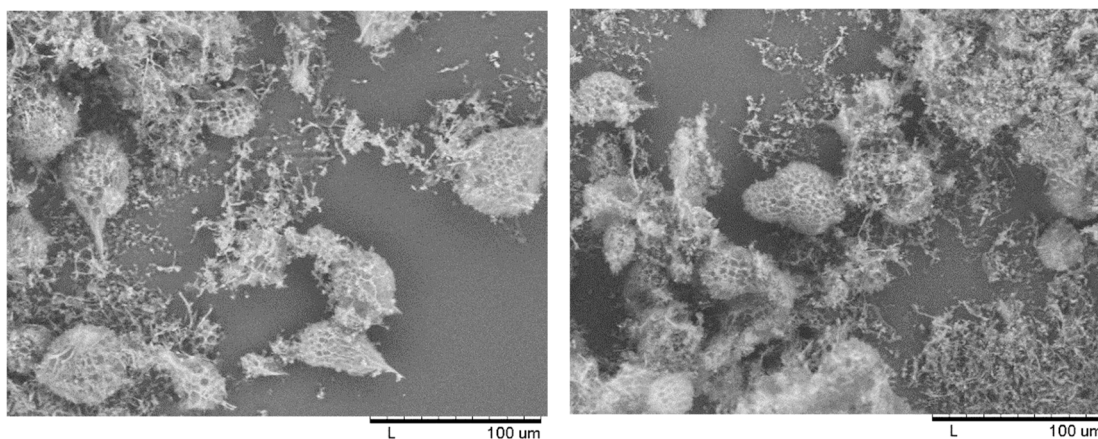


Figure 4.54. SEM images of freeze-dried gelatin microgel suspension, after dialysis.

4.2.6.6 Centrifugation

The use of centrifugation, as a purification method has the advantage to be an easy method which allows to sediment the majority of the microgels while keeping the continuous phase as supernatant. It has

already been used in many other studies to purify microgel suspensions (Eichenbaum, Kiser, Shah, Simon, & Needham, 1999; Shivkumar V. Ghugare et al., 2012; Murthy et al., 2003; Schachschal et al., 2011).

In our work, the microgel suspension was centrifuged for 10 min at 2000 rpm and at 10 °C to assure that the gelatin droplets remain in gel form and don't melt. The microgels sedimented to the bottom of the tube during the centrifugation process, and the continuous phase remained on the top (Figure 4.55 a). As the maltodextrin phase is diluted to a third of their initial concentrations (~5-10 wt %, depending on the initial emulsion composition) their density is lower than the ones of gelatin microgels, with a concentration of ~10-20 wt % (depending on the initial emulsion composition) (see density graph of polymers in Figure 4.21). In between each centrifugation step, the supernatant was replaced by fresh solvent (if not otherwise commented, water) and the centrifugation tube was agitated by vortex to resuspend the microgels.

After the first centrifugation process, the supernatant contained barely no microgels and consisted mainly of some solid polymer precipitate (Figure 4.55 c). Strong mechanical agitation, by vortexing, in the resuspended fresh water solutions, allowed to maintain the microgels as individual particles (Figure 4.55 d) and prevented to a big extent them from aggregating to each other or form a continuous hydrogel.

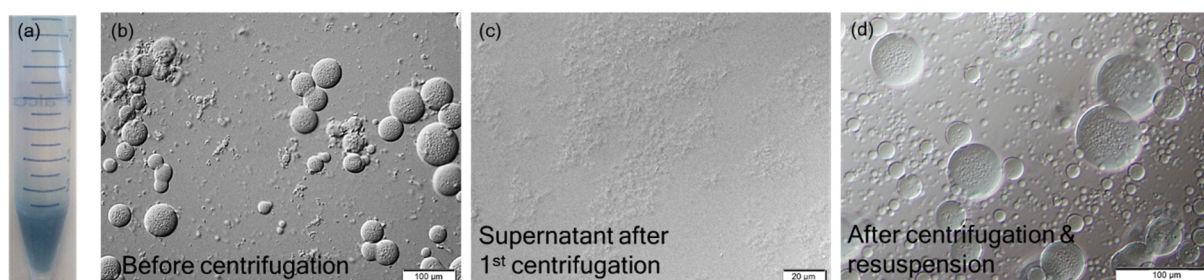


Figure 4.55. (a) Centrifuge tube after first centrifugation shows that crosslinked gelatin microgels sedimented to bottom of the tube and the upper phase consisted of the continuous phase, into which the microgels were suspended. (b) Microgel suspension (prepared from a 4.5% Gel /13 MD (1mM Genipin) emulsion) before purification by centrifugation and after purification by twice centrifugation and resuspension in water (d). (c) shows that the supernatant after the first centrifugation was free from microgels and consisted mainly of solid precipitate of the polymers.

SEM images after lyophilisation of the samples purified by centrifugation showed a high density of spherical or leaf-like shaped porous particles with only few solid aggregates which might have originated from remaining polymers in the surrounding continuous phase (Figure 4.56). In contrast to the other purification methods barely no other material was found surrounding the microgel particles.

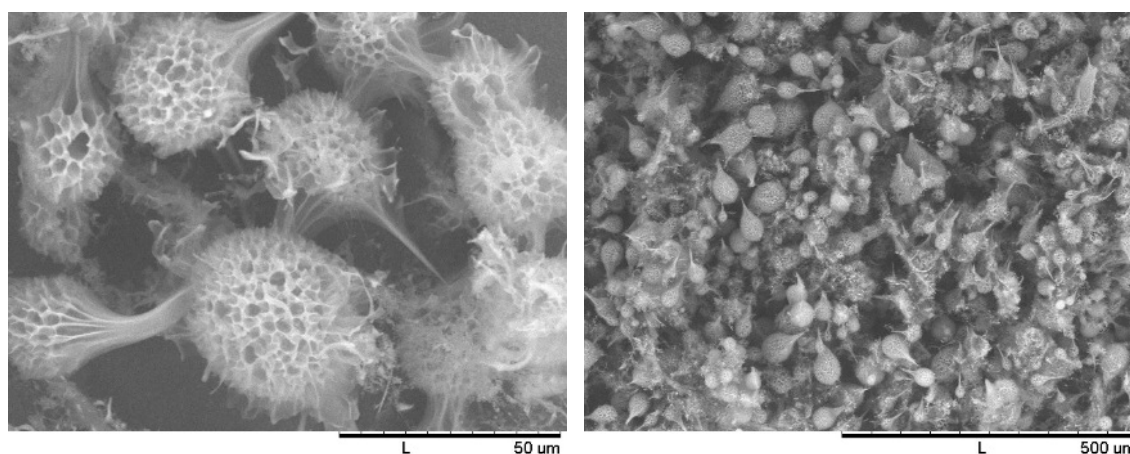


Figure 4.56. SEM images of freeze-dried gelatin microgel suspension, after purification by centrifugation and resuspension.

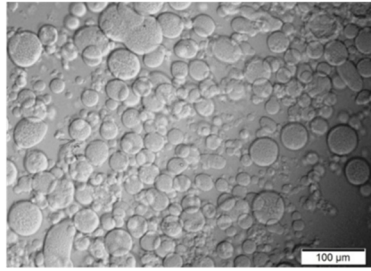
The effectiveness of purification by centrifugation was moreover tested by measuring the optical rotation of the supernatant after the first and the second centrifugation-resuspension cycles. The optical rotation of the supernatant at the wavelengths 365, 405 and 546 nm can be found in Table 4.7. As commented in the above section about optical rotation, optical rotation can only be used qualitatively in our case, since the experimental error is rather large. However, the results of optical rotation can still provide conclusions about the presence of the two polymers. Table 4.7 shows that between the first and second centrifugation and purification step, most of the (optically active) polymers, thus maltodextrin and gelatin, have been removed from the microgel external medium. The second supernatant had very low optical rotation angles. By calculating theoretical approximate sample compositions (from equations (4.4) and (4.5)) in the dispersing medium, the second centrifugation and purification process lead to removal of most polymers in the dispersing medium. Gelatin concentration got reduced from approximately 0.85 wt% to 0.45 wt% and maltodextrin from approximately 4.7 wt% to 0.41 wt%. Thus, after the second centrifugation and redispersion of the microgels into purified water, polymer concentration in the continuous phase of the microgel suspension may have been relatively low.

Table 4.7. Optical rotation measurement at 365 and 546 nm of the supernatants of centrifuged microgel suspensions (obtained from a 4.5% Gel /13 MD (1 mM Genipin) emulsion). ¹Theoretical composition of sample calculated over measured optical rotations at 365 nm and 546 nm (see equations (4.4) and (4.5)).

| | $\alpha(\lambda=365 \text{ nm})$ | $\alpha(\lambda=546 \text{ nm})$ | Calculated sample composition ¹ |
|---|----------------------------------|----------------------------------|--|
| Supernatant after first centrifugation | 18.6 ° | 7.5 ° | 0.85 % Gel 4.7 % MD |
| Supernatant after second centrifugation | 0.53 ° | 0.18 ° | 0.45 % Gel 0.41 % MD |

4.2.6.7 Summary

From the three purification methods, centrifugation and dialysis gave valuable results, while filtering seemed to aggregate the sample and did not purify the samples effectively. Centrifugation was finally chosen to purify our microgel suspension, as this method was simple and SEM images indicated the most effective removal of polymers from the continuous phase into which the microgels were suspended. Figure 4.57 and Figure 4.58 compare the three different purification methods.



(Gelatin: 50 kDa
Maltodextrin: 3.6 kDa)

Before Purification
4.5 Gelatin / 13 % Maltodextrin
(1mM Genipin)

Filtration

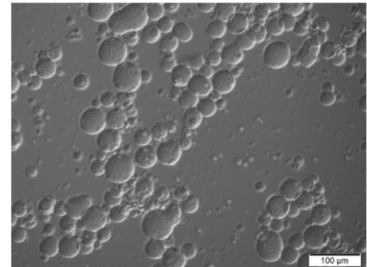
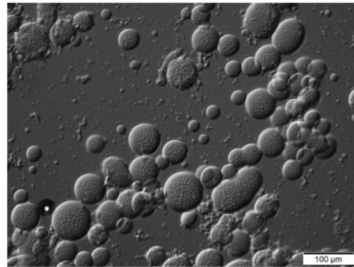
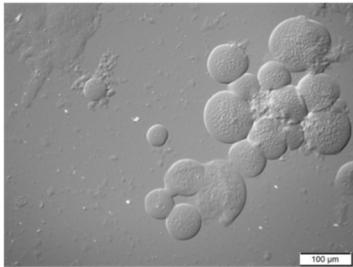
Centrifugation

Dialysis

Polycarbonate Filter
(10 μm pore size)

2x 2000 rpm
(10min, 0°C)

In Water at 25°C
(Pore Size 12 kDa)



- Microgel particles **block filter pores** → only small volumes are filtered
- Microgels in remaining in filter **bigger than average**
- Maltodextrin impurities still observable

- Microgels **keep shape**
- Simple, rapid method (20 min)
- Risk of partial aggregation of particles.

- Microgels **keep shape**
- Long-lasting method (min. 1 day)
- Mild conditions

Figure 4.57. Comparison of the different purification methods of a gelatin/maltodextrin emulsion, after gelling of the droplets and dilution of the continuous maltodextrin-rich phase.

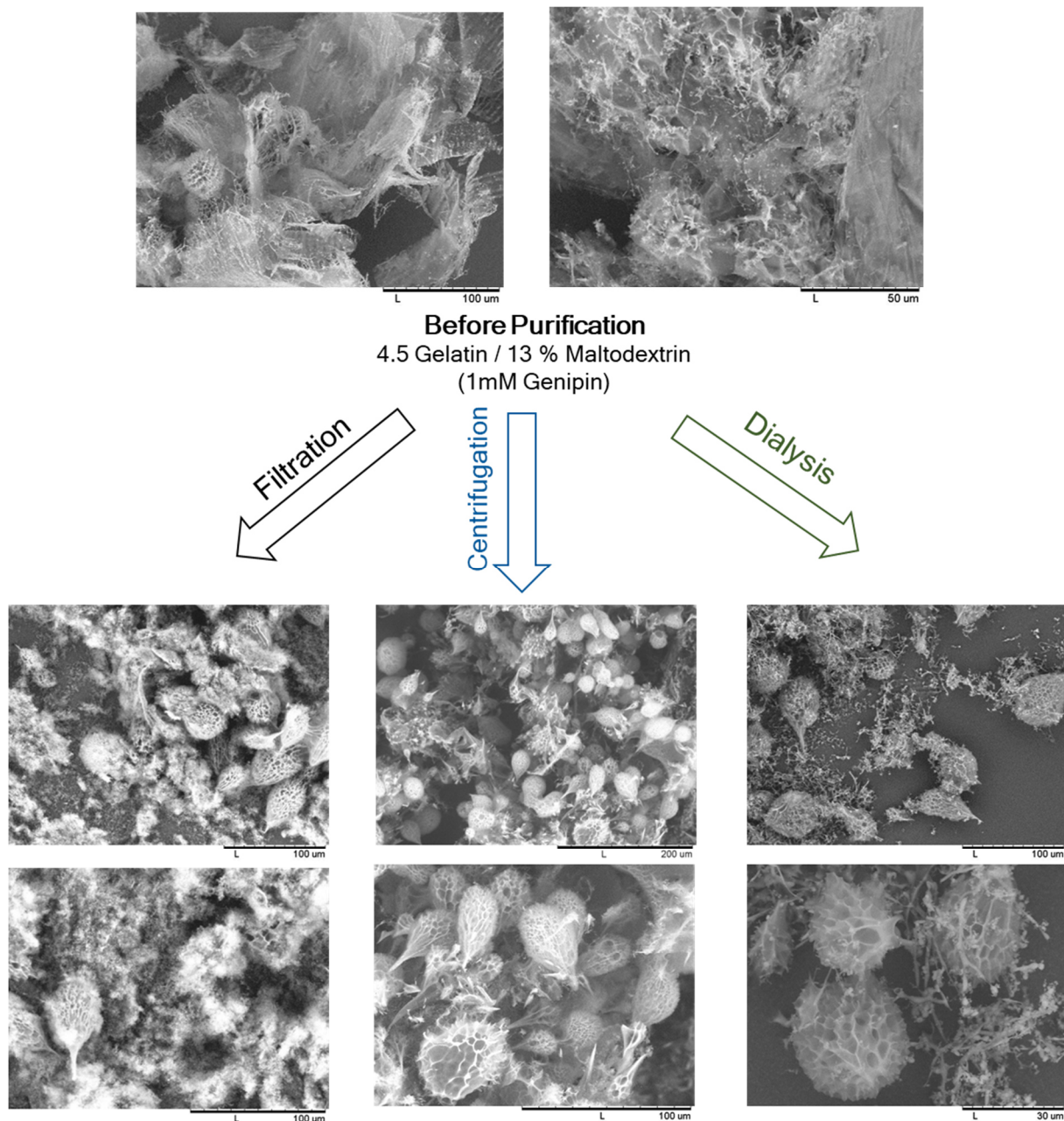


Figure 4.58. SEM images of microgel suspensions (obtained from 4.5% Gel /13% MD (1 mM Genipin)) before and after purification. The solid samples were observed after freeze-drying.

4.2.7 Freeze-Drying of Microgels

Gelatin microgel solutions, in absence of antimicrobial agents, could not be stored at room temperature at long periods of time, since growth of microorganisms was observed after 1-2 weeks at room temperature. Addition of a biocide, such as sodium azide, should be required if the product is aimed to be stored at room temperature. Another option is to store the microgels as a dry powder. In the present work, we opted for freeze-drying to properly preserve the microgels, and the results are described in the next section. Freeze-drying of microgels was performed on aqueous suspensions of purified microgels.

Therefore, they were (in most cases, see below) frozen by CO₂ ice and then lyophilised in the freeze-drier. The final dried microgels, in form of a white powder, were observed by SEM imaging (Figure 4.59 b,e,h).

4.2.7.1 Morphology of Microgels after Freeze-Drying

SEM images of freeze-dried microgels (Figure 4.59 b,e,h) showed that microgels remained stable upon the freezing and vacuum drying, by sublimation of the liquid present in the microgel suspension. Moreover, the size of the microgels remained similar, to when they were dissolved in water. As can be observed in the SEM images, the microgels however, experienced a deformation to a leaf-like morphology and macropores of few micrometers (~1-3 μm) were formed. Other reports in the literature describe a similar effect on microgels or microspheres after the freeze-drying process (Cheng, Chu, Zhang, Wang, & Wei, 2008; Lin, Chen, & Run-Chu, 1999; Mou et al., 2014; Petrusic et al., 2012). The pores originate from the sublimation of the frozen water, which was dispersed in the interconnected polymeric network of gelatin. The direction of the pores might have originated from the orientation of ice crystals, which were oriented because of either the temperature gradient while freezing or the agitation applied during freezing. The size of the pores after drying might be a concern for delivery of active ingredients suspended in the microgels. If the physicochemical interactions with the polymer are not strong enough, they might get released from the microgels during the drying process. Potential loss of active ingredient during drying was thus tested in our case (details in section 4.3.6).

Explanation for the leaf-like shape might be directional sublimation of water inside the microgels (Cheng et al., 2008; Lin et al., 1999). As the top of the microgels was frozen, some water might have been pressed to flow downwards. The streaming water was then gradually frozen, forming hereby the leaf-like structure.

Those effects can be minimised by using a critical-point drying method. Lin et al. compared different drying methods and concluded that the critical-point drying method maintained the spherical and smooth topography of the microgels (Lin et al., 1999). Critical point drying relies on drying of the sample above the critical point of a solvent, at which physical characteristics of liquid and gaseous are not distinguishable. The critical point of water lies at 374 °C and 229 bar, which would destroy the sample. Therefore, water is usually replaced with liquid CO₂, whose critical point lies at 31 °C and 74 bar. This is however not straightforward, as it requires the replacement of water by liquid CO₂, which is done over several dehydration steps, by replacing first water by ethanol and acetone. This method was not tested for our case. That the microgels are porous in the dried state is not of a problem, if its encapsulated active agent is not lost during the drying process, and if it can recover its original morphology after redispersion into the solvent. Both detailed in Section 4.2.7.4 and 4.3.6.

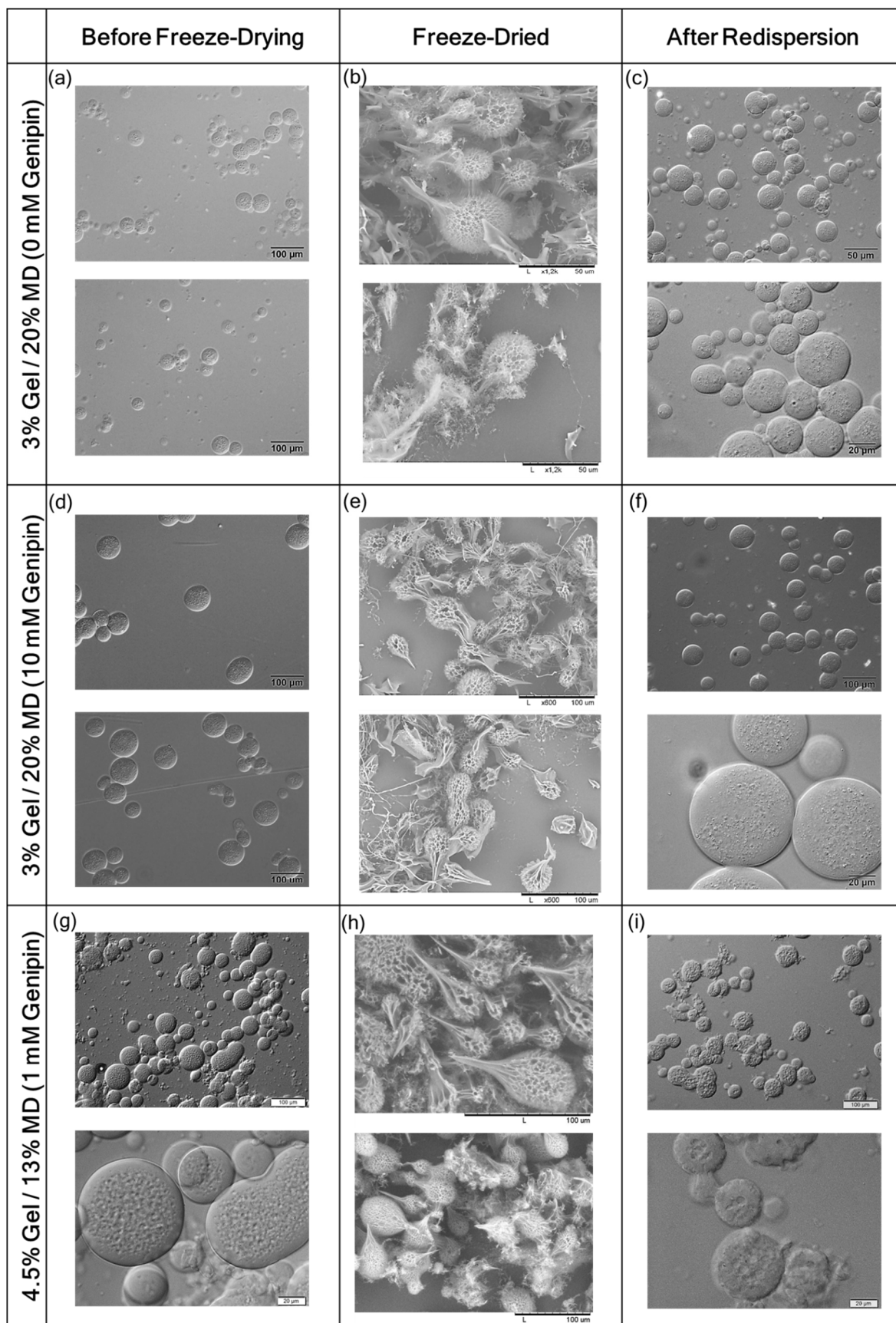


Figure 4.59. Freeze-drying and resuspension of the dry microgel powder, originating from 3% Gel / 20 % MD and 4.5 % Gel / 13% MD emulsions with different concentrations of crosslinker genipin. (a,d,g) show the microgels before freeze-drying, (b,e,h) are SEM images of freeze-dried microgel suspensions and (c,f,i) show the morphology of the microgels after resuspension in water. The samples in (a-f) contain enzyme, which explains the small particles observed in (a) and (f).

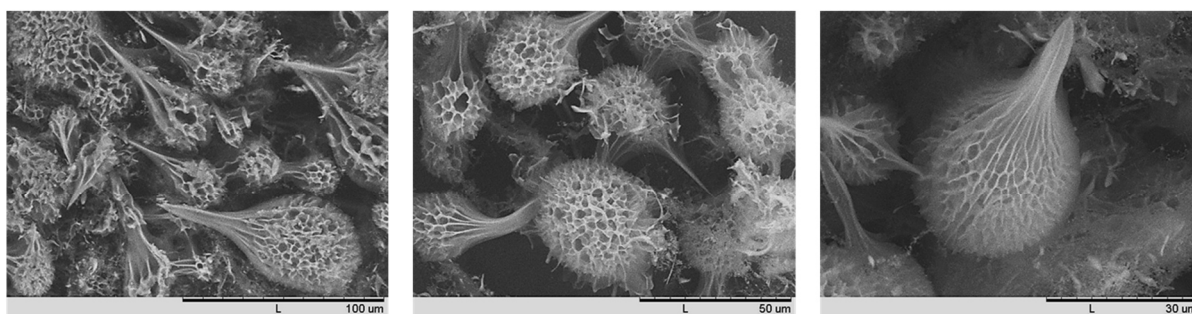
4.2.7.2 Influence of Freeze-Drying Conditions on Freeze-Dried Product

By changing the method of freezing the microgel suspension, before lyophilisation at $-85\text{ }^{\circ}\text{C}$ and ~ 0.03 mbar, it was aimed at reducing deformation of the microgels to a leaf-like structure after the lyophilisation process. Therefore, the morphology of the resulting microgels were compared by freezing them in one case by CO_2 ice/acetone mixture, as usually for the other experiments, and in the other case by liquid nitrogen.

The comparison of these two freezing methods is shown in Figure 4.60. Particles frozen by liquid nitrogen have a more spherical shape than microgels frozen by CO_2 ice / acetone. Still, particles prepared with N_2 are not perfectly spherical, and the tip formation could not be avoided. The tips were however thinner, indicating that less polymer was dragged into this part of the microgel during the freezing process. Tip formation is only possible, as long as water is still in its liquid form, which depends on the freezing temperature. Thus it makes sense that freezing the microgels in liquid nitrogen minimizes this type of deformation. The fact that N_2 is more appropriate for freeze-drying could be related to its much lower temperature, in comparison to CO_2 ice / acetone. In any case, pore formation could not be avoided by freezing under colder conditions, as they originate from sublimated ice crystals, which are formed in both cases.

As tip formation in the dried form of the microgels could not significantly be avoided, samples in further experiments will be dried in CO_2 ice / acetone, for practical reasons. In our lab facilities (liquid nitrogen was not directly available to our lab, while carbon ice it was fully available).

Frozen by Carbon-ice ($-78.5\text{ }^{\circ}\text{C}$)



Frozen by Liquid Nitrogen ($-210\text{ }^{\circ}\text{C}$)

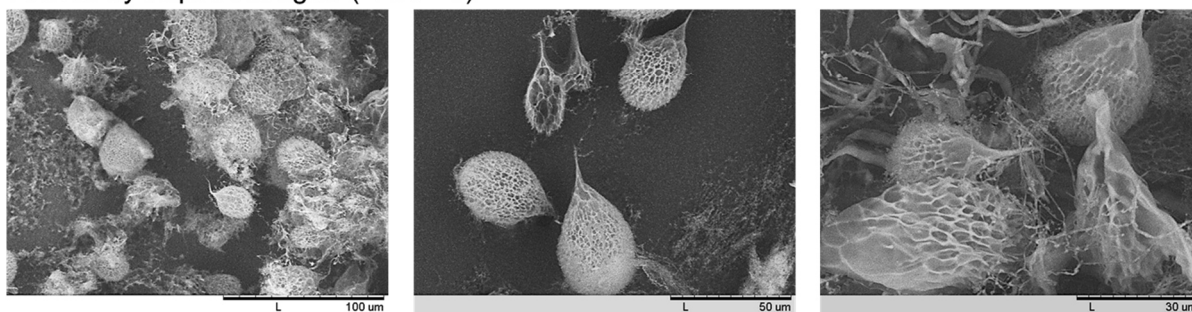


Figure 4.60. Comparison of dried microgel morphology (observed by SEM imaging) of microgels (produced from 4.5% Gel/13% (1 mM Genipin) emulsion) frozen either by CO_2 ice or liquid nitrogen.

4.2.7.3 Influence of Microgel Composition on Freeze-Drying

The influence of the emulsion composition and crosslinker concentration, used to prepare the microgels, on microgel size will be discussed in section 4.2.8.4.1 and 4.2.8.4.5. Herein, the influence of composition parameters on the morphology of freeze-dried microgels will be investigated.

Microgels made from emulsion compositions, lying closer to the binodal line of the gelatin/maltodextrin phase diagram show the aspect of a multiple emulsion, with some primary inner droplets within the microgels (e.g. 4.5 % Gel /13 % MD (1 mM Genipin) emulsion in Figure 4.59 g). This may originate from a secondary phase separation happening near the binodal line. There was however no difference in morphology of the dried microgels observed, which could be correlated to the composition of the emulsion from which the microgels were made (Figure 4.59 and Figure 4.61).

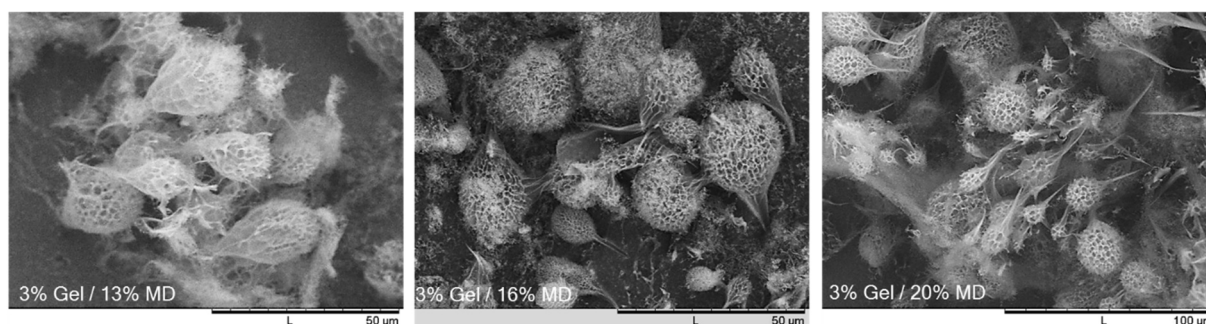


Figure 4.61. Morphology of freeze-dried microgels, prepared with different gelatin/maltodextrin compositions, without crosslinking of gelatin, observed by SEM imaging.

Regarding the influence of crosslinker concentration, it did not produce effects on pore size or particle size of the dried microgels, as seen for the 3% Gel / 20% MD based microgel with 0 and 10 mM genipin (crosslinked 2 h at 35 °C) in Figure 4.59 (b) and (e). Petrusic et al. observed the same in their studies, showing that crosslinking did not affect pore size of freeze-dried PNIPAAm microgels (Petrusic et al., 2012). This result is unexpected as crosslinking serves usually to reduce pore size in polymeric microgels. No detailed porosimetry analysis of the dried microgels was undertaken, as the high surface area of the dried leaf-like microgel tips would have contributed to a big error into porosity calculation of the spherical part of the dried microgel. Crosslinking would only affect the stability of the network, but not its morphology. Similar results on effect of crosslinking on microgel size can be found further below (Figure 4.70).

4.2.7.4 Redispersion of Freeze-Dried Microgels

When rehydrating the freeze-dried porous microgels by redispersing in water (Figure 4.59 c,f,i), they recovered the spherical morphology, as before the drying step (Figure 4.59 a,d,g). The leaf-like structure, as observed under the SEM imaging of the dried product (Figure 4.59 b,e,h), was not observed anymore. This may mainly be ascribed to the flexible and elastic characteristics of the crosslinked gelatin networks. Remarkably, the particle size distribution after rehydration seems to remain approximately the same as before freeze-drying and changes in particle morphology seem to be small.

In contrast to the microgels originating from 3% Gel / 20% MD emulsions, the microgels from 4.5 % Gel /13% emulsions (Figure 4.59 i) did not regain an identical morphology as before freeze-drying, but

instead the surface of the particles after rehydration seemed to have higher roughness. Schachschal et al. obtained similar results for PNIPAAm microgels, as seen in the figures of their article (Schachschal et al., 2011). We suppose that this difference originates from the fact, that the amount of gelatin polymer in gelatin microgels produced from 4.5 % Gel /13% MD emulsions is lower than the one produced from 3% Gel / 20% MD emulsion. This hypothesis comes from the assumption that the tie lines could be more or less perpendicular to the 50:50 phase volume line in the phase diagram of gelatin/maltodextrin (Figure 4.31). Thus, the gelatin concentration of the dispersed gelatin-rich droplets might be ~20 wt% for the 3% Gel / 20% MD emulsion, and ~10 wt% for the 4.5 % Gel /13% MD emulsion (composition of both phases in emulsion determined by intersection of tie line with binodal line). As a consequence, less polymer might be present in 4.5 % Gel /13% MD emulsion-based microgels, to cover completely the surface-lying pores of the porous microgels. When redispersing those emulsions, interestingly, the interior gelled droplets of the microgels remained present. This hypothesis should be confirmed with a more systematic study.

In conclusion, the results clearly demonstrate that crosslinked gelatin microgels can be freeze-dried and later redispersed in purified water, without producing major effects on the microgels. Consequently, freeze-drying was selected in our work for the preservation of the microgels, instead of more complex methods such as critical-point drying, as used by Lin et al (Lin et al., 1999).

4.2.8 Characterisation of Microgel Particles

4.2.8.1 Flocculation of Microgels in Suspension

As microgels were purified by applying centrifugation-resuspension cycles, after each centrifugation treatment, it was observed by optical microscopy that microgel particles presented partial aggregation (Figure 4.64). This was attributed to the mechanical force applied to particles during centrifugation. Weak flocculation of the microgels, may also be attributed to a low zeta potential of the microgels. We intended to measure zeta potential of microgel suspensions in water, to get a better understanding of their colloidal stability and investigate the influence of crosslinking on net charge. As the zeta potential is concentration-dependent, the sample concentration threshold at which the zeta potential keeps a constant value was searched for. Figure 4.62 (a) shows that no such concentration could be found and that the zeta potential varied strongly with concentration, and resulted in positive or negative values. The rapid sedimentation of the microgels in the measuring cell (Figure 4.62 (b)), explained those inconclusive results, and signified that the zeta potential of those microgels suspensions could not be precisely measured. The actual mechanism of colloidal stability was not in the scope of the present work, and it was thus not studied in more detail. Previous studies (P. A. Turner et al., 2017; A. Wang et al., 2012) found values between -9 and -12 mV for similar gelatin microgels at physiologic pH, above the isoelectric point of gelatin ($pI \approx 4.7-5.2$). They are close to the values measured in Figure 4.62 (a), for low microgel concentrations. Those values are not high enough to provide colloidal stability to the particles solution and may thus explain the flocculation we observe. Moreover, they found that crosslinking gelatin reduces the zeta potential slightly, mainly due to the consumption of primary amines of gelatin (P. A. Turner et al., 2017).



Figure 4.62. Microgels, here blue as crosslinked with genipin, started to sediment after few seconds inside the measuring cell, making zeta potential measurement not possible.

Microgels aggregation resulted also for longer time periods between the moment the emulsion, used as template for the microgel, was stopped to mix and the moment it was cooled down to 0 °C to form microgels.

Figure 4.63 shows representative parts of the emulsions (stirred at 30 °C) cooled down 0, 0.5, 1 or 5 min after stopping the agitation of the emulsion. As it can be seen, aggregation increases with increasing rest time. The emulsion was prepared at 30 °C, close to the gelling point of gelatin. Therefore, arresting

the mixing lead presumably rather to aggregation of viscous/ gel-like droplets instead of coalescence of the liquid droplets. No increase in droplet size was observed, within this time period. Coalescence would have been more probable at higher temperature, at which the gelatin droplets have lower viscosity and can thus more easily break the liquid film at the droplet-droplet interface.

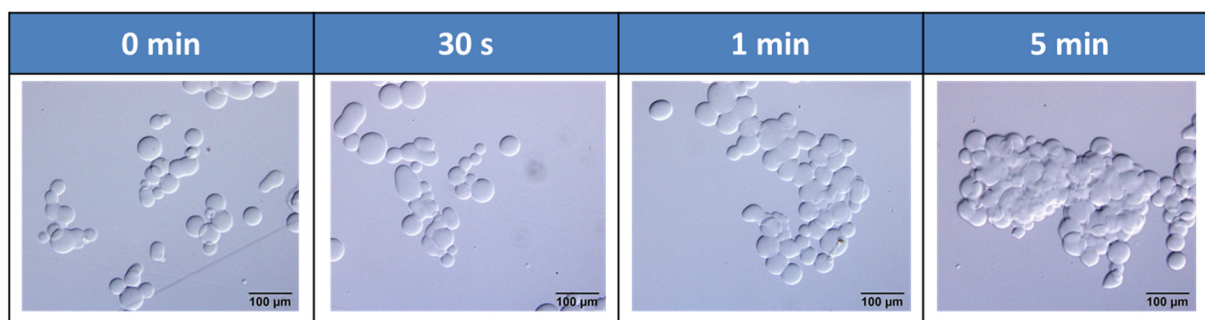


Figure 4.63. Microgels aggregation for 0, 0.5, 1 and 5 min of waiting between stopping emulsion (3% Gel / 20% MD) agitation at 30 °C and its cooling down to form microgel.

4.2.8.2 Deflocculating aggregated Microgel by Sonication of Microgels

To counteract aggregation, samples were sonicated, applying a power of 80 W, with 4 on/off cycles with a duration of 5s/20s each cycle. The energy from sonication allowed deflocculating the microgels (Figure 4.64), without affecting or modifying microgel morphology. This was successfully performed, as for non-crosslinked, as well as for crosslinked microgels. Within few minutes the microgels sediment to the bottom of the vial, however no aggregation was observed over a period of several days after sonication of the samples.

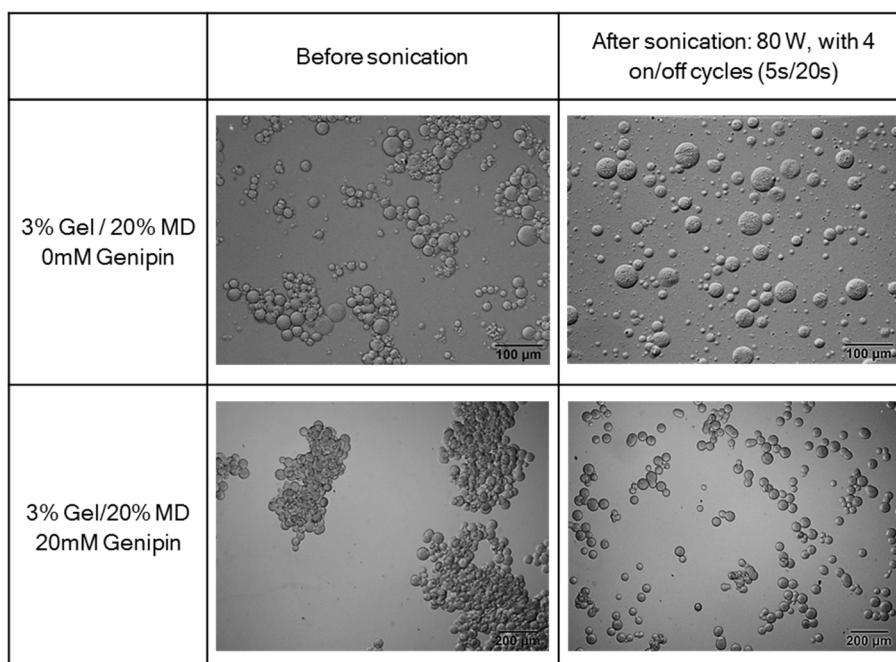


Figure 4.64. Sonication of gelatin/maltodextrin emulsions lead to deflocculation of the aggregated crosslinked and non-crosslinked gelatin droplets.

4.2.8.3 Size Determination of Microgels: Microscopy versus Laser Diffraction

An alternative to the time-consuming size determination of microgel particles, by size analysis of micrographs (measuring of over 300 droplets per sample), is size determination by laser diffraction measurements. This technique is based on the analysis of the diffraction intensity of monochromatic light inciting onto the sample. The bigger the diffraction angle is, the smaller the particle size.

Size distribution of crosslinked microgels, prepared from a 3 % Gel / 20 % MD (1 mM Genipin) emulsion, was followed during a period of 1 month, by light scattering. Results were compared with size distributions obtained by microscopic analysis of the samples.

From the scattering profile obtained, the particle size distribution has been calculated. The transformation from scattering data to size, depends on the refractive indices of dispersant (microgels) and continuous medium, and as well the absorption index of the particle. The refractive indices were measured and known (microgels RI=1.341, water RI=1.33). However the absorption index had to be estimated, based on values from literature (Kong et al., 2011), and comparing the residual (measure of fit between calculated and measured scattering profile of sample) for different indices. Finally, an absorption index of 0.1 was chosen.

The volume size distribution of the particles can be seen in Figure 4.65, for the laser light diffraction and Figure 4.66, shows the histograms of the values obtained from microscopic size analysis. To obtain these values, the number size distribution (Figure 8.2) was transformed into volume size distribution.

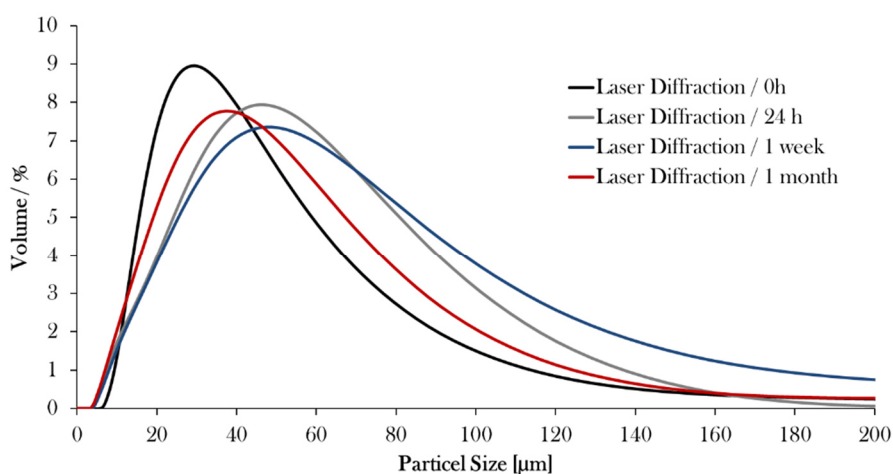


Figure 4.65. Volume Size distribution of crosslinked microgels, (prepared from a 3 % Gel / 20 % MD (1 mM Genipin) emulsion), measured by light diffraction, at time 0 h, 24 h, 1 week and 1 month.

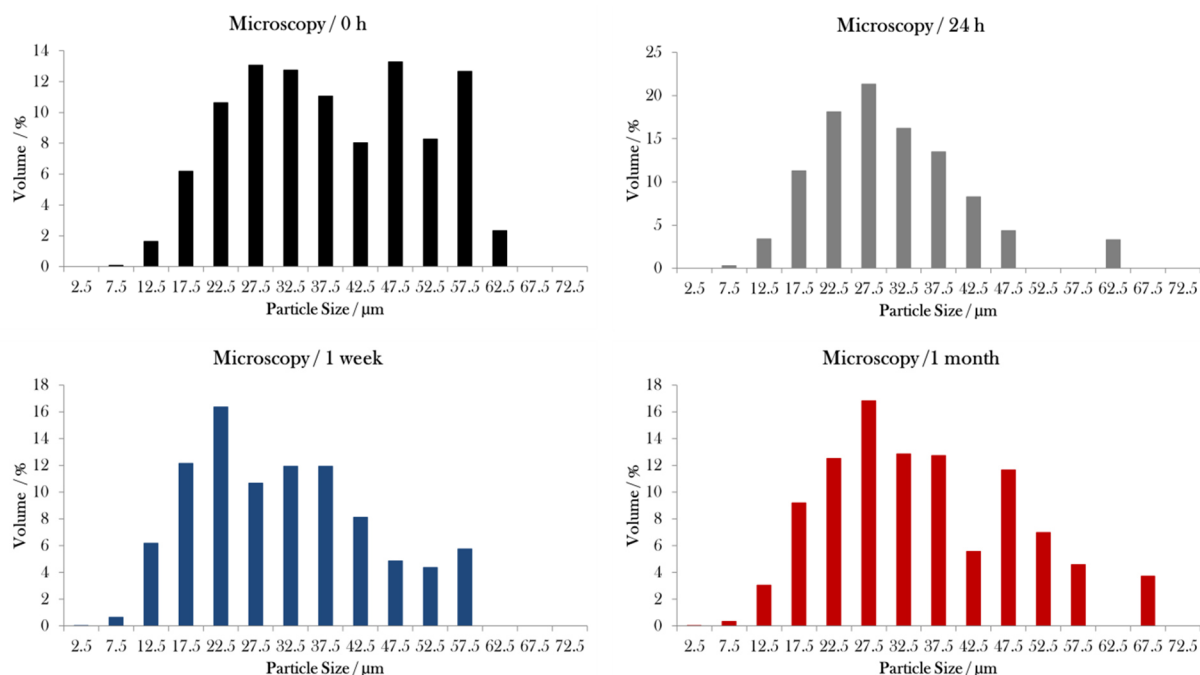


Figure 4.66. Volume Size distribution of crosslinked microgels, (prepared from a 3 % Gel / 20 % MD (1 mM Genipin) emulsion), measured by analysis of microscopic images with the imaging software Image J., at time 0 h, 24 h, 1 week and 1 month. For better comparison, number distribution was transformed to volume distribution.

Table 4.8 summarises the results by comparing the evolution of the volume mean diameter, $D[4,3]$, over a period of 1 month, measured by laser diffraction particle size analysis and by size analysis by microscopy. The polydispersity is represented by the *Span*.

Table 4.8. Volume mean diameter, $D[4,3]$, evolution over 1 month of crosslinked microgels (prepared from a 3 % Gel / 20 % MD (1 mM Genipin) emulsion), measured by light diffraction and microscopic particle analysis. Moreover, *Span* for the different measurement methods, and the median of the microscopic analysis are indicated. Microgel sizes are indicated in μm .

| | Laser Diffraction | | Optical Microscopy | |
|----------------|-------------------|------|--------------------|------|
| | $D[4,3]$ | Span | $D[4,3]$ | Span |
| 0 h | 43.4 | 1.8 | 45.1 | 1.0 |
| 24 h | 60.2 | 2.0 | 30.0 | 1.2 |
| 1 week | 59.3 | 2.3 | 34.5 | 1.3 |
| 1 month | 51.1 | 2.1 | 35.1 | 1.2 |

Based on those results, both techniques will be compared to select the most appropriate technique for further experiments.

From Table 4.8 it can be seen, that for most samples, the $D[4,3]$ obtained from microscopic analysis do not coincide with the values obtained from laser diffraction measurements, and are generally smaller. Furthermore, the *Span* is lower for the volume size distribution measured by optical microscopy. The

lower Span, polydispersity, is explained, that analysing micrographs, droplets of small size can not be detected, while they are detected by laser diffraction. On the other hand, laser diffraction may consider aggregated microgels as a single particle of increased diameter, leading thus to displacement of the volume size distribution towards higher particle sizes. This does not only affect the *Span*, but also the volume mean diameter. $D[4,3]$ determined by laser diffraction measurements were, for most samples, larger than if obtained by microscopic analysis. Moreover, the transformation from the number distribution of the particle size, obtained by microscope (Figure 8.2), to the volume distribution, may also add some error, as perfectly spherical microgel particles are assumed. This is not the case for all particles.

Following size development, by both techniques, over a period of 1 months, laser diffraction measurements shows particle size increase in the first 24 h and then remain more or less constant. Microscopic analysis indicate, in contrast, that in the first 24h, the particle size diminishes and then stays constant.

Another source of error to be considered in light diffraction measurements is the quality of the fit, the residual. For instance, volume mean diameter, $D[4,3]$, at 0 h, had the biggest residual (1.3) compared to the measurements at other time points (0.2). This means that the size distribution at $t=0$ h is not a perfect fit to the corresponding scattering profile obtained and the result has to be considered with caution. For the same scattering profile, when changing the absorption index from 0.1 to 0.01 (resulting in even higher residual values), the calculated diameter for $t=0$ h, resulted bigger than the ones obtained at later time periods. Results from optical microscopy are thus more reliable as they do not depend on unknown material parameters (needed to transform the scattering profile to the size distribution, using Mie's Theory), such as the absorption index. Moreover, those droplets are large enough to be observed precisely under the microscope.

As a conclusion, size determination by laser diffraction is not recommended for this system as the obtained size distribution might not reflect the real one. From now, only optical microscopy will be used for size determination of microgel sizes.

Results, from microscopic size analysis, indicate that microgel remain stable over at least 30 days and their size remains constant. Changes in the first 24 h are probably due to ongoing crosslinking processes, which make the polymer network more compact and thus diminish microgel particle size. More in detail follow-up of microgel size during 30 days is presented in section 4.2.8.4.5 .

4.2.8.4 Influence of Preparation Parameters on Microgel Size

To understand parameters, which influence the gelatin droplet size of a gelatin-in-maltodextrin emulsion, the effect of emulsion composition, stirring speed, stirring temperature, solvent and crosslinker concentration was tested on resulting gelatin droplet size.

4.2.8.4.1 Composition of W/W Emulsion

As mentioned in section 4.2.5, the composition in the multiphase region of gelatin/maltodextrin mixtures determines if gelatin-in-maltodextrin, maltodextrin-in-gelatin or bicontinuous structures are obtained. Of

interest is to know whether the composition influences, not only the morphology of the emulsions, but also the droplet size. Therefore, gelatin-in-maltodextrin emulsions of three different gelatin and three different maltodextrin concentrations were prepared by homogenising them by Ultra-Turrax® during 1 min at 9,500 rpm. After cooling and dilution with ice-cold water, their size distribution was analysed. The results indicate that droplet size was quite independent on either gelatin or maltodextrin concentration in the emulsion (Figure 4.67). Previous studies in gelatin/PEG emulsions, obtained smaller droplet size with increasing viscosity of the continuous and dispersed phase (Kong et al., 2011), thus increasing concentrations of both polymers. In our case, other experimental conditions, such as mixing temperature and stirring speed seem to have a more important influence on droplet size, than emulsion composition. The distribution of droplet size in Figure 4.67 shows that the difference in median size (11-19 μm) can be related to polydispersity within the samples.

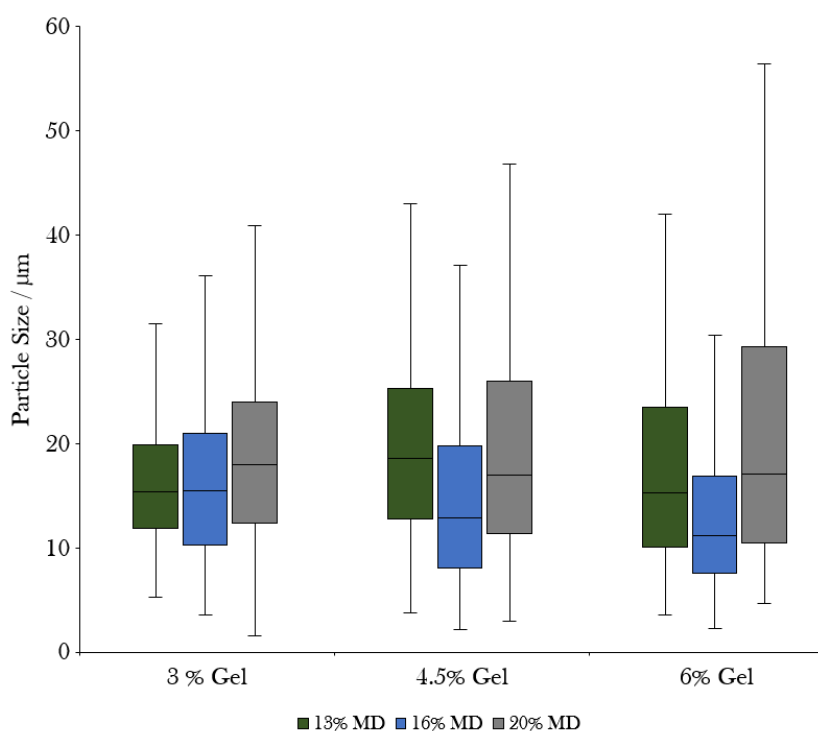


Figure 4.67. Median size of microgel particles prepared from emulsions of varying gelatin/maltodextrin emulsion compositions. The box represents the data lying within the IQR and the median is marked by a horizontal line. The whiskers outside the box indicate the range of data up to d(5) or d(95).

4.2.8.4.2 Stirring Speed

Increased mechanical stirring with higher energies leads to reduced droplet sizes, which is of interest in application of microgels in drug or food delivery applications. Stokes et al. confirmed this previously for the gelatin/maltodextrin emulsion system (Stokes et al., 2001).

The emulsions were thus prepared by homogenisation by ultraturaxing to reduce not only droplet size, but also polydispersity amongst the sample. To find the adequate rotation speed, a 8% Gel / 20% MD mixture, which contained gelatin droplets as dispersed phase, was used as a model sample. By changing rotation speed, it could be shown that higher rotation speeds reduced average droplet sizes from 33 to 19 μm (Table 4.9). Polydispersity was reduced as well, by comparing the size distribution and the

interquartile range amongst the samples. No big difference could be observed between the values for the rotation speeds of 9,500 rpm and above. It should be noted that rotation speeds above 9,500 rpm lead rapidly to strong foam formation within the sample. To reduce this phenomenon, agitation time was half (from 1 min to 30s for the samples homogenised at 13,500 and 19,500 rpm. It can thus be concluded that a rotation speed 9,500 rpm was most effective and will thus be used in the experiments, which have the objective to obtain small and less polydisperse samples.

Table 4.9. Influence of rotation speed on droplet size of 8% Gel / 20% MD emulsion. The interquartile range (IQR) is defined as $d(75)-d(25)$.

| Rotation Speed [rpm] | Median [μm] | IQR [μm] |
|-------------------------|-----------------------------|--------------------------|
| 7,500 | 33 | 22 |
| 9,500 | 21 | 10 |
| 13,500 | 24 | 12 |
| 19,500 | 19 | 12 |

4.2.8.4.3 Temperature during emulsification

One important factor in the emulsification of the gelatin/maltodextrin mixture was the temperature, at which the emulsion was stirred. To examine the influence of temperature on droplet size, the emulsion was stirred for 30 min at three different temperatures: 30, 45 and 60 °C.

As can be seen from the results in Table 4.10 droplet size was lower at 45 °C (18 μm) and 60 °C (19 μm), compared to 30 °C (25 μm), while the polydispersity increased with increasing temperature. Similar results can be seen in Table 4.11. This can be explained by the variations in viscosity of gelatin droplets, which is lower at increased temperatures, which is favourable for droplet break-up during emulsification. Droplet size decreased at higher temperatures, since droplet break-up was favoured by agitation. However, coalescence might also be promoted at increased temperature, and thus this could explain the higher polydispersity at increased temperature.

Temperature is an important factor in emulsification, as it does not affect only emulsion size, but also crosslinking kinetics of gelatin by genipin and enzyme activity.

Table 4.10. Influence of mixing temperature (500 rpm for 30 min) on droplet size of 3% Gel / 20% MD emulsion. The interquartile range (IQR) is defined as $d(75)-d(25)$.

| Temperature [°C] | Median [μm] | IQR [μm] |
|---------------------|-----------------------------|--------------------------|
| 30 | 25 | 7 |
| 45 | 18 | 11 |
| 60 | 19 | 14 |

4.2.8.4.4 Medium (Water or PEM buffer)

All previous microgels were prepared in water. In order to assure favourable conditions for the enzyme, the solvent of the microgel must be PEM buffer (composition detailed in Table 3.1). Therefore, microgels were prepared by the same procedure as before, but instead of using water, all polymers were dissolved in PEM buffer. Microgels could be prepared in the PEM buffer, as can be seen in Figure 4.68, which compares microgels prepared under same conditions, just with a different medium. If preparing the emulsions in PEM buffer, gelatin droplet size were however smaller than if prepared in water (Figure 4.68 and Table 4.11). All emulsions in Table 4.11 were mixed during 30 min at 500 rpm, no Ultra-Turrax[®] homogeniser was used, which would have reduced droplet size additionally.

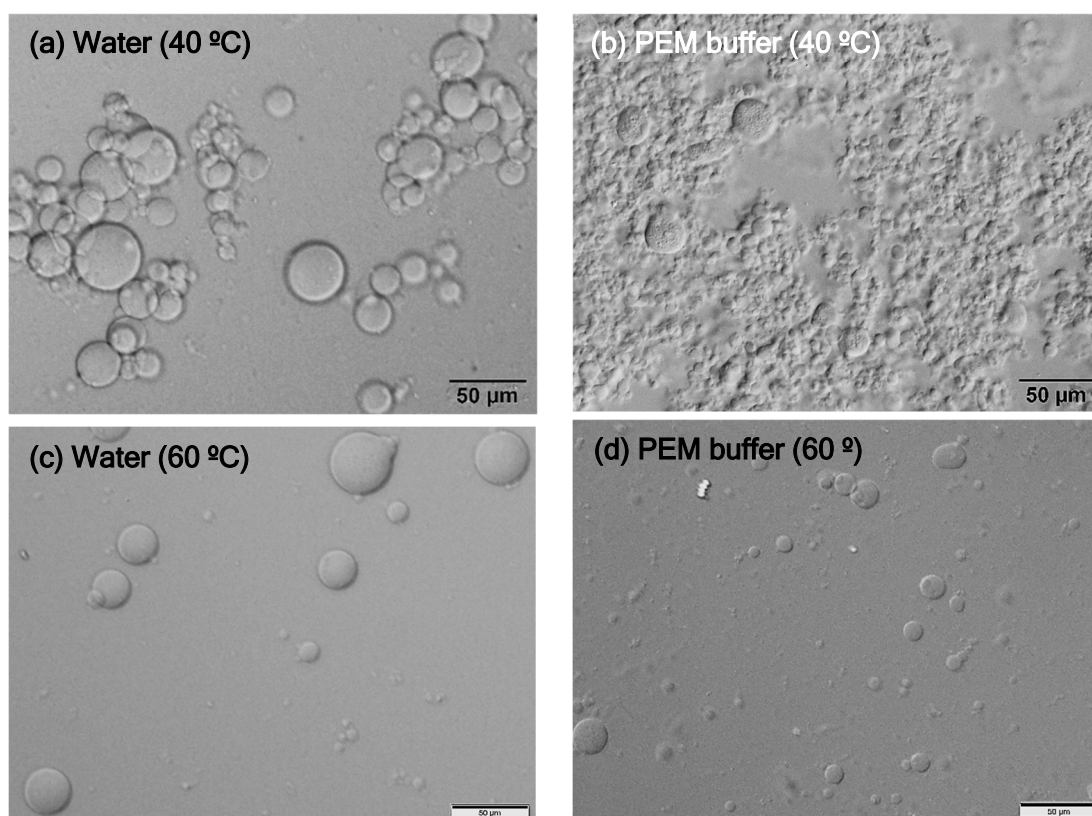


Figure 4.68. Comparison of gelatin droplet size, produced from 3 % Gel / 20% MD, with (a, c) water or (b, d) PEM buffer.

It could be shown, as in Table 4.10, that increasing temperature during emulsification, from 30 to 60 °C, decreases droplet size from 25 μm to 19 μm (in the case of water) or from 17 to 13 μm (with PEM buffer). The reasons therefore, are detailed in the previous section.

Furthermore, preparing the emulsion in PEM buffer decreased droplet size of emulsions, from 19-25 μm down to 10-17 μm (Table 4.11), in the case of 3% Gel / 20% MD prepared with magnetic stirring. The pH of both solvents is similar (pH 6.5), however PEM buffer possesses a higher ionic strength. This might influence on hydration of the two polymer and consequently could have a strong effect on interfacial tension.

Table 4.11. Droplet size, expressed as median, and polydispersity, indicated as the interquartile range, as a function of temperature for the two aqueous systems used. Composition was 3% Gel / 20% MD, prepared with magnetic stirring at 500 rpm, during 30 min, with ≈ 6 g total sample weight. After emulsion formation, samples were cooled down to 0°C, and finally diluted with cold solvent, as described previously.

| System | | 30°C | 40°C | 60°C |
|------------|---------------------------------------|------|------|------|
| Water | Droplet size (median) / μm | 25 | 21 | 19 |
| | Polydispersity (IQR) / μm | 7 | 11 | 14 |
| PEM buffer | Droplet size (median) / μm | 17 | 10 | 13 |
| | Polydispersity (IQR) / μm | 6 | 4 | 8 |

Thus, preparing emulsions at higher temperatures, in PEM buffer and increased stirring speed, one could obtain droplets with smaller size, and consequently smaller microgels. As those conditions affect also crosslinking kinetics and enzyme stability, they have therefore to be carefully selected.

4.2.8.4.5 Crosslinker Concentration

Crosslinking of gelatin by genipin was performed to ensure higher stability against degradation or dissolution of the polymer at for example high temperatures, extreme pH conditions or from enzymatic degradation. However, if microgels were too strongly crosslinked (high crosslinker concentration or long crosslinking) intercrosslinks between microgels, formation of aggregates (Figure 4.69 b), or even formation of one single macrogel occurred. Therefore, crosslinking concentrations and times were selected to avoid merging between microgel particles.

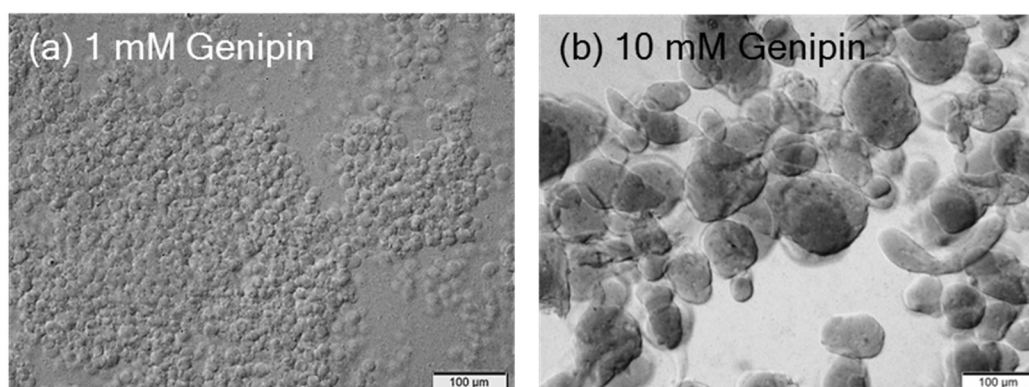


Figure 4.69. Microgels, prepared from 4.5 % / 13 % Gel, were crosslinked with (a) 1 mM Genipin or (b) 10 mM Genipin during 24 h at 30 °C. 10 mM genipin leads the droplets to merge and form bigger aggregates, due to interparticle crosslinks (b). At lower concentrations the microgels are crosslinked, however with much less particle merging between the individual microgels (a).

Gelatin microgels were prepared in PEM buffer applying Ultra-Turrax® homogenisation of the emulsion, and then samples were stirred for 30 min at 40 °C with various amounts of crosslinking agent (genipin), and were diluted as described. Finally, microgel suspensions were stored in water at 4°C and their size was followed over a period of 1 month (Figure 4.70).

These conditions were selected in order to obtain microgels with the smallest particle size. The results showed that particle size of this sample remained constant during the 1 month period, for all crosslinking concentrations (between 0 and 5 mM genipin). After 30 days, the size did not vary more than 5 %, in comparison to the initial size at zero time.

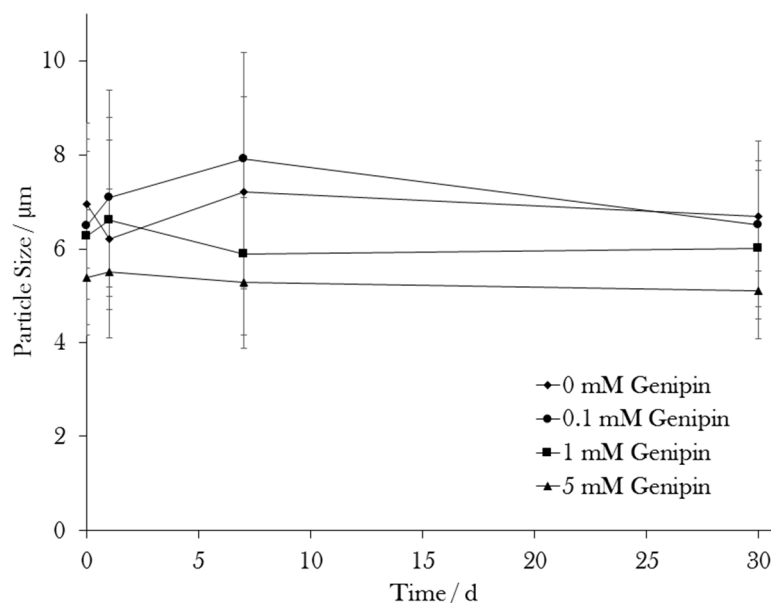


Figure 4.70. Microgel size evolution over a period of 1 month at 4 °C and at various crosslinking concentrations. The error bars indicate the interquartile range (IQR) of the particle size distribution.

Figure 4.70 also shows that microgels crosslinked with 5 mM Genipin were smaller (5-5.5 μm) than the ones with lower genipin concentrations (6-8 μm), which can be explained by contraction of the crosslinked gelatin matrix and syneresis at increased crosslinker concentration. But for lower genipin concentrations, crosslinking barely influenced microgel size, which is in agreement with previous studies (Annan et al., 2007).

It has further to be noted that no shrinkage in the first 24 h is observed, as in previous experiments, such as those shown in Table 4.8 and Figure 4.72, in which the microgels were crosslinked during 20 min at 60 °C with 1 mM Genipin. From Figure 4.16 it can be seen that crosslinking under those conditions leads to a higher crosslinking ratio, and thus may explain why those microgels got reduced in size in the first 24 h and not in this (Figure 4.70) case. The reduced size at $t = 0$ h for 5 mM Genipin (Figure 4.70) may indicate that this shrinkage started during the crosslinking process in the emulsion.

4.2.8.5 Long Term Stability of Microgels

From Figure 4.70 and Table 4.8 it can be seen that microgel sizes remain constant over a period of 1 month. Microgels remain stable over far longer time, if stored in the fridge. Figure 4.71 shows microgels, prepared from a 4.5 % Gel / 13 % MD (1 mM Genipin) emulsion, which were followed up to 500 days. As can be seen, microgels did not dissolve or aggregate over this prolonged time and can thus be kept in solution for over a year. The only issue is bacterial growth starting to occur, even at 4°C after several months. This could be avoided by either using biocides, such as sodium azide, or sterilising the solution after preparation. An alternative, as mentioned in section 4.2.7, is freeze-drying the microgels and keeping them in a dry state.

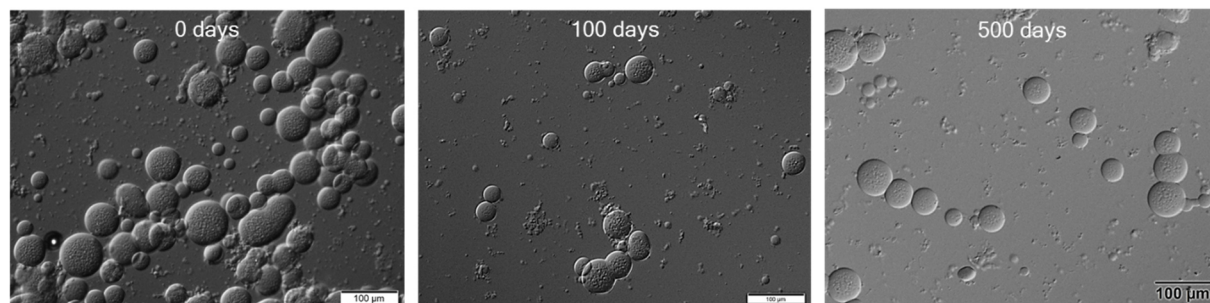


Figure 4.71. Microgels, prepared from a 4.5 % Gel / 13% MD (1 mM Genipin) emulsion, remained stable over many months (here tested up to 500 days), if stored in the fridge at 4 °C.

4.2.8.6 Influence of pH on Microgel size

The aim was to investigate the influence of pH on the swelling behavior of the microgels. Solutions with pH between pH 2-11 were prepared, based on an universal pH Buffer, the Davies buffer (Davies, 1959). Microgels, prepared from 3% Gel / 20% MD (1 mM Genipin) emulsions, were dispersed into those buffer solutions and one sample into water. The solutions were kept at 4 °C and their size was followed during a period of 2 weeks, with sample analysis at 0 h, 3.5 h, 24 h and 2 weeks (Figure 4.72 and Table 4.12).

Table 4.12. Size development, for a period of 2 weeks, of microgels dispersed in solutions of pH 2 –pH 11, and water. Median [μm] and the upper and lower quartile (in brackets) are shown.

| | Water | pH 2 | pH 3 | pH 4 | pH 5 | pH 8 | pH 11 |
|----------------|---------------|---------------|---------------|---------------|---------------|---------------|---------------|
| 0 h | 23 (15-32) | 12 (7-24) | 17 (9-32) | 15 (9-25) | 16 (9-25) | 13 (8-22) | 11 (7-18) |
| 3.5 h | 17 (11-25) | 23 (13-34) | 12 (8-19) | 10 (3-21) | 14 (7-23) | 17 (10-24) | 10 (6-16) |
| 24 h | 20 (13-31) | 25 (14-40) | 25 (16-37) | 11 (7-20) | 20 (13-28) | 21 (24-29) | 17 (9-26) |
| 2 weeks | 18 (11-24) | - | 30 (21-44) | 19 (12-26) | 17 (11-26) | 18 (12-25) | 19 (11-27) |

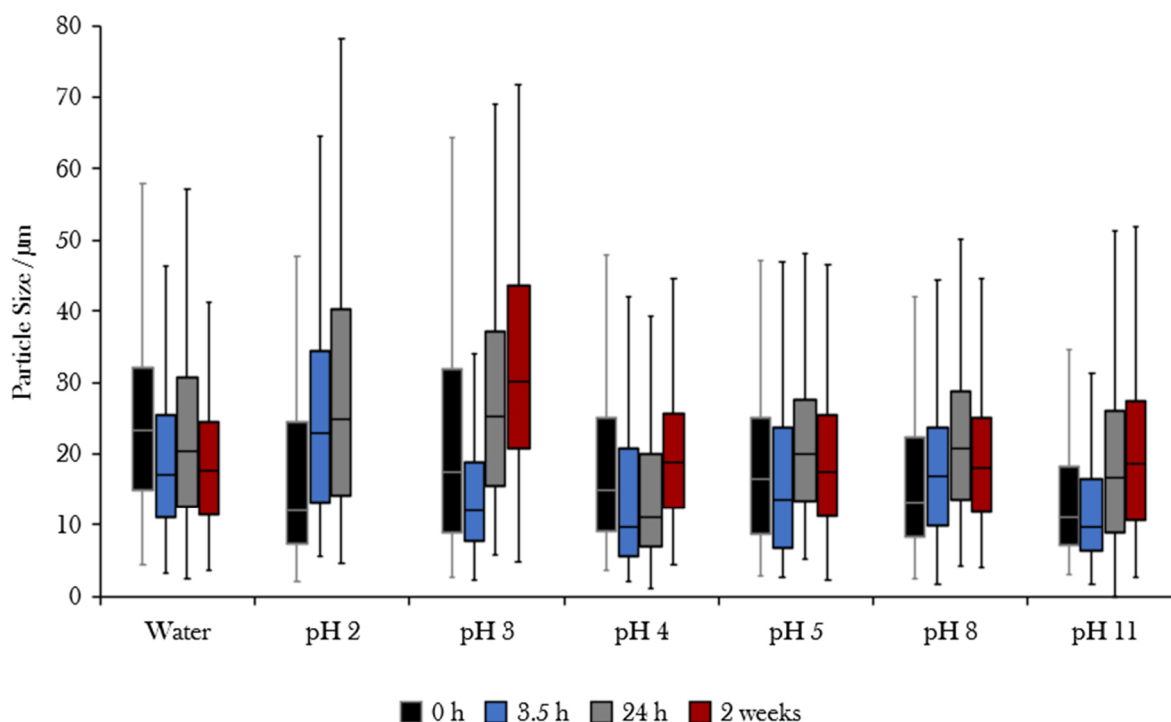


Figure 4.72. Size development, for a period of 2 weeks, of microgels dispersed in solutions of pH 2 –pH 11, and water. The box represents the data lying within the IQR and the median is marked by a horizontal line. The lines outside the box indicate the range of data up to d(5) or d(95).

Swelling of microgels has been observed after 2 weeks for pH 2, 3, 8 and 11, however not for the microgels prepared at pH 4 and 5 and water (pH 6.5). The reason is that at the pH values far from the isoelectric point (4.7-5.2) gelatin proteinaceous chains are electrostatically charged, leading to repulsion between adjacent chains and producing expansion of the microgel network. If microgels were dispersed at pH 2, they strongly swelled and finally got dissolved after 24 h (between 24-48 h). The polymer crosslinks were not strong enough to maintain the polymer network connected and covalent bonds within the network might have been hydrolyzed at those acidic pH conditions.

It can also be assumed that for most samples there was a competition between microgel shrinkage due to ongoing crosslinking, observed before (Table 4.8), and microgel swelling, due to electrostatic repulsion of polymer chains, if pH was far away from the pI.

Furthermore, the microgels dispersed in water had, at time = 0h a higher initial diameter, than the microgels dispersed in the Davies buffer. In contrast to the studies in section 4.2.8.4.4, those microgels were all prepared in emulsions with as medium water. The difference in size is thus not due to the influence of another medium, the Davies buffer, which could have influenced the droplet size during preparation of the microgels. The difference rather may have been caused by suspending the microgels in the new solvent. This was caused probably by the higher ionic strength of the buffer solutions, and not by pH. The buffer solutions had an increased ionic strength, in comparison to water (ionic strengths between 0.12-0.31 M, depending on the pH) and higher osmolality (0.19-0.4 osmol/L). Those two factors may have reduced microgel size, as explained in next section. As seen in Figure 4.73 ionic strength or osmolality of this strength could have been part of the reason that has induced those size differences. Furthermore, we hypothesize that size difference between microgels dispersed in water and

those in the Davies buffer, may have been caused by multivalent ions, such as tetraborate or citrate, in the buffer.

4.2.8.7 Influence of Salt concentration on Microgel size

Ionic strength and osmolality differences between the solvent inside the microgel and the one they are dispersed in, could lead to change in microgel size. When dispersing the microgels in solutions of higher ionic strength, the ions may shield charges on the polymeric network, reduce ionic repulsions between them and thus lead to reduced microgel size. Osmotic pressure differences between the solvent, in which the microgels were prepared in and the surrounding medium, might also contribute to shrinkage of the microgels, as water can diffuse from the microgels towards the solvent of increased osmotic pressure, could lead to microgel shrinking.

Therefore, microgels prepared in water, were centrifuged, the supernatant removed and then, the microgels redispersed into solution of water, 0.1 or 0.2 M NaCl. Microgel size development was followed during 24 h (stored at 4 °C).

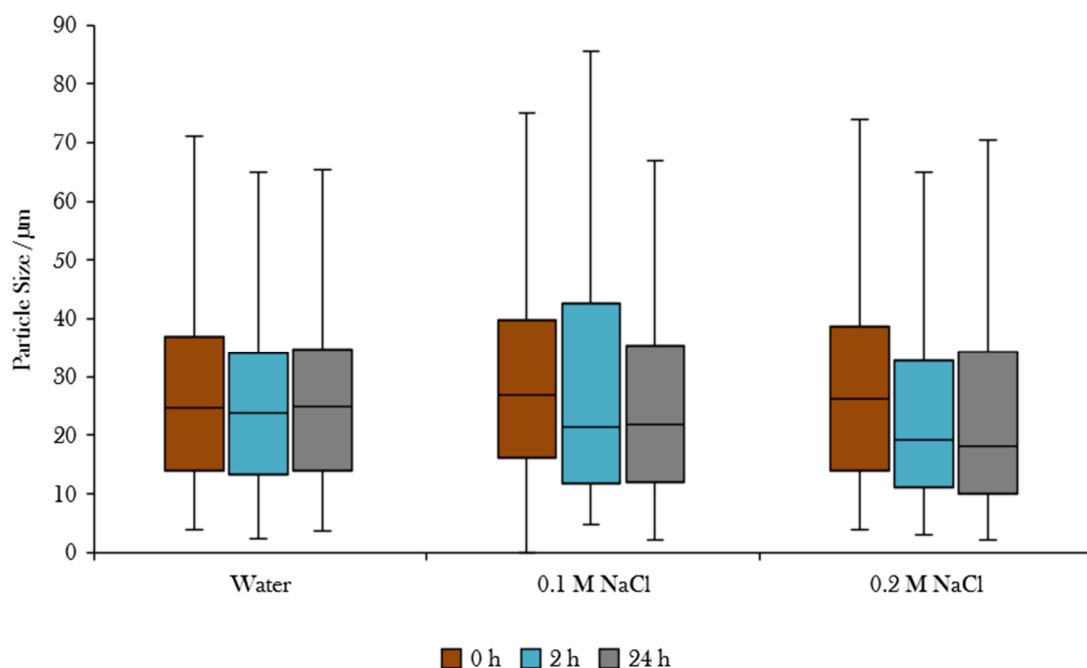


Figure 4.73. Influence of salinity (0, 0.1 M and 0.2 M NaCl) on microgel size during 24h of storage at 4 °C. The box represents the data lying within the IQR and the median is marked by a horizontal line. The whiskers outside the box indicate the range of data up to d(5) or d(95).

Few difference between samples immersed into water to the ones in salt solutions were observed (Figure 4.73). Microgel size was similar at time=0 h (~25-27 µm) for all samples, and remained constant for microgels dispersed into water. In contrast, after 2-24 h, particle size diminished for microgels immersed into salt solutions, down to 19 µm in 0.1 M NaCl and 16 µm for 0.2 M NaCl. Charge shielding of the ions might have also increased aggregation of the microgels, due to a possible smaller electrostatic repulsion. This was however not observed in our case.

Wang et al. showed that at increased salt concentrations (0.2-1 M NaCl), the gelatin microgel shrank within seconds to half their size, they worked however with gelatin microgels of lower polymer density (microgels prepared on porous CaCO₃ nanoparticles as templates) (A. Wang et al., 2012).

4.2.8.8 Stability of Microgels at 37 °C and in Simulated Gastric Fluid

The microgels were introduced for 2 h at 37 °C in either water or simulated gastric fluid (pH≈3) to test their stability under those conditions, simulating temperature and pH conditions of the gastric environment. Non-crosslinked microgels dissolved shortly after heating them to 37 °C (Figure 4.74). Gelatin liquefies at those temperatures, if not crosslinked sufficiently. The crosslinked microgels were crosslinked during 90 min at 30 °C. As it can be seen, increasing genipin concentration, increases the stability of the microgels at 37 °Cs and under acidic pH conditions. Microgels crosslinked with 1 mM genipin swelled at 37 °C, but remained stable, while at pH 3 in the SGF most of the microgel dissolved. At 5 mM genipin, the microgels remained stable under simulated gastric conditions. Crosslinking has thus an important impact on microgel stability under acidic conditions and at 37 °C.

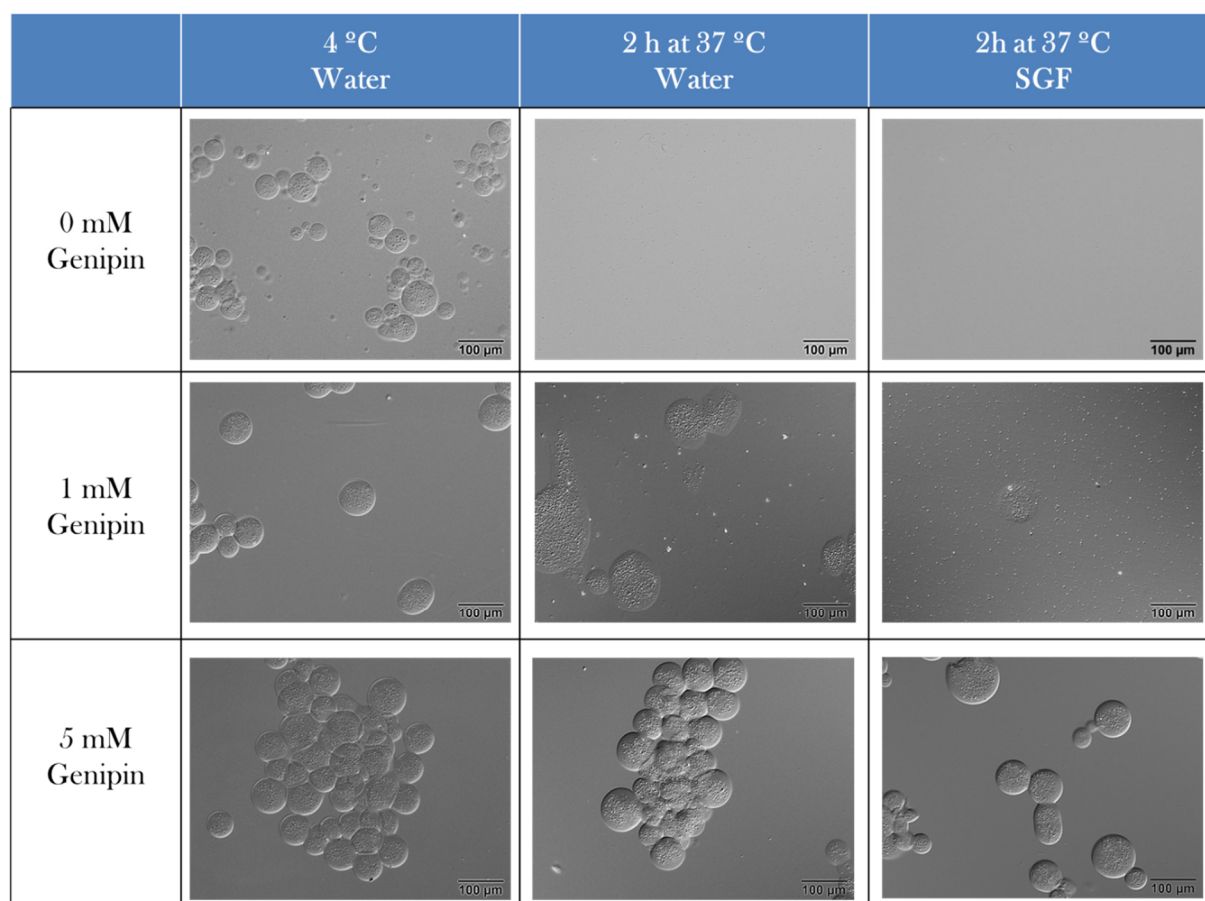


Figure 4.74. Stability of microgel crosslinked with various concentrations of genipin (crosslinking 90 min at 30 °C) , at 4 °C, dissolved in water, after 2 h at 37 °C in water and 2 h at 37 °C in simulated gastric fluid (SGF) at pH 3. Microgels tested in this experiment were loaded with enzymes. The internal structure observed inside the microgels is attributed to the presence of the enzyme (Figure 4.84 second part results).

4.3 Enzyme Encapsulation into Crosslinked Gelatin Microgels

The best method to encapsulate the enzyme into the microgels was studied. Four different encapsulation methods will be tested, as explained in further details in the experimental section:

- **Method Gen(E)/Enz(M):** Crosslinking the emulsion, forming microgels and adding the enzyme to the microgels in two ways:
 - b) Adding enzymes to a microgel suspension
 - c) Rehydrating freeze-dried microgels with an enzyme solution
- **Method Gen(E)/Enz(E):** Adding the enzyme and genipin during the emulsification process and then forming microgels
- **Method Gen(M)/Enz(E):** Adding the enzyme during the emulsification process, form microgels and crosslink microgels by mixing them with a genipin solution.

Of interest, when encapsulating enzyme is to get a high encapsulation yield and high activity recovery. This means, that a high percentage of enzyme added during the preparation of the microgels, remains inside the enzyme, and that a high proportion of them remain active.

The best method to quantify those two values would be to measure on one hand enzyme concentration in the supernatant and inside the microgels, and on the other hand enzyme activity in those two regions. Based on those values, encapsulation yield and activity recovery can be calculated.

In addition, we will label the enzyme fluorescently to be able to track its location inside the microgel suspension.

4.3.1 *Analyzing Enzyme Concentration, Activity and Location*

4.3.1.1 *Determination of Enzyme Concentration*

4.3.1.1.1 Protein Absorption at 280 nm

A common, simple method to quantify proteins in solution is to measure their UV-absorbance at 280 nm, which is a characteristic peak for amino acids with aromatic rings. A calibration curve of β -Gal enzyme in PEM buffer showed that its absorbance at 280 nm relates linearly to its concentration (Figure 4.75). This method might be thus adequate to quantify enzyme concentration in solution. However this method cannot be applied if the absorption of other molecules in solution overlap with the one of β -Gal at 280 nm. Our aim was to quantify the enzyme concentration in the supernatant of a microgel suspension, produced from a cooled-down gelatin-in-maltodextrin emulsion, into which enzyme was added. Polymers in the emulsion had however also strong UV-absorption at 280 nm (Figure 4.76), which made it impossible to use this method as assay for quantifying the enzyme in our system. As a consequence, the Bradford assay was tested as a possible assay to quantify β -Gal concentration in the microgel dispersions.

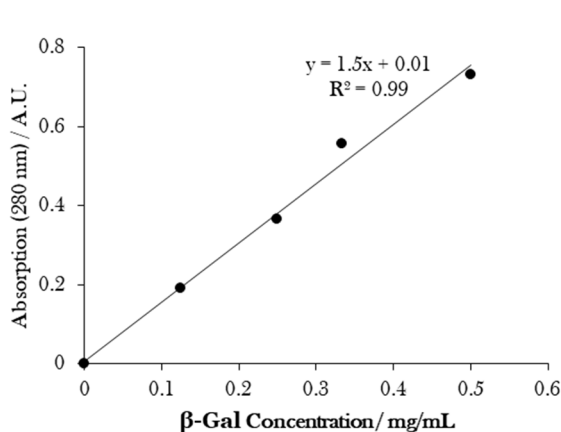


Figure 4.75. Calibration Curve of β -Gal enzyme concentration, quantified by UV-absorption measurement at 280 nm, in PEM buffer.

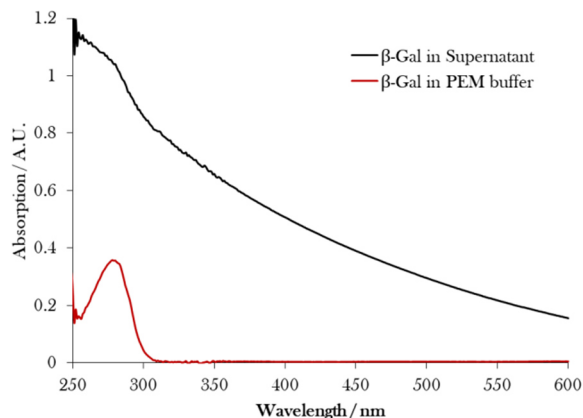


Figure 4.76. UV-absorption of enzyme at 280 nm overlaps with absorption bands of polymers in the supernatant of the gelatin microgels, after the first purification step.

Enzyme concentration was determined next with the Bradford Protein Assay, which is based on the absorbance peak shift from 465 to 595 nm, when Coomassie Brilliant Blue G-250 binds to proteins. First, its applicability was tested by measuring calibration curves of the standard protein Bovine Serum Albumin (BSA) and the enzyme β -Gal (Figure 4.77).

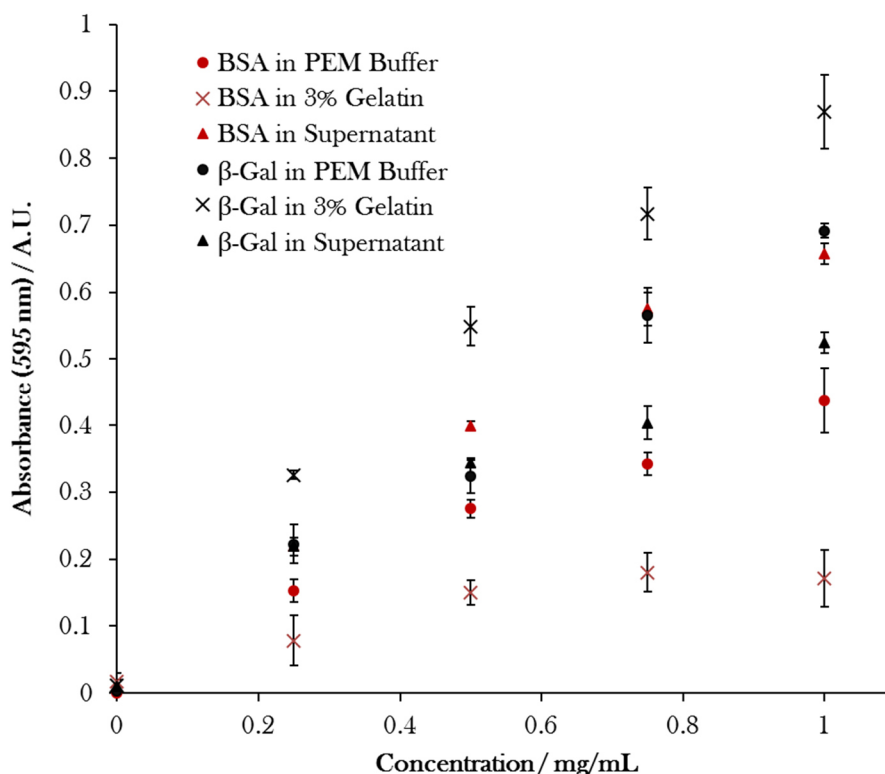


Figure 4.77. Calibration curve of the proteins BSA and β -Gal in three different solvents: PEM buffer, the supernatant of cooled down gelatin-in-maltodextrin emulsions, and 3 wt% gelatin.

Table 4.13. Assay data to determine protein concentration (y) from the absorbance at 595 nm (x). R² stands for the correlation coefficient of the linear regression.

| | β-Gal | BSA |
|--------------------|------------------------------------|------------------------------------|
| PEM Buffer | $y = 0.69x + 0.02$ $R^2 = 0.99$ | $y = 0.43x + 0.03$ $R^2 = 0.98$ |
| 3 % Gelatin | $y = 0.84x + 0.07$ $R^2 = 0.98$ | $y = 0.16x + 0.04$ $R^2 = 0.87$ |
| Supernatant | $y = 0.49x + 0.06$ $R^2 = 0.96$ | $y = 0.68x + 0.03$ $R^2 = 0.98$ |

The proteins were dissolved in the three different solvents, PEM buffer, supernatant and gelatin, which are the ones into which the enzymes are dissolved during encapsulation (Table 3.1): The PEM buffer is the solvent, in which the enzymes are dissolved before adding the enzyme to the emulsion/microgel and it's the solvent of the continuous medium of the purified microgel suspensions. The supernatant is the solution into which enzymes are dissolved after the first washing step of cooled down gelatin-in-maltodextrin emulsions, into which the enzyme was introduced. The 3 wt% gelatin solution is the solvent, corresponding to the gelatin microgels.

Usually BSA is used as a standard sample, from which concentration of protein solutions of unknown concentrations are determined. As it can be seen in Table 4.13 Figure 4.77, this does not hold true for the enzyme used in our assays, β-Gal. The calibration curves between the two proteins do not coincide, thus it explains that the assay, and thus the binding capacity of Coomassie Brilliant Blue G-250 to proteins depends on the nature of the functional groups in the protein. From Table 4.13 and the error bars in Figure 4.77 it can be seen that protein concentration determination in the gelatin microgels, will be difficult, as gelatin does also react with the Bradford reagent leading to some error in the measurements. In general, the composition of the solvent affects strongly the outcome of the assay. The other calibration curves are close to linear, with best linear fit for β-Gal in PEM buffer.

Therefore, the Bradford assay will be first tried on the encapsulation method Gen(E)/Enz(M) (Table 3.5), in which encapsulation yield can be calculated from enzyme quantification in solutions containing mainly PEM buffer, thus minimising sources of errors.

Enzymes were added to purified crosslinked (1 mM genipin) and non-crosslinked microgel suspensions dispersed in PEM buffer and stirred for 2 h. It was expected that some enzyme remain inside or on top of the microgels due to non-covalent interactions between the enzyme and the microgels. Total enzyme added to the microgels, and quantity remaining in the supernatants after purification by centrifugation, was determined with the Bradford assay. By subtracting the amount of enzyme in the supernatant from total enzyme added, the amount of enzyme remaining inside the microgel was calculated. The amount of enzyme inside the microgel could not be directly measured, as the Bradford assay reacts as well with gelatin, from which the microgels are made from (Table 4.13). Before making any analysis from the results obtained, or showing them, it has to be noted that unrealistic negative values were obtained for enzyme quantity remaining inside the crosslinked microgels. The experiment was repeated twice and the result remained the same. This indicates that some components in the solution of the supernatants of the microgels interfere with the Bradford assay leading to erroneous enzyme concentration measurements. The supernatant should theoretically only consist of PEM buffer and enzymes, as the microgel suspensions was purified twice, before addition of enzymes. Enzyme concentration measurement inside pure PEM buffer, did not seem to present a problem, as seen in Figure 4.77. Traces

of free genipin might have interfered with the assay, it is known that many of components have incompatibilities with the Bradford assay. Furthermore, genipin-crosslinked gelatin microgels absorb in the same region as stable Coomassie Brilliant Blue G-250 (Figure 4.15). Few microgels might have remained in the supernatant and contributed to absorption at 595 nm, the contribution would be however minimal: The supernatant got diluted 50-fold in the Coomassie Brilliant Blue G-250 solution, and within the supernatant a very low amount of crosslinked microgels might have been present.

Another error in this experimental method is the determination of total enzyme quantity. During the experimental process, enzyme might get lost by adsorption of protein to the glass wall. More correct would thus be to quantify total enzyme as the sum of enzyme in the supernatant and in the microgels. As commented above, enzyme can not be quantified inside the microgels, therefore enzyme activity measurements will be used to determine encapsulation yield.

By using appropriate control samples, in which no enzyme activity gets lost (free from genipin), the total enzyme activity in those control samples (sum of activity in supernatants and microgel) can be taken as a reference for subsequent calculations of encapsulation yield and activity recovery in treated samples (details in experimental section).

Therefore, the total enzyme activity for the different encapsulation methods was measured, to study the activity loss during the encapsulation process, due to interaction with genipin.

4.3.1.2 Enzyme Activity Measurement

Lactase activity was determined with the Ortho-Nitrophenyl- β -galactoside (ONPG) assay, which is based on the cleavage of ONPG into glucose and ortho-nitrophenol (ONP), which can be determined spectrophotometrically, by measuring absorbance at $\lambda=420\text{nm}$. Various dilutions of the enzyme stock solution in PEM buffer were tested and a linear relation between the enzyme activity and the absorption of ONP was found (Figure 4.78). The outcome of the measurement, thus the production of ONP, is time dependent, and the exact calculation to obtain enzyme activity can be found in the experimental section (equation 3.10). Those enzyme activity measurements can serve, not only to verify if the enzyme remains active, but also for quantifying total enzyme concentration, if activity loss under certain conditions is determined in preliminary experiments.

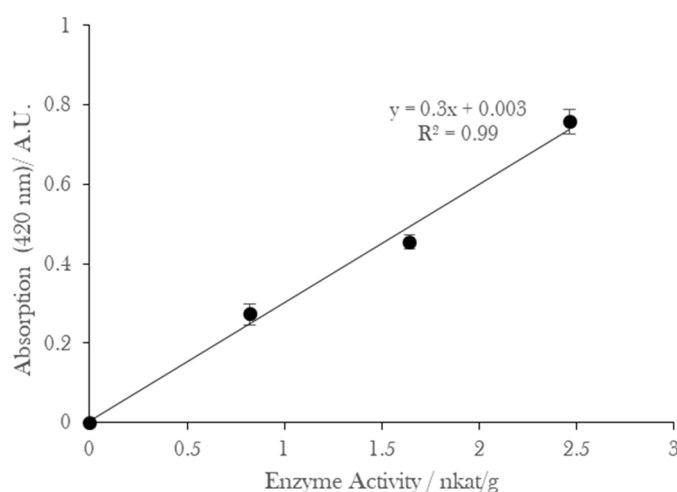


Figure 4.78. Calibration Curve of enzyme activity in PEM buffer, tested with the ONPG assay (10 min reaction time). The absorption of the product ONP is linearly proportional to enzyme activity.

4.3.1.3 Fluorescence Labelling of Lactase with FITC

To locate the enzyme lactase inside the microgel suspension, by microscopy, it was labelled by the fluorescent dye FITC. To test whether labelling was successful, the absorbance of the labelled enzyme was measured and the degree of labelling calculated. Figure 4.79 shows that the labelled lactase (Lactase-FITC) has characteristic peaks at 280 and 494 nm. 280 nm is the peak absorption for most proteins, and at 494 nm is the absorption peak of FITC. Based on those data and equation 3.12 the degree of labelling, which corresponds to the molar ratio between FITC and lactase, was calculated. It corresponded to 4.13, which means that in average 4.13 mol FITC is bound per mol lactase. The labelling was thus successful and can be used to study the location of the enzyme. The protein concentration of labelled lactase was calculated, using equation 3.11, and is 0.04 mM, corresponding to 4.8 mg/mL (molecular weight of lactase=117619 Da, data from manufacturer).

The purpose of labelling the enzyme was to get a qualitative understanding of the distribution of the enzyme. Furthermore, it has to be noted, that the labelling protocol implies dissolving the enzyme in a buffer at pH 10, which deactivated the enzyme. As a consequence activity measurements, can only be performed with non-labelled lactase.

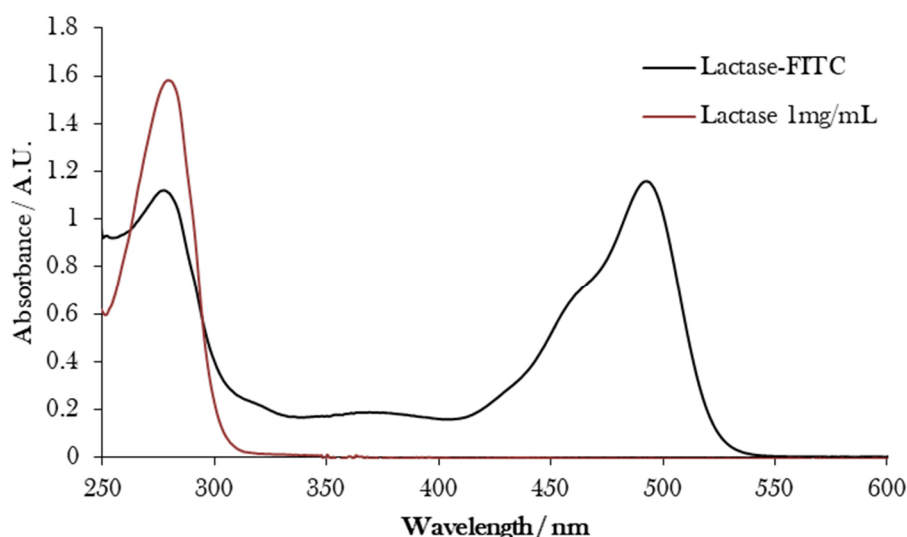


Figure 4.79. Absorbance spectra of labelled lactase (Lactase-FITC) and non-labelled lactase, used to determine the degree of labelling of Lactase-FITC.

4.3.2 Enzyme Compatibility with Crosslinker and Microgels

4.3.2.1 Enzyme Activity in Presence of Genipin and Gelatin

A challenge when introducing lactase into the microgels will be the compatibility of the enzyme with the other molecules. Of concern could be genipin, which acts as a crosslinker of amino groups and might thus create covalent bonds within the enzyme, producing a reduction in enzyme activity.

As an initial study, the enzyme was mixed during a period of 30 min at 37 °C inside solutions of PEM buffer containing up to 10 mM genipin and 10 wt% gelatin. The solutions/macrogels were stocked at 4 °C and their specific activity measured after 3 h (Figure 4.80).

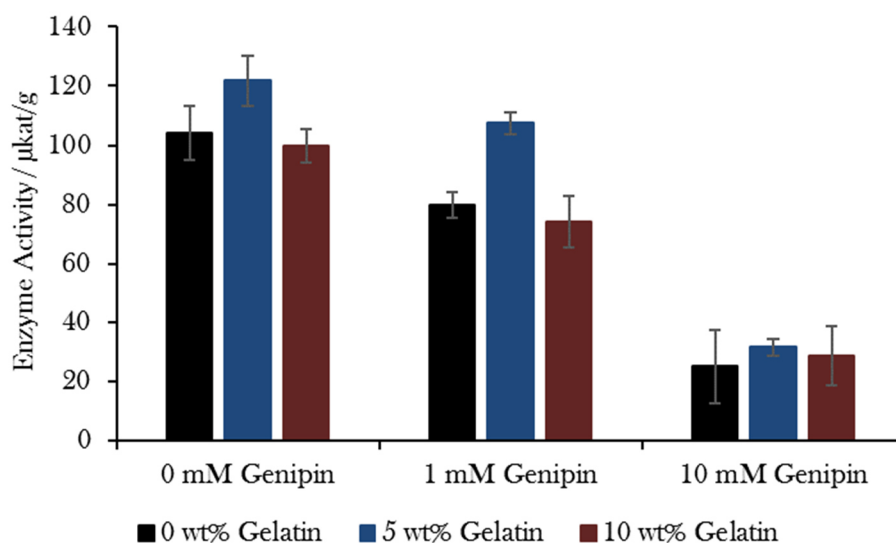


Figure 4.80. Influence of crosslinker genipin and continuous medium (Gelatin in PEM buffer) composition on enzyme activity. Components were stirred during 30 min at 37°C and stored 3h at 4°C, before measuring their activity.

Increasing genipin concentration lead to specific activity loss of the enzyme, from 104 µkat/g (0 mM genipin) to 25 µkat/g (10 mM genipin) if dissolved in PEM buffer. In solutions of 10 wt% gelatin, it was assumed, that genipin might react not only with the enzyme, but also with the amino groups of gelatin and thus reduce activity loss, compared to enzyme dissolved into PEM buffer free from gelatin. Contrary to the expectation, similar loss in activity were observed if β-Gal is dissolved in gelatin (Figure 4.80). Gelatin seemed however not to affect enzyme activity. As a consequence of those results, a compromise in crosslinking concentration has to be found in order, on one hand to assure sufficient crosslinking to obtain stable microgels, and on the other hand prevent activity loss of the enzyme in the presence of high crosslinker concentrations.

In order to avoid reaction between the enzyme with genipin, an option is to separate the crosslinking steps of gelatin from the encapsulation of the enzyme into the gelatin microgels.

4.3.2.2 Enzyme Activity in Suspension of Crosslinked Microgels

β-Gal was added to a suspension of microgel, either crosslinked with 10 mM genipin (crosslinking 20 min at 40 °C) or non-crosslinked and its activity compared to the case, of suspended into PEM buffer. Enzyme activity was followed during a period of 2 weeks (Figure 4.81). No activity decrease was measured, if the enzyme was added to the microgel suspensions. Independent, if they were crosslinked or not. It seems that free genipin was washed away during the purification process of the microgels or was entirely consumed during the crosslinking reaction with gelatin, and thus microgels crosslinked with 10 mM genipin do not affect enzyme activity.

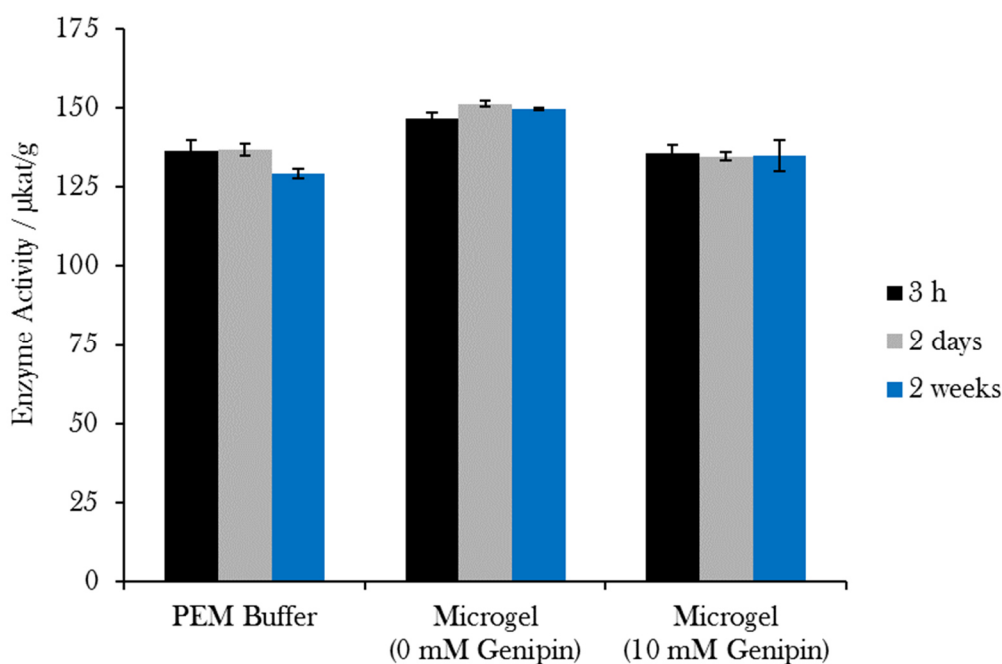


Figure 4.81. Enzyme activity in PEM buffer solutions free from microgel or containing non-crosslinked or crosslinked (10 mM Genipin) microgels.

4.3.3 Activity Loss of Enzymes during Encapsulation Process

Similar to the studies in section 4.3.2 the enzyme activity loss under the different encapsulation process methods was studied. Adding enzymes with an initial activity of 70 nkat/g to a genipin solution, without both gelatin and maltodextrin, affects its activity, as can be seen in Table 4.14 (free enzyme solution). Previously crosslinked microgel solutions (method Gen(E)/Enz(M)) did not affect enzyme activity negatively (Table 4.14), as the merely physical interactions between the enzymes and the microgels and low concentration of free genipin in solution, did probably lead to no or minor conformational changes of the enzyme. Those two results confirms the results obtained above (Figure 4.81).

Table 4.14. Enzyme activity (nkat/g) for the different preparation methods of enzyme-loaded microgels (based on 3% Gel / 20 % MD emulsions). In all samples, enzyme activity was 70 nkat/g, in absence of genipin. Crosslinking conditions: ¹ 30 min at 30°C, ² 60 min at 30°C, ³ 90 min at 30°C, ⁴ 180 min at 25 °C.

| | Free enzyme | Method Gen(E)/Enz(M) | Method Gen(E)/Enz(E) | Method Gen(M)/Enz(E) |
|---------------------|-----------------|----------------------|---|----------------------|
| 0 mM Genipin | 70 | 70 | 70 | 70 |
| 5 mM Genipin | 64 ³ | 69 ³ | 69 ¹ /67 ² /50 ³ | 63 ⁴ |

Crosslinking gelatin in presence of β -Gal (method Gen(E)/Enz(E) and Gen(M)/Enz(E)), lead to higher activity loss. This is illustrated by showing the influence of crosslinking time (30, 60 and 90 min) in method Gen(E)/Enz(E), which reduces the activity (69, 67 and 50 nkat/g, respectively). Supposedly, genipin did not only crosslink gelatin, but also reacted with the amino groups of the enzyme, creating intra- and inter-crosslinks between gelatin and β -Gal, which could have affected the enzyme.

Methods Gen(E)/Enz(M) and Gen(E)/Enz(E), the latter with 30 min crosslinking at 30°C, allow the maximum activity after addition of 5 mM genipin, achieving 69 nkat/g in both cases (Table 4.14). If the enzyme-loaded microgel was crosslinked, once formed (method Gen(M)/Enz(E), at 25 °C), the enzyme lost 10 % of its activity, from 70 to 63 nkat/g. In the case of methods Gen(E)/Enz(E) and Gen(M)/Enz(E) (addition of enzyme before microgel formation), one might assume that gelatin might have protected the enzyme, preventing genipin from reacting with the enzyme, and thus, preserving a relatively high activity.

Higher activity loss is observed when genipin reacts simultaneously with gelatin and the enzyme (down to 50 nkat/g for method Gen(E)/Enz(E) and 63 nkat/g for method Gen(M)/Enz(E)). In comparison, if genipin reacts only with the free enzyme, the activity is 64 nkat/g. The difference might be due to intercrosslinks between gelatin and the enzyme, in addition to intracrosslinks in the enzyme. Both types of crosslinking could affect the enzyme active site and thus reduce enzyme activity. In any case, covalent crosslinking is supposed to be needed, in order to prevent an early desorption of the enzyme, since enzymes loosely adsorbed to the microgels might be easily released, as described in previous studies (Schachschal et al., 2011).

4.3.4 Encapsulation Yield and Activity Recovery of different Encapsulation Methods

4.3.4.1 Addition of enzyme after microgel formation (Method Gen(E)/Enz(M)):

4.3.4.1.1 Adding enzymes to a microgel suspension:

Enzyme was added to the 0°C cold PEM buffer, in the last step of microgel production, the dilution of cooled-down emulsions. The solution was consequently stirred with a magnet during 3h at 25 °C. After washing twice the microgel suspension, 10 % of initially added enzyme remained in non-crosslinked and 7 % in crosslinked (5 mM Genipin) microgel suspensions (Table 4.15). Lower amount of enzyme associated the microgels, may be caused by the fact that crosslinking reduces mesh size of polymer network and lowers number of charged groups, which contribute to attraction of the enzyme to the microgel.

Table 4.15. Encapsulation yield for Method Gen(E)/Enz(M). ¹Crosslinking during 90 min at 30°C

| | Method Gen(E)/Enz(M) |
|--------------|-------------------------|
| 0 mM Genipin | 10 % |
| 5 mM Genipin | 7 % ¹ |

To verify where the enzymes are located, whether they penetrated the microgels or just adsorb on its surface, the same encapsulation method was applied, using labelled enzyme (Lactase-FITC) (Figure 4.82).

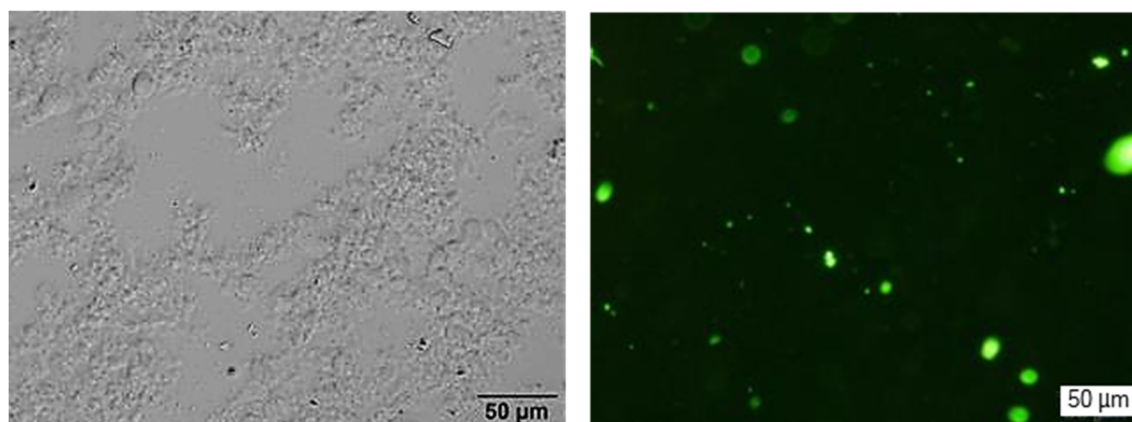


Figure 4.82. Optical microscopy images of microgels, produced in 3% Gel / 20% MD emulsion, with labelled enzyme in absence of genipin. If labelled enzyme was added after microgel formation no enzyme could be observed to penetrate the microgels, nor was a higher fluorescent intensity observed on the surface of the microgels. Green spots in the image origin probably from insoluble FITC particles, which can also be observed in the microscopy image on the left.

It was observed that enzymes did neither penetrate nor adsorb to the microgels. The enzyme seemed to be equally distributed in the microgel suspension, leading to the conclusion that adding the enzyme to already formed microgels, does not lead to sufficient strong interaction between the particle and the enzyme, to produce high encapsulation/adsorption rates. Most of the enzyme was probably loosely associated to the microgels and would have been removed with several additional washing steps.

4.3.4.1.2 Rehydrating freeze-dried microgels with an enzyme solution

A variation of this method, which might be more successful is freeze drying first the microgels and mixing the powder with the enzyme solution in PEM buffer. The dried gelatin microgels, when rehydrating may act like a sponge, entrapping the enzyme into them by the “breathing-in” technique, which has been used previously to entrap solutes in hydrogel networks (Nolan et al., 2006). This technique was tried with freeze-dried crosslinked microgels (0.1 mM Genipin, crosslinked 30 min at 40 °C).

After mixing the freeze-dried microgels during 2 h at 0 °C with the enzyme solution, the suspension was centrifuged and redispersed into fresh buffer solution twice. The enzyme activity in the continuous phases after washing and inside the microgels was determined and resulted that surprisingly only 3 % of enzyme remained associated to the microgels. Due to the low encapsulation yield this encapsulation method was not studied in further details. The reason for the low amount of enzyme associated to the microgels may be that despite a possible sponge-like absorption of microgels during rehydration, no chemical interactions were strong enough to retain the enzyme associated to gelatin matrix of the microgel. Freeze-drying might have affected conformational changes in the polymer, which reduced interaction between the enzyme and the microgel.

4.3.4.2 Addition of the enzyme together with the gelatin solution

Enzyme was mixed during 3 h at 35 °C with the gelatin solution, to allow the enzyme to form bonds with gelatin, before formation of the emulsion with maltodextrin. Using this method, thus addition of the enzyme in the early stages of the microgel preparation, lead to higher encapsulation yields (Table 4.16), compared to the previous method.

Table 4.16. Encapsulation yield for the two different encapsulation methods, when adding the enzyme together with the gelatin solution into the emulsions. ¹Crosslinking during 90 min at 30°C ²Crosslinking during 180 min at 25 °C.

| | Method Gen(E)/Enz(E) | Method Gen(M)/Enz(E) |
|--------------|-------------------------|-------------------------|
| 0 mM Genipin | 16 % | 13 % |
| 5 mM Genipin | 64 % ¹ | 19 % ² |

This was also illustrated by fluorescently marking the enzyme and tracking its position after encapsulation. A big amount of the FITC-marked lactase localised inside the microgels, as shown in Figure 4.83. After one month enzymes remained inside the microgel, as can be shown with the fluorescently marked enzymes (Figure 4.83). More detailed results on long-term stability of the enzyme inside microgels are shown in next section.

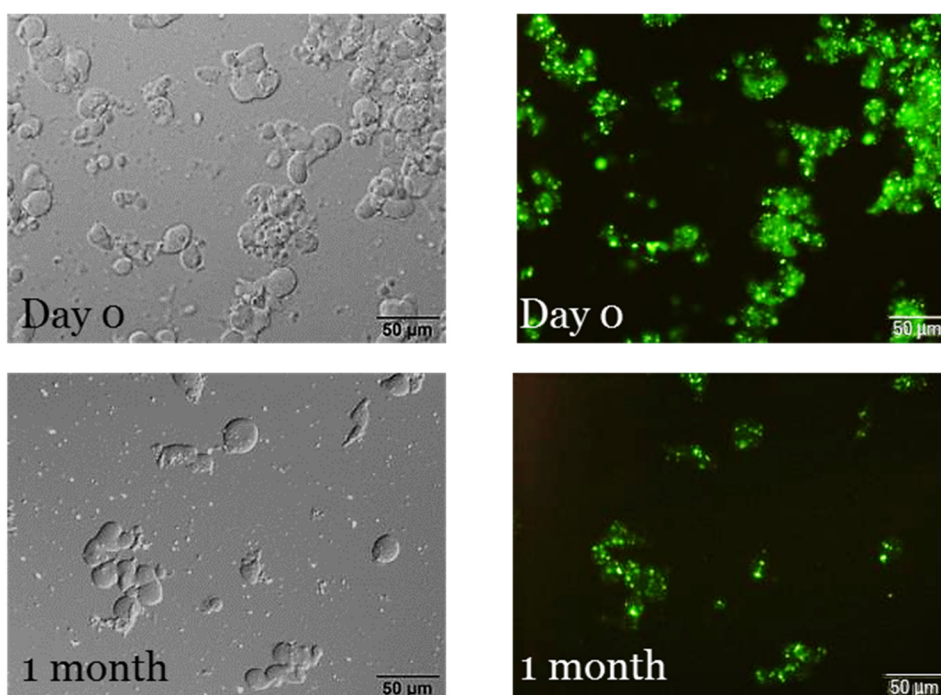


Figure 4.83. Location of labelled β -Gal inside the non-crosslinked microgel suspension, when added to gelatin, before emulsification. After purification of the samples, it is observed that the enzyme was encapsulated into the microgels and remained there for a period of at least 1 month.

Moreover, the presence of enzymes could be observed from the microstructure of the microgels. Black particles, normally not present in enzyme-free microgels, can be observed inside the enzyme-loaded microgels (Figure 4.84). Those origin probably form aggregates of the enzyme, as single β -Gal enzymes have an approximate diameter of 14 nm.

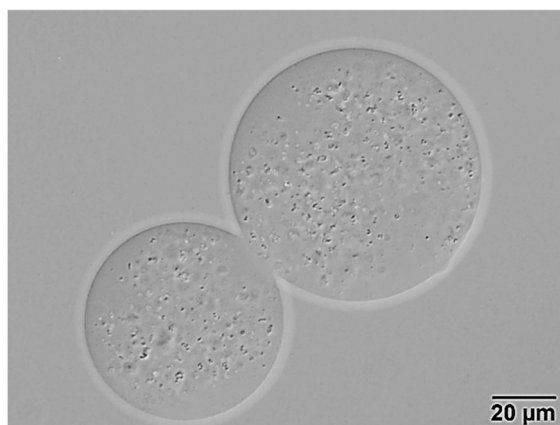


Figure 4.84. The presence of enzymes inside the microgels, could be observed from the microstructure of microgels. The black particles inside the microgels origin from the enzyme solution.

To increase enzyme retention inside the microgels, they were crosslinked by the two different methods (Method Gen(E)/Enz(E) and Gen(M)/Enz(E)). Results (Table 4.16) indicated that crosslinking during emulsification (Method Gen(E)/Enz(E)) achieved the highest encapsulation yield (64 %). In contrast, if the microgels were crosslinked after encapsulation of the enzyme (Method Gen(M)/Enz(E)), encapsulation yield was lower (19 %). Non-covalently associated enzymes might dissociate from the microgels into the aqueous surrounding medium, in which it is soluble, during the crosslinking process (3 h stirring at 25 °C). In both crosslinking methods (Gen(E) and Gen(M)) crosslinking increased encapsulation yield of the enzyme, compared to the same preparation procedure without genipin: 64 % vs. 16 % for crosslinking during the emulsification process and 19 % vs. 13 % for crosslinking of gelatin after microgel formation.

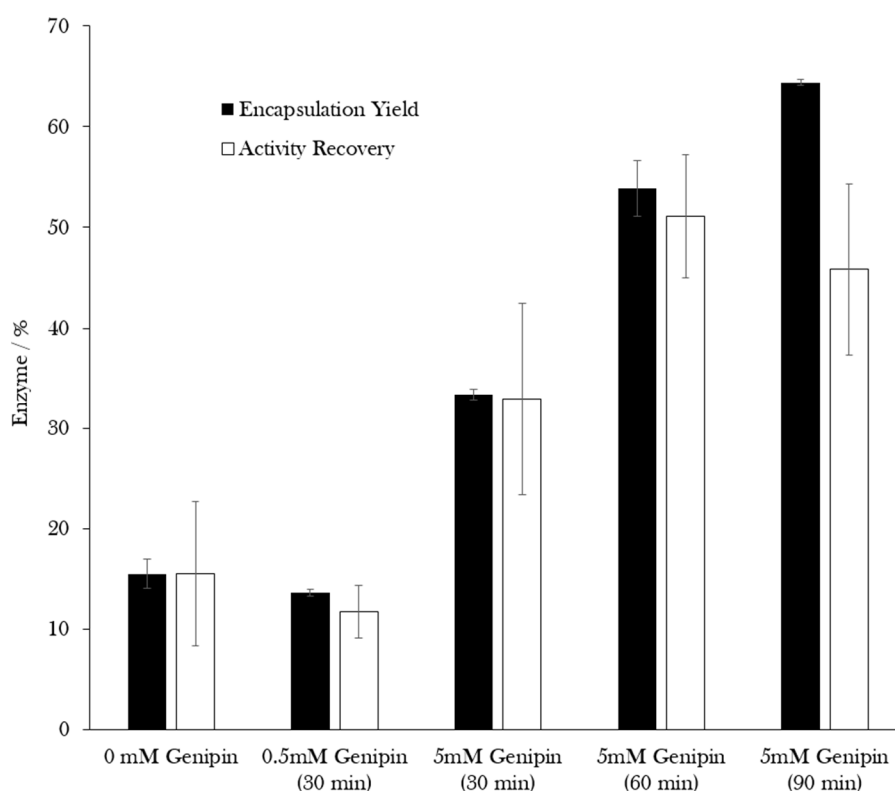


Figure 4.85. Encapsulation yield and activity recovery of enzymes encapsulated under varying crosslinking conditions. The microgels were prepared by method Gen(E)/Enz(E).

The influence of amount of crosslinking on encapsulation yield was tested for Method Gen(E)/Enz(E), the method with the highest encapsulation yields. As expected, with higher crosslinking concentration and time, bigger amounts of enzymes could be incorporated into the microgels (Figure 4.85). These results can be attributed to the fact that crosslinking might decrease the mesh size of the polymer network from where enzymes might diffuse into the aqueous surrounding medium. Furthermore, genipin might covalently link β -gal to the microgels, increasing retention within the particles.

Despite higher encapsulation yields at higher crosslinking concentrations, it has to be considered that not only high encapsulation yield is of interest, but especially high activity recovery. Thus that the portion of enzyme remaining encapsulated has the highest activity. Higher genipin concentrations/crosslinking times, which lead to higher encapsulation yields, lead however as well to increased deactivation of the enzyme (Table 4.14). The percentage of active enzyme remaining inside the microgels, the activity recovery, was calculated for the different conditions and are shown in Figure 4.85. Microgels crosslinked with 5 mM genipin during 1 h had the highest activity recovery (51 %). As a conclusion, from all tested encapsulation methods, these condition are the optimal to get a high activity recovery. Besides the high activity recovery, the interest is that the enzyme remains inside the microgels over a prolonged period of time and that the microgel protects it from harsh environmental factors.

4.3.5 Enzyme Long-Term Stability in Microgels

Of interest is the storage stability of the enzyme-loaded microgels in the fridge at 4 °C. Therefore, activity of a selection of crosslinked enzyme-loaded microgel suspensions was followed for a period of 1 month (Figure 4.86). Enzyme activity remained stable over this period, under both conditions, crosslinking with 5 mM genipin during 30 and 90 min. This means that no component inside those solutions was harmful for the enzyme.

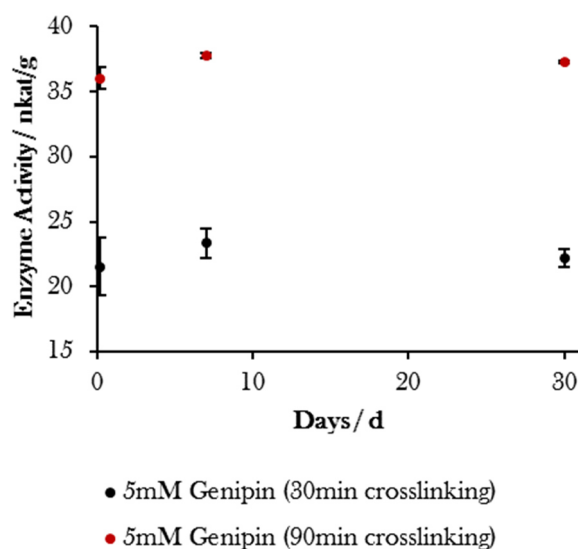


Figure 4.86. Enzyme activity of enzyme-loaded crosslinked microgel suspension during a period of 1 month. The solutions were stored in the fridge at 4 °C.

In Figure 4.83 it was seen, using fluorescently labelled lactase that after 1 month the enzyme remained within the microgel. Of interest is to know the amount of enzyme remaining inside the microgel and how much diffused in this time period out of the microgels. A detailed study was performed after 1 week storage for various amounts of crosslinking conditions. After 1 week storage at 4 °C, the microgel solutions were centrifuged and the enzyme activities in the supernatant and within the microgels were measured. Results indicated that fewer enzymes were released from the stronger crosslinked microgels (Figure 4.87), with 88 % of enzymes remaining within the microgels for crosslinking them 90 min with 5 mM genipin (Method Gen(E)/Enz(E)). If the microgels were not crosslinked fewer than 50 % of the enzyme remained in the microgels. Those results go in line with afore-mentioned explanations that crosslinking retains the enzyme within the gelatin microgels due to covalent crosslinking to the delivery vehicle and reduced pore sizes of crosslinked microgels. One method to prevent enzyme diffusion out of the microgels, which happens during storage in solution, may be to freeze-dry the enzyme-loaded microgels, which was tested in next section.

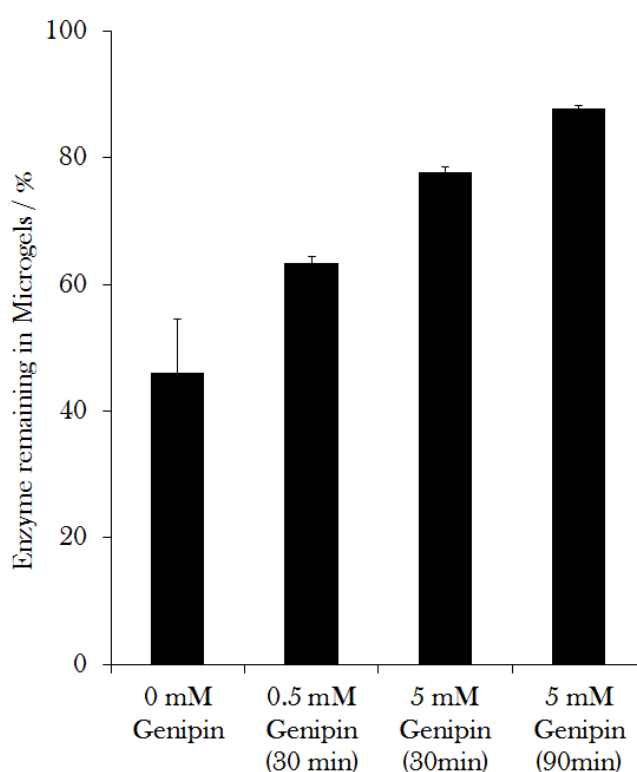


Figure 4.87. Enzymes remaining in microgels after 1 week dispersed in water at 4°C. The microgels were prepared by method Gen(E)/Enz(E).

4.3.6 Freeze-Drying and Rehydration of Enzyme-Loaded Microgels

To prevent enzyme diffusion out of the microgels, which happens during storage in solution, enzyme-loaded microgels were freeze-dried. After their freeze drying, they were redispersed into the same amount of solvent and their activity compared to before freeze-drying (Figure 4.88).

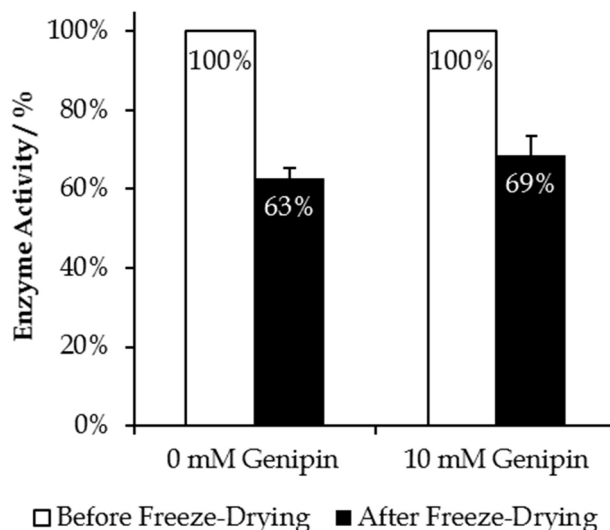


Figure 4.88. Enzyme activity after freeze-drying and rehydration, compared to the activity before freeze-drying. Crosslinked (10 mM genipin) and non-crosslinked microgels were tested.

The freeze-drying process leads to some deformation of the microgel network, which can induce irreversible conformational changes in the protein structure, which in turn may lead to reduction of enzyme activity. The microgel, after rehydrating, took again the same morphology, as before freeze-drying (Figure 4.59). Freeze-drying affected enzyme activity, which was measured after rehydrating the dry microgels. 37 % of activity was lost for non-crosslinked and 31 % for crosslinked (10 mM Genipin, 90 min crosslinking) microgels (Figure 4.88). Similar amounts of enzyme (laccase) activity were lost in PNIPAAm microgels (Schachschal et al., 2011) or in other studies for free enzyme (Amid, Manap, & Zohdi, 2014; Sawada & Akiyoshi, 2010). Low temperature stress, dehydration stress, ice crystal formation or deformation of the microgel network, which can induce irreversible conformational changes in the protein structure are factors, which have been shown to deactivate and destabilize the enzyme during freeze-drying (Arakawa, Prestrelski, Kenney, & Carpenter, 2001).

Nevertheless this activity loss can be tolerated, considering that, if stored in liquid suspension, up to 50 % of enzyme was lost due to diffusion out of the microgels (Figure 4.87). Keeping the microgels as a freeze-dried powder may be therefore be a better option, allowing them to be kept over a prolonged period without enzyme loss or microbial growth in the solution.

4.3.7 Enzyme stability under simulated gastric pH and body temperature conditions

The influence of mixing ratios of microgels, dispersed in water or in PEM buffer, with SGF can be found in Table 4.17.

Table 4.17. pH of simulated gastric fluid (SGF), PEM buffer, water and mixtures of microgels dispersed in water or PEM buffer with SGF. Measured at 25 °C.

| Solvent | pH |
|-----------------------------|-----|
| SGF | 3.0 |
| PEM | 6.5 |
| Water | 6.4 |
| Microgel (PEM):SGF (1:5) | 6.4 |
| Microgel (PEM):SGF (1:10) | 5.8 |
| Microgel (PEM):SGF (1:25) | 5.7 |
| Microgel (Water):SGF (1:5) | 3.8 |
| Microgel (Water):SGF (1:10) | 3.3 |
| Microgel (Water):SGF (1:25) | 3.2 |

The stability of the enzyme-loaded microgels in SGF (1:10 dilution ratios) was investigated by suspending them into SGF (pH 3) at 37 °C, during 120 min, which is the recommended time for digestion. (Minekus et al., 2014) Two distinct microgel dispersions were used therefore: First, microgels dispersed in water (final pH of the mixture with SGF was ≈ 3.3 .) and second, microgels dispersed in PEM buffer (final pH of the mixture with SGF was ≈ 5.8).

In the first case (pH ≈ 3.3), free and encapsulated β -Gal enzyme were introduced into SGF and their activity tested directly after mixing. Microgels, prepared with method Gen(E)(Enz(E) with crosslinking concentrations up to 20 mM genipin, were tested. For both, free and encapsulated enzymes, the enzyme became instantaneously deactivated after few seconds. The time between mixing the microgels with SGF, taking the sample and reacting it with the ONPG-solution was sufficient to deactivate the enzyme. Encapsulating the enzyme into the microgels did not protect it from direct deactivation under low pH conditions. Increasing crosslinker concentration up to 20 mM genipin did not either. The pH of the solutions were raised to pH 6.5 with a NaOH solution, to verify whether the pH-mediated deactivation of the enzyme is reversible. Adaptation of the pH did however not lead to reactivation of β -Gal activity.

In the second case, when microgels were dispersed in PEM buffer and diluted into SGF at a ratio 1:10, (pH ≈ 5.8), activity decreased sharply over the 120 min and final activity, compared to the activity at time = 0 min, was 6 % for the microgels with 0 and 5 mM genipin, 3 % for the microgels crosslinked with 10 mM genipin and 1 % for the free enzyme (Figure 4.89).

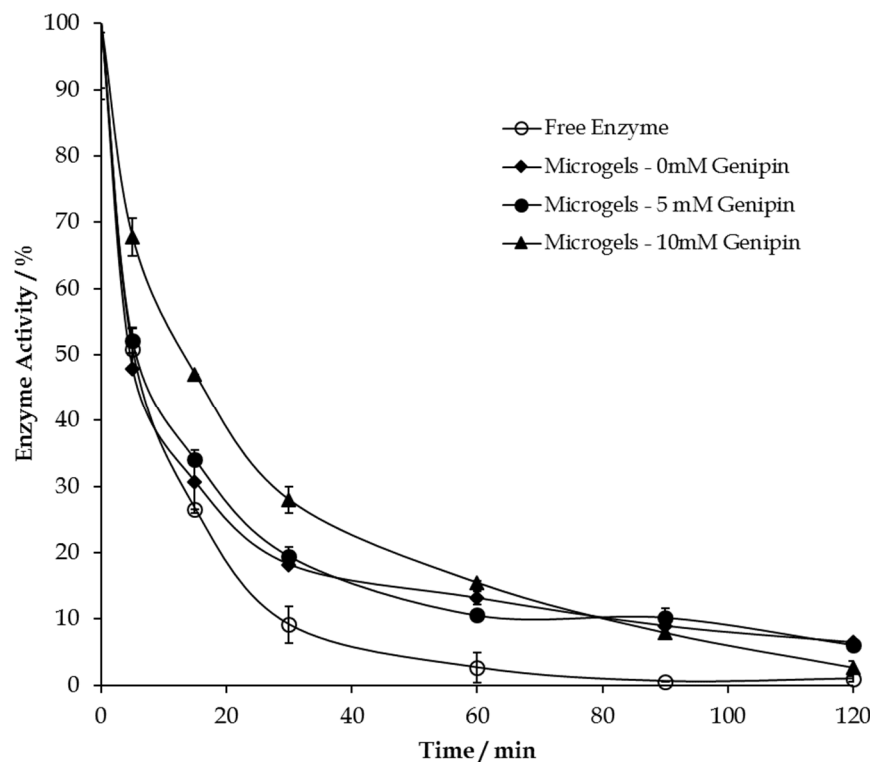


Figure 4.89. β -Gal Enzyme activity at $\text{pH} \approx 5.8$ and 37°C . Free enzyme rapidly lost activity. Encapsulating the enzyme inside the microgels allows having a higher enzyme activity.

Kinetics of enzyme deactivation was however slower in the crosslinked microgels compared to the free enzyme. Time till enzyme activity reached 50 % after 5 min for the free enzyme and after 14 min for the samples crosslinked with 10 mM genipin. Moreover, it took 17 min for the free enzyme and 37 min for the crosslinked microgels (10 mM) to reach 25 % of enzyme activity. Those results indicate that encapsulating the enzyme into the microgel, conveys a protective effect for the enzyme, as higher activity is retained after 120 min. Encapsulating could however not prevent activity diminution under those conditions, as the crosslinked gelatin network might allow diffusion of protons or other electrolytes into microgel particles, which might harm the enzyme. Figure 3.2 shows the activity profile of the enzyme at various pH conditions and indicates that at pH 5.8 enzyme activity is strongly (70 %) diminished, compared to its pH optimum at pH 6.5.

On the other hand, crosslinking promoted stability of the microgels under those conditions. Non-crosslinked microgels become mainly dissolved after 120 min, whereas the crosslinked microgels did remain stable under those conditions (Figure 4.90).

Those results show that there are serious limitations in using microgels as protective delivery vehicles of enzymes in acidic pH conditions. Mesh size of microgels are 5-500 nm (Z. Zhang, Zhang, Chen, Tong, & McClements, 2015), even if crosslinking the polymer or coating them with biopolymer layers (Srivastava, Brown, Zhu, & McShane, 2005; Taqieddin & Amiji, 2004). With this pore size, the small hydrogen ions (H^+) can easily diffuse through the polymer network into the microgels, inducing enzyme deactivation.

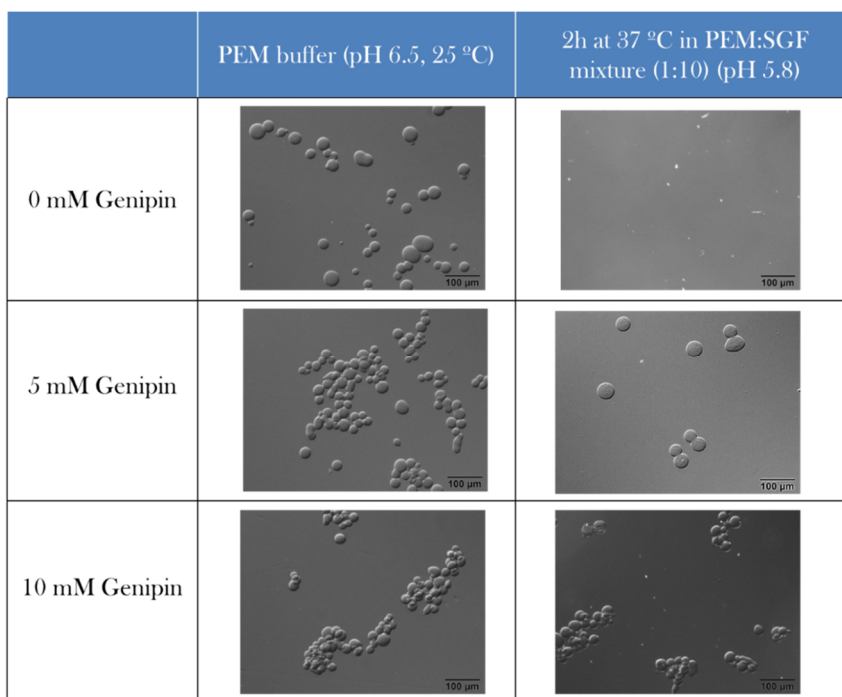


Figure 4.90. Optical microscopy images of non-sonicated microgels, prepared in a 3% Gel / 20% MD emulsion. Crosslinking gelatin microgels, with genipin, provide stability at 37°C and pH 5.8 to the microgels. Non-crosslinked gelatin microgels dissolve under those conditions.

Besides this, *in vivo* digestive enzymes and mechanical forces during digestion can further affect microgel and enzyme integrity. As commented in the introduction, many other approaches were tested to encapsulate lactase and make them resistant to acidic environments, but most of them were unsuccessful (Jin et al., 2008; Nichele et al., 2011). Only few studies managed to form protective immobilisation environments for lactase, such as alginate-carboxymethyl cellulose gels (Mai et al., 2013) or chocolate-coated agarose carriers (Nussinovitch et al., 2012). An elegant approach was used by Zhang et al., in which they co-encapsulated with magnesium hydroxide ($\text{Mg}(\text{OH})_2$), a basic buffer, inside carrageenan-based hydrogel beads (Z. Zhang et al., 2017). $\text{Mg}(\text{OH})_2$ is insoluble at neutral and basic pH values, but soluble at acidic pH values. The hydrogel beads, when dispersed into an acidic solution, kept a close to neutral internal pH for an extended period.

Another approach could be to use acid-resistant lactase, extracted from fungi, which have a pH optimum between 3.5 and 4 (Saqib et al., 2017). However, the challenge using those types of lactase is that in the intestinal environment, where lactose should be digested, the pH lies at around pH 7, which deactivates the enzymes.

Taking into consideration that our enzyme-loaded microgels are not suitable as protective agents under acidic environment, those results at pH 5.8 and 37 °C (Figure 4.89) should be considered as preliminary results for the possible use of those β -Gal-loaded microgels in e.g. industrial production of lactose-hydrolyzed milk, which has similar pH and temperature conditions. (Grosová et al., 2008) This application is of a great interest according to the annual growth rate of lactose-free products worldwide.

Chapter 5
CONCLUSIONS

5 Conclusions

NaCMC/BSA System

- The phase behaviour of Sodium carboxymethylcellulose (NaCMC) / Bovine Serum Albumin (BSA) mixtures at 25 °C and pH 13 was studied. At high biopolymer concentrations, segregative phase separation into two liquid phases was observed.
- NaCMC/BSA emulsions were formed and were shown to be kinetically stable over long periods of times (observed up to 20 days), if stored at 4°C. Under those conditions, viscosity is higher, reducing coalescence of emulsion droplets. Electrostatic repulsion between the negatively charged NaCMC droplets could have also improved colloidal stability.
- The crosslinking capabilities of the bivalent Ca^{2+} or trivalent Al^{3+} and Fe^{3+} ions were tested for NaCMC, BSA and NaCMC-in-BSA emulsions. Ca^{2+} could selectively crosslink NaCMC, while the trivalent ions crosslinked both components, NaCMC and BSA.
- Crosslinking time controlled whether NaCMC beads (with a gelled interior) or capsules (with a liquid interior) were obtained. This was due to diffusion of the crosslinking ions from the external medium to the interior, thus obtaining beads at longer crosslinking times.
- NaCMC-in-BSA emulsions were crosslinked with trivalent Al^{3+} and Fe^{3+} ions, to obtain gelled capsules with W/W emulsions in its interior (denoted as encapsulated emulsions). It can be regarded as a form of multiple emulsion. These particles may be interesting as delivery vehicles, due to their double protection capabilities, by the two polymers: BSA beads containing NaCMC droplets in the core, which could be loaded with an active component.
- Freeze-drying of encapsulated emulsions lead to particles with pores, whose size corresponded to that of the emulsion droplets. Therefore, the emulsion droplets template the formation of macropores inside the beads.
- The size of the encapsulated emulsions was reduced by electro spraying the emulsions into the crosslinker solution. Beads of the size down to 600 μm were obtained with this technique.
- Encapsulated Al^{3+} -crosslinked NaCMC/BSA emulsions remained stable under pH conditions simulating the passage from food, to the gastric and finally intestinal pH environment.
- Different methods of immobilising the enzyme lactase into the encapsulated Al^{3+} -crosslinked NaCMC/BSA emulsions have been studied, and it was concluded that the crosslinker solution (pH 2.8-3.5) and the emulsion (pH 11-13) have pH conditions unfavourable for the enzyme.

Gelatin/Maltodextrin System

- The detailed phase behaviour of water/gelatin/maltodextrin mixtures at 50 °C was analysed. Four distinct regions could be found, depending on concentration of polymer components: L: One liquid phase, L+S: One liquid and a solid phase, L₁+L₂: Two liquid phases and finally L₁+L₂+S: Two liquid phases coexisting with a solid phase.
- The solid formed at the interphase between both liquid phases and gradually sedimented to the bottom of the sample. It was analysed by Raman spectroscopy and it was found that the solid is composed of either maltodextrin or a mixture of maltodextrin and gelatin, depending on the composition of the gelatin/maltodextrin mixture.
- Gelatin-in-maltodextrin, maltodextrin-in-gelatin and bicontinuous emulsions were obtained.
- Multiple emulsions were also formed by secondary phase separation inside the already formed droplets. Three factors affected their formation: rate of cooling of the emulsion, the concentration distance to the binodal line and the nature of the dispersed phase.
- Microgels were formed from gelatin-in-maltodextrin emulsions by gelling and crosslinking the dispersed gelatin droplets with genipin. They were successfully purified by centrifugation and resuspension in water.
- Higher stirring speeds and temperatures, and preparation of the emulsions in a PEM buffer reduced the microgel particle size. Microgels down to 6 µm could be prepared and maintained their particle size during a period of at least 1 month at 4 °C. Moreover, qualitative observations by optical microscopy had shown that crosslinked microgel suspensions could remain stable at least during ≈500 days, if kept at 4°C.
- Swelling of the gelatin microgels was observed for pH conditions at pH values different from the isoelectric point of gelatin (pI≈4.7-5). Higher ionic strengths reduced microgel size.
- The stability of microgels under simulated gastric temperature and pH conditions was tested, and it was shown that crosslinking increases the stability of the microgels at pH 2 and 37 °C, while non-crosslinked microgels dissolved under those conditions.
- Microgel freeze-drying lead to deformation to a leaf-like morphology and macropores of few micrometers. It was shown that microgels, despite their deformation in the dried form, regained their original morphology after rehydration.
- The lactase enzyme was localised inside the microgels, by labelling the enzyme with the fluorescent dye FITC.
- Enzyme encapsulation yield into the microgels reached a maximum of 64 %. Encapsulation yield increased with crosslinking degree. These conditions lead however also to the highest activity loss, due to direct contact between genipin and the enzyme, which partly deactivated

the enzyme. Considering the activity loss, the highest activity recovery (51 %), which corresponds to active enzyme remaining inside the microgels, was achieved for microgels crosslinked with 5 mM genipin during 1h at 30 °C.

- Total enzyme activity in the microgel suspension remained almost constant for at least 1 month, if stored at 4°C.
- Crosslinking reduces diffusion of enzyme out of the microgels. Non-crosslinked microgels maintained 50 % of encapsulated enzyme, after one week, whereas crosslinked microgels were able to retain up to 90 % of enzyme.
- After freeze-drying the enzyme-loaded microgels, ~65 % of original enzyme activity could be maintained. Keeping the delivery vehicle in a dried state has the advantage to minimise enzyme loss due to diffusion out of the microgel, and may avoid microbial growth.
- Enzyme-loaded crosslinked gelatin microgels were not able to keep the enzyme active under simulated gastric fluid temperature and pH conditions (37 °C, pH 3). The polymer network was probably not a sufficient barrier against proton diffusion, leading to deactivation of the enzyme.
- However, crosslinked microgels have some protective effect on enzyme activity at pH 5.8 and 37 °C. After 30 min only 10 % of free enzyme remains active, while activity increases to 30 %, if the enzyme is immobilised into the crosslinked microgel. This can be considered as a preliminary result for the use of those β -Gal-loaded microgels in e.g. industrial production of lactose-hydrolyzed milk, which has similar pH and temperature conditions.

Chapter 6

RECOMMENDATIONS FOR
FUTURE RESEARCH

6 Recommendations for Future Research

In this Thesis two systems were studied. In the first one, the NaCMC/BSA mixture, emulsions were obtained, which were crosslinked with trivalent ions, Fe^{3+} and Al^{3+} to obtain gelled beads containing encapsulated emulsions. Those beads showed stability under acidic and neutral pH conditions found in food, the gastric and intestinal regions.

In the second system, gelatin/maltodextrin W/W emulsions were obtained and their properties analyzed. Those emulsions were used as templates for formation of genipin-crosslinked gelatin microgels, into which the enzyme lactase was encapsulated with a good encapsulation yield and enzyme activity. The enzyme-loaded microgels could be stored over long periods of time, without losing activity. The results suggest that these microgels could be eventually used as enzyme immobilizer in industrial lactase-free milk production.

For possible future continuation of the research, the following recommendations are given.

General recommendations

- Obtain higher colloidal stability of W/W emulsions, by for example using particles as stabilizers (Pickering emulsions).
- Achieve precise control of droplet size obtained from W/W emulsions (for instance W/W nano-emulsions have not been described yet in the literature).
- Study in details interfacial properties of W/W emulsions, which are distinct to conventional W/O interphases.
- Form microgels with biopolymers able to protect labile molecules in unfavorable pH conditions.
- Study the use of W/W emulsions and microgels for applications in food formulation (low calorie food and beverage products), enhancing food texture.

Specific Recommendations

1. NaCMC/BSA Emulsion System

- Study chemical crosslinking methods selective to NaCMC, in order to isolate NaCMC microgels from the NaCMC/BSA emulsion.
- Study in details swelling behavior of encapsulated emulsions under different pH conditions.
- Measure trivalent ion concentration in the solvent to understand under which conditions they dissociate from the polymer network.
- Improve electrospraying conditions to obtain beads from even smaller droplets. Consider alternative methods to reduce bead sizes (e.g. high-pressure spraying, atomization etc.)
- Investigate whether the emulsion beads provide sufficient protection to keep the acid-stable enzymes active in neutral pH conditions.

- Addition of encapsulated emulsion, free from enzyme, into a solution of an enzyme solution and study the encapsulation efficiency.
- Use other model drugs to study the use of this system as a sustained delivery system.

2. Gelatin/Maltodextrin Emulsion System

- More detailed studies of the formation of the solid phase in gelatin/maltodextrin mixture should be done to fully understand its composition and rate of formation under different gelatin/maltodextrin concentration ratios.
- Determine the concentration of both polymers in gelatin/maltodextrin mixtures, to obtain tie lines of the phase diagram and know the exact composition of dispersed droplets and the microgels.
- Understand why the change of solvent composition leads to smaller droplet size, by studying the phase behavior and interfacial properties of the gelatin/maltodextrin mixtures under different pH and ionic strength conditions.
- Study in further details the spontaneous formation of multiple emulsions, from simple gelatin-in-maltodextrin emulsions upon cooling.
- Swelling studies of microgels under different temperatures might be of interest, to understand whether they show some temperature-mediated swelling.
- Test stability of microgels in presence of proteolytic enzymes found in the digestive tract.
- Coat gelatin microgels with a second polymer, which may allow conveying electrostatic and steric stability to microgel suspensions, increasing protection from acidic pH and reducing diffusion of enzyme out of the microgel during storage.
- Incorporate a solid buffer, such as $\text{Mg}(\text{OH})_2$, into the microgels which allows to keep a neutral pH microenvironment inside the microgels, when immersed into acidic medium. This allows to prevent enzyme deactivation in gastric environments.
- Test the long term stability of dried enzyme-loaded microgels.
- Study the use of the crosslinked, food-grade gelatin microgels as immobilizer of lactase during the production of lactose-hydrolyzed milk.

Chapter 7
BIBLIOGRAPHY

7 Bibliography

- Abbasi, N., Navi, M., & Tsai, S. S. H. (2017). Microfluidic Generation of Particle-Stabilized Water-in-Water Emulsions. *Langmuir*, acs.langmuir.7b03245.
- Agarwal, T., Narayana, S. N. G. H., Pal, K., Pramanik, K., Giri, S., & Banerjee, I. (2015). Calcium alginate-carboxymethyl cellulose beads for colon-targeted drug delivery. *International Journal of Biological Macromolecules*, 75, 409–417.
- Akao, T., Kobashi, K., & Aburada, M. (1994). Enzymic studies on the animal and intestinal bacterial metabolism of geniposide. *Biological & Pharmaceutical Bulletin*, 17, 1573–6.
- Alemán, J. V., Chadwick, A. V., He, J., Hess, M., Horie, K., Jones, R. G., ... Stepto, R. F. T. (2007). Definitions of terms relating to the structure and processing of sols, gels, networks, and inorganic-organic hybrid materials (IUPAC Recommendations 2007). *Pure and Applied Chemistry*, 79, 1801–1829.
- Alevisopoulos, S., & Kasapis, S. (1999). Molecular weight effects on the gelatin/maltodextrin gel. *Carbohydrate Polymers*, 40, 83–87.
- Alevisopoulos, S., Kasapis, S., & Abeysekera, R. (1996). Formation of kinetically trapped gels in the maltodextrin—gelatin system. *Carbohydrate Research*, 293, 79–99.
- Almog, J., Cohen, Y., Azoury, M., & Hahn, T.-R. (2004). Genipin: A Novel Fingerprint Reagent with Colorimetric and Fluorogenic Activity. *Journal of Forensic Sciences*, 49, 1–3.
- Amid, M., Manap, Y., & Zohdi, N. K. (2014). Microencapsulation of Purified Amylase Enzyme from Pitaya (*Hylocereus polyrhizus*) Peel in Arabic Gum-Chitosan using Freeze Drying. *Molecules*, 19, 3731–3743.
- Annan, N. T., Borza, a, Moreau, D. L., Allan-Wojtas, P. M., & Hansen, L. T. (2007). Effect of process variables on particle size and viability of *Bifidobacterium lactis* Bb-12 in genipin-gelatin microspheres. *Journal of Microencapsulation*, 24, 152–62.
- Antonov, Y. ., Grinberg, Vy., & Tolstoguzov, V. (1976). Thermodynamic compatibility of proteins and polysaccharides. *SVyssokomol. Soyed.*, 18B, 566–569.
- Apostolov, A. A., Boneva, D., Vassileva, E., Mark, J. E., & Fakirov, S. (2000). Mechanical properties of native and crosslinked gelatins in a bending deformation. *Journal of Applied Polymer Science*, 76, 2041–2048.
- Aragon Artigas, J. (2016). *Influence of electrolytes and pH on the phase behaviour of gelatin/maltodextrin aqueous mixtures, for water-in-water emulsion formation*. Final Grade Thesis, Universitat de Barcelona.
- Arakawa, T., Prestrelski, S. J., Kenney, W. C., & Carpenter, J. F. (2001). Factors affecting short-term and long-term stabilities of proteins. *Advanced Drug Delivery Reviews*, 46, 307–26.
- Asakura, S., & Oosawa, F. (1954). On Interaction between Two Bodies Immersed in a Solution of Macromolecules. *The Journal of Chemical Physics*, 22, 1255–1256.
- Asano, I., So, S., & Lodge, T. P. (2016). Oil-in-Oil Emulsions Stabilized by Asymmetric Polymersomes Formed by AC + BC Block Polymer Co-Assembly. *Journal of the American Chemical Society*, 138, 4714–4717.

- Asenjo, J. A., & Andrews, B. A. (2011). Aqueous two-phase systems for protein separation: A perspective. *Journal of Chromatography A*, *1218*, 8826–8835.
- Aveyard, R., Binks, B. P., & Clint, J. H. (2003). Emulsions stabilised solely by colloidal particles. *Advances in Colloid and Interface Science*, *100–102*, 503–546.
- Aydın, D., & Kızılel, S. (2017). Water-in-Water Emulsion Based Synthesis of Hydrogel Nanospheres with Tunable Release Kinetics. *Jom*, *69*, 1185–1194.
- Aymard, P., Williams, M. a. K., Clark, a. H., & Norton, I. T. (2000). A Turbidimetric Study of Phase Separating Biopolymer Mixtures during Thermal Ramping. *Langmuir*, *16*, 7383–7391.
- Balakrishnan, G., Nicolai, T., Benyahia, L., & Durand, D. (2012). Particles Trapped at the Droplet Interface in Water-in-Water Emulsions.
- Baler, K., Michael, R., Szleifer, I., & Ameer, G. A. (2014). Albumin hydrogels formed by electrostatically triggered self-assembly and their drug delivery capability. *Biomacromolecules*, *15*, 3625–3633.
- Bancroft, W. D. (1912). The Theory of Emulsification, V. *The Journal of Physical Chemistry*, *17*, 501–519.
- Banerjee, S., Singh, S., Bhattacharya, S. S., & Chattopadhyay, P. (2013). Trivalent ion cross-linked pH sensitive alginate-methyl cellulose blend hydrogel beads from aqueous template. *International Journal of Biological Macromolecules*, *57*, 297–307.
- Beijerinck, M. W. (1896). Ueber eine Eigentümlichkeit der löslichen Stärke. *Zentralblatt Für Bakteriologie, Parasitenkunde Und Infektionskrankheiten*, *2*, 697–699.
- Beijerinck, M. W. (1910). Ueber emulsionsbildung bei der vermischung wässriger Lösungen gewisser gelatinierender kolloide. *Zeitschr. Chem. Ind. Kolloide (Kolloid Z)*, *7*, 16.
- Bellé, A. S., Hackenhaar, C. R., Spolidoro, L. S., Rodrigues, E., Klein, M. P., & Hertz, P. F. (2018). Efficient enzyme-assisted extraction of genipin from genipap (*Genipa americana* L.) and its application as a crosslinker for chitosan gels. *Food Chemistry*, *246*, 266–274.
- Bhattacharya, S., Eckert, F., Boyko, V., & Pich, A. (2007). Temperature-, pH-, and magnetic-field-sensitive hybrid microgels. *Small (Weinheim an Der Bergstrasse, Germany)*, *3*, 650–7.
- Bhattacharya, S. S., Ghosh, A. K., Banerjee, S., Chattopadhyay, P., & Ghosh, A. (2012). Al³⁺ ion cross-linked interpenetrating polymeric network microbeads from tailored natural polysaccharides. *International Journal of Biological Macromolecules*, *51*, 1173–1184.
- Bhattacharya, S. S., Shukla, S., Banerjee, S., Chowdhury, P., Chakraborty, P., & Ghosh, A. (2013). Tailored IPN Hydrogel Bead of Sodium Carboxymethyl Cellulose and Sodium Carboxymethyl Xanthan Gum for Controlled Delivery of Diclofenac Sodium. *Polymer - Plastics Technology and Engineering*, *52*, 795–805.
- Bigi, A., Cojazzi, G., Panzavolta, S., Roveri, N., & Rubini, K. (2002). Stabilization of gelatin films by crosslinking with genipin. *Biomaterials*, *23*, 4827–4832.
- Bigi, A., Cojazzi, G., Panzavolta, S., Rubini, K., & Roveri, N. (2001). Mechanical and thermal properties of gelatin films at different degrees of glutaraldehyde crosslinking. *Biomaterials*, *22*, 763–8.
- Bock, N., Woodruff, M. A., Hutmacher, D. W., & Dargaville, T. R. (2011). Electrospraying, a reproducible method for production of polymeric microspheres for biomedical applications. *Polymers*, *3*, 131–149.

- Bonham, J. A., Faers, M. A., & van Duijneveldt, J. S. (2014). Non-aqueous microgel particles: synthesis, properties and applications. *Soft Matter*, *10*, 9384–9398.
- Borza, A. D., Annan, N. T., Moreau, D. L., Allan-Wojtas, P. M., Ghanem, A., Rousseau, D., Paulson, A.T., Hansen, L. T. (2010). Microencapsulation in genipin cross-linked gelatine-maltodextrin improves survival of *Bifidobacterium adolescentis* during exposure to in vitro gastrointestinal conditions. *Journal of Microencapsulation*, *27*, 387–399.
- Boyko, V., Pich, A., Lu, Y., Richter, S., Arndt, K.-F., & Adler, H.-J. P. (2003). Thermo-sensitive poly(N-vinylcaprolactam-co-acetoacetoxyethyl methacrylate) microgels: 1—synthesis and characterization. *Polymer*, *44*, 7821–7827.
- Bradford, M. M. (1976). A Rapid and Sensitive Method for the Quantitation of Microgram Quantities of Protein Utilizing the Principle of Protein-Dye Binding. *ANALYTICAL BIOCHEMISTRY*, *72*, 248–254.
- Bromberg, L., Temchenko, M., Alakhov, V., & Hatton, T. A. (2005). Kinetics of swelling of polyether-modified poly(acrylic acid) microgels with permanent and degradable cross-links. *Langmuir : The ACS Journal of Surfaces and Colloids*, *21*, 1590–8.
- Brown, C. R., Madsen, R. A., Norton, I. T., & Wesdorp, L. H. (1993). EP0574973. Retrieved from <https://encrypted.google.com/patents/EP0574973B1?cl=tr>
- Brüssow, H. (2013). Nutrition, population growth and disease: a short history of lactose. *Environmental Microbiology*, *15*, 2154–61.
- Burgess, D. J., & Carless, J. E. (1985). Manufacture of gelatin/gelatin cocervate microcapsules. *International Journal of Pharmaceutics*, *27*, 61–70.
- Butler, M. F., & Heppenstall-Butler, M. (2001). Phase separation in gelatin/maltodextrin and gelatin/maltodextrin/gum arabic mixtures studied using small-angle light scattering, turbidity, and microscopy. *Biomacromolecules*, *2*, 812–823.
- Butler, M. F., & Heppenstall-Butler, M. (2003). Phase separation in gelatin/dextran and gelatin/maltodextrin mixtures. *Food Hydrocolloids*, *17*, 815–830.
- Butler, M. F., Ng, Y. F., & Pudney, P. D. a. (2003). Mechanism and kinetics of the crosslinking reaction between biopolymers containing primary amine groups and genipin. *Journal of Polymer Science, Part A: Polymer Chemistry*, *41*, 3941–3953.
- Bütschli, O. (1898). Untersuchungen über Strukturen: insbesondere über Strukturen nichtzelliger Erzeugnisse des Organismus und über ihre Beziehungen zu Strukturen, welche ausserhalb des Organismus entstehen (p. 251). Leipzig: Verlag Von Wilhelm Engelmann.
- Buttler, M. F. (2002). Phase separation in a sheared gelatin/maltodextrin mixture studied by small-angle light scattering. *Biomacromolecules*, *3*, 1208–1216.
- Buzza, D. M. a, Fletcher, P. D. I., Georgiou, T. K., & Ghasdian, N. (2013). Water-in-water emulsions based on incompatible polymers and stabilized by triblock copolymers-templated polymersomes. *Langmuir*, *29*, 14804–14814.
- Bysell, H., Månsson, R., Hansson, P., & Malmsten, M. (2011). Microgels and microcapsules in peptide and protein drug delivery. *Advanced Drug Delivery Reviews*, *63*, 1172–85.
- Cacace, D. N., Rowland, A. T., Stapleton, J. J., Dewey, D. C., & Keating, C. D. (2015). Aqueous Emulsion Droplets Stabilized by Lipid Vesicles as Microcompartments for Biomimetic Mineralization. *Langmuir*, *31*, 11329–11338.

- Capron, I., Costeux, S., & Djabourov, M. (2001). Water in water emulsions: phase separation and rheology of biopolymer solutions. *Rheologica Acta*, *40*, 441–456.
- Cavaliere, F., Chiessi, E., Villa, R., Viganò, L., Zaffaroni, N., Telling, M. F., ... Paradossi, G. (2008). Novel PVA-based hydrogel microparticles for doxorubicin delivery. *Biomacromolecules*, *9*, 1967–1973.
- Chang, C., & Zhang, L. (2011). Cellulose-based hydrogels: Present status and application prospects. *Carbohydrate Polymers*, *84*, 40–53.
- Chang, W.-H., Chang, Y., Lai, P.-H., & Sung, H.-W. (2003). A genipin-crosslinked gelatin membrane as wound-dressing material: in vitro and in vivo studies. *Journal of Biomaterials Science. Polymer Edition*, *14*, 481–95.
- Chen, Y.-S., Chang, J.-Y., Cheng, C.-Y., Tsai, F.-J., Yao, C.-H., & Liu, B.-S. (2005). An in vivo evaluation of a biodegradable genipin-cross-linked gelatin peripheral nerve guide conduit material. *Biomaterials*, *26*, 3911–3918.
- Cheng, C. J., Chu, L. Y., Zhang, J., Wang, H. D., & Wei, G. (2008). Effect of freeze-drying and rehydrating treatment on the thermo-responsive characteristics of poly(N-isopropylacrylamide) microspheres. *Colloid and Polymer Science*, *286*, 571–577.
- Cheung Shum, A. H., Varnell, J., & Weitz, D. A. (2012). Microfluidic fabrication of water-in-water (w/w) jets and emulsions. *Biomicrofluidics*, *6*, 12808.
- Chronakis, I. S. (1998). On the molecular characteristics, compositional properties, and structural-functional mechanisms of maltodextrins: a review. *Critical Reviews in Food Science and Nutrition*, *38*, 599–637.
- Chu, C.-H., Sakiyama, T., & Yano, T. (1995). pH-Sensitive Swelling of a Polyelectrolyte Complex Gel Prepared from Xanthan and Chitosan. *Bioscience, Biotechnology, and Biochemistry*, *59*, 717–719.
- Clark, A. H. (2000). Direct analysis of experimental tie line data (two polymer – one solvent systems) using Flory – Huggins theory. *Carbohydrate Polymers*, *42*, 337–351.
- Corvo, L. (2017). *Emulsion des Carboxymetilcelulosa sódica (NaCMC) y Albúmina de Suero Bovino (BSA) iónicamente entrecruzadas como sistemas de liberación de enzimas*. Final Grade Thesis, Universitat Autònoma de Barcelona.
- Das, M., Mardiyani, S., Chan, W. C. W., & Kumacheva, E. (2006). Biofunctionalized pH-Responsive Microgels for Cancer Cell Targeting: Rational Design. *Advanced Materials*, *18*, 80–83.
- Davies, M. T. (1959). A universal buffer solution for use in ultra-violet spectrophotometry. *The Analyst*, *84*, 248.
- De Geest, B. G., Déjugnat, C., Prevot, M., Sukhorukov, G. B., Demeester, J., & De Smedt, S. C. (2007). Self-Rupturing and Hollow Microcapsules Prepared from Bio-polyelectrolyte-Coated Microgels. *Advanced Functional Materials*, *17*, 531–537.
- de Boer, G. B. J., de Weerd, C., Thoenes, D., & Goossens, H. W. J. (1987). Laser Diffraction Spectrometry: Fraunhofer Diffraction Versus Mie Scattering. *Particle & Particle Systems Characterization*, *4*, 14–19.
- De Gussem, K., Vandenabeele, P., Verbeken, A., & Moens, L. (2005). Raman spectroscopic study of Lactarius spores (Russulales, Fungi). *Spectrochimica Acta - Part A: Molecular and Biomolecular Spectroscopy*, *61*, 2896–2908.
- De Veij, M., Vandenabeele, P., De Beer, T., Remon, J. P., & Moens, L. (2009). Reference database of

- Raman spectra of pharmaceutical excipients. *Journal of Raman Spectroscopy*, 40, 297–307.
- Deng, Y., Misselwitz, B., Dai, N., & Fox, M. (2015). Lactose intolerance in adults: Biological mechanism and dietary management. *Nutrients*, 7, 8020–8035.
- Dewey, D. C., Strulson, C. A., Cacace, D. N., Bevilacqua, P. C., & Keating, C. D. (2014). Bioreactor droplets from liposome-stabilized all-aqueous emulsions. *Nature Communications*, 5, 4670.
- Dickinson, E. (2015). Exploring the frontiers of colloidal behaviour where polymers and particles meet. *Food Hydrocolloids*, 52, 497–509.
- Dickinson, E., & Bergenstahl, B. (1997). Food colloids : proteins, lipids and polysaccharides, 428.
- Ding, P., Wolf, B., Frith, W. J., Clark, a H., Norton, I. T., & Pacek, a W. (2002). Interfacial tension in phase-separated gelatin/dextran aqueous mixtures. *Journal of Colloid and Interface Science*, 253, 367–76.
- Djabourov, M. (1988). Gelation of aqueous gelatin solutions. I. Structural investigation. *Journal de Physique*, 49, 319–332.
- Djabourov, M., Maquet, J., Theveneau, H., Leblond, J., & Papon, P. (1985). Kinetics of gelation of aqueous gelatin solutions. *British Polymer Journal*, 17, 169–174.
- Dobry, M. A. (1948). Sur l'incompatibilité des macromolécules en solution aqueuse. *Bulletin Des Sociétés Chimiques Belges*, 57, 280–285.
- Doi, K. (1965). Formation of amylopectin granules in gelatin gel as a model of starch precipitation in plant plastids. *Biochimica et Biophysica Acta (BBA) - Biophysics Including Photosynthesis*, 94, 557–565.
- Doublier, J. L., Garnier, C., Renard, D., & Sanchez, C. (2000). Protein-polysaccharide interactions. *Current Opinion in Colloid and Interface Science*, 5, 202–214.
- Drude, P. (1900). *Lehrbuch der Optik* (1st ed.). Leipzig: Hirzel.
- Dumetz, A. C., Chockla, A. M., Kaler, E. W., & Lenhoff, A. M. (2008). Effects of pH on protein–protein interactions and implications for protein phase behavior. *Biochimica et Biophysica Acta (BBA) - Proteins and Proteomics*, 1784, 600–610.
- Duval, S., Chung, C., & McClements, D. J. (2015). Protein-Polysaccharide Hydrogel Particles Formed by Biopolymer Phase Separation, 334–341.
- Edelman, M. W., Tromp, R. H., & van der Linden, E. (2003). Phase-separation-induced fractionation in molar mass in aqueous mixtures of gelatin and dextran. *Physical Review E - Statistical Physics, Plasmas, Fluids, and Related Interdisciplinary Topics*, 67, 11.
- Edelman, M. W., Van der Linden, E., De Hoog, E., & Tromp, R. H. (2001). Compatibility of gelatin and dextran in aqueous solution. *Biomacromolecules*, 2, 1148–1154.
- Ehren, J., Govindarajan, S., Morón, B., Minshall, J., & Khosla, C. (2008). Protein engineering of improved prolyl endopeptidases for celiac sprue therapy. *Protein Engineering, Design and Selection*, 21, 699–707.
- Eichenbaum, G. M., Kiser, P. F., Shah, D., Simon, S. a., & Needham, D. (1999). Investigation of the swelling response and drug loading of ionic microgels: The dependence on functional group composition. *Macromolecules*, 32, 8996–9006.
- Espigulé, C. M. (2016). *Novel biocompatible microgels for functional food, obtained in water-in-water emulsions*. Final Grade Thesis, Universitat de Barcelona.

- Esquena, J. (2016). Water-in-water (W/W) emulsions. *Current Opinion in Colloid and Interface Science*, 25, 109–119.
- Esteghlal, S., Niakosari, M., Hosseini, S. M. H., Mesbahi, G. R., & Yousefi, G. H. (2016). Gelatin-hydroxypropyl methylcellulose water-in-water emulsions as a new bio-based packaging material. *International Journal of Biological Macromolecules*, 86, 242–249.
- Fernandez-Nieves, A., Wyss, H. M., Mattsson, J., & Weitz, D. A. (2011). *Microgel suspensions: fundamentals and applications*. (A. Fernandez-Nieves, H. M. Wyss, J. Mattsson, & D. A. Weitz, Eds.). Weinheim, Germany: Wiley-VCH Verlag GmbH & Co. KGaA. doi:10.1002/9783527632992
- Firoozmand, H., Murray, B. S., & Dickinson, E. (2007). Fractal-type particle gel formed from gelatin + starch solution. *Langmuir*, 23, 4646–4650.
- Firoozmand, H., & Rousseau, D. (2015). Food-grade bijels based on gelatin-maltodextrin-microbial cell composites. *Food Hydrocolloids*, 48, 208–212.
- Flory, P. J., & Krigbaum, W. R. (1951). Thermodynamics of High Polymer Solutions. *Annual Review of Physical Chemistry*.
- Foster, T. J., Brown, C. R. T., & Norton, I. T. (1996). Phase inversion of water-in-water emulsions. In P. A. Williams, G. O. Phillips, & D. J. Wedlock (Eds.), *Gums and Stabilisers for the Food Industry 8*, (pp. 297–306). Oxford, UK: IRL Press.
- Frank, C. (2001). Polymer Science and Engineering. Retrieved from <http://web.stanford.edu/class/cheme160/lectures/lecture9.pdf>
- Franssen, O., & Hennink, W. E. (1998). A novel preparation method for polymeric microparticles without the use of organic solvents. *International Journal of Pharmaceutics*, 168, 1–7.
- Frei-Rutishauser, B., Muehlenfeld, C., Watson, T., & Warnke, G. (2016). Factors Affecting Sterile Filtration of Sodium-Carboxymethylcellulose–Based Solutions. *BioProcess International*.
- Frith, W. J. (2010). Mixed biopolymer aqueous solutions--phase behaviour and rheology. *Advances in Colloid and Interface Science*, 161, 48–60.
- Fuhrmann, G., & Leroux, J.-C. (2014). Improving the stability and activity of oral therapeutic enzymes--recent advances and perspectives. *Pharmaceutical Research*, 31, 1099–105.
- Fujikawa, S., Yokota, T., & Koga, K. (1988). Immobilization of β -glucosidase in calcium alginate gel using genipin as a new type of cross-linking reagent of natural origin. *Applied Microbiology and Biotechnology*, 28, 440–441.
- Ghugare, S., Chiessi, E., Fink, R., & Gerelli, Y. (2011). Structural investigation on thermoresponsive PVA/poly (methacrylate-co-N-isopropylacrylamide) microgels across the volume phase transition. *Macromolecules*, 4470–4478.
- Ghugare, S. V., Chiessi, E., Cerroni, B., Telling, M. T. F., Sakai, V. G., & Paradossi, G. (2012). Biodegradable dextran based microgels: a study on network associated water diffusion and enzymatic degradation. *Soft Matter*, 8, 2494.
- Ghugare, S. V., Chiessi, E., Sakai, V. G., Telling, M. T. F., Wadgaonkar, P. P., & Paradossi, G. (2013). Thermoresponsive and biodegradable dextran based microgels: Synthesis and structural investigation. *Macromolecular Symposia*, 329, 27–34.
- Ghugare, S. V., Mozetic, P., & Paradossi, G. (2009). Temperature-sensitive poly(vinyl alcohol)/poly(methacrylate-co-N-isopropyl acrylamide) microgels for doxorubicin delivery.

Biomacromolecules, 10, 1589–1596.

- Godard, P., Biebuyck, J. J., Daumerie, M., Naveau, H., & Mercier, J. P. (1978). Crystallization and melting of aqueous gelatin. *Journal of Polymer Science: Polymer Physics Edition*, 16, 1817–1828.
- González Flecha, F. L., & Levi, V. (2003). Determination of the molecular size of BSA by fluorescence anisotropy. *Biochemistry and Molecular Biology Education*, 31, 319–322.
- Grinberg, V. Y., & Tolstoguzov, V. B. (1997). Thermodynamic incompatibility of proteins and polysaccharides in solutions. *Food Hydrocolloids*, 11, 145–158.
- Grosová, Z., Rosenberg, M., & Rebroš, M. (2008). Perspectives and applications of immobilised β -galactosidase in food industry - A review. *Czech Journal of Food Sciences*, 26, 1–14.
- Gupta, S., Jain, A., Chakraborty, M., Sahni, J. K., Ali, J., & Dang, S. (2013). Oral delivery of therapeutic proteins and peptides: a review on recent developments. *Drug Delivery*, 20, 237–46.
- Haffner, F. B., Van de Wiele, T., & Pasc, A. (2017). Original behavior of *L. rhamnosus* GG encapsulated in freeze-dried alginate-silica microparticles revealed upon simulated gastrointestinal conditions. *J. Mater. Chem. B*, 5, 7839–7847.
- Harding, S. E. (1997). Biopolymer Mixtures. *Food / Nahrung*, 41. doi:10.1002/food.19970410130
- Haug, I., Williams, M. A. K., Lundin, L., Smidsrød, O., & Draget, K. I. (2003). Molecular interactions in, and rheological properties of, a mixed biopolymer system undergoing order/disorder transitions. In *Food Hydrocolloids* (Vol. 17, pp. 439–444). Elsevier.
- Hecht, L., Blanch, E. W., Bell, A. F., & Day, L. A. (1999). Raman optical activity instrument for studies of biopolymer structure and dynamics. *Journal of Raman Spectroscopy*, 30, 815–825.
- Hoey, A., Ryan, J. T., Fitzsimons, S. M., & Morris, E. R. (2016). Segregative Interactions in Single-Phase Mixtures of Gelling (Potato) Maltodextrin with Other Hydrocolloids. In *Gums and Stabilisers for the Food Industry 18 Hydrocolloid Functionality for Affordable and Sustainable Global Food Solutions* (pp. 305–312).
- Horst, R., & Wolf, B. A. (2002). Thermodynamics of polymer solutions. Retrieved from http://wolf.chemie.uni-mainz.de/Internet/Students/thermodynamics_of_polymer_solutions.pdf
- Huang, K. S., Lu, K., Yeh, C. S., Chung, S. R., Lin, C. H., Yang, C. H., & Dong, Y. S. (2009). Microfluidic controlling monodisperse microdroplet for 5-fluorouracil loaded genipin-gelatin microcapsules. *Journal of Controlled Release*, 137, 15–19.
- Huggins, M. L. (1942). Theory of Solutions of High Polymers. *Journal of the American Chemical Society*, 64, 1712–1719.
- Husain, Q. (2010). β Galactosidases and their potential applications: A review. *Critical Reviews in Biotechnology*, 30, 41–62.
- Imhof, A., & Pine, D. J. (1997). Stability of Nonaqueous Emulsions. *Journal of Colloid and Interface Science*, 192, 368–374.
- Impellitteri, N. A., Toepke, M. W., Lan Levensgood, S. K., & Murphy, W. L. (2012). Specific VEGF sequestering and release using peptide-functionalized hydrogel microspheres. *Biomaterials*, 33, 3475–3484.
- Ingram, C. J. E., Mulcare, C. A., Itan, Y., Thomas, M. G., & Swallow, D. M. (2009). Lactose digestion and the evolutionary genetics of lactase persistence. *Human Genetics*, 124, 579–591.
- Itmonline.org. (2003). GARDENIA: Key Herb for Dispelling Dampness and Heat Via the Triple Burner.

Retrieved January 4, 2018, from <http://www.itmonline.org/arts/gardenia.htm>

- Ito, Y., Casolaro, M., Kono, K., & Imanishi, Y. (1989). An insulin-releasing system that is responsive to glucose. *Journal of Controlled Release*, *10*, 195–203.
- Jenkins, H. P., & Clarke, J. S. (1945). Gelatin Sponge, a new hemostatic substance. *Archives of Surgery*, *51*, 253.
- Jin, T., Zhu, J., Wu, F., Yuan, W., Geng, L. L., & Zhu, H. (2008). Preparing polymer-based sustained-release systems without exposing proteins to water-oil or water-air interfaces and cross-linking reagents. *Journal of Controlled Release : Official Journal of the Controlled Release Society*, *128*, 50–9.
- Johansson, H.-O., Karlström, G., Tjerneld, F., & Haynes, C. a. (1998). Driving forces for phase separation and partitioning in aqueous two-phase systems. *Journal of Chromatography B: Biomedical Sciences and Applications*, *711*, 3–17.
- Jones, O. G., & McClements, D. J. (2010). Functional Biopolymer Particles: Design, Fabrication, and Applications. *Comprehensive Reviews in Food Science and Food Safety*, *9*, 374–397.
- Joseph, I., & Venkataram, S. (1995). Indomethacin sustained release from alginate-gelatin or pectin-gelatin coacervates. *International Journal of Pharmaceutics*, *126*, 161–168.
- Kaijanen, L., Paakkunainen, M., Pietarinen, S., Jernström, E., & Reinikainen, S.-P. (2015). Ultraviolet Detection of Monosaccharides: Multiple Wavelength Strategy to Evaluate Results after Capillary Zone Electrophoretic Separation. *Int. J. Electrochem. Sci*, *10*, 2950–2961.
- Kamel, S., Ali, N., Jahangir, K., Shah, S. M., & El-Gendy, A. A. (2008). Pharmaceutical significance of cellulose: A review. *Express Polymer Letters*, *2*, 758–778.
- Kamide, K., & Kamide, K. (2005). 1 – Introduction. In *Cellulose and Cellulose Derivatives* (pp. 1–23). Elsevier.
- Kang, C. H., & Sandler, S. I. (1987). Phase behavior of aqueous two-polymer systems. *Fluid Phase Equilibria*, *38*, 245–272.
- Kang, J., Wu, F., Cai, Y., Xu, M., He, M., & Yuan, W. (2014). Development of Recombinant Human Growth Hormone (rhGH) sustained-release microspheres by a low temperature aqueous phase/aqueous phase emulsion method. *European Journal of Pharmaceutical Sciences : Official Journal of the European Federation for Pharmaceutical Sciences*, *62*, 141–7.
- Kasapis, S., Morris, E. R., Norton, I. T., & Brown, C. R. T. (1993). Phase equilibria and gelation in gelatin/maltodextrin systems — Part III: phase separation in mixed gels. *Carbohydrate Polymers*, *21*, 261–268.
- Kasapis, S., Morris, E. R., Norton, I. T., & Clark, A. H. (1993a). Phase equilibria and gelation in gelatin/maltodextrin systems — Part I: gelation of individual components. *Carbohydrate Polymers*, *21*, 243–248.
- Kasapis, S., Morris, E. R., Norton, I. T., & Clark, A. H. (1993b). Phase equilibria and gelation in gelatin/maltodextrin systems — Part IV: composition-dependence of mixed-gel moduli. *Carbohydrate Polymers*, *21*, 269–276.
- Kasapis, S., Morris, E. R., Norton, I. T., & Gidley, M. J. (1993). Phase equilibria and gelation in gelatin/maltodextrin systems — Part II: polymer incompatibility in solution. *Carbohydrate Polymers*, *21*, 249–259.
- Kawaguchi, H. (2013). Micro hydrogels: preparation, properties, and applications. *Journal of Oleo*

Science, 62, 865–71.

- Kennedy, J. F., Noy, R. J., Stead, J. A., & White, C. A. (1986). Factors Affecting, and Prediction of, the Low Temperature Precipitation of Commercial Low DE Maltodextrins. *Starch - Stärke*, 38, 273–281.
- Khan, A., Othman, M. B. H., Chang, B. P., & Akil, H. M. (2015). Preparation, physicochemical and stability studies of chitosan-PNIPAM based responsive microgels under various pH and temperature conditions. *Iranian Polymer Journal*, 24, 317–328.
- Khan, A. Y., Talegaonkar, S., Iqbal, Z., Ahmed, F. J., & Khar, R. K. (2006). Multiple emulsions: an overview. *Current Drug Delivery*, 3, 429–43.
- Khan, R. S., Nickerson, M. T., Paulson, A. T., & Rousseau, D. (2011). Release of fluorescent markers from phase-separated gelatin-maltodextrin hydrogels. *Journal of Applied Polymer Science*, 121, 2662–2673.
- Kim, J. J., & Park, K. (2001). Modulated insulin delivery from glucose-sensitive hydrogel dosage forms. *Journal of Controlled Release*, 77, 39–47.
- Kim, M. S., Park, S. J., Gu, B. K., & Kim, C.-H. (2012). Ionically crosslinked alginate–carboxymethyl cellulose beads for the delivery of protein therapeutics. *Applied Surface Science*, 262, 28–33.
- Kirchmayer, D. M., Watson, C. a., Ranson, M., & Panhuis, M. in Het. (2013). Gelapin, a degradable genipin cross-linked gelatin hydrogel. *RSC Advances*, 3, 1073.
- Kiser, P. F., Wilson, G., & Needham, D. (2000). Lipid-coated microgels for the triggered release of doxorubicin. *Journal of Controlled Release*, 68, 9–22.
- Klapper, M., Nenov, S., Haschick, R., Müller, K., & Müllen, K. (2008). Oil-in-Oil Emulsions: A Unique Tool for the Formation of Polymer Nanoparticles. *Accounts of Chemical Research*, 41, 1190–1201.
- Klein, M. P., Hackenhaar, C. R., Lorenzoni, A. S. G., Rodrigues, R. C., Costa, T. M. H., Ninow, J. L., & Hertz, P. F. (2016). Chitosan crosslinked with genipin as support matrix for application in food process: Support characterization and β -d-galactosidase immobilization. *Carbohydrate Polymers*, 137, 184–190.
- Kong, Y. Q., Li, D., Wang, L. J., & Adhikari, B. (2011). Preparation of gelatin microparticles using water-in-water (w/w) emulsification technique. *Journal of Food Engineering*, 103, 9–13.
- Koo, H. J., Lim, K. H., Jung, H. J., & Park, E. H. (2006). Anti-inflammatory evaluation of gardenia extract, geniposide and genipin. *Journal of Ethnopharmacology*, 103, 496–500.
- Krishna Rao, K. S. V, Vijaya Kumar Naidu, B., Subha, M. C. S., Sairam, M., & Aminabhavi, T. M. (2006). Novel chitosan-based pH-sensitive interpenetrating network microgels for the controlled release of cefadroxil. *Carbohydrate Polymers*, 66, 333–344.
- Kronberg, B., Holmberg, K., & Lindman, B. (2014). *Surface Chemistry of Surfactants and Polymers*. Chichester, UK: John Wiley & Sons, Ltd. doi:10.1002/9781118695968
- Lamprecht, A., Schäfer, U. F., & Lehr, C. M. (2000). Characterization of microcapsules by confocal laser scanning microscopy: Structure, capsule wall composition and encapsulation rate. *European Journal of Pharmaceutics and Biopharmaceutics*, 49, 1–9.
- Lau, T. T., Wang, C., & Wang, D. A. (2010). Cell delivery with genipin crosslinked gelatin microspheres in hydrogel/microcarrier composite. *Composites Science and Technology*, 70, 1909–1914.
- Leisner, D., Blanco, M., & Quintela, L. (2002). Phase separation mechanism in gelling aqueous

- biopolymer mixture probed by light scattering. *Macromolecular Symposia*, 115, 93–115.
- Lekkerkerker, H. N. W., & Tuinier, R. (2011). *Colloids and the depletion interaction*. Springer.
- Levett, C. (2011). Coaching the nursing and midwifery teams. *Australian Nursing Journal (July 1993)*, 18, 56.
- Levitt, M., Wilt, T., & Shaukat, A. (2013). Clinical Implications of Lactose Malabsorption Versus Lactose Intolerance. *Journal of Clinical Gastroenterology*, 47, 471–480.
- Li, B., Wang, L., Li, D., Adhikari, B., & Mao, Z. (2012). Preparation and characterization of crosslinked starch microspheres using a two-stage water-in-water emulsion method. *Carbohydrate Polymers*, 88, 912–916.
- Li, Y., Norde, W., & Kleijn, J. M. (2012). Stabilization of protein-loaded starch microgel by polyelectrolytes. *Langmuir: The ACS Journal of Surfaces and Colloids*, 28, 1545–51.
- Li, Y., Zhang, Z., van Leeuwen, H. P., Cohen Stuart, M. a., Norde, W., & Kleijn, J. M. (2011). Uptake and release kinetics of lysozyme in and from an oxidized starch polymer microgel. *Soft Matter*, 7, 10377.
- Liang, D., Fu, X., Liao, M., Yuan, W., & Su, J. (2013). Development of dextran microparticles loaded with IL-1Ra of high-encapsulation efficiency and high-bioactivity by a novel method without exposing IL-1Ra to water–oil interfaces. *Powder Technology*, 235, 299–302.
- Liang, H.-C., Chang, W.-H., Lin, K.-J., & Sung, H.-W. (2003). Genipin-crosslinked gelatin microspheres as a drug carrier for intramuscular administration: in vitro and in vivo studies. *Journal of Biomedical Materials Research. Part A*, 65, 271–282.
- Lien, S.-M., Li, W.-T., & Huang, T.-J. (2008). Genipin-crosslinked gelatin scaffolds for articular cartilage tissue engineering with a novel crosslinking method. *Materials Science and Engineering: C*, 28, 36–43.
- Lii, C. Y., Tomasik, P., Zaleska, H., Liaw, S. C., & Lai, V. M. F. (2002). Carboxymethyl cellulose-gelatin complexes. *Carbohydrate Polymers*, 50, 19–26.
- Lin, S.-Y., Chen, K.-S., & Run-Chu, L. (1999). Drying methods affecting the particle sizes, phase transition, deswelling/reswelling processes and morphology of poly(N-isopropylacrylamide) microgel beads. *Polymer*, 40, 6307–6312.
- Logees.com. (2018). Gardenia ‘Prostrata’ (Gardenia jasminoides). Retrieved January 4, 2018, from <https://www.logees.com/gardenia-prostrata-gardenia-jasminoides.html>
- Lohani, A., Singh, G., Bhattacharya, S. S., Rama Hegde, R., & Verma, A. (2016). Tailored-interpenetrating polymer network beads of κ-carrageenan and sodium carboxymethyl cellulose for controlled drug delivery, 31, 53–64.
- Lopez, V. C., Hadgraft, J., & Snowden, M. J. (2005). The use of colloidal microgels as a (trans)dermal drug delivery system. *International Journal of Pharmaceutics*, 292, 137–47.
- Lopez, V. C., Raghavan, S. L., & Snowden, M. J. (2004). Colloidal microgels as transdermal delivery systems. *Reactive and Functional Polymers*, 58, 175–185.
- Lorén, N., & Hermansson, A. M. (2000). Phase separation and gel formation in kinetically trapped gelatin/maltodextrin gels. *International Journal of Biological Macromolecules*, 27, 249–262.
- Lorén, N., Hermansson, A. M., Williams, M. A. K., Lundin, L., Foster, T. J., Hubbard, C. D., Clark, A. H., Norton, I. T., Bergström, E. T., Goodall, D. M. (2001). Phase separation induced by

- conformational ordering of gelatin in gelatin/maltodextrin mixtures. *Macromolecules*, *34*, 289–297.
- Lorén, N., Langton, M., & Hermansson, A. (1999). Confocal laser scanning microscopy and image analysis of kinetically trapped phase-separated gelatin/maltodextrin gels. *Food Hydrocolloids*, *13*, 185–198.
- Loret, C., Meunier, V., Frith, W. J., & Fryer, P. J. (2004). Rheological characterisation of the gelation behaviour of maltodextrin aqueous solutions. *Carbohydrate Polymers*, *57*, 153–163.
- Loret, C., Schumm, S., Pudney, P. D. A., Frith, W. J., & Fryer, P. J. (2005). Phase separation and molecular weight fractionation behaviour of maltodextrin/agarose mixtures. In *Food Hydrocolloids* (Vol. 19, pp. 557–565).
- Lundin, L., Norton, I., Foster, T. J., Williams, M. A. K., Hermansson, A.-M., & Bergström, E. (2000). Phase Separation in Mixed Biopolymer Systems. *Gums and Stabilisers for the Food Industry 10*, 167–180.
- Lundin, L., Williams, M. A. K., & Foster, T. J. (2003). Phase separation in foods. In *Texture in Food* (Volume 1; pp. 63–85). Woodhead.
- Mai, T. H. A., Tran, V. N., & Le, V. V. M. (2013). Biochemical studies on the immobilized lactase in the combined alginate-carboxymethyl cellulose gel. *Biochemical Engineering Journal*, *74*, 81–87.
- Mariod, A. A., & Adam, H. F. (2013). Review: Gelatin, source, extraction and industrial applications. *Acta Scientiarum Polonorum, Technologia Alimentaria*, *12*, 135–147.
- Matalanis, A., Jones, O. G., & McClements, D. J. (2011). Structured biopolymer-based delivery systems for encapsulation, protection, and release of lipophilic compounds. *Food Hydrocolloids*, *25*, 1865–1880.
- Matalanis, A., Lesmes, U., Decker, E. A., & McClements, D. J. (2010). Fabrication and characterization of filled hydrogel particles based on sequential segregative and aggregative biopolymer phase separation. *Food Hydrocolloids*, *24*, 689–701.
- Matalanis, A., & McClements, D. J. (2012). Factors Influencing the Formation and Stability of Filled Hydrogel Particles Fabricated by Protein/Polysaccharide Phase Separation and Enzymatic Cross-Linking. *Food Biophysics*, *7*, 72–83.
- McClements, D. (2014). *Nanoparticle- and Microparticle-based Delivery Systems*. CRC Press. doi:10.1201/b17280
- McClements, D. J. (2010). Emulsion design to improve the delivery of functional lipophilic components. *Annual Review of Food Science and Technology*, *1*, 241–69.
- Medronho, B., Romano, A., Miguel, M. G., Stigsson, L., & Lindman, B. (2012). Rationalizing cellulose (in)solubility: Reviewing basic physicochemical aspects and role of hydrophobic interactions. *Cellulose*, *19*, 581–587.
- Mi, F.-L., Shyu, S.-S., & Peng, C.-K. (2005). Characterization of ring-opening polymerization of genipin and pH-dependent cross-linking reactions between chitosan and genipin. *Journal of Polymer Science Part A: Polymer Chemistry*, *43*, 1985–2000.
- Mi, F., Sung, H., & Shyu, S. (2000). Synthesis and Characterization of a Novel Chitosan-Based Network Prepared Using Naturally Occurring Crosslinker, 2804–2814.
- Michon, C., Cuvelier, G., Launay, B., Parker, A., & Takerkart, G. (1995). Study of the compatibility/incompatibility of gelatin/t-carrageenan/water mixtures. *Carbohydrate Polymers*,

28, 333–336.

- Mie, G. (1908). Beiträge zur Optik trüber Medien, speziell kolloidaler Metallösungen. *Annalen Der Physik*, 330, 377–445.
- Minekus, M., Alminger, M., Alvito, P., Ballance, S., Bohn, T., Bourlieu, C., Brodkorb, a. (2014). A standardised static in vitro digestion method suitable for food - an international consensus. *Food & Function*, 5, 1113–24.
- Misselwitz, B., Pohl, D., Frühauf, H., Fried, M., Vavricka, S. R., & Fox, M. (2013). Lactose malabsorption and intolerance: pathogenesis, diagnosis and treatment. *United European Gastroenterology Journal*, 1, 151–9.
- Miyata, T., Asami, N., & Uragami, T. (1999). A reversibly antigen-responsive hydrogel. *Nature*, 399, 766–9.
- Mladenovska, K., Cruaud, O., Richomme, P., Belamie, E., Raicki, R. S., Venier-julienne, M., Goracinova, K. (2007). 5-ASA loaded chitosan – Ca – alginate microparticles : Preparation and physicochemical characterization, 345, 59–69.
- Montalto, M., Curigliano, V., Santoro, L., Vastola, M., Cammarota, G., Manna, R., Gasbarrini, A., Gasbarrini, G. (2006). Management and treatment of lactose malabsorption. *World Journal of Gastroenterology*, 12, 187.
- Moon, B. U., Abbasi, N., Jones, S. G., Hwang, D. K., & Tsai, S. S. H. (2016). Water-in-Water Droplets by Passive Microfluidic Flow Focusing. *Analytical Chemistry*, 88, 3982–3989.
- Morris, E. R. (2009). Functional Interactions in Gelling Biopolymer Mixtures. In *Modern Biopolymer Science* (First Edit, pp. 167–198). Elsevier.
- Mou, C.-L., Ju, X.-J., Zhang, L., Xie, R., Wang, W., Deng, N.-N., Wei, J., Chen, Q., Chu, L.-Y. (2014). Monodisperse and Fast-Responsive Poly(*N* -isopropylacrylamide) Microgels with Open-Celled Porous Structure. *Langmuir*, 30, 1455–1464.
- Murray, B. S., & Phisarnchananan, N. (2014, December 15). The effect of nanoparticles on the phase separation of waxy corn starch + locust bean gum or guar gum. *Food Hydrocolloids*, pp. 92–99.
- Murray, B. S., & Phisarnchananan, N. (2016). Whey protein microgel particles as stabilizers of waxy corn starch + locust bean gum water-in-water emulsions. *Food Hydrocolloids*, 56, 161–169.
- Murthy, N., Xu, M., Schuck, S., Kunisawa, J., Shastri, N., & Fréchet, J. M. J. (2003). A macromolecular delivery vehicle for protein-based vaccines: acid-degradable protein-loaded microgels. *Proceedings of the National Academy of Sciences of the United States of America*, 100, 4995–5000.
- Navarra, G., Giacomazza, D., Leone, M., Librizzi, F., Militello, V., & San Biagio, P. L. (2009). Thermal aggregation and ion-induced cold-gelation of bovine serum albumin. *European Biophysics Journal*, 38, 437–446.
- Nayak, S., Lee, H., Chmielewski, J., & Lyon, L. A. (2004). Folate-mediated cell targeting and cytotoxicity using thermoresponsive microgels. *Journal of the American Chemical Society*, 126, 10258–9.
- Nguyen, B. T., Nicolai, T., & Benyahia, L. (2013). Stabilization of water-in-water emulsions by addition of protein particles. *Langmuir*, 29, 10658–10664.
- Nguyen, B. T., Wang, W., Saunders, B. R., Benyahia, L., & Nicolai, T. (2015). pH-Responsive Water-in-Water Pickering Emulsions. *Langmuir*, 150317102048003.

- Nichele, V., Signoretto, M., & Ghedini, E. (2011). β -Galactosidase entrapment in silica gel matrices for a more effective treatment of lactose intolerance. *Journal of Molecular Catalysis B: Enzymatic*, *71*, 10–15.
- Nickerson, M. T., Farnworth, R., Wagar, E., Hodge, S. M., Rousseau, D., & Paulson, a T. (2006). Some physical and microstructural properties of genipin-crosslinked gelatin-maltodextrin hydrogels. *International Journal of Biological Macromolecules*, *38*, 40–4.
- Nickerson, M. T., Patel, J., Heyd, D. V., Rousseau, D., & Paulson, A. T. (2006). Kinetic and mechanistic considerations in the gelation of genipin-crosslinked gelatin. *International Journal of Biological Macromolecules*, *39*, 298–302.
- Nickerson, M. T., Paulson, a T., Wagar, E., Farnworth, R., Hodge, S. M., & Rousseau, D. (2006). Some physical properties of crosslinked gelatin–maltodextrin hydrogels. *Food Hydrocolloids*, *20*, 1072–1079.
- Nicolai, T., & Murray, B. (2017). Particle stabilized water in water emulsions. *Food Hydrocolloids*, *68*, 157–163.
- Nolan, C. M., Gelbaum, L. T., & Lyon, L. A. (2006). ¹H NMR investigation of thermally triggered insulin release from poly(N-isopropylacrylamide) microgels. *Biomacromolecules*, *7*, 2918–22.
- Norton, I. T., & Frith, W. J. (2001). Microstructure design in mixed biopolymer composites. *Food Hydrocolloids*, *15*, 543–553.
- Nussinovitch, A., Chapnik, N., Gal, J., & Froy, O. (2012). Delivery of lactase using chocolate-coated agarose carriers. *Food Research International*, *46*, 41–45.
- O’connell, S., & Walsh, G. (2006). Physicochemical characteristics of commercial lactases relevant to their application in the alleviation of lactose intolerance. *Applied Biochemistry and Biotechnology*, *134*. Retrieved from <http://link.springer.com/article/10.1385/ABAB:134:2:179>
- O’Connell, S., & Walsh, G. (2007). Purification and properties of a beta-galactosidase with potential application as a digestive supplement. *Applied Biochemistry and Biotechnology*, *141*, 1–14.
- O’Connell, S., & Walsh, G. (2010). A novel acid-stable, acid-active beta-galactosidase potentially suited to the alleviation of lactose intolerance. *Applied Microbiology and Biotechnology*, *86*, 517–24.
- Ogawa, K., Wang, B., & Kokufuta, E. (2001). Enzyme-regulated microgel collapse for controlled membrane permeability. *Langmuir*, *17*, 4704–4707.
- Oh, J. K., Drumright, R., Siegwart, D. J., & Matyjaszewski, K. (2008). The development of microgels/nanogels for drug delivery applications. *Progress in Polymer Science*, *33*, 448–477.
- Oh, J. K., Lee, D. I., & Park, J. M. (2009). Biopolymer-based microgels/nanogels for drug delivery applications. *Progress in Polymer Science*, *34*, 1261–1282.
- Oh, J. K., Siegwart, D. J., & Matyjaszewski, K. (2007). Synthesis and biodegradation of nanogels as delivery carriers for carbohydrate drugs. *Biomacromolecules*, *8*, 3326–31.
- Olde Damink, L. H. H., Dijkstra, P. J., Van Luyn, M. J. A., Van Wachem, P. B., Nieuwenhuis, P., & Feijen, J. (1995). Glutaraldehyde as a crosslinking agent for collagen-based biomaterials. *Journal of Materials Science: Materials in Medicine*, *6*, 460–472.
- Oss-Ronen, L., & Seliktar, D. (2010). Photopolymerizable Hydrogels Made from Polymer-Conjugated Albumin for Affinity-Based Drug Delivery. *Advanced Engineering Materials*, *12*, B45–B52.
- Ostwald, V. W., & Hertel, R. H. (1929). Kolloidchemische reaktionen zwischen solen von

eiweisskörpern und polymeren kohlehydraten. *Kolloid-Zeitschrift*, 47, 258–268.

- Park, T. G., & Hoffman, a S. (1990). Immobilization and characterization of beta-galactosidase in thermally reversible hydrogel beads. *Journal of Biomedical Materials Research*, 24, 21–38.
- Parker, N. G., & Povey, M. J. W. (2012). Ultrasonic study of the gelation of gelatin: Phase diagram, hysteresis and kinetics. *Food Hydrocolloids*, 26, 99–107.
- Parlato, M., Johnson, A., Hudalla, G. A., & Murphy, W. L. (2013). Adaptable poly(ethylene glycol) microspheres capable of mixed-mode degradation. *Acta Biomaterialia*, 9, 9270–9280.
- Patil, J. S., Marapur, S. C., Gurav, P. B. C., & Banagar, A. V. (2015). Ionotropic Gelation and Polyelectrolyte Complexation Technique: Novel Approach to Drug Encapsulation. *Handbook of Encapsulation and Controlled Release*, 273–296.
- Pawar, V. K., Gopal, J., Singh, Y., Chaurasia, M., Reddy, B. S., & Chourasia, M. K. (2014). Targeting of gastrointestinal tract for amended delivery of protein / peptide therapeutics : Strategies and industrial perspectives. *Journal of Controlled Release*, 196, 168–183.
- Peddireddy, K. R., Nicolai, T., Benyahia, L., & Capron, I. (2016). Stabilization of Water-in-Water Emulsions by Nanorods. *ACS Macro Letters*, 5, 283–286.
- Peng, S., & Wu, C. (2000). Poly(N-vinylcaprolactam) microgels and its related composites. *Macromolecular Symposia*, 159, 179–186.
- Pereira de Sousa, I., & Bernkop-Schnürch, A. (2014). Pre-systemic metabolism of orally administered drugs and strategies to overcome it. *Journal of Controlled Release : Official Journal of the Controlled Release Society*, 192, 301–9.
- Pereira, L., Sousa, A., Coelho, H., Amado, A. M., & Ribeiro-Claro, P. J. A. (2003). Use of FTIR, FT-Raman and ¹³C-NMR spectroscopy for identification of some seaweed phycocolloids. In *Biomolecular Engineering* (Vol. 20, pp. 223–228).
- Pereltsvaig, A. (2013). Global Geography of Milk Consumption and Lactose (In)Tolerance. Retrieved from <http://www.languagesoftheworld.info/uncategorized/global-geography-milk-consumption-lactose-intolerance.html>
- Petrusic, S., Jovancic, P., Lewandowski, M., Giraud, S., Bugarski, B., Djonlagic, J., & Koncar, V. (2012). Synthesis, characterization and drug release properties of thermosensitive poly(N-isopropylacrylamide) microgels. *Journal of Polymer Research*, 19, 9979.
- Pich, A., & Adler, H. (2007). Encapsulation Technologies for Active Food Ingredients and Food Processing. *Polymer International*. Retrieved from <http://onlinelibrary.wiley.com/doi/10.1002/pi.2142/full>
- Piculell, L., & Lindman, B. (1992). Association and Segregation in Aqueous Polymer/Polymer, Polymer Surfactant, and Surfactant Surfactant Mixtures - Similarities and Differences. *Advances In Colloid And Interface Science*, 41, 149–178.
- Poortinga, A. T. (2008). Microcapsules from self-assembled colloidal particles using aqueous phase-separated polymer solutions. *Langmuir*, 24, 1644–1647.
- PubChem: Open Chemistry Database. (2004). Compound Summary for CID 24380: Iron trichloride. Retrieved from https://pubchem.ncbi.nlm.nih.gov/compound/ferric_chloride#section=Top
- PubChem: Open Chemistry Database. (2018a). Aluminum Sulfate. Retrieved from <https://pubchem.ncbi.nlm.nih.gov/compound/24850#section=Top>

- PubChem: Open Chemistry Database. (2018b). Potassium Alum Anhydrous. Retrieved from https://pubchem.ncbi.nlm.nih.gov/compound/Potassium_alum#section=Top
- Qiu, X., & Hu, S. (2013). “Smart” materials based on cellulose: A review of the preparations, properties, and applications. *Materials*, *6*, 738–781.
- Ramesh Babu, V., Krishna Rao, K. S. V., Sairam, M., Naidu, B. V. K., Hosamani, K. M., & Aminabhavi, T. M. (2006). pH sensitive interpenetrating network microgels of sodium alginate-acrylic acid for the controlled release of ibuprofen. *Journal of Applied Polymer Science*, *99*, 2671–2678.
- Rangel-Rodríguez, A. M., Conxita, S., Susana, V., Flores-Gallardo, S. G., Contreras-Esquível, J. C., & Licea-Jiménez, L. (2014). Immobilization of Pectinesterase in Genipin-Crosslinked Chitosan Membrane for Low Methoxyl Pectin Production. *Applied Biochemistry and Biotechnology*, *174*, 2941–2950.
- Ratzinger, G., Wang, X., Wirth, M., & Gabor, F. (2010). Targeted PLGA microparticles as a novel concept for treatment of lactose intolerance. *Journal of Controlled Release: Official Journal of the Controlled Release Society*, *147*, 187–92.
- Rault, I., Frei, V., Herbage, D., Abdul-Malak, N., & Huc, A. (1996). Evaluation of different chemical methods for cross-linking collagen gel, films and sponges. *Journal of Materials Science: Materials in Medicine*, *7*, 215–221.
- Reddy, T., & Tammishetti, S. (2002). Gastric resistant microbeads of metal ion cross-linked carboxymethyl guar gum for oral drug delivery. *Journal of Microencapsulation*, *19*, 311–318.
- Rose, J., Pacelli, S., Haj, A., Dua, H., Hopkinson, A., White, L., & Rose, F. (2014). Gelatin-Based Materials in Ocular Tissue Engineering. *Materials*, *7*, 3106–3135.
- Rubino, O. P., Kowalsky, R., & Swarbrick, J. (1993). Albumin microspheres as a drug delivery system: relation among turbidity ratio, degree of cross-linking, and drug release. *Pharmaceutical Research*, *10*, 1059–65.
- Sagis, L. M. C. (2008). Dynamics of controlled release systems based on water-in-water emulsions: a general theory. *Journal of Controlled Release: Official Journal of the Controlled Release Society*, *131*, 5–13.
- Samuel, L. (2012). How does lactose affect gastrointestinal function? Retrieved February 6, 2018, from <http://www.interactive-biology.com/4025/how-lactose-affects-gi-function/>
- Santonocito, C., Scapaticci, M., Guarino, D., Annicchiarico, E. B., Lisci, R., Penitente, R., Gasbarrini, A., Zuppi, C., Capoluongo, E. (2015). Lactose intolerance genetic testing: Is it useful as routine screening? Results on 1426 south-central Italy patients. *Clinica Chimica Acta*, *439*, 14–17.
- Saqib, S., Akram, A., Halim, S. A., & Tassaduq, R. (2017). Sources of β -galactosidase and its applications in food industry. *3 Biotech*, *7*, 1–7.
- Sawada, S., & Akiyoshi, K. (2010). Nano-Encapsulation of Lipase by Self-Assembled Nanogels: Induction of High Enzyme Activity and Thermal Stabilization. *Macromolecular Bioscience*, *10*, 353–358.
- Schachschal, S., Adler, H.-J., Pich, A., Wetzels, S., Matura, A., & van Pee, K.-H. (2011). Encapsulation of enzymes in microgels by polymerization/cross-linking in aqueous droplets. *Colloid and Polymer Science*, *289*, 693–698.
- Schmitt, C., Sanchez, C., Desobry-Banon, S., & Hardy, J. (1998). Structure and technofunctional properties of protein-polysaccharide complexes: a review. *Critical Reviews in Food Science and Nutrition*, *38*, 689–753.

- Scholten, E., Visser, J. E., Sagis, L. M. C., & van der Linden, E. (2004). Ultralow interfacial tensions in an aqueous phase-separated gelatin/dextran and gelatin/gum Arabic system: a comparison. *Langmuir : The ACS Journal of Surfaces and Colloids*, *20*, 2292–7.
- Schrader, B. (1995). *Infrared and Raman Spectroscopy: Methods and Applications*. Weinheim, Germany: Wiley-VCH Verlag GmbH. doi:10.1002/9783527615438.fmatter
- Semenova, M. G. (1996). Factors determining the character of biopolymer-biopolymer interactions in multicomponent aqueous solutions modeling food systems. In *Macromolecular Interactions in Food Technology* (pp. 37–49).
- Semenova, M. G., & Dickinson, E. (2010). Biopolymers in Food Colloids: Thermodynamics and Molecular Interactions. doi:10.1163/ej.9789004171862.i-370
- Sheldon, R. A., & van Pelt, S. (2013). Enzyme immobilisation in biocatalysis: why, what and how. *Chem. Soc. Rev.*, *42*, 6223–6235.
- Shewan, H. M., & Stokes, J. R. (2013). Review of techniques to manufacture micro-hydrogel particles for the food industry and their applications. *Journal of Food Engineering*, *119*, 781–792.
- Shumilina, E. V., & Shchipunov, Y. A. (2002). Chitosan–Carrageenan Gels. *Colloid Journal*, *64*, 372–378.
- Sibel, R., & Jones, S. A. (1996). *Handbook of Fat Replacers*. CRC Press.
- Singer, Yamamoto, & Latella. (1992). 5171603. U.S. patent: US.
- Singh, P., Medronho, B., Miguel, M. G., & Esquena, J. (2018). On the encapsulation and viability of probiotic bacteria in edible carboxymethyl cellulose-gelatin water-in-water emulsions. *Food Hydrocolloids*, *75*, 41–50.
- Solorio, L., Zwolinski, C., Lund, A. W., Farrell, M. J., & Jan, P. (2011). Gelatin microspheres crosslinked with genipin for local delivery of growth factors, *4*, 514–523.
- Song, Y., Sauret, A., & Shum, H. C. (2013). All-aqueous multiphase microfluidics. *Biomicrofluidics*, *7*. doi:10.1063/1.4827916
- Southwest Research Institute Website. (2015). Spinning Disk Atomisation. Retrieved from <http://www.swri.org/4org/d01/microenc/microen/atomization.htm>
- Srivastava, R., Brown, J. Q., Zhu, H., & McShane, M. J. (2005). Stable Encapsulation of Active Enzyme by Application of Multilayer Nanofilm Coatings to Alginate Microspheres. *Macromolecular Bioscience*, *5*, 717–727.
- Stenekes, R. J., Franssen, O., van Bommel, E. M., Crommelin, D. J., & Hennink, W. E. (1998, April). The preparation of dextran microspheres in an all-aqueous system: effect of the formulation parameters on particle characteristics. *Pharmaceutical Research*.
- Stenekes, R. J., Franssen, O., van Bommel, E. M., Crommelin, D. J., & Hennink, W. E. (1999). The use of aqueous PEG/dextran phase separation for the preparation of dextran microspheres. *International Journal of Pharmaceutics*, *183*, 29–32.
- Stokes, J. R., Wolf, B., & Frith, W. J. (2001). Phase-separated biopolymer mixture rheology: Prediction using a viscoelastic emulsion model. *Journal of Rheology*, *45*, 1173.
- Sui, Z., King, W. J., & Murphy, W. L. (2007). Dynamic Materials Based on a Protein Conformational Change. *Advanced Materials*, *19*, 3377–3380.
- Sundararaghavan, H. G., Monteiro, G. A., Lapin, N. A., Chabal, Y. J., Miksan, J. R., & Shreiber, D. I.

- (2008). Genipin-induced changes in collagen gels: Correlation of mechanical properties to fluorescence. *J Biomed Mater Res*, 87, 308–320.
- Sung, H.-W., Huang, D.-M., Chang, W.-H., Huang, R.-N., & Hsu, J.-C. (1999). Evaluation of gelatin hydrogel crosslinked with various crosslinking agents as bioadhesives: In vitro study. *Journal of Biomedical Materials Research*, 46, 520–530.
- Sung, H.-W., Huang, R.-N., Huang, L. L. H., & Tsai, C.-C. (1999). In vitro evaluation of cytotoxicity of a naturally occurring cross-linking reagent for biological tissue fixation. *Journal of Biomaterials Science, Polymer Edition*, 10, 63–78.
- Sungur, S. (1999). Investigations on drug release systems using CMC crosslinked with ferric ions. *Artificial Cells, Blood Substitutes, and Immobilization Biotechnology*, 27, 279–90.
- Swallow, D. M. (2003). Genetics of Lactase Persistence and Lactose Intolerance. *Annual Review of Genetics*, 37, 197–219.
- Tadros, T. F. (Ed.). (2009). *Emulsion Science and Technology*. Weinheim, Germany: Wiley-VCH Verlag GmbH & Co. KGaA. doi:10.1002/9783527626564
- Tadros, T. F. (2013). Emulsion Formation, Stability, and Rheology. In *Emulsion Formation and Stability* (pp. 1–75). Weinheim, Germany: Wiley-VCH Verlag GmbH & Co. KGaA.
- Tadros, T., Izquierdo, P., Esquena, J., & Solans, C. (2004). Formation and stability of nano-emulsions. *Advances in Colloid and Interface Science*, 108–109, 303–318.
- Tan, J. P. K., & Tam, K. C. (2007). Application of drug selective electrode in the drug release study of pH-responsive microgels. *Journal of Controlled Release*, 118, 87–94.
- Tanriseven, A., & Doğan, Ş. (2002). A novel method for the immobilization of β -galactosidase. *Process Biochemistry*, 38, 27–30.
- Taqiuddin, E., & Amiji, M. (2004). Enzyme immobilization in novel alginate-chitosan core-shell microcapsules. *Biomaterials*, 25, 1937–1945.
- Tolstoguzov, V. (2003). Some thermodynamic considerations in food formulation. *Food Hydrocolloids*, 17, 1–23.
- Tombs, M. P., & Peacocke, A. R. (1974). The Osmotic Pressure of Biological Macromolecules. doi:10.1016/0307-4412(75)90013-8
- Touyama, R., Takeda, Y., Inoue, K., Kawamura, I., Yatsuzuka, M., Ikumoto, T., ... Inouye, H. (1994). Studies on the blue pigments produced from genipin and methylamine. I. Structures of the brownish-red pigments, intermediates leading to the blue pigments. *Chemical and Pharmaceutical Bulletin*, 42, 668–673.
- Tromp, R. H., Rennie, A. R., & Jones, R. A. L. (1995). Kinetics of the Simultaneous Phase Separation and Gelation in Solutions of Dextran and Gelatin. *Macromolecules*, 28, 4129–4138.
- Tuinier, R. (1999). Phase behavior of casein micelles/exocellular polysaccharide mixtures: Experiment and theory. *Journal of Chemical Physics*, 110, 9296–9304.
- Tuinier, R., Fan, T. H., & Taniguchi, T. (2015). Depletion and the dynamics in colloid-polymer mixtures. *Current Opinion in Colloid and Interface Science*, 20, 66–70.
- Turgeon, S. L., Beaulieu, M., Schmitt, C., & Sanchez, C. (2003). Protein-polysaccharide interactions: Phase-ordering kinetics, thermodynamic and structural aspects. *Current Opinion in Colloid and Interface Science*, 8, 401–414.

- Turner, K. M., Pasut, G., Veronese, F. M., Boyce, A., & Walsh, G. (2011). Stabilization of a supplemental digestive enzyme by post-translational engineering using chemically-activated polyethylene glycol. *Biotechnology Letters*, *33*, 617–621.
- Turner, P. A., Thiele, J. S., & Stegemann, J. P. (2017). Growth factor sequestration and enzyme-mediated release from genipin-crosslinked gelatin microspheres. *Journal of Biomaterials Science, Polymer Edition*, *28*, 1826–1846.
- Vesa, T. H., Marteau, P., & Korpela, R. (2000). Lactose Intolerance. *Journal of the American College of Nutrition*, *19*, 165S–175S.
- Vilchez, S., Samitier, V., Porras, M., Esquena, J., & Erra, P. (2009). Chitosan Hydrogels Covalently Crosslinked with a Natural Reagent. *Tenside Surfactants Detergents*, *46*, 13–17.
- Vis, M., Opdam, J., Vant Oor, I. S. J., Soligno, G., Van Roij, R., Tromp, R. H., & Ern , B. H. (2015). Water-in-Water Emulsions Stabilized by Nanoplates. *ACS Macro Letters*, *4*, 965–968.
- Vold, R. D. (1965). Emulsions: Theory and practice (Becher, Paul). *Journal of Chemical Education*, *42*, 692.
- Vrij, A. (1976). Polymers at Interfaces and the Interactions in Colloidal Dispersions. *Pure and Applied Chemistry*, *48*, 471–483.
- Wang, A., Cui, Y., Li, J., & Van Hest, J. C. M. (2012). Fabrication of gelatin microgels by a “cast” strategy for controlled drug release. *Advanced Functional Materials*, *22*, 2673–2681.
- Wang, L., Wang, Y., Qu, J., Hu, Y., You, R., & Li, M. (2013). The Cytocompatibility of Genipin-Crosslinked Silk Fibroin Films. *Journal of Biomaterials and Nanobiotechnology*, *04*, 213–221.
- Wang, S., Van Dijk, J. A. P. P., Odijk, T., & Smit, J. A. M. (2001). Depletion-induced demixing in aqueous protein-polysaccharide solutions. *Biomacromolecules*, *2*, 1080–1088.
- Welsch, N., Becker, A. L., Dzubiella, J., & Ballauff, M. (2012). Core-shell microgels as “smart” carriers for enzymes. *Soft Matter*, *8*, 1428.
- Welsch, N., Wittemann, A., & Ballauff, M. (2009). Enhanced activity of enzymes immobilized in thermoresponsive core-shell microgels. *Journal of Physical Chemistry B*, *113*, 16039–16045.
- Williams, M., Fabri, D., & Hubbard, C. (2001). Kinetics of droplet growth in gelatin/maltodextrin mixtures following thermal quenching. *Langmuir*, 3412–3418.
- Wills, P. R., Jacobsen, M. P., & Winzor, D. J. (1996). Direct analysis of solute self-association by sedimentation equilibrium. *Biopolymers*, *38*, 119–130.
- Wolf, B., Scirocco, R., Frith, W., & Norton, I. (2000a). Shear-induced anisotropic microstructure in phase-separated biopolymer mixtures. *Food Hydrocolloids*, *14*, 217–225.
- Wolf, B., Scirocco, R., Frith, W., & Norton, I. (2000b). Shear-induced anisotropic microstructure in phase-separated biopolymer mixtures. *Food Hydrocolloids*, *14*, 217–225.
- Wu, Y.-T., Lin, D.-Q., & Zhu, Z.-Q. (1998). Thermodynamics of aqueous two-phase systems—the effect of polymer molecular weight on liquid–liquid equilibrium phase diagrams by the modified NRTL model. *Fluid Phase Equilibria*, *147*, 25–43.
- Xia, H., Li, B.-Z., & Gao, Q. (2017). Effect of molecular weight of starch on the properties of cassava starch microspheres prepared in aqueous two-phase system. *Carbohydrate Polymers*, *177*, 334–340.
- Xiao, C., Li, H., & Gao, Y. (2009). Preparation of fast pH-responsive ferric

- carboxymethylcellulose/poly(vinyl alcohol) double-network microparticles. *Polymer International*, 58, 112–115.
- Yao, C. H., Liu, B. S., Chang, C. J., Hsu, S. H., & Chen, Y. S. (2004). Preparation of networks of gelatin and genipin as degradable biomaterials. *Materials Chemistry and Physics*, 83, 204–208.
- Yasukawa, M., Kamio, E., & Ono, T. (2011). Monodisperse water-in-water-in-oil emulsion droplets. *ChemPhysChem*, 12, 263–266.
- Yu, M., & Arons, J. . (1994). Phase behaviour of aqueous solutions of neutral and charged polymer mixtures. *Polymer*, 35, 3499–3502.
- Yuan, W., Yang, J., Kopecková, P., & Kopecek, J. (2008). Smart hydrogels containing adenylate kinase: translating substrate recognition into macroscopic motion. *Journal of the American Chemical Society*, 130, 15760–1.
- Zhang, H., Mardyani, S., Chan, W. C. W., & Kumacheva, E. (2006). Design of biocompatible chitosan microgels for targeted pH-mediated intracellular release of cancer therapeutics. *Biomacromolecules*, 7, 1568–72.
- Zhang, Y., Sun, G., Wang, X., Wang, L., Hu, M., Wang, Z., & Tao, Y. (2014). Efforts on membrane properties and enzymes by adding divalent cations and sodium carboxymethyl cellulose. *Carbohydrate Polymers*, 106, 94–100.
- Zhang, Y., Zhu, W., Wang, B., & Ding, J. (2005). A novel microgel and associated post-fabrication encapsulation technique of proteins. *Journal of Controlled Release*, 105, 260–268.
- Zhang, Z., Zhang, R., Chen, L., & McClements, D. J. (2016). Encapsulation of lactase (β -galactosidase) into κ -carrageenan-based hydrogel beads: Impact of environmental conditions on enzyme activity. *Food Chemistry*, 200, 69–75.
- Zhang, Z., Zhang, R., Chen, L., Tong, Q., & McClements, D. J. (2015). Designing hydrogel particles for controlled or targeted release of lipophilic bioactive agents in the gastrointestinal tract. *European Polymer Journal*, 72, 698–716.
- Zhang, Z., Zhang, R., & McClements, D. J. (2017). Lactase (B-galactosidase) encapsulation in hydrogel beads with controlled internal pH microenvironments: Impact of bead characteristics on enzyme activity. *Food Hydrocolloids*, 67, 85–93.
- Zhivkov, A. M. (2013). Electric properties of carboxymethyl cellulose. *Cellul.: Fundam. Aspects*, 197–226.

Chapter 8
ANNEXES

8 Annexes

8.1 Calibration Curve of Ortho-Nitrophenol

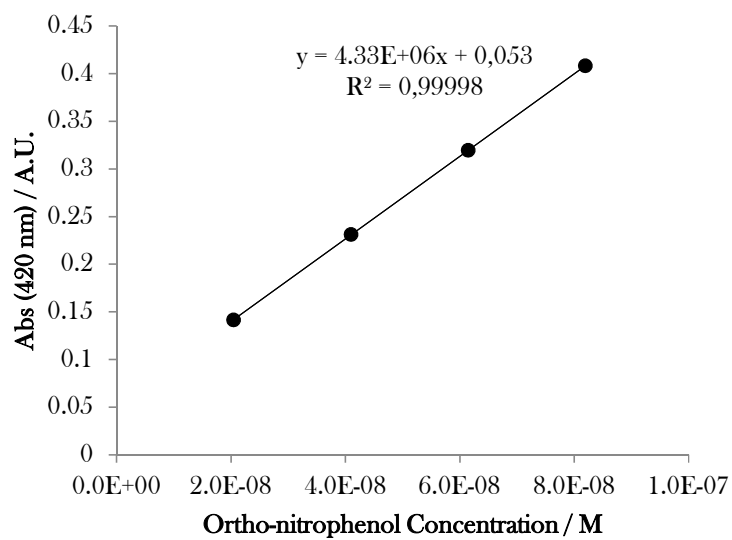


Figure 8.1. Absorption at 420 nm of different ortho-nitrophenol concentrations.

8.2 Size Determination of Microgels: Microscopy versus Laser Diffraction - Number Size Distribution of crosslinked Microgels

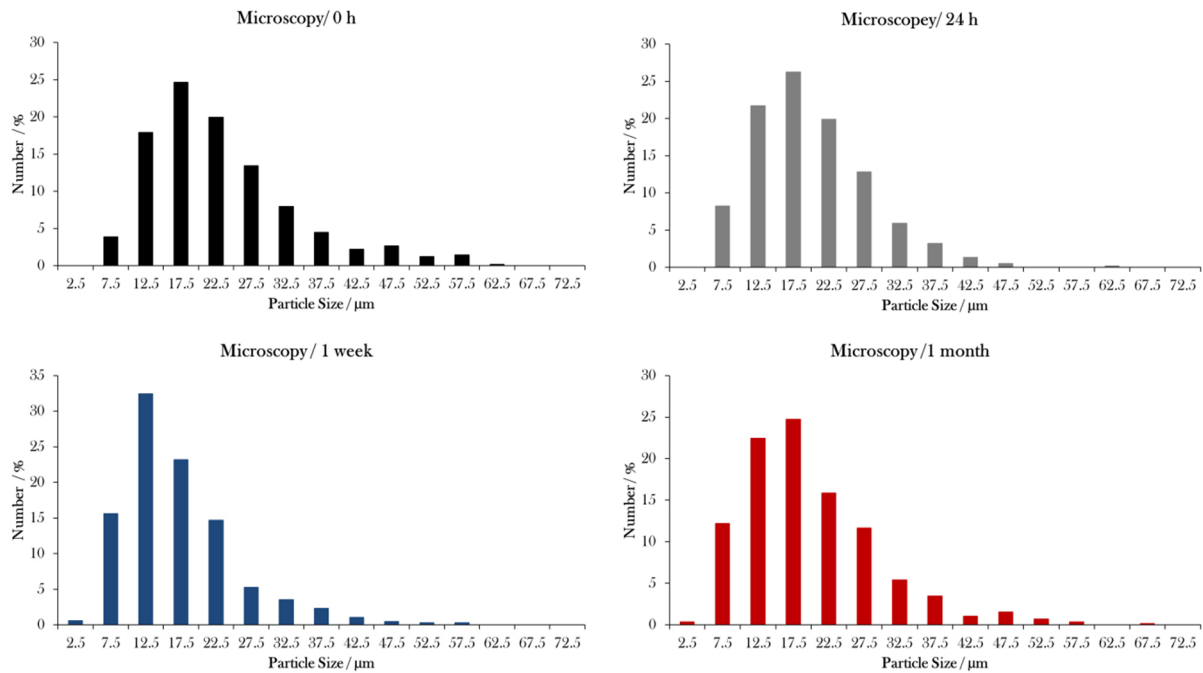


Figure 8.2. Number Size distributions of crosslinked microgels, (prepared from a 3 % Gel / 20 % MD (1 mM Genipin) emulsion), measured by microscopy, at time 0 h, 24 h, 1 week and 1 month. Data used for transformation into volume size distribution and comparison with data obtained from laser diffraction measurements.

8.3 Publications

During his PhD Thesis, Yoran Beldengrün contributed to the following publications:

- Y. Beldengrün, J. Aragon, S. Prazeres, G. Montalvo, J. Miras, J. Esquena, *Gelatin-Maltodextrin Water-in-Water (W/W) Emulsions for the Preparation of Crosslinked Enzyme-Loaded Microgels*, Langmuir, 2018 (article accepted for publication)
- J. Esquena, Y. Beldengrün, *Formulación y Aplicaciones de Nuevas Emulsiones de Tipo Agua-en-Agua (W/W)*, Noticias de Cosmética y Perfumería (NCP), editado por la Sociedad Española de Químicos Cosméticos (SEQC) nº 357, octubre 2017.

This document is confidential and is proprietary to the American Chemical Society and its authors. Do not copy or disclose without written permission. If you have received this item in error, notify the sender and delete all copies.

Gelatin-Maltodextrin Water-in-Water (W/W) Emulsions for the Preparation of Crosslinked Enzyme-Loaded Microgels

| | |
|-------------------------------|---|
| Journal: | <i>Langmuir</i> |
| Manuscript ID | la-2018-01599k |
| Manuscript Type: | Article |
| Date Submitted by the Author: | 14-May-2018 |
| Complete List of Authors: | Beldengrün, Yoran; Spanish Council for Scientific Research (CSIC), Institute of Advanced Chemistry of Catalonia (IQAC) Aragon, Jordi; Spanish Council for Scientific Research (CSIC), Institute of Advanced Chemistry of Catalonia (IQAC) Prazeres, Sofia; University of Alcalá, Physical Chemistry Montalvo, Gemma; University of Alcalá, Physical Chemistry Miras, Jonathan; Spanish Council for Scientific Research (CSIC), Institute of Advanced Chemistry of Catalonia (IQAC) Esquena, Jordi; Spanish Council for Scientific Research (CSIC), Institute of Advanced Chemistry of Catalonia (IQAC) |
| | |

SCHOLARONE™
Manuscripts

Gelatin-Maltodextrin Water-in-Water (W/W) Emulsions for the Preparation of Crosslinked Enzyme-Loaded Microgels

Yoran Beldengrün¹, Jordi Aragon¹, Sofia F. Prazeres², Gemma Montalvo², J. Miras¹, Jordi Esquena^{1,*}

¹*Institute of Advanced Chemistry of Catalonia, Spanish National Research Council (IQAC-CSIC) and Networking Research Center on Bioengineering, Biomaterials and Nanomedicine (CIBER-BBN), Barcelona, Spain*

²*University of Alcalá, Department of Analytical Chemistry, Physical Chemistry and Chemical Engineering, Alcalá de Henares, Madrid, Spain*

Corresponding author: jordi.esquena@iqac.csic.es

Keywords: *W/W Emulsion, Phase Behavior, Microgel Formation, Genipin, β -Galactosidase, encapsulation.*

Abstract

Crosslinked gelatin microgels were formed in gelatin-in-maltodextrin water-in-water (W/W) emulsions and evaluated as carriers of the enzyme β -Galactosidase. The phase behaviour of aqueous gelatin/maltodextrin mixtures was studied in detail, focusing in the multiphase region of the phase diagram that is constituted by three equilibrium phases: two immiscible aqueous phases plus one solid phase. The solid phase was analysed by Raman spectroscopy, and water-in-water emulsions were formed within the multiphase region. Gelation of the dispersed gelatin droplets was induced by cooling and crosslinking with genipin, which is a natural crosslinking reagent of low toxicity, leading to the formation of gelatin microgel particles. These microgels were studied as delivery vehicles for the enzyme lactase, used as a model active component. Various incorporation methods of the enzyme were tested, to achieve highest encapsulation yield and activity recovery. Microgel particles, loaded with the enzyme, can be freeze-dried, and the enzyme remained active after a complete cycle of freeze-drying and rehydration. The stability of the enzyme at 37 °C under gastric and neutral pH conditions was tested and led to the conclusion that the crosslinked microgels could be suitable for use in food-industry, where β -Gal carriers are of interest for hydrolysing lactose in milk products.

INTRODUCTION

Water-in-oil (W/O) or oil-in-water (O/W) emulsions have since long time been preferential templates for nano- and microparticles, despite the fact that using surfactants can be a disadvantage for drug delivery where good biocompatibility is required. To assure biocompatibility of Drug Delivery Systems (DDS), an interesting alternative is using water-in-water (W/W) emulsions as templates to obtain DDS.¹ Water-in-water emulsions are colloidal dispersions made of two immiscible aqueous phases that are in thermodynamic equilibrium, in absence of both oil and surfactant.²

Mixtures of two hydrophilic polymers in aqueous solution can produce three different situations in phase behavior: (a) Complete miscibility, in the case of weak interactions between the two kinds of polymers; (b) Associative phase separation, with formation of a precipitate/coacervate, because of strong attractive interactions between the two polymers; or (c) Segregative phase separation induced by repulsive interactions between the polymers. The latter case leads to the formation of Aqueous Two-Phase Systems, in which two aqueous solutions in thermodynamic equilibrium are formed, where each phase is enriched with one of the polymers and saturated with the other polymer. In these biphasic aqueous systems, W/W emulsion droplets can be formed by dispersing one phase into the other phase.²

More than 100 mixed aqueous mixtures, containing proteins and polysaccharides in aqueous solution, are known to experience phase separation.³ This segregative phase separation can occur by thermodynamic incompatibility between a charged protein and a neutral or similarly charged polysaccharide.⁴ Two main factors can contribute to the thermodynamic incompatibility between the two macromolecules, and the main one is their difference in hydration, which can be explained in terms of the Flory-Huggins interaction parameters between the two polymers and their respective interactions with water.⁵ Usually, the most charged polymer is highly hydrated, and it expels the less hydrated polymer. The second factor that induces phase segregation in two immiscible aqueous phases is the “excluded volume” or “steric exclusion” effect. It implies that, above a critical concentration of polymers, there is an osmotic driving force that favours separation of the system into two aqueous phases, each one enriched in one of the polymers.^{6,7} Because of that, phase segregation is promoted by differences in molecular weight, and many systems that show aqueous phase segregation consist of a charged polymer with very high molecular weight, mixed with a non-charged polymer with lower molecular weight.

W/W emulsions can be obtained by applying agitation in such aqueous biphasic systems, simply by dispersing the phase with smaller volume fraction, forming droplets into the phase that has a larger volume fraction. W/W emulsions are governed by the same physical principles as W/O or O/W emulsions, including the rules for droplet break up and coalescence.⁸ However, typically for W/W emulsions, partial miscibility of the two polymers occurs, and interfacial tension is often extremely low: in the order of 0.01 mN/ m for a gelatin-maltodextrin interface, compared to around 50 mN/ m for a typical hydrocarbon-water interface.^{9,10} Such low tensions are due to the small differences in composition across water/water interfaces, a consequence of the fact that both phases have water as the same solvent. Moreover, interfacial tensions decrease as the phase compositions become close to the critical point.

1
2
3 Surfactants, due to their amphiphilic nature, having both hydrophilic and hydrophobic groups,
4 are not suitable for stabilising the water-water interface of W/W emulsions. Therefore, effective
5 stabilization of emulsions is an important challenge for physical chemists. One method is
6 adsorption of particles, such as silica, nanorods, nanoplates, microgels etc.,¹¹ at the water-water
7 interface. Preparation of water-in-water Pickering emulsions was first reported in 2008 by
8 Poortinga,¹² and later, it has been studied in great detail by Nicolai, Murray and their
9 coworkers.¹³ For a proper stabilization of W/W Pickering emulsions, the particles have to
10 become partially wetted by both aqueous phases, allowing the formation of a stabilizing layer of
11 particles that are adsorbed on the interface. For example, recent results from Benyahia and co-
12 workers have shown that particles coated with polysaccharides can strongly adsorb on W/W
13 emulsions interfaces, and thus, these surface functionalized particles can stabilize W/W
14 emulsion droplets.¹⁴

15
16
17 Another method is adding a crosslinking agent or changing environmental conditions such as
18 temperature, pH or solvent quality, to allow solidification/gelling and thus stabilisation of the
19 emulsion and formation of polymer particles, in surfactant-free conditions. Over this way,
20 microgels can be formed in a completely mild aqueous system by this simple and effective
21 method. Microgels, defined as gel particles of any shape with an equivalent diameter of
22 approximately 0.1 to 100 μm ,¹⁵ can be obtained by chemical crosslinking in the disperse phase
23 of W/W emulsions, and might have the ability to swell in response to changes (temperature,
24 ionic strength, osmotic pressures, etc.) in the external medium.

25
26
27 An early report on formation of microgels, by this method based on polymer-polymer
28 immiscibility and free from organic solvents, was described in 1998 by Franssen and Hennink¹⁶
29 and since then, it has been reported with a variety of different polymer systems. Most emulsions
30 were based on PEG or PVA, mixed with dextran or starch, in which the polymer in the
31 dispersed phase was crosslinked by photo initiation or ionic complexation.¹⁷⁻²³ However very
32 few studies reported microgel formation, based on emulsions free from synthetic
33 polymers.^{16,24,25} Natural biopolymers are of great interest in the field of food science and drug
34 delivery as they are intrinsically biodegradable, abundant in nature, renewable, nontoxic, and
35 relatively cheap.

36
37
38 In this study, we examined the possibility of forming gelatin microgels, crosslinked with
39 genipin, obtained from gelatin-maltodextrin emulsions. Gelatin/maltodextrin mixtures have
40 been studied in detail because of the easy formation of both gelatin-in-maltodextrin or
41 maltodextrin-in-gelatin emulsions, which can be kinetically trapped thanks to the gelling
42 properties of gelatin,²⁶ allowing the formation of microgels with controlled size and morphology
43 detail.^{1,9,27-35}

44
45
46 Our aim is using the crosslinked gelatin microgels as carriers of β -Galactosidase (β -Gal). β -Gal,
47 is usually produced within the brush border of the small intestine and catalyzes the hydrolysis of
48 lactose (β -D-galactopyranosyl-(1 \rightarrow 4)-D-glucose) into D-glucose and D-galactose. Lactose
49 intolerant persons (70% of the world population³⁶) have a deficiency in β -Gal and as a
50 consequence are dependent on exogenous supply of this enzyme to allow the digestion of dairy
51 products. As β -Gal in its free form is usually deactivated under gastrointestinal tract
52 conditions,³⁷ encapsulation of the enzyme into protective matrices of various materials has been
53 subject of previous studies.³⁸⁻⁴¹

1
2
3
4
5
6
7
8
9
10
11
12
13
14
15
16
17
18
19
20
21
22
23
24
25
26
27
28
29
30
31
32
33
34
35
36
37
38
39
40
41
42
43
44
45
46
47
48
49
50
51
52
53
54
55
56
57
58
59
60

Gelatin microgels are very suitable for delivery of enzymes, as they are hydrophilic and contain a large amount of water. This allows the enzymes to be incorporated with only moderate conformational changes and with limited aggregation^{42,43} preserving the stability of the enzyme protecting it and acting as a buffer to the acidic environment of the acidic gastric pH.

MATERIALS AND METHODS

Materials

Gelatin (abbreviated as Gel) was from bovine skin, gel strength ~225 g Bloom, Type B, with 50-100 kDa molecular mass. Its gelation occurs below 30-35°C approximate temperature range. Maltodextrin (abbreviated as MD), with dextrose equivalent 4.0-7.0, had a molecular mass of 3.6 kDa. Gelatin, Maltodextrin, Fluorescein isothiocyanate isomer I ($\geq 90\%$) (FITC), KCl, HCl, MgCl₂, NaCl, Na₂CO₃, (NH₄)₂CO₃ and NaOH, were all supplied by Sigma-Aldrich (Spain). Genipin was purchased from Challenge Bioproducts Co. (Taiwan). EDTA and MgSO₄ were purchased at Fluka. NaHCO₃ was purchased at Panreac, KH₂PO₄, CaCl₂ and DMSO at Merck Millipore and K₂HPO₄·3H₂O was obtained from CalbioChem. The enzyme lactase, β -galactosidase (denoted as β -gal), extracted from *K. lactis*, EC 3.2.1.23, was provided by Chr. Hansen (Denmark) with activity of 5200 NLU/ g (= 113 μ kat/ g) in a concentration of 25 mg of protein/mL. The enzyme was supplied in a mixture of PEM buffer solution (prepared with 1 mM MgSO₄, 0.05 mM EDTA, 65 mM KH₂PO₄, 35 mM K₂HPO₄·3H₂O in water, with a total pH 6.5) and glycerol (1:1 w/w). Ortho-Nitrophenyl- β -galactoside (ONPG) was obtained from Carbosynth. All water used was filtered by the water purification system Millipore model Synergy Smart UV (resistivity at 25 °C: 18.2 M Ω · cm; conductivity 0.056 μ S/ cm, water quality: type I, ion concentration < 1 μ g/ L).

Phase Behaviour

Mixtures of gelatin and maltodextrin of different concentrations were prepared in order to study their phase behaviour in water. The mixture had a pH of approximately 5. The 25 wt % gelatin stock solutions were prepared by dispersing gelatin into cold water and then stirred continuously at 60 °C during 30 min. For the 30 wt % maltodextrin stock solutions, maltodextrin was dispersed into cold water and stirred continuously at 95 °C during 30 min in tightly sealed glass vial to avoid solvent evaporation. The gelatin and maltodextrin stock solutions at 50 °C were mixed together with water to obtain samples of gelatin concentrations ranging between 0-12 wt% and maltodextrin of 0-22 wt%. The samples were vortexed during 10 seconds and then placed into a thermostated bath at 50 °C constant temperature, for a period of 5 days. Phase behaviour was consequently observed.

The samples are denoted from now on as x % Gel/ y % MD (z mM Genipin). For example, 3 % Gel/ 20 % MD (5 mM Gen) denotes a mixture of 3 wt % gelatin / 20 wt % maltodextrin (5 mM genipin). If no genipin was used, the brackets are omitted.

Furthermore, stability of some samples was assessed from multiple light scattering measurements by means of a Turbiscan™ Lab Expert (Formulaction) at constant temperature (50 °C) and $\lambda = 880$ nm. For this purpose, 18 g of sample were introduced in a glass measurement cell tightly stoppered to avoid solvent evaporation. Transmission and

1
2
3
4
5
6
7
8
9
10
11
12
13
14
15
16
17
18
19
20
21
22
23
24
25
26
27
28
29
30
31
32
33
34
35
36
37
38
39
40
41
42
43
44
45
46
47
48
49
50
51
52
53
54
55
56
57
58
59
60

backscattering data were acquired for a period of 5 days. Raman spectra were obtained at room temperature using a confocal micro-Raman (Jobin-Yvon LabRam HR 800), coupled to an optical microscope (Olympus BXFM). The micro-Raman was equipped with a Laser Diode (TEC-120 de Sacher Lasertechnik) emitting at $\lambda = 785$ nm. Radiation power was 0.5-4 mW.

For the identification of the phases in the emulsions, gelatin was previously labelled by adding 0.1 wt % FITC solution (2 % w/v in Dimethyl sulfoxide) directly to a 25 wt % gelatin solution and stirring during 2 h at 40 °C.

Formation and Purification of Microgels

For the formation of microgels, 3 % Gel/ 20 % MD emulsions with a given amount of genipin were prepared. The solvents were either water or PEM buffer, having the latter more favourable pH and ionic conditions for β -Gal activity. In a typical experiment, gelatin-in-maltodextrin emulsions (volume of 6 mL) were formed by homogenisation for 1 min at 9500 rpm, using an IKA ULTRA-TURRAX[®] homogenizer equipped with a S25N-10G dispersing element. Then, the dispersions were continuously stirred at ~500 rpm with a magnet stirrer, in order to allow gelatin-genipin crosslinking reactions to occur. Different conditions, varying genipin concentration, stirring temperature and time, were tested. In order to improve colloidal stability, preventing particle aggregation, sample tubes were subsequently placed at 0 °C in ice bath for 1 min, and then samples were diluted by adding 0 °C cold solvent (either water or PEM buffer) at 2:1 ratio with respect to the initial sample volume.

Microgels were purified by a simple centrifugation-resuspension method. First, gelatin microgel suspensions were sedimented by centrifugation at soft conditions (10 min, 2500 rpm, 5 °C) and the supernatant, rich in maltodextrin, was removed. Preliminary experiments showed that these conditions were sufficient for the controlled sedimentation of particles, which did not become irreversibly aggregated. Then, the microgels were redispersed, by vortex agitation, in the same volume of purified milliQ water. This purification procedure was repeated once more. Finally, to deflocculate the partially aggregated microgels, the samples were ultrasonicated (applying a power of 80 W, with 4 on/off cycles with a duration of 5 s/ 20 s for each cycle) by means of the Sonoplus Ultrasonic homogenizer HD3200 (Bandelin). Some selected samples were freeze-dried by freezing them in a carbon-ice/acetone mixture and consequently introduced into the freeze dryer (Christ Alpha 2-4 LD Plus) and kept there till they were totally dried.

Particle size, expressed as the median of the number size distribution, was determined by using an optical microscope (Olympus model BX51TRF-6, coupled to a digital camera Olympus DP73) fitted with a calibrated micrometer scale. Image analysis of the micrographs was performed using Image J software and number size distribution was obtained from measuring a minimum of 300 particles. The polydispersity was calculated as the interquartile range (IQR, which is the difference between 75 and 25 percentiles) of the number size distribution. The polydispersity is indicated in the size plots, as the error bars.

Incorporation of β -Gal Enzyme into Microgels

For the purpose of introducing the enzyme lactase into the microgel particles, 3 % Gel/ 20 % MD emulsions in PEM buffer were used and homogenised by stirring at 500 rpm. The temperatures of treatment were selected taking into account the temperature sensitiveness of gelatin gelation and enzyme activity. For this reason, solutions of gelatin and enzyme were mixed at 35 °C, emulsions were treated with genipin at 30 °C, and gelatin microgels were treated at 25 °C. The rest of the preparation procedure (gelation of gelatin droplets and purification of microgel suspension) was the same, as detailed above.

Three different methods (summarised in Table 1) were tested to incorporate enzymes into the microgels, with the main objective to maximise encapsulation yield and minimising activity loss of enzyme. In all cases, the final enzyme concentration in the microgel suspension corresponded to approximately 1610x dilution of the enzyme stock solution, which results in an enzyme activity of 70 nkat/g. The differences between the methods are the moment at which the enzymes or genipin was added.

Table 1. Preparation methods of enzyme loaded microgels. Details in the text.

| | Method A | Method B1 | Method B2 |
|--------------------------------------|----------|------------------|-----------|
| Addition to Emulsion at 30 °C | Genipin | Genipin + Enzyme | Enzyme |
| Addition to Microgel at 25 °C | Enzyme | - | Genipin |

- *Method A: Addition of enzyme after microgel formation*
The enzyme was added to the 0 °C cold PEM buffer, in the last step of microgel production. The solution was consequently stirred with a magnet, at ~500 rpm, during 3 h at 25 °C.
- *Methods B1 and B2: Addition of the enzyme together with the gelatin solution*
 - *Method B1: Addition of genipin during emulsification.*
The enzyme was stirred together with the gelatin stock solution during 3 h at 35 °C. After addition of maltodextrin and genipin solutions, at 30 °C, emulsions were formed, crosslinking with genipin occurred, and microgels were obtained.
 - *Method B2: Addition of genipin after microgel formation.*
The enzyme was also stirred together with the gelatin stock solution during 3 h at 35 °C, but in this case, genipin was added to the 0 °C cold PEM buffer, after cooling down emulsions and forming microgels. Therefore, genipin was added to microgels that had been previously loaded with the enzyme. Afterwards, the mixture was placed at 25 °C, and stirred with a magnet during 3 h, to allow crosslinking reactions.

Finally, in all three cases, samples were cooled down at 0 °C and purified as detailed before, by centrifugation, extraction of supernatant and redispersion of microgels in PEM buffer.

Activity of β -Gal-loaded microgels

To evaluate the encapsulation yield, β -Gal enzymes were fluorescently labelled with FITC. β -Gal solutions were dissolved in a 0.1 M sodium carbonate buffer (pH 10) at an enzyme:buffer ratio of 10:1, and 5 vol % FITC solution (0.2 %, w/v) was added and stirred during 2h at 20°C. Excess free fluorescent dye was removed by passing the mixture through a Sephadex G-25 size-exclusion chromatography column.

β -Gal activity was determined by reacting 0.5 mL of the sample with 2.5 mL of 40 mM ortho-Nitrophenyl- β -galactoside (ONPG) at 30 °C. β -Gal catalyses the cleavage of ONPG into glucose and ortho-nitrophenol (ONP), which can be determined spectrophotometrically, by measuring absorbance at $\lambda = 420\text{nm}$. Samples were diluted accordingly in order to reach absorption between 0.2-1, in less than 25min. When reaching these conditions, the reaction was stopped with a 1mL of a pH 11 solution containing 0.5 M Na_2CO_3 and 0.13 M EDTA. The specific activity was determined as the formation rate of the product ONP, by using Lambert-Beers law and dividing by reaction time. Initial total enzyme activity was 70 nkat/ g in the solutions. **Error! Reference source not found.** illustrates the distribution of active and inactive enzyme in microgel solution, on basis of which the percentage of active enzyme, the encapsulation yield, and the activity recovery were calculated. The definitions of these parameters were adapted from literature.⁴⁴

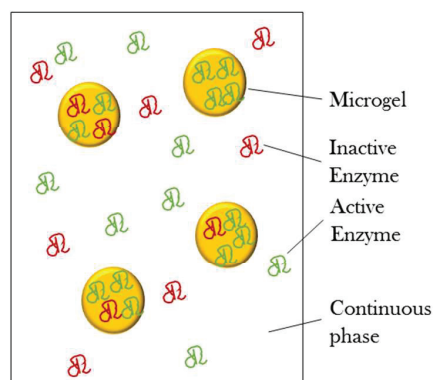


Figure 1. Illustration of a microgel solution, before purification, containing active and inactive enzymes within the microgels and the continuous phase (supernatant, when purifying by centrifugation).

The percentage of active enzyme was calculated as the ratio of the total enzyme activity (A_{tot}) in the sample containing the crosslinker genipin, with respect to the total enzyme activity in the control sample (without genipin) ($A_{tot}(\text{control})$).

$$\text{Percentage of active enzyme (\%)} = \frac{A_{tot}}{A_{tot}(\text{control})} \cdot 100 \quad (1)$$

The encapsulation yield of the enzyme was determined by calculating the ratio of the enzyme activity within the microgel A_{mg} dispersions in respect to the total enzyme activity A_{tot} (calculated as the sum of the activities of supernatants A_{sn} and microgel particles A_{mg}). This calculation assumes that the ratio of active/inactive enzyme is the same inside and outside the microgel particles.

$$\text{Encapsulation yield (\%)} = \frac{A_{mg}}{A_{sn} + A_{mg}} \cdot 100 = \frac{A_{mg}}{A_{tot}} \cdot 100 \quad (2)$$

Finally, activity recovery of encapsulated enzyme was calculated as the product of encapsulation yield and percentage of active enzyme.

$$\text{Activity recovery (\%)} = \frac{A_{mg}}{A_{tot}} \cdot \frac{A_{tot}}{A_{tot(\text{control})}} \cdot 100 = \frac{A_{mg(\text{sample})}}{A_{tot(\text{control})}} \cdot 100 \quad (3)$$

Stability of encapsulated enzyme

The influence of exposure to gastric pH and temperature conditions on the stability of microgels and β -Gal was investigated. Therefore enzyme-loaded microgel dispersions (prepared either in water or in PEM buffer) were added at 37 °C to the simulated gastric fluid (SGF) at a ratio of 1:10 (w/w). The SGF (pH 3) was formulated according to Minekus *et al.*,⁴⁵ in absence of gastric enzymes, with following ion concentrations; K^+ (7.8 mM), Na^+ (72.2 mM), Cl^- (70.2 mM), $H_2PO_4^-$ (0.9 mM), HCO_3^- (25.5 mM), Mg^{2+} (0.1 mM), NH_4^+ (1 mM), Ca^{2+} (0.15 mM). 6 M HCl was added to adjust the pH to 3. This mixture was then stirred for 2 h at 37 °C and activity was determined as a function of time.

RESULTS AND DISCUSSION

Phase Behaviour

After 5 days at 50 °C, mixtures (final pH \approx 5) of gelatin and maltodextrin solutions in water, showed three different types of phase behaviour depending on the composition of the mixtures: At lower concentrations, the biopolymers experienced perfect miscibility; producing a single liquid phase (L). At slightly increased concentrations of the biopolymers, a precipitate forms resulting in a liquid coexisting with a solid phase, which slowly sediments on the vial bottom (L+S). Above a certain concentration threshold, phase separation of the liquid phase occurs, and two liquid phases and a solid precipitate co-exist (L_1+L_2+S). Figure 2 depicts the aqueous phase diagram of gelatin-maltodextrin mixtures, with some examples of emulsions observed under fluorescence optical microscopy.

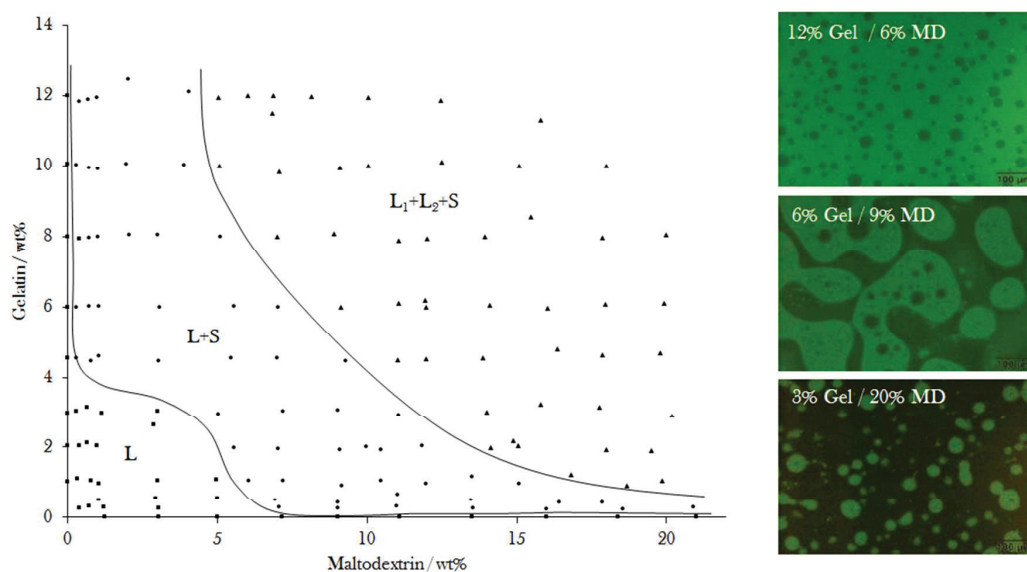


Figure 2. Phase diagram of the water/gelatin/maltodextrin system (pH \approx 5), observed at 50°C after 5 days of equilibration. The phase diagram can be divided into three regions: One liquid phase (L), a solid coexisting with a liquid phase (L+S) and a region, where two liquid phases and a solid phase coexist (L_1+L_2+S). Depending on the concentrations of the different biopolymers gelatin-in-maltodextrin (3 % Gel / 20 % MD), bicontinuous (6% Gel/ 9% MD) or maltodextrin-in-gelatin (12 % Gel/ 6 % MD) microstructures can be obtained, as observed by fluorescence optical microscopy (Green: FITC-labeled gelatin).

The nature of the emulsions (gelatin-in-maltodextrin, maltodextrin-in-gelatin or bicontinuous) can be clearly observed by fluorescence optical microscopy images of emulsions prepared with FITC-labeled gelatin (images in Fig. 2). Maltodextrin-in-gelatin emulsions were obtained in the case of 12 % Gel/ 6 % MD composition, whereas a gelatin-in-maltodextrin was formed at 12 % Gel/ 6 % MD composition. This was expected, and already described in the literature¹⁰, being known that the nature of the emulsion depends on the relative volumes of the two liquid phases. After applying agitation, the phase with the greater volume defines the continuous phase. Consequently, samples with a larger phase volume of gelatin solution tend to form maltodextrin-in-gelatin droplets, and vice versa. In the case of compositions that result in two phases with similar volumes (e.g. 6 % Gel/ 9 % MD), bicontinuous structures can also be observed, as also shown in Fig. 2. As expected, this bicontinuous emulsion was a transient unstable system, which could only be observed for a short period.

Comparing the obtained phase diagram with other previously described in the literature the tendency of the binodal line is similar, but depending on the reports, the curve is shifted from higher concentrations to lower concentrations^{1,10,46} or vice versa.³¹ This originates from the fact that different studies use different types of gelatin and maltodextrin polymers and physicochemical properties might differ on sources and from batch to batch. Moreover, temperature at which the phase diagram was studied also differed from study to study.

As mentioned before, our experiments show that a third phase is formed as solid-like sediment, which slowly appears. Turbidity measurements (results in supporting information, Fig. S1) indicated that formation of precipitate and starts to be detected after 2.5-4.5 days, depending on

1
2
3 the biopolymer ratio. With our system, we thus could not reproduce a previous report, where
4 precipitation of the biopolymers was only observed after centrifugation of the freshly prepared
5 sample at 45 °C.³¹
6

7
8 It should be noted that the phase behaviour of gelatin/maltodextrin system has been studied in
9 previous works.^{1,10,31,34} However, only few studies^{31,47} have reported about the existence of the
10 third solid phase that forms a precipitate in this biopolymer mixture. Precipitation, at a
11 temperature where both individual biopolymers are perfectly soluble in water, is unexpected and
12 unusual. The possibility of Maillard-type reactions should be ruled out since our conditions
13 (aqueous solutions at 50 °C) are not adequate for such reactions. Kasapis *et al.* analysed the
14 precipitate by optical rotation and indicated that it is mainly composed of maltodextrin,³¹ and
15 suggested that this insoluble solid phase formed by changes in conformation of the polymers.
16 We confirmed those results by analysing the precipitate extracted from a mixture of 3 % Gel/ 20
17 % MD with Raman Spectroscopy (Fig. 3). First, the reference Raman spectra of gelatin and
18 maltodextrin were obtained. The bands in the spectra are assigned to characteristic vibrational
19 modes as shown in Fig. 3. The Raman spectrum of maltodextrin⁴⁸ has a characteristic sharp
20 band around 485 cm⁻¹, which can be assigned to the $\nu(\text{C-C})$ backbone stretch⁴⁹ modes of
21 pyranose rings. The glycosidic stretching modes, $\nu(\text{C-O-C})$ and $\nu(\text{C-C,})$ appear in the region
22 950–1200 cm⁻¹; and the $\delta(\text{CH}_2)$ and $\delta(\text{C-OH})$ deformations region is from 1200 to 1500 cm⁻¹
23 ^{50,51}. The Raman spectrum of gelatin had main bands at 1440 cm⁻¹ and 1656 cm⁻¹, corresponding
24 to the Amide II ($\delta(\text{NH})$, $\nu(\text{CN})$) and I ($\nu(\text{C=O})$) bands, respectively. Those are typical
25 assignments for protein backbone vibrations⁵². The spectrum is also in agreement with the
26 previously reported for Gelatin⁴⁸. Raman bands between 800 and 950 cm⁻¹ could correspond to
27 $\nu(\text{C-O-C})$ stretching vibrations, while the Raman bands in the range of 1000 to 1100 cm⁻¹ can
28 be corresponded to the deformation $\delta(\text{CH}_2)$ and stretching vibrations of $\nu(\text{C-C})$ and $\nu(\text{C-O})$.
29
30

31 The solid phase of the gelatin-in-maltodextrin emulsion (3 % Gel/ 20% MD), which was
32 obtained after centrifugation of the emulsion, removal of the liquid and lyophilisation of the
33 remaining solid phase, strongly resembled the maltodextrin spectra. This, together the absence
34 of the amide bands make us conclude that the solid phase of the 3 % Gel/ 20 % MD
35 composition is mainly made of maltodextrin, confirming previous studies³¹.
36
37
38
39
40
41
42
43
44
45
46
47
48
49
50
51
52
53
54
55
56
57
58
59
60

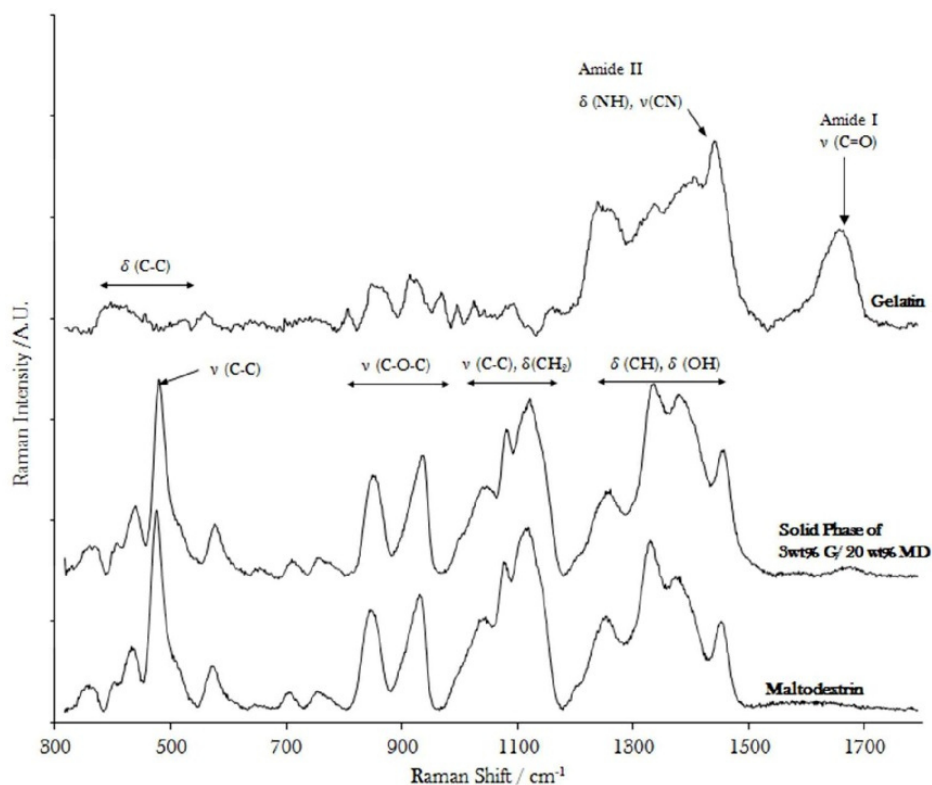


Figure 3. Confocal micro-Raman spectra of gelatin, maltodextrin and the solid phase found in the 3 % Gelatin/ 20 % Maltodextrin emulsion after 5 days at 50 °C.

Formation of the solid phase has been proposed to originate from segregative interactions of maltodextrin with disordered gelatin leading to conformational ordering of maltodextrin from 2 coils to double helix. This in turn leads to hydrophobic interactions and aggregation of the uncharged helices forming an insoluble precipitate.⁴⁷ Kasapis et al. analysed the precipitate quantitatively by optical rotation and confirmed that gelatin promoted maltodextrin precipitation, proportionally to its concentration and to the square of the concentration of maltodextrin³¹. Furthermore, this process is time and temperature dependent, and thus the phase boundary line separating the L form L+S phase is moving towards lower concentrations of the diagram over time and for lower temperatures (results not shown). In the present work, no precipitate was observed when forming microgels in freshly prepared gelatin-in-maltodextrin emulsions. As described before, the solid phase has a rather slow kinetics of formation. It might occur that precipitation of maltodextrin has a high activation energy, and thus, its presence can be neglected at short times after emulsions preparation. In any case, the formation of the solid phase is not in the scope of the present paper and thus, and it will be the subject of a future work.

Influence of preparation parameters on emulsion droplet size

Emulsion composition of 3% Gel/ 20 % MD was selected, as template for the preparation of gelatin microgels. At this composition, gelatin makes up the dispersed phase of the emulsion, and gelatin-in-maltodextrin emulsions can be obtained (inset Fig. 2). Similar compositions were also studied, and concentrations of gelatin or maltodextrin did not influence gelatin droplet size (Supporting information, Figure S2). However, it affected gelatin droplet morphology. Depending on composition, either simple emulsions or multiples emulsions were formed (Fig. 4).

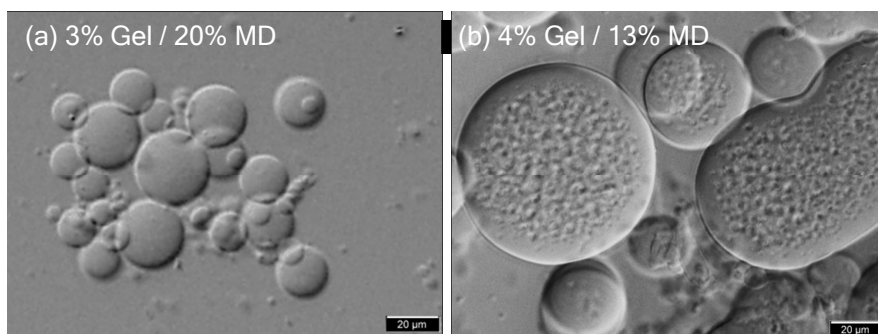


Figure 4. Illustrative examples of two emulsions with different morphology. (a) Simple Gelatin-in-maltodextrin emulsion, obtained in 3 % Gel/ 20 % MD. (b) Multiple emulsion, obtained in 4.5 % Gel/ 13% MD, closer to the binodal line.

Observations by optical microscopy clearly have shown that emulsions in 3 % Gel/ 20% MD composition consisted of gelatin droplets dispersed in maltodextrin solution, as shown in Fig. 1.

However, at compositions closer to the binodal line, for example, 4.5 % Gel/ 13% MD, multiple emulsions were observed (Fig. 4 (b)). Such multiple emulsions have already been described elsewhere for gelatin/maltodextrin mixtures.⁵³ It is supposed that the multiple emulsions are formed by secondary phase separation within the already formed droplets. Lowering the temperature leads to increased incompatibility between the two polymers due to entropic reasons, inducing phase separation of mixtures in the case of compositions close to the bimodal line.

Regarding the droplet size of emulsions, we have observed that increasing temperature during emulsification, from 30 to 60 °C, decreases droplet size from 25 µm to 19 µm (in the case of water) or from 17 to 13 µm (with PEM buffer). Those results are given in Table 2. This can be explained by the variations in viscosity of gelatin droplets, which is lower at increased temperatures, which is favourable for droplet break-up during emulsification. Droplet size decreased at higher temperatures since droplet break-up was favoured by agitation. However, coalescence might also be promoted at increased temperature, and thus this could explain the higher polydispersity at increased temperature.

Table 2. Droplet size, expressed as median diameter (d), and polydispersity, indicated as the interquartile range (IQR), as a function of temperature for the two aqueous systems used. Composition was 3% Gel / 20% MD, prepared with magnetic stirring at 500 rpm, during 30 min, with ≈ 6 g total sample weight. After emulsion formation, samples were cooled down to 0°C, and finally diluted with cold solvent, as described previously.

| System | | 30 °C | 40 °C | 60 °C |
|------------|----------------------------------|------------|-------------|-------------|
| Water | $d \pm \text{IQR} / \mu\text{m}$ | 25 \pm 7 | 21 \pm 11 | 19 \pm 14 |
| PEM buffer | $d \pm \text{IQR} / \mu\text{m}$ | 17 \pm 6 | 10 \pm 4 | 13 \pm 8 |

Furthermore, preparing the emulsion in PEM buffer decreased droplet size of emulsions, from 19-25 μm down to 10-17 μm (Table 2), in the case of 3 % Gel/ 20% MD prepared with magnetic stirring. The pH of both solvents is similar (pH 6.5), however PEM buffer possesses a higher ionic strength. This might influence on hydration of the two polymers and consequently could have a strong effect on interfacial tension.

Thus, preparing emulsions at higher temperatures, in PEM buffer and increased stirring speed, one could obtain droplets with smaller size, and consequently, smaller microgels. As those conditions affect also crosslinking kinetics and enzyme stability, they have therefore to be carefully selected.

Formation and properties of microgels

As described in more detail in the experimental section, gelatin microgels were prepared by homogenisation with an Ultra-Turrax[®] stirrer, of gelatin-in-maltodextrin emulsions. Then, emulsion droplets were crosslinked with genipin and samples were cooled down in ice-water. Afterwards, microgels were diluted and purified by centrifugation, extraction of the supernatant and resuspension in the solvent. This purification procedure has been shown to be the most effective and simple method, compared to dialysis and membrane filtration, as observed by optical microscopy and SEM microscopy on freeze-dried samples (results not shown). Centrifugation under mild conditions (2000 rpm) did not lead to deformation or non-reversible aggregation of the microgels.

Figure 5 shows the particle size of microgels prepared from a 3 % Gel/ 20 % MD emulsion in PEM buffer, homogenised and crosslinked for 30 min at 40 °C with various amounts of crosslinking agent (genipin). These conditions were selected in order to obtain microgels with the smallest particle size.

Finally, purified microgel suspensions were stored in PEM buffer at 4 °C and their stability was tested over a period of 1 month (Figure 5). The results showed that particle size of this sample remained constant during the 1 month period, for all crosslinking concentrations (between 0 and 5 mM genipin). After 30 days the size did not vary more than 5 %, in comparison to the initial size at zero time. All microgel samples remained stable and did not dissolve for over 500 days (results not shown).

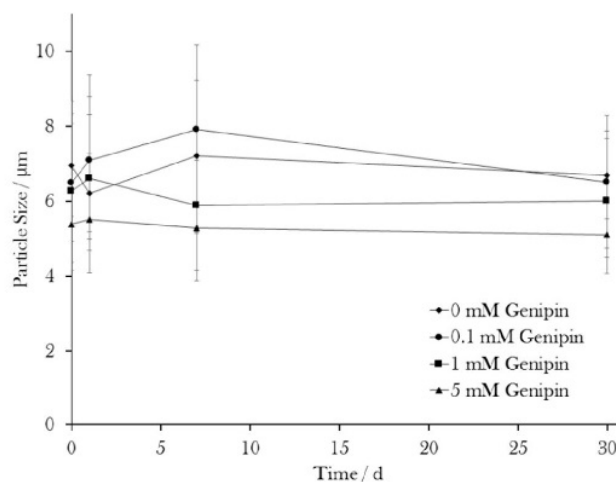


Figure 5. Microgel size evolution over a period of 1 month at 4 °C and at various crosslinking concentrations. The error bars indicate the interquartile range (IQR) of the particle size distribution.

Fig. 5 also shows that microgels crosslinked with 5 mM Genipin were smaller (5-5.5 μm) than the ones with lower genipin concentrations (6-8 μm), which can be explained by contraction of the crosslinked gelatin matrix and syneresis at increased crosslinker concentration. But for lower genipin concentrations, crosslinking barely influenced microgel size, which is in agreement with previous studies.⁵⁴

Probably, zeta potential plays an important role in the colloidal stability of the microgels. Zeta potential of microgels dispersed in water could not be precisely measured, because of rapid sedimentation. However, an approximate value of -8 mV was obtained, which is consistent to expectations of a relatively small negative value of zeta potential.⁵⁵ This zeta potential might be the reason for the presence of some weak flocculation, as observed in Fig. 6(a). However, it should be remarked that this flocculation was reversible, since apparently it was avoided by applying the ultrasonication treatment described in the experimental section (applying a power of 80 W, with 4 on/ off cycles with duration of 5 s/ 20 s each cycle). The actual mechanism of colloidal stability was not in the scope of the present paper, and it was not studied in more detail.

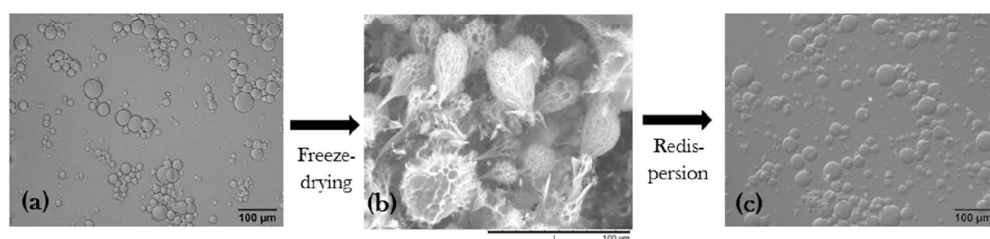
Microgels were purified by applying centrifugation-resuspension cycles. After each centrifugation treatment, it was observed by optical microscopy that microgel particles presented partial aggregation (results in supporting information, Fig. S3). This was attributed to the mechanical force applied to particles during centrifugation. However, it was also observed that sonication allowed deflocculating the microgels and thus, non-aggregated microgels were obtained after the sonication treatment (Fig. S3).

Gelatin microgel solutions, in absence of antimicrobial agents, could not be stored at room temperature at long periods since growth of microorganisms was observed after 1-2 weeks at

1
2
3 room temperature. Addition of a biocide, such as sodium azide, should be required if the
4 product is aimed to be stored at room temperature. Another option is to store the microgels as a
5 dry powder. In the present work, we opted for freeze-drying to properly preserve the microgels,
6 and the results are described in the next section.
7
8
9

10 Freeze Drying and resuspension of Microgels

11 Fig. 6 shows an example of crosslinked microgels (Fig. 6a), the particles observed after freeze-
12 drying (Fig. 6b) and the final microgels obtained after resuspending the dried sample in water
13 (Fig. 6c). This process was performed on microgels prepared from a 3 % Gel/ 20 % MD (1 mM
14 Genipin) emulsion, crosslinked during 20 min at 60 °C. The SEM images of freeze-dried
15 microgels (Fig. 6b) showed that microgels experienced a deformation to a leaf-like morphology
16 and macropores were formed. Other reports in the literature describe a similar effect on
17 microgels or microspheres after the drying process.^{56,57} The pores originate from the sublimation
18 of the frozen water, which was dispersed in the interconnected polymeric network of gelatin.
19 Explanation for the leaf-like shape might be directional sublimation of water inside the
20 microgels.^{56,57} As the top of the microgels was frozen, some water might have been pressed to
21 flow downwards. The streaming water was then gradually frozen, forming hereby the leaf-like
22 structure. Interestingly, crosslinking did not affect pore size (results not shown).
23
24
25



35 **Figure 6.** (a) Microgels, prepared from a 3 % Gel/ 20 % MD (1 mM Genipin) emulsion, observed under
36 optical microscopy, before freeze-drying. (b) After freeze-drying, microgels showed leaf-like morphology
37 and large pores. When redispersed in water (c), the microgels preserve their initial size and spherical
38 morphology.
39
40

41 When rehydrating the freeze-dried porous microgels by adding water (Fig. 6c), they recovered
42 the spherical morphology, as before the drying step (Fig. 6a). This may mainly be ascribed to
43 the flexible and elastic characteristics of the crosslinked gelatin networks. Remarkably, the
44 particle size distribution after rehydration seems to remain approximately the same as before
45 freeze-drying and changes seem to be small.
46

47 In conclusion, the results clearly demonstrate that crosslinked gelatin microgels can be freeze-
48 dried and later can be rehydrated, without producing major effects on the microgels.
49 Consequently, freeze-drying was selected in our work for the preservation of the microgels,
50 instead of more complex methods such as critical-point drying, as used by Lin *et al.*⁵⁷
51
52
53
54
55
56
57
58
59
60

β -Gal enzyme-loaded microgels

We studied the encapsulation yield and activity recovery of the β -Gal enzyme-loaded microgels, prepared by three different methods, explained in Table 1. In all samples in absence of genipin, the activity value for the free enzyme enzyme was 70 nkat/ g, since this is independent on the method used for introducing the enzyme into the microgels. However, the presence of genipin affects the enzyme activity, and its final activity depends on preparation method, as it can be seen in Table 3.

Table 3. Enzyme activity (nkat/g) in absolute values for the different methods of enzyme-loading (based on 3% Gel / 20 % MD emulsions). Crosslinking conditions: ¹ 30 min at 30°C, ² 60 min at 30°C, ³ 90 min at 30°C, ⁴ 180 min at 25 °C.

| | Free enzyme | Method A | Method B1 | Method B2 |
|---------------------|-----------------|-----------------|---|-----------------|
| 0 mM Genipin | 70 | 70 | 70 | 70 |
| 5 mM Genipin | 64 ³ | 69 ³ | 69 ¹ / 67 ² / 50 ³ | 63 ⁴ |

Previously crosslinked microgel solutions (Method A) did not affect enzyme activity (Table 3), as the merely physical interactions between the enzymes and the microgels and low concentration of free genipin in solution, did probably lead to no or minor changes of the active ingredient. Opposite, the values shown in Table 3 clearly show that crosslinker (genipin) reduces enzyme activity. Crosslinking gelatin in presence of β -Gal (Methods B1 and B2), lead to higher activity loss. This is illustrated by showing the influence of crosslinking time (30, 60 and 90 min) in Method B1, which reduces the activity (69, 67 and 50 nkat/g, respectively). Supposedly, genipin did not only crosslink gelatin, but also reacted with the amino groups of the enzyme, creating intra- and inter-crosslinks between gelatin and β -Gal, which could have affected the enzyme.

Methods A and B1, the latter with only 30 min crosslinking at 30 °C, allow the maximum activity after addition of 5 mM genipin, achieving 69 nkat/ g in both cases (Table 3). If the enzyme-loaded microgel was crosslinked, once formed (Method B2, at 25 °C), the enzyme lost 10 % of its activity, from 70 to 63 nkat/ g. In the case of methods B1 and B2 (addition of enzyme before microgel formation), one might assume that gelatin might have protected the enzyme, preventing genipin from reacting with the enzyme, and thus, preserving a relatively high activity.

The higher activity loss if genipin reacts simultaneously with gelatin and the enzyme (down to 50 nkat/g for Method B1 and 63 nkat/ g for method B2), compared to reacting only with the free enzyme (64 nkat/ g) might be due to intercrosslinks between gelatin and the enzyme, in addition to intracrosslinks in the enzyme. Both types of crosslinking could affect the enzyme active site and thus reducing enzyme activity. In any case, covalent crosslinking is supposed to be beneficial, in order to prevent an early desorption of the enzyme, since enzymes loosely adsorbed to the microgels might be easily released, as described in previous studies.⁵⁸

Encapsulation yield of the three methods was thus tested. First, β -Gal was added after microgel formation (Method A). After washing twice, the microgel suspension, 10 % of initially added enzyme remained in non-crosslinked and 7 % in crosslinked (5 mM Genipin) microgel suspensions (Table 4). Those enzymes, however, did not penetrate or adsorb to the microgels, as was observed by labelling the enzyme (optical microscopy images in supporting information, Fig S4). Enzyme was equally distributed in the microgel suspension, leading to the conclusion that adding the enzyme to already formed microgels, does not lead to sufficient strong interaction between the particle and the enzyme, to produce high encapsulation/adsorption rates. Most of the enzyme was probably loosely associated to the microgels and would have been removed with several additional washing steps.

Table 4. Encapsulation yield for different encapsulation methods. ¹Crosslinking during 90 min at 30°C for Methods A and B. ²Crosslinking during 180 min at 25 °C.

| | Method A Adding enzyme to microgel suspension | Method B1 Crosslinking during microgel formation | Method B2 Crosslinking after microgel formation |
|--------------|---|--|---|
| 0 mM Genipin | 10 % | 16 % | 13 % |
| 5 mM Genipin | 7 % ¹ | 64 % ¹ | 19 % ² |

Therefore, the enzyme was mixed with non-gelified gelatin during the emulsification process (Method B1 and B2). This, in contrast, lead to sufficiently strong bonds between both proteins, and the enzyme remained encapsulated inside gelatin microgels, as it can be seen in Figure 7. Furthermore, labelled enzyme stayed within the microgels for at least 1 month (Fig. 7).

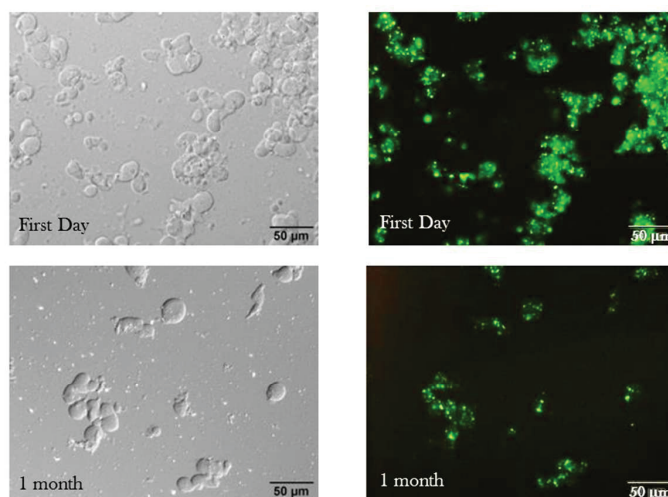
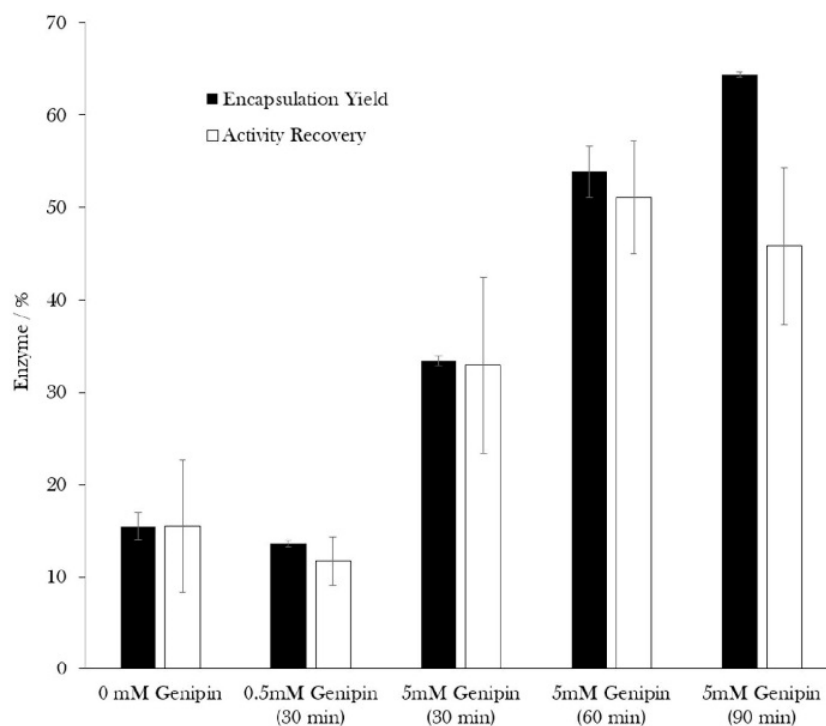


Figure 7. Location of labelled β -Gal when added during formation of non-crosslinked microgels (prepared by Method B1, in absence of genipin). After purification of the samples, it is observed that enzyme was encapsulated into the microgels and remained there for a period of at least 1 month.

To increase enzyme retention inside the microgels, they were crosslinked by the two different methods (Method B1 and B2). Results (Table 4) indicated that crosslinking during emulsification (Method B1) achieved the highest encapsulation yield (64 %), as during the crosslinking procedure in Method B2 non-covalently linked enzymes might dissociate from the microgels into the aqueous surrounding medium, in which it is soluble. In both preparation

1
2
3 methods (B1 and B2), crosslinking increased encapsulation yield of the enzyme, compared to
4 the same preparation procedure without genipin: 64 % vs. 16 % for crosslinking during the
5 emulsification process (Method B1) and 19 % vs. 13 % for crosslinking of gelatin after
6 microgel formation (Method B2). Additionally, as expected, with higher crosslinking
7 concentration and time, bigger amounts of enzymes could be incorporated into the microgels
8 (Fig. 8). These results can be attributed to the fact that crosslinking might diminish the mesh
9 size of the polymer network from where enzymes might diffuse into the aqueous surrounding
10 medium. Furthermore, genipin might covalently link β -gal to the microgels, increasing retention
11 within the particles.
12

13
14 Taking deactivation of the enzyme by genipin into account (Table 3), the percentage of active
15 enzyme remaining inside the microgels, the activity recovery, was calculated and is shown in
16 Figure 8. Microgels crosslinked with 5 mM Genipin (60 min) had the highest activity recovery
17 (51 %).
18



47
48
49
50
51
52
53
54
55
56
57
58
59
60

Figure 8. Encapsulation yield and activity recovery of enzymes encapsulated under varying crosslinking conditions.

Moreover, microgels were stored for 1 week at 4 °C to assess how much of the enzyme remains encapsulated during this period. After 1 week, the microgel solutions were centrifuged and the enzyme activities in the supernatant and within the microgels were measured. Results indicated that fewer enzymes were released from the stronger crosslinked microgels (Fig. 9), with 88 % of enzymes remaining within the microgels that were crosslinked during 90 min with 5 mM genipin (Method B1). If the microgels were not crosslinked, less than 50 % enzyme remained in the microgels. All these results go in line with afore-mentioned explanations that crosslinking retains the enzyme within the gelatin microgels, due to entrapment of enzyme molecules into the crosslinked polymer network.

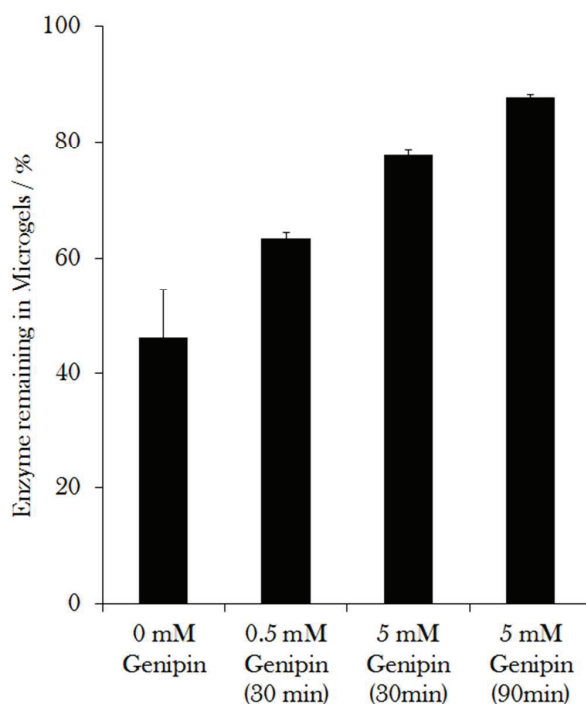


Figure 9. Release of enzyme from microgels after 1 week dispersed in water at 4 °C. The microgels were prepared by Method B1.

To prevent enzyme diffusion out of the microgels, which might happen during storage in solution, enzyme-loaded microgels were freeze-dried. Freeze-drying did not much affect enzyme activity, which was measured after rehydrating the dry microgels. 37 % of activity was lost for non-crosslinked and 31 % for crosslinked (10 mM Genipin, 90 min crosslinking) microgels. Considering up to 50 % of enzyme was lost due to diffusion out of the microgels in solution, keeping the microgels as a freeze-dried powder may be a better option, allowing them to be preserved over a prolonged period, without enzyme loss or bacterial contamination.

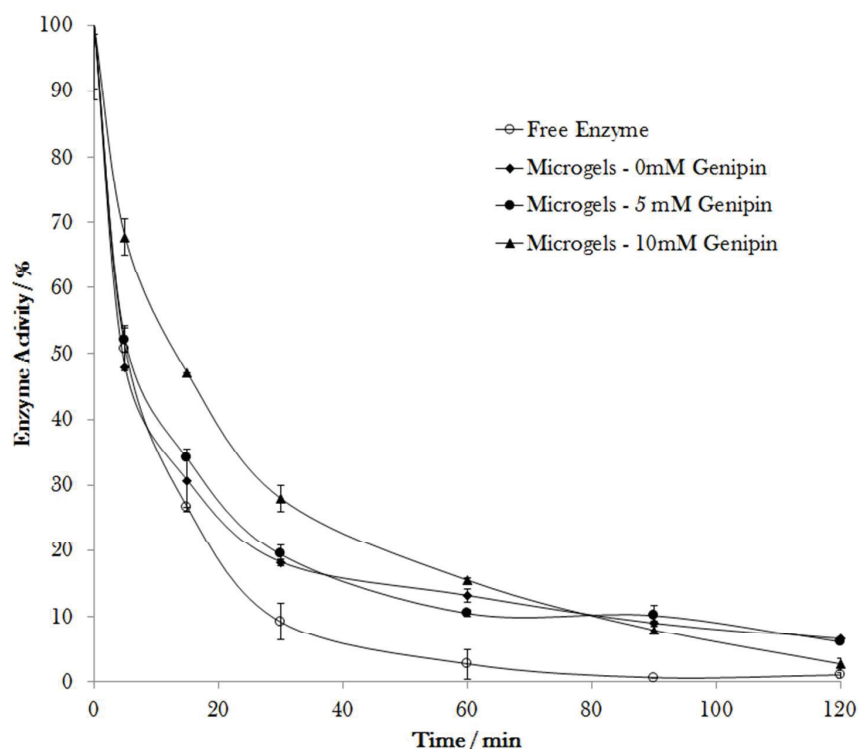
Enzyme stability under simulated gastric pH and body temperature conditions

The stability of the enzyme-loaded microgels in SGF (1:10 dilution ratios) was investigated by suspending them into SGF (pH 3) at 37 °C, during 120 min, which is the recommended time for digestion.⁴⁵ Two distinct microgel dispersions were used therefore: First, microgels dispersed in water (final pH of the mixture with SGF was \approx 3) and second, microgels dispersed in PEM buffer (final pH of the mixture with SGF was \approx 6).

In the first case (pH \approx 3), free and encapsulated β -Gal enzyme become instantaneously deactivated after a few seconds (results not shown). Encapsulating the enzyme into the microgels did not protect it from direct deactivation under low pH conditions.

In the second case (pH \approx 6), activity diminished sharply over the 120 min and final activity, compared to the activity at time = 0 min, was 6 % for the microgels with 0 and 5 mM genipin, 3

1
2
3 % for the microgels crosslinked with 10 mM genipin and 1 % for the free enzyme (Fig. 10).
4 Kinetics of enzyme deactivation was however slower in the crosslinked microgels compared to
5 the free enzyme. Time till enzyme activity reached 50 % was 5 min for the free enzyme and 14
6 min for the samples crosslinked with 10 mM genipin. Moreover, it took 17 min for the free
7 enzyme and 37 min for the crosslinked microgels (10 mM) to reach 25 % of enzyme activity.
8 Those results indicate that encapsulating the enzyme into the microgel, conveys a protective
9 effect for the enzyme, as higher activity is retained after 120 min. Encapsulating could however
10 not prevent activity diminution under those conditions, as the crosslinked gelatin network might
11 allow diffusion of protons or other electrolytes into microgel particles, which might harm the
12 enzyme.
13
14



15
16
17
18
19
20
21
22
23
24
25
26
27
28
29
30
31
32
33
34
35
36
37
38
39
40
41
42 **Figure 10.** β -Gal Enzyme activity at $\text{pH}\approx 6$ and $37\text{ }^\circ\text{C}$. Free enzyme rapidly lost activity. Encapsulating
43 the enzyme inside the microgels allows a higher enzyme activity.
44
45

46
47 On the other hand, crosslinking promoted stability of the microgels under those conditions.
48 Non-crosslinked microgels become mainly dissolved after 120 min, whereas the crosslinked
49 microgels did remain stable under those conditions (results in supporting information, Fig S5).
50 One can predict that, under *in vivo* conditions, gastric juice would assure that the pH would
51 remain acid, even if the microgels are prepared in PEM buffer. As a consequence, those results
52 at pH 5.8 and $37\text{ }^\circ\text{C}$ should be considered as preliminary results for the possible use of those β -
53 Gal-loaded microgels in e.g. industrial production of lactose-hydrolyzed milk, which has similar
54 pH and temperature condition.⁵⁹ This application is of great interest according to the annual
55 growth rate of lactose-free products worldwide.
56
57
58
59
60

CONCLUSIONS

The phase behaviour of gelatin-in-maltodextrin W/W emulsions has been studied in detail and the solid precipitate, which is formed after several days, has been identified by Raman spectroscopy as maltodextrin. These emulsions have been successfully used as templates to prepare enzyme-loaded gelatin microgels. The influence of solvent and stirring temperature of the emulsion was studied on droplet size, showing that microgels as low as $\approx 5 \mu\text{m}$ can be obtained. Crosslinking of gelatin with genipin, a natural crosslinker much less toxic than conventional crosslinkers, has allowed the formation of gelatin microgels. Suspensions of such microgel particles remain stable for a minimum of one month, without major variations in particle size. The microgel particles can be preserved in the form of a freeze-dried powder. It has been observed that microgels can recover their original size and shape, after one cycle of freeze-drying followed by rehydration.

Lactose enzyme has been successfully loaded into the microgels by several methods, achieving the highest encapsulation yield and lowest enzyme activity loss by enzyme-addition and polymer crosslinking during emulsification (Method B1). Moreover, it was shown that the enzyme can remain inside the microgels for a period of at least 1 month, in PEM buffer solution. The encapsulation yield and the activity recovery have been studied. The results showed that increasing crosslinking concentration and time has improved the encapsulation yield of enzyme into the microgels, up to 64 %. Encapsulation of the enzyme into microgels has preserved the enzyme activity over a prolonged time, and interestingly, crosslinking of the microgels with genipin did only slightly affect enzyme activity.

The use of those gelatin microgels as oral delivery vehicles for β -Gal had to be discarded, as they did not offer robust protection to the encapsulated enzyme at gastric pH. However, considering the results at pH 5.8 and 37 °C, the microgels crosslinked with genipin could be suitable for enzyme immobilization during industrial production of lactose-hydrolyzed milk.

As an alternative for taking β -Gal supplementation, lactose intolerant persons can consume dairy products, in which lactose has externally been hydrolyzed. Immobilising β -Gal is of interest in industrial production of lactose-hydrolyzed milk, as direct addition of β -Gal to the substrate is economically unacceptable. Immobilised enzyme can be reused several times, decreasing the costs of the process. Furthermore, the application of encapsulated biocatalyst compared to free enzyme has other benefits such as easy separation from reaction solution, no contamination of product by the enzyme, long-term stability and continuous processing.^{39,59-61} Our crosslinked, food-grade gelatin microgels may thus be studied as a strategy for encapsulation of lactase during the production of lactose-hydrolyzed milk. Furthermore, the microgels formed might have potential applications as fat or starch mimetics for production of low calorie foods and beverages, and as texture modifiers. These hypotheses can be studied in future publications.

ASSOCIATED CONTENT

Supporting Information. Fig. S1: Turbidity measurements of gelatin/maltodextrin mixtures over a period of 5 days; Fig. S2: Influence of W/W emulsion composition on gelatin droplet size; Fig. S3: Effect of sonication on gelatin droplets flocculation; Fig. S4: Optical microscopy images of microgels with labelled enzyme, produced by Method A; Fig. S5: Colloidal stability of non-crosslinked and crosslinked gelatin microgels at different temperature and pH.

ACKNOWLEDGEMENTS

The authors greatly acknowledge financial support from the Spanish Ministry of Economy and Competitiveness (CTQ2014-52687-C3-1-P project) and Marie Skłodowska Curie Initial Training Networks (FP7-PEOPLE-2013-ITN-606713, BIBAFOODS project). Support from Generalitat de Catalunya (2014SGR1655 and TECCIT15-1-0009) and Centro de Investigación Biomédica en Red de Bioingeniería, Biomateriales y Nanomedicina (CIBER-BBN), is also acknowledged.

Phase behaviour, microscopy observations and particle size determinations have been performed by the Nanostructured Liquid Characterization Unit, located at the Institute of Advanced Chemistry of Catalonia (IQAC), belonging to the Spanish National Research Council (CSIC) and affiliated to the NANBIOSIS ICTS of the Biomedical Networking Center (CIBER-BBN).

The authors also greatly thank Allan Mackie and Josep Bonet (Universitat Rovira i Virgili, Spain) and Carlos Rodríguez-Abreu (IQAC-CSIC) for useful discussions.

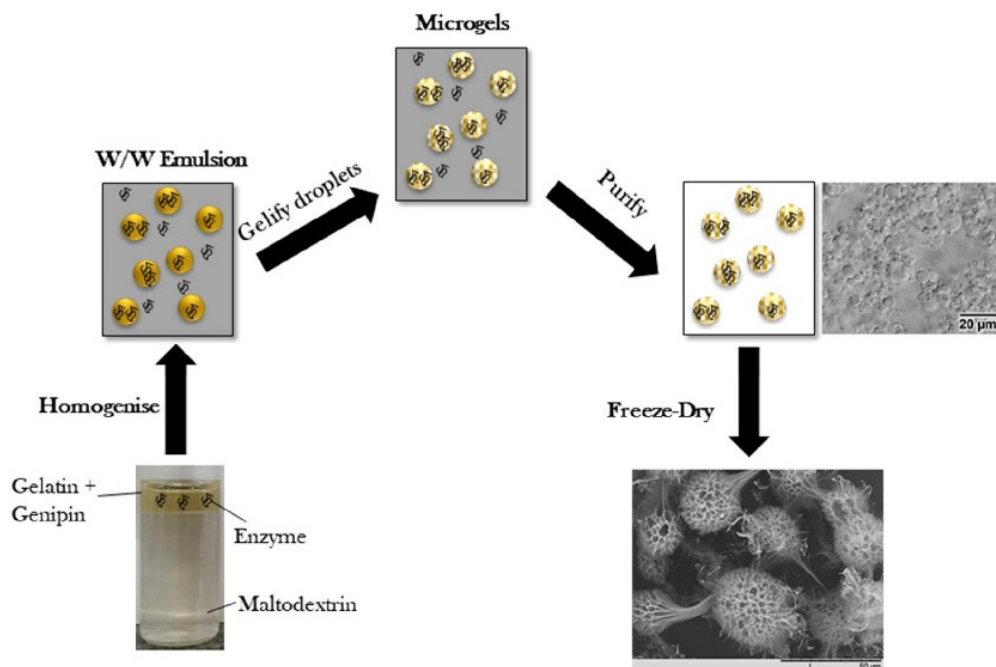
REFERENCES

- (1) Khan, R. S.; Nickerson, M. T.; Paulson, A. T.; Rousseau, D. Release of Fluorescent Markers from Phase-Separated Gelatin-Maltodextrin Hydrogels. *J. Appl. Polym. Sci.* **2011**, *121* (5), 2662–2673.
- (2) Esquena, J. Water-in-Water (W/W) Emulsions. *Curr. Opin. Colloid Interface Sci.* **2016**, *25*, 109–119.
- (3) Grinberg, V. Y.; Tolstoguzov, V. B. Thermodynamic Incompatibility of Proteins and Polysaccharides in Solutions. *Food Hydrocoll.* **1997**, *11* (2), 145–158.
- (4) Doublier, J. L.; Garnier, C.; Renard, D.; Sanchez, C. Protein-Polysaccharide Interactions. *Curr. Opin. Colloid Interface Sci.* **2000**, *5* (3-4), 202–214.
- (5) Clark, A. H. Direct Analysis of Experimental Tie Line Data (two Polymer – One Solvent Systems) Using Flory – Huggins Theory. *Carbohydr. Polym.* **2000**, *42* (4), 337–351.
- (6) McClements, D. *Nanoparticle- and Microparticle-Based Delivery Systems*; CRC Press, 2014.
- (7) Semenova, M. G.; Dickinson, E. Biopolymers in Food Colloids: Thermodynamics and Molecular Interactions. **2010**.
- (8) Shewan, H. M.; Stokes, J. R. Review of Techniques to Manufacture Micro-Hydrogel Particles for the Food Industry and Their Applications. *J. Food Eng.* **2013**, *119* (4), 781–792.
- (9) Stokes, J. R.; Wolf, B.; Frith, W. J. Phase-Separated Biopolymer Mixture Rheology: Prediction Using a Viscoelastic Emulsion Model. *J. Rheol. (N. Y. N. Y.)* **2001**, *45* (5), 1173.
- (10) Norton, I. T.; Frith, W. J. Microstructure Design in Mixed Biopolymer Composites. *Food Hydrocoll.* **2001**, *15* (4-6), 543–553.
- (11) Esquena, J. Water-in-Water (W/W) Emulsions. *Curr. Opin. Colloid Interface Sci.* **2016**, *25*, 109–119.
- (12) Poortinga, A. T. Microcapsules from Self-Assembled Colloidal Particles Using Aqueous Phase-Separated Polymer Solutions. **2008**, *24* (5), 1644–1647.
- (13) Nicolai, T.; Murray, B. Particle Stabilized Water in Water Emulsions. *Food Hydrocoll.* **2017**, *68*, 157–163.
- (14) de Freitas, R. A.; Nicolai, T.; Chassenieux, C.; Benyahia, L. Stabilization of Water-in-Water Emulsions by Polysaccharide-Coated Protein Particles. *Langmuir* **2016**, *32*, 1227–1232.
- (15) Alemán, J. V.; Chadwick, A. V.; He, J.; Hess, M.; Horie, K.; Jones, R. G.; Kratochvil, P.; Meisel, I.; Mita, I.; Moad, G.; et al. Definitions of Terms Relating to the Structure and Processing of Sols, Gels, Networks, and Inorganic-Organic Hybrid Materials (IUPAC Recommendations 2007). *Pure Appl. Chem.* **2007**, *79* (10), 1801–1829.
- (16) Franssen, O.; Hennink, W. E. A Novel Preparation Method for Polymeric Microparticles without the Use of Organic Solvents. *Int. J. Pharm.* **1998**, *168* (1), 1–7.
- (17) Li, B.; Wang, L.; Li, D.; Adhikari, B.; Mao, Z. Preparation and Characterization of Crosslinked Starch Microspheres Using a Two-Stage Water-in-Water Emulsion Method. *Carbohydr. Polym.* **2012**, *88* (3), 912–916.
- (18) Impellitteri, N. A.; Toepke, M. W.; Lan Levensgood, S. K.; Murphy, W. L. Specific VEGF Sequestering and Release Using Peptide-Functionalized Hydrogel Microspheres. *Biomaterials* **2012**, *33* (12), 3475–3484.
- (19) Parlato, M.; Johnson, A.; Hudalla, G. A.; Murphy, W. L. Adaptable Poly(ethylene Glycol) Microspheres Capable of Mixed-Mode Degradation. *Acta Biomater.* **2013**, *9* (12), 9270–9280.
- (20) Xia, H.; Li, B.-Z.; Gao, Q. Effect of Molecular Weight of Starch on the Properties of Cassava Starch Microspheres Prepared in Aqueous Two-Phase System. *Carbohydr. Polym.* **2017**, *177* (August), 334–340.
- (21) Ghugare, S. V.; Mozetic, P.; Paradossi, G.; Tor, R. Temperature-Sensitive Poly (Vinyl Alcohol)/ Poly (Methacrylate- Co - N -Isopropyl Acrylamide) Microgels for Doxorubicin Delivery. **2009**, 1589–1596.
- (22) Cavalieri, F.; Chiessi, E.; Villa, R.; Viganò, L.; Zaffaroni, N.; Telling, M. F.; Paradossi, G.; Viganò, L.; Zaffaroni, N.; Telling, M. F.; et al. Novel PVA-Based Hydrogel Microparticles for Doxorubicin Delivery. *Biomacromolecules* **2008**, *9* (7), 1967–1973.
- (23) Stenekes, R. J.; Franssen, O.; van Bommel, E. M.; Crommelin, D. J.; Hennink, W. E. The Use of Aqueous PEG/dextran Phase Separation for the Preparation of Dextran Microspheres. *Int. J. Pharm.* **1999**, *183* (1), 29–32.
- (24) Duval, S.; Chung, C.; McClements, D. J. Protein-Polysaccharide Hydrogel Particles Formed by Biopolymer Phase Separation. **2015**, 334–341.

- 1
2
3 (25) Firoozmand, H.; Murray, B. S.; Dickinson, E. Fractal-Type Particle Gel Formed from Gelatin + Starch
4 Solution. *Langmuir* **2007**, *23* (8), 4646–4650.
- 5 (26) Djabourov, M. Gelation of Aqueous Gelatin Solutions. I. Structural Investigation. *J. Phys.* **1988**, *49* (2),
6 319–332.
- 7 (27) Alevisopoulos, S.; Kasapis, S.; Abeyssekera, R. Formation of Kinetically Trapped Gels in the Maltodextrin—
8 gelatin System. *Carbohydr. Res.* **1996**, *293* (1), 79–99.
- 9 (28) Kasapis, S.; Morris, E. R.; Norton, I. T.; Brown, C. R. T. Phase Equilibria and Gelation in
10 Gelatin/maltodextrin Systems — Part III: Phase Separation in Mixed Gels. *Carbohydr. Polym.* **1993**, *21* (4),
11 261–268.
- 12 (29) Kasapis, S.; Morris, E. R.; Norton, I. T.; Clark, A. H. Phase Equilibria and Gelation in Gelatin/maltodextrin
13 Systems — Part IV: Composition-Dependence of Mixed-Gel Moduli. *Carbohydr. Polym.* **1993**, *21* (4), 269–
14 276.
- 15 (30) Kasapis, S.; Morris, E. R.; Norton, I. T.; Clark, A. H. Phase Equilibria and Gelation in Gelatin/maltodextrin
16 Systems — Part I: Gelation of Individual Components. *Carbohydr. Polym.* **1993**, *21* (4), 243–248.
- 17 (31) Kasapis, S.; Morris, E. R.; Norton, I. T.; Gidley, M. J. Phase Equilibria and Gelation in Gelatin/maltodextrin
18 Systems — Part II: Polymer Incompatibility in Solution. *Carbohydr. Polym.* **1993**, *21* (4), 249–259.
- 19 (32) Lorén, N.; Hermansson, A. M.; Williams, M. A. K.; Lundin, L.; Foster, T. J.; Hubbard, C. D.; Clark, A. H.;
20 Norton, I. T.; Bergström, E. T.; Goodall, D. M. Phase Separation Induced by Conformational Ordering of
21 Gelatin in Gelatin/maltodextrin Mixtures. *Macromolecules* **2001**, *34* (2), 289–297.
- 22 (33) Lorén, N.; Langton, M.; Hermansson, A. Confocal Laser Scanning Microscopy and Image Analysis of
23 Kinetically Trapped Phase-Separated Gelatin/maltodextrin Gels. *Food Hydrocoll.* **1999**, *13*, 185–198.
- 24 (34) Lundin, L.; Norton, I.; Foster, T. J.; Williams, M. A. K.; Hermansson, A.-M.; Bergström, E. Phase
25 Separation in Mixed Biopolymer Systems. *Gums Stabilisers Food Ind.* **10** **2000**, 167–180.
- 26 (35) Williams, M.; Fabri, D.; Hubbard, C. Kinetics of Droplet Growth in Gelatin/maltodextrin Mixtures
27 Following Thermal Quenching. *Langmuir* **2001**, 3412–3418.
- 28 (36) Lomer, M. C. E.; Parkes, G. C.; Sanderson, J. D. Review Article: Lactose Intolerance in Clinical Practice—
29 Myths and Realities. *Aliment. Pharmacol. Ther.* **2008**, *27* (2), 93–103.
- 30 (37) O’connell, S.; Walsh, G. Physicochemical Characteristics of Commercial Lactases Relevant to Their
31 Application in the Alleviation of Lactose Intolerance. *Appl. Biochem. Biotechnol.* **2006**, *134*.
- 32 (38) Zhang, Z.; Zhang, R.; McClements, D. J. Lactase (B-Galactosidase) Encapsulation in Hydrogel Beads with
33 Controlled Internal pH Microenvironments: Impact of Bead Characteristics on Enzyme Activity. *Food*
34 *Hydrocoll.* **2017**, *67*, 85–93.
- 35 (39) Fujikawa, S.; Yokota, T.; Koga, K. Immobilization of α -Glucosidase in Calcium Alginate Gel Using
36 Genipin as a New Type of Cross-Linking Reagent of Natural Origin. *Appl. Microbiol. Biotechnol.* **1988**, *28*
37 (4-5), 440–441.
- 38 (40) Nussinovitch, A.; Chapnik, N.; Gal, J.; Froy, O. Delivery of Lactase Using Chocolate-Coated Agarose
39 Carriers. *Food Res. Int.* **2012**, *46* (1), 41–45.
- 40 (41) Ratzinger, G.; Wang, X.; Wirth, M.; Gabor, F. Targeted PLGA Microparticles as a Novel Concept for
41 Treatment of Lactose Intolerance. *J. Control. Release* **2010**, *147* (2), 187–192.
- 42 (42) Fernandezinnnoo-Nieves, A.; Wyss, H.; Mattsson, J.; Weitz, D. *Microgel Suspensions: Fundamentals and*
43 *Applications*; 2011.
- 44 (43) Bysell, H.; Månsson, R.; Hansson, P.; Malmsten, M. Microgels and Microcapsules in Peptide and Protein
45 Drug Delivery. *Adv. Drug Deliv. Rev.* **2011**, *63* (13), 1172–1185.
- 46 (44) Sheldon, R. A.; van Pelt, S. Enzyme Immobilisation in Biocatalysis: Why, What and How. *Chem. Soc. Rev.*
47 **2013**, *42* (15), 6223–6235.
- 48 (45) Minekus, M.; Alving, M.; Alvito, P.; Ballance, S.; Bohn, T.; Bourlieu, C.; Carrière, F.; Boutrou, R.;
49 Corredig, M.; Dupont, D.; et al. A Standardised Static in Vitro Digestion Method Suitable for Food - an
50 International Consensus. *Food Funct.* **2014**, *5* (6), 1113–1124.
- 51 (46) Aymard, P.; Williams, M. a. K.; Clark, a. H.; Norton, I. T. A Turbidimetric Study of Phase Separating
52 Biopolymer Mixtures during Thermal Ramping. *Langmuir* **2000**, *16* (19), 7383–7391.
- 53 (47) Hoey, A.; Ryan, J. T.; Fitzsimons, S. M.; Morris, E. R. Segregative Interactions in Single-Phase Mixtures of
54 Gelling (Potato) Maltodextrin with Other Hydrocolloids. In *Gums and Stabilisers for the Food Industry 18*
55 *Hydrocolloid Functionality for Affordable and Sustainable Global Food Solutions*; 2016; pp 305–312.
- 56 (48) De Veij, M.; Vandenabeele, P.; De Beer, T.; Remon, J. P.; Moens, L. Reference Database of Raman Spectra
57
58
59
60

- of Pharmaceutical Excipients. *J. Raman Spectrosc.* **2009**, *40* (3), 297–307.
- (49) De Gussem, K.; Vandenaabeele, P.; Verbeke, A.; Moens, L. Raman Spectroscopic Study of Lactarius Spores (Russulales, Fungi). *Spectrochim. Acta - Part A Mol. Biomol. Spectrosc.* **2005**, *61* (13-14), 2896–2908.
- (50) Pereira, L.; Sousa, A.; Coelho, H.; Amado, A. M.; Ribeiro-Claro, P. J. A. Use of FTIR, FT-Raman and ¹³C-NMR Spectroscopy for Identification of Some Seaweed Phycocolloids. In *Biomolecular Engineering*; 2003; Vol. 20, pp 223–228.
- (51) Hecht, L.; Blanch, E. W.; Bell, A. F.; Day, L. A. Raman Optical Activity Instrument for Studies of Biopolymer Structure and Dynamics. *J. Raman Spectrosc.* **1999**, *30* (9), 815–825.
- (52) Schrader, B. *Infrared and Raman Spectroscopy: Methods and Applications*; Wiley-VCH Verlag GmbH: Weinheim, Germany, 1995.
- (53) Foster, T. J.; Brown, C. R. T.; Norton, I. T. Phase Inversion of Water-in-Water Emulsions. In *Gums and Stabilisers for the Food Industry 8*; Williams, P. A., Phillips, G. O., Wedlock, D. J., Eds.; IRL Press: Oxford, UK, 1996; pp 297–306.
- (54) Annan, N. T.; Borza, a; Moreau, D. L.; Allan-Wojtas, P. M.; Hansen, L. T. Effect of Process Variables on Particle Size and Viability of Bifidobacterium Lactis Bb-12 in Genipin-Gelatin Microspheres. *J. Microencapsul.* **2007**, *24* (2), 152–162.
- (55) Turner, P. A.; Thiele, J. S.; Stegemann, J. P. Growth Factor Sequestration and Enzyme-Mediated Release from Genipin-Crosslinked Gelatin Microspheres. *J. Biomater. Sci. Polym. Ed.* **2017**, *28* (16), 1826–1846.
- (56) Cheng, C. J.; Chu, L. Y.; Zhang, J.; Wang, H. D.; Wei, G. Effect of Freeze-Drying and Rehydrating Treatment on the Thermo-Responsive Characteristics of poly(N-Isopropylacrylamide) Microspheres. *Colloid Polym. Sci.* **2008**, *286* (5), 571–577.
- (57) Lin, S.-Y.; Chen, K.-S.; Run-Chu, L. Drying Methods Affecting the Particle Sizes, Phase Transition, Deswelling/reswelling Processes and Morphology of poly(N-Isopropylacrylamide) Microgel Beads. *Polymer (Guildf)*. **1999**, *40* (23), 6307–6312.
- (58) Schachschal, S.; Adler, H.-J.; Pich, A.; Wetzel, S.; Matura, A.; van Pee, K.-H. Encapsulation of Enzymes in Microgels by Polymerization/cross-Linking in Aqueous Droplets. *Colloid Polym. Sci.* **2011**, *289* (5-6), 693–698.
- (59) Grosová, Z.; Rosenberg, M.; Rebroš, M. Perspectives and Applications of Immobilised β -Galactosidase in Food Industry - A Review. *Czech J. Food Sci.* **2008**, *26* (1), 1–14.
- (60) Tanriseven, A.; Doğan, Ş. A Novel Method for the Immobilization of β -Galactosidase. *Process Biochem.* **2002**, *38* (1), 27–30.
- (61) Klein, M. P.; Hackenhaar, C. R.; Lorenzoni, A. S. G.; Rodrigues, R. C.; Costa, T. M. H.; Ninow, J. L.; Hertz, P. F. Chitosan Crosslinked with Genipin as Support Matrix for Application in Food Process: Support Characterization and β -D-Galactosidase Immobilization. *Carbohydr. Polym.* **2016**, *137*, 184–190.

Table of Contents (TOC) Graphic



Formulación y aplicaciones de nuevas emulsiones de tipo agua-en-agua (W/W)

Jordi Esquena y Yoran Beldengrün

Instituto de Química Avanzada de Cataluña (IQAC), Consejo Superior de Investigaciones Científicas (CSIC) y Centro de Investigaciones Biomédicas en Red (CIBER-BBN) en Bioingeniería, Biomateriales y Nanomedicina (CIBER-BBN)

Las emulsiones de tipo agua-en-agua (W/W) constituyen un tipo de sistema coloidal muy novedoso y que está despertando un gran interés. Las emulsiones W/W están constituidas por gotas de una fase acuosa que están dispersadas en el seno de otra fase acuosa, sin aceite y sin tensioactivo. En el presente artículo se describe cómo formular y preparar estas emulsiones, sus propiedades, principales características y sus posibles aplicaciones en cosmética. Se describen ejemplos de la utilización de las emulsiones W/W para incorporar principios activos.

Introducción

Las emulsiones de tipo agua-en-agua (abreviadas como W/W) son sistemas muy novedosos que consisten en gotas de una solución acuosa, dispersadas en el seno de otra solución acuosa⁽¹⁻⁴⁾. Por lo tanto, las emulsiones W/W son dispersiones coloidales sin fase oleosa. Las emulsiones W/W poseen propiedades interesantes, como la biocompatibilidad, ausencia de toxicidad y elevada transparencia, y por ello pueden ser de gran interés en una gran variedad de aplicaciones comerciales.

Recientemente, las emulsiones W/W están siendo objeto de un gran interés científico, aunque la existencia de este tipo de emulsiones se conoce desde hace mucho tiempo. La primera vez que se describieron fue en 1896, cuando un microbiólogo, Beijerinck, observó la formación de gotas en un medio de cultivo para bacterias, preparado mezclando gelatina y almidón de bajo peso molecular^(5,6). Actualmente, se conoce que las emulsiones de tipo agua-en-agua pueden formarse en una gran variedad de sistemas bifásicos acuosos ("Aqueous Two-Phase Systems")^(7,8). La formación de emulsiones agua-en-agua se basa en la inmiscibilidad de dos componentes solubles en agua, que posean una incompatibilidad mutua y que dichos componentes generen una repulsión suficiente para mantenerse segregados en dos fases acuosas en equilibrio termodinámico.

Generalmente, las emulsiones agua-en-agua se preparan en sistemas constituidos por mezclas de dos polímeros mutuamente incompatibles, siendo ambos polímeros hidrofílicos y solubles en agua^(1,8-10). El comportamiento típico, en un estos sistema constituidos por agua, un polímero hidrofílico (P_A) y otro polímero hidrofílico (P_B), siendo ambos polímeros mutuamente incompatibles, se presenta en la Figura 1. El sistema separa en dos fases acuosas inmiscibles: una fase contiene la mayor parte del polímero A, y está saturada con el polímero B, mientras que la segunda fase contiene principalmente el polímero B, y está saturada con el polímero A. Las composiciones que están mutuamente en equilibrio termodinámico se relacionan mediante las líneas de reparto en el diagrama de fases. Las líneas de reparto convergen en el punto crítico (P_c).

Las emulsiones de tipo agua-en-agua se forman cuando las fuerzas de interacción entre los dos polímeros hidrosolubles son repulsivas⁽¹¹⁾. Ello puede manifestarse en una gran variedad de sistemas, con la condición que los dos polímeros no posean cargas de signos opuestos. Generalmente, las fuerzas de repulsión entre polímeros están causadas por efectos de hidratación⁽⁸⁾. Por lo tanto, la formación de emulsiones W/W es posible en una gran variedad de mezclas de polímeros hidrosolubles, excepto cuando los dos polímeros poseen cargas de signos opuestos. En el caso de mezclas de polímeros iónicos, o bien un polímero iónico y otro no iónico, la

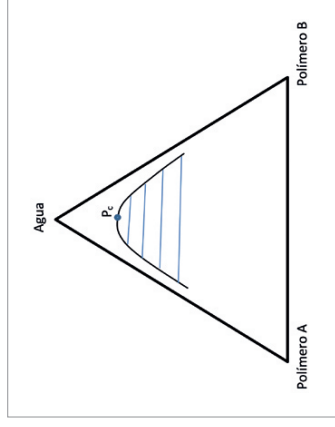


Figura 1. Diagrama de fases ternario esquemático, en un sistema acuoso en presencia de dos polímeros hidrosolubles. Se indica la región de inmiscibilidad, donde es posible formar gotas de emulsiones agua-en-agua (W/W), las líneas de reparto y el punto crítico.

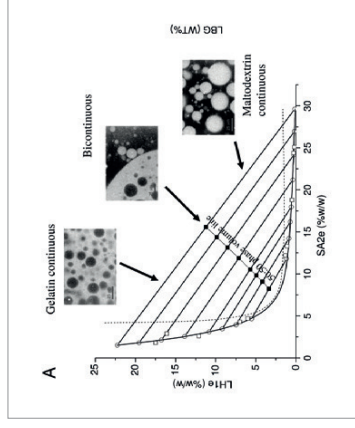


Figura 2. Diagrama de fases del sistema agua/gelatina/maltodextrina, a 45°C (Reproducción de la referencia⁽¹⁷⁾, con permiso de Elsevier).

separación de fases depende del pH y de la fuerza iónica del medio.

Normalmente los diagramas de fases se representan en función de la concentración de un polímero y la concentración del segundo polímero. En la Figura 2 se muestra un ejemplo representativo. Se muestra la región bifásica, donde se pueden formar las emulsiones, en función de las concentraciones de los dos polímeros. Las concentraciones en equilibrio se relacionan mediante las líneas de reparto ("tie-lines")⁽¹¹⁾.

En el ejemplo de la Figura 2, del sistema agua/gelatina/maltodextrina, se muestran los distintos tipos de emulsiones. Las emulsiones de Maltodextrina-en-gelatina se preparan en composiciones ricas en gelatina, y las emulsiones de gelatina-en-maltodextrina se preparan en composiciones con mayor contenido de maltodextrina. En

composiciones intermedias es posible observar emulsiones bicontinuas, cuya estabilidad suele ser muy reducida.

Formación de emulsiones

Las emulsiones agua-en-agua se pueden preparar mezclando dos soluciones acuosas, que contienen polímeros mutuamente inmiscibles⁽¹⁾. Estas emulsiones se obtienen sin añadir tensioactivo y sin aceite, en sistemas acuosos bifásicos. La Figura 3 muestra un esquema de este proceso de preparación.

En las emulsiones W/W, la diferencia de índices de refracción entre la fase dispersa y la continua suele ser muy pequeña, y por lo tanto, las emulsiones W/W son translúcidas. Como ejemplo, en la Figura 4 se muestra el

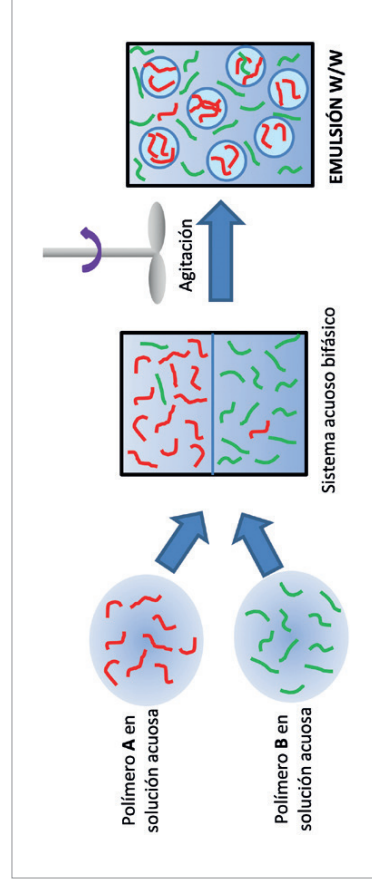


Figura 3. Esquema de la preparación de emulsiones W/W.

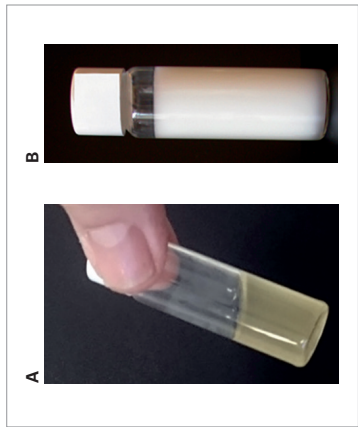


Figura 4. Imágenes ilustrativas de una emulsión de tipo agua-en-agua (W/W), mostrando poca turbidez, y de una emulsión convencional de tipo aceite-en-agua (O/W), cuyo turbidez es mayor.

aspecto macroscópico de una emulsión W/W, donde se observa que la emulsión posee una baja turbidez. Como comparación, se muestra el aspecto típico de una emulsión convencional de tipo O/W.

Las emulsiones W/W se pueden preparar en una gran variedad de mezclas de polímeros solubles en agua (dextrano, gelatina, almidón, polietilenglicol, etc). Como ejemplos, se pueden citar los sistemas almidón/agar⁽⁶⁾, PEG/dextrano⁽¹³⁾ y gelatina/maltodextrina⁽¹⁴⁾. La principal dificultad en la formulación de emulsiones agua-en-agua es conseguir una buena estabilidad. Esta limitación ha sido un problema importante durante mucho tiempo. Sin embargo, recientemente se han desarrollado nuevos métodos que permiten conseguir una buena estabilidad de las dispersiones.

Estabilización de las emulsiones

Las emulsiones W/W suelen presentar coalescencia, que puede disminuir su estabilidad coloidal. Por razones obvias, las moléculas de tensioactivo no se adsorben en las interfases W/W. Por lo tanto, las emulsiones de tipo W/W se deben estabilizar utilizando mecanismos distintos de las emulsiones convencionales.

Algunas emulsiones W/W pueden ser estables, gracias a la repulsión electrostática entre las gotas que previene el contacto entre las gotas. Otro mecanismo es la estabilización mediante partículas adsorbidas en la superficie de las gotas. Se conoce que estas emulsiones estables, denominadas emulsiones de Pickering⁽¹⁵⁾, pueden ser de tipos aceite-en-agua (O/W) o agua-en-aceite (W/O). Sin embargo, recientemente se ha descrito que las

emulsiones de Pickering también pueden ser de tipo agua-en-agua^(17,21).

La energía de adsorción, ΔG , de una partícula esférica en una interfase es función de su radio R, la tensión interfacial γ , y el ángulo de contacto en la interfase θ . Esta energía de adsorción viene determinada por la ecuación 1⁽⁶⁾.

$$\Delta G = \pi R^2 \gamma (1 - \cos \theta)^2 \quad (Eq. 1)$$

En emulsiones W/W, la energía de adsorción, ΔG , es pequeña porque el valor de tensión, γ , suele ser muy bajo. Sin embargo, la energía de adsorción aumenta con R^2 . Por lo tanto, cuando el tamaño de las partículas es relativamente grande, entonces la energía de adsorción es suficiente para mantener a las partículas en la interfase. En la Figura 5 se muestran dos ejemplos de emulsiones de tipo agua-en-agua, estabilizadas mediante partículas.

Durante los últimos años, se han escrito emulsiones W/W estabilizadas mediante distintas partículas, que incluyen arcillas⁽²²⁾, cristales de celulosa⁽²³⁾ y liposomas⁽²⁴⁾. Por lo tanto, los estabilizantes para las emulsiones W/W pueden ser muy variados, considerando partículas hidrofílicas.

Aplicaciones de las emulsiones W/W

Las emulsiones W/W pueden poseer propiedades muy interesantes, como biocompatibilidad, ausencia de toxicidad y elevada transparencia; y por ello pueden ser de gran interés en una gran variedad de aplicaciones comerciales. Cabe destacar que las emulsiones W/W se pueden preparar utilizando mezclas de proteínas y polisacáridos biocompatibles⁽²⁵⁾. Por ello, se considera de gran importancia la utilización de las emulsiones W/W para incorporar principios activos, y estudiar la liberación controlada de productos para aplicaciones farmacéuticas y alimentarias⁽²⁶⁾. Además, las emulsiones W/W pueden ser de gran interés para formulaciones alimentarias ("free-fat emulsions")⁽²⁷⁾, cuyo interés comercial es muy elevado, considerando la formulación de emulsiones alimentarias sin grasas y con muy bajas calorías. Es importante señalar que algunas emulsiones de tipo agua-en-agua ya existen comercialmente en el mercado, aunque la naturaleza coloidal de estas formulaciones no sea conocida⁽²⁸⁾.

Una aplicación muy interesante de las emulsiones agua-en-agua es su utilización como precursores para la obtención de microgeles. Los microgeles son partículas formadas por una red tridimensional fuertemente

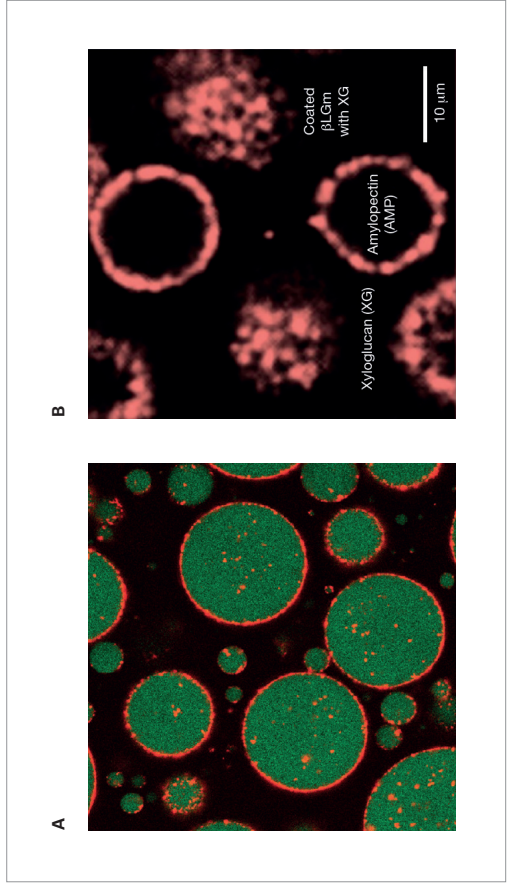


Fig. 5. Ejemplos de emulsiones W/W estabilizadas mediante partículas. (a) gotas que contienen dextrano, dispersadas en una solución de polietilenglicol. (b) gotas con amilopectina, dispersadas en una solución de aliglucano. En ambos casos, los partículas estabilizantes se han preparado a partir de *Psittaculobolus*. Las imágenes se han obtenido mediante microscopía confocal de fluorescencia, utilizando marcadores fluorescentes (Imágenes reproducidas de los referencias^(22,23), con permiso de la American Chemical Society).

hidratada, y que es capaz de retener una elevada cantidad de agua (>95%). Generalmente, las partículas de microgeles están constituidas por un polímero, muy hidrófilo, entrecruzado mediante enlaces covalentes^(29,30).

Esta estructura permite que las partículas de microgeles puedan hincharse y/o encogerse de forma totalmente reversible, absorbiendo y/o expulsando agua. Este comportamiento de hinchamiento/encogimiento puede depender de estímulos externos (temperatura, pH, fuerza iónica, presión osmótica, etc). Por este motivo, los microgeles pueden permitir la liberación



Figura 6. Ejemplo de microgeles de gelatina, obtenidos mediante la gelificación de la fase dispersa en emulsiones de tipo agua-en-agua.

"inteligente" de principios activos, en función de dichos estímulos externos. La Figura 6 muestra un ejemplo de microgeles de gelatina, obtenidos en emulsiones de tipo gelatina-en-maltodextrina.

Después del proceso de emulsificación el polímero que se encuentra en la fase dispersa se puede reticular y así formar un microgel. La formación de microgeles a partir de emulsiones W/W presenta una serie de ventajas ya que no es necesaria la adición de tensioactivos ni de fase oleosa. Además se evita el uso de solventes orgánicos los cuales pueden afectar a la estabilidad de las proteínas y a la biocompatibilidad del sistema. Como resultado se puede obtener un microgel biocompatible de fácil fabricación que puede ser empleado en el sector farmacéutico como vehículo para la liberación de fármacos y en el sector alimentario o cosmético para impartir las características necesarias de viscosidad al producto.

Otra aplicación de las emulsiones W/W es su utilización como microreactores para la síntesis de moléculas de alto valor añadido. Las emulsiones W/W presentan las ventajas que mantienen medios confinados, permitiendo la entrada/salida de reactivos y productos, en condiciones acuosas suaves y biocompatibles. Por ejemplo, se han descrito reacciones de síntesis orgánica en gotas de solución de dextrano, dispersas en una solución de polietilenglicol⁽³¹⁾. Otro ejemplo es la

utilización de emulsiones W/W para la síntesis de partículas de CaCO₃²⁴.

Todos estos ejemplos ilustran que las emulsiones agua-en-agua son sistemas biocompatibles y biomiméticos, que se pueden formular con una gran variedad de componentes hidrófilos. Evidentemente, un aspecto muy importante es que no contienen ni aceite ni tensioactivo, es decir, son sistemas obtenidos exclusivamente con moléculas solubles en agua.

Hasta el momento, se han desarrollado pocas aplicaciones en cosmética. Ello es debido al poco conocimiento sobre estos sistemas y las dificultades en conseguir una buena estabilidad. Sin embargo, descubrimientos recientes han permitido conocer nuevas formas de estabilización de las emulsiones, y alcanzar una buena estabilidad a largo plazo. Sin duda, las emulsiones W/W son muy prometedoras y es previsible que próximamente aparezcan nuevas aplicaciones, con el lanzamiento de nuevos productos al mercado, basados en dispersiones W/W.

Conclusiones

Las emulsiones agua-en-agua (W/W) son dispersiones coloidales muy interesantes que consisten en gotas de una solución acuosa, dispersas en otra solución acuosa. Las emulsiones W/W se preparan en mezclas acuosas de dos polímeros hidrosolubles, formando dos fases líquidas inmiscibles. Por lo tanto, las emulsiones W/W no contienen ni aceite ni tensioactivo. Se pueden obtener utilizando componentes biocompatibles y de grado alimentario, como por ejemplo proteínas (albúmina, gelatina, lactoglobulina, etc.) y polisacáridos (almidón, agar, maltodextrina, etc.). Por lo tanto, las posibles aplicaciones pueden ser muy variadas. Actualmente, se están desarrollando emulsiones W/W para la encapsulación y liberación de principios activos hidrofílicos. Una aplicación desarrollada recientemente es la utilización de las emulsiones W/W para la síntesis de microgeles.

La estabilización de las emulsiones W/W ha sido un aspecto que ha limitado la utilización de estas emulsiones para aplicaciones comerciales. Sin embargo, recientes descubrimientos han demostrado que las emulsiones W/W se pueden estabilizar a largo plazo, gracias a mecanismos de repulsión electrostática o de estabilización mediante adsorción de partículas. Ello puede permitir el desarrollo de nuevas e interesantes aplicaciones en cosmética. Actualmente, el rango de posibles aplicaciones se expande muy rápidamente, y se están desarrollando investigaciones de gran interés.

Es de esperar que en un futuro aparezcan nuevas aplicaciones en una gran variedad de campos tecnológicos, tales como biomedicina, farmacia, cosmética y/o formulaciones alimentarias, etc.

Agradecimientos

Los autores agradecen el apoyo del Ministerio de Economía y Competitividad (Proyecto CTQ2014-52687-C3-1-P) y de la Comisión Europea (ayudas Marie Skłodowska Curie, FP7-PEOPLE-2013-ITN). Los autores también agradecen el apoyo de la Generalitat de Catalunya (2014SGR1655 and TECCT15-10009) y del Centro de Investigación Biomédica en Red de Biogeriería, Biomateriales y Nanomedicina (CIBER-BBN). Los autores también agradecen a Sarah Poletti por las imágenes de microgeles de gelatina.

Referencias

1. J. Esquerdo, "Water-in-water (W/W) emulsions," *Curr. Opin. Colloid Interface Sci.*, vol. 25, pp. 109-119, 2016.
2. I. Capron, S. Costeux, and M. Djibourou, "Water in water emulsions: phase separation and rheology of biopolymer solutions," *Rheol. Acta*, vol. 40, no. 5, pp. 441-456, Sep. 2001.
3. T. Nicolai and B. Murray, "Particle stabilized water in water emulsions," *Food Hydrocol.*, vol. (in press), 2016.
4. A. H. Cheung Shum, J. Yamell, and D. A. Weitz, "Microfluidic fabrication of water-in-water (w/w) jets and emulsions," *Biomicrofluidics*, vol. 6, no. 1, p. 12808, 2012.
5. M. W. Beijerinck, "Ueber eine Eigentümlichkeit der löslichen Stärke," *Zentralblatt für Bakteriologie, Parasitenkunde und Infekt.*, vol. 2, no. 22, pp. 697-699, 1896.
6. M. W. Beijerinck, "Ueber emulsionsbildung bei der vermischung wässriger Lösungen gewisser gelatinierender Kolloide," *Zeitschr. Chem. Ind. Kolloide (KolloidZ)*, vol. 7, p. 16, 1910.
7. R. Hatti-Kaul, "Aqueous Two-Phase Systems: A General Overview," *Mol. Biotechnol.*, vol. 19, pp. 269-277, 2001.
8. C. Kang and S. Sandler, "Phase behavior of aqueous two-polymer systems," *Fluid Phase Equilib.*, vol. 38, pp. 245-272, 1987.
9. V. Y. Grinberg and V. B. Tolstoguzov, "Thermodynamic incompatibility of proteins and polysaccharides in solutions," *Food Hydrocol.*, vol. 11, no. 2, pp. 145-158, 1997.
10. S. L. Turgeon, C. Schmitt, and C. Sanchez, "Protein-polysaccharide complexes and concentrates," *Curr. Opin. Colloid Interface Sci.*, vol. 12, no. 4-5, pp. 166-178, 2007.
11. A. H. Clark, "Direct analysis of experimental tie line data (two polymer - one solvent systems) using Flory - Huggins theory," *Carbohydr. Polym.*, vol. 42, pp. 337-351, 2000.
12. I. T. Norton and W. J. Frith, "Microstructure design in mixed biopolymer composites," *Food Hydrocol.*, vol. 15, no. 4-6, pp. 543-553, Jul. 2001.
13. R. J. Steinko, O. Fransson, E. M. van Bommel, D. J. Commin, and W. E. Hennink, "The use of aqueous PEG/dextran phase separation for the

31. D. C. Dewey, C. A. Stoulsen, D. N. Cacace, P. C. Bevilacqua, and C. D. Keating, "Bioreactor droplets from liposome-stabilized all-aqueous emulsions," *Mt. Commun.*, vol. 5, no. May, pp. 1-9, 2014.
32. J. K. Oh, R. Drumright, D. J. Siegwart, and K. Matyjaszewski, "The development of microgels/nanogels for drug delivery applications," *Prog. Polym. Sci.*, vol. 33, no. 4, pp. 448-477, 2008.
33. J. Rubio-Retama, F. M. Tamini, M. Henrich, and E. López-Cabarcos, "Synthesis and Characterization of Poly (magnesium acrylate) Microgels," *Langmuir*, no. 23, pp. 8538-8543, 2007.
34. S. Alexopoulos, S. Kasapis, and R. Abeysekera, "Formation of kinetically trapped gels in the maltodextrin-gelatin system," *Carbohydr. Res.*, vol. 293, no. 1, pp. 79-99, Oct. 1996.
35. S. Alexopoulos and S. Kasapis, "Molecular weight effects on the gelatin/maltodextrin gel," *Carbohydr. Polym.*, vol. 40, pp. 83-97, 1999.
36. S. Kasapis, E. R. Morris, I. T. Norton, and A. H. Clark, "Phase equilibria and gelation in gelatin/maltodextrin systems - Part I: gelation of individual components," *Carbohydr. Polym.*, vol. 21, no. 4, pp. 243-249, Jan. 1993.
37. S. Kasapis, E. R. Morris, I. T. Norton, and M. J. Gidley, "Phase equilibria and gelation in gelatin/maltodextrin systems - Part II: polymer incompatibility in solution," *Carbohydr. Polym.*, vol. 21, no. 4, pp. 249-259, Jan. 1993.
38. S. Kasapis, E. R. Morris, I. T. Norton, and C. R. T. Brown, "Phase equilibria and gelation in gelatin/maltodextrin systems - Part III: phase separation in mixed gels," *Carbohydr. Polym.*, vol. 21, no. 4, pp. 261-268, Jan. 1993.
39. S. Kasapis, E. R. Morris, I. T. Norton, and A. H. Clark, "Phase equilibria and gelation in gelatin/maltodextrin systems - Part IV: composition-dependence of mixed-gel moduli," *Carbohydr. Polym.*, vol. 21, no. 4, pp. 269-276, Jan. 1993.
40. L. Lundin, I. T. Norton, T. J. Foster, M. A. K. Williams, A. M. Hermansson, and E. Bergström, "Phase separation in mixed biopolymer systems," in *10th International Gums and Stabilizers for the Food Industry. The Past, Present and Future of Food Hydrocolloids*, 1999, pp. 167-180.
41. J. R. Stokes, B. Wolf, and W. J. Frith, "Phase-separated biopolymer mixture rheology: Prediction using a viscoelastic emulsion model," *J. Rheol.* (N. Y. N. Y.), vol. 45, no. 5, p. 1173, 2001.
42. H. M. Shewan and J. R. Stokes, "Review of techniques to manufacture micro-hydrogel particles for the food industry and their applications," *J. Food Eng.*, vol. 119, no. 4, pp. 781-792, 2013.
43. G. V. N. Redna and P. R. Chatterji, "Controlled Drug Release from Gelatin-Sodium Carboxymethylcellulose Interpenetrating Polymer Networks," *J. Macromol. Sci.*, vol. 1325, no. 6, pp. 629-639, 2003.
44. D. Aydın and S. Kizilel, "Water-in-Water Emulsion Based Synthesis of Hydrogel Nanospheres with Tunable Release Kinetics," *J. Miner. Met. Mater. Soc.*, vol. (in press), 2016.
45. A. Matralanis, U. Lesmes, E. A. Decker, and D. J. McClements, "Fabrication and characterization of filled hydrogel particles based on sequential segregative and aggregative biopolymer phase separation," vol. 24, no. 8, pp. 689-701, 2010. ●

8.4 Contributions at Conferences

During his PhD Thesis, Yoran Beldengrün contributed to the following list of oral presentations and posters at scientific conferences. For the oral presentations, the speaker is underlined.

Oral Presentations

- Y. Beldengrün, J. Aragón-Artigas, C. Miguel-Espigulé, M. Ros-González, L. Corvo- Alguacil, J. Esquena-Moret: “*Designing Enzyme Carriers: Water-in-Water Emulsions as templates for Microgels and Encapsulated Emulsions*”. ESC2017, 19-22 June 2017, Florence.
- Y. Beldengrün, J. Aragón-Artigas, C. Miguel-Espigulé, M. Ros-González, L. Corvo- Alguacil, J. Esquena-Moret: “*Use of water-in-water emulsions for encapsulation of enzymes*”. 47 Jornadas del Comité Español de la Detergencia, Tensioactivos y Productos Afines (CED47), Barcelona, 3-4 March 2017.
- Y. Beldengrün: “*Cross-Linked microgels, produced by water-in-water-emulsions, as delivery system for enzymes*”. III Meeting of Young Researchers on Colloids and Interfaces (JICI III), Madrid, Spain, 13-14 October 2016.
- Y. Beldengrün, J. Aragón-Artigas, J. E. Moret: “*Formation of responsive enzyme-loaded gelatin microgels using water-in-water emulsions*”. 30th European Colloid and Interface Society (ECIS), Rome, Italy, 4-9 September 2016.
- Y. Beldengrün, “*Formation of responsive enzyme-loaded gelatin microgels using water-in-water emulsions*”. Workshop CBN16, Barcelona, October 2016.
- Yoran Beldengrün; Jordi Aragón; Laura Corvo; Cristina Miquel; Maite Ros; Jordi Esquena, “*Water-in-water (W/W) emulsions for preparing microgels*”. 31th Conference of the European Colloid and Interface Society (ECIS 2017), Madrid, 3-8 September 2017.
- Y. Beldengrün, J. Aragón, L. Corvo, C. Miquel, M. Ros, J. Esquena, “*Microgels obtained in water-in-water (W/W) emulsions*”. 7th Iberian Meeting on Colloids and Interfaces (RICI7), Madrid, 4-7 July 2017.
- Y. Beldengrün, J. Esquena, “*Water-in-water (W/W) emulsions*”. ”. 48 Jornadas del Comité Español de la Detergencia, Tensioactivos y Productos Afines (CED47), Barcelona, 7-8 March 2018.
- Y. Beldengrün, L. Corvo, C. Jaén, C. Miquel, M. Ros, N. Salinas, J. Esquena, “*Water-in-Water (W/W) emulsions for preparation of microgels and encapsulation of active components*”, 16th Conference of the International Association of Colloid and Interface Scientists (16th IACIS), Rotterdam, Netherlands, 21-25 May, 2018.

Posters

- Y. Beldengrün: “*Cross-Linked Microgels, produced by water-in-water-emulsions, as delivery system for enzymes*”. Formula VIII/ CED47 Congress, Barcelona, Spain, 4-7 July 2016.

8.5 Undergraduate Students Supervised

During his PhD Thesis, Yoran Beldengrün supervised the following six undergraduate students.

- Laura Corvo
Emulsion des Carboxymetilcelulosa sódica (NaCMC) y Albúmina de Suero Bovino (BSA) iónicamente entrecruzadas como sistemas de liberación de enzimas.
Type of Work: Final Grade Thesis (TFG)
Codirectors: Yoran Beldengrün; Jordi Esquena
Universitat Autònoma de Barcelona
Year: 2017
- Maite Ros González
Preparación y caracterización de microgeles en emulsiones agua-en-agua
Type of Work: Internship
Codirectors: Yoran Beldengrün; Jordi Esquena
Universitat de Barcelona
Year: 2016
- Juan Maldonado
Enzyme Encapsulation into Microgels
Type of Work: Internship
Codirectors: Yoran Beldengrün; Jordi Esquena
University of Austin, Texas
Year: 2016
- Jordi Aragón Artigas
Influence of electrolytes and pH on the phase behaviour of gelatin/maltodextrine mixtures, for water-in-water emulsion formation
Type of Work: Final Grade Thesis (TFG)
Codirectors: Yoran Beldengrün; Jordi Esquena Universitat de Barcelona
Year: 2016
- Cristina Miquel Espigulé
Novel Biocompatible microgels for functional food, obtained in water-in-water emulsions
Type of Work: Final Grade Thesis (TFG)
Codirectors: Yoran Beldengrün; Jordi Esquena
Universitat de Barcelona
Year: 2016
- Sarah Poletti
Preparation and Characterization of microgels
Type of Work: Internship
Codirectors: Yoran Beldengrün; Jordi Esquena
University of Austin, Texas
Year: 2015